

2014

Improved Synthesis, Separation, Transition Metal Coordination and Reaction Chemistry of a New Binucleating Tetrphosphine Ligand

Ekaterina Kalachnikova

Louisiana State University and Agricultural and Mechanical College, kat_kalach@hotmail.com

Follow this and additional works at: https://digitalcommons.lsu.edu/gradschool_dissertations



Part of the [Chemistry Commons](#)

Recommended Citation

Kalachnikova, Ekaterina, "Improved Synthesis, Separation, Transition Metal Coordination and Reaction Chemistry of a New Binucleating Tetrphosphine Ligand" (2014). *LSU Doctoral Dissertations*. 1105.
https://digitalcommons.lsu.edu/gradschool_dissertations/1105

This Dissertation is brought to you for free and open access by the Graduate School at LSU Digital Commons. It has been accepted for inclusion in LSU Doctoral Dissertations by an authorized graduate school editor of LSU Digital Commons. For more information, please contact gradetd@lsu.edu.

IMPROVED SYNTHESIS, SEPARATION, TRANSITION METAL
COORDINATION AND REACTION CHEMISTRY OF A NEW
BINUCLEATING TETRAPHOSPHINE LIGAND

A Dissertation

Submitted to the Graduate Faculty of the
Louisiana State University and
Agricultural and Mechanical College
in partial fulfillment of the
requirement for the degree of
Doctor of Philosophy

in

The Department of Chemistry

by
Ekaterina Kalachnikova
B.S. University of South Alabama, 2007
May 2015

Acknowledgements

I am very grateful to Prof. George Stanley for providing me with the opportunity to join his research group, for his guidance, encouragement, and constant support. Thank you for dedicating your time and energy to help me be an individual I am today. Thank you for always being available and ready to help.

I thank my doctoral committee members: Profs. Andrew Maverick, Evgueni Nesterov, Jun Xu for all their time and helpful suggestions.

I am especially thankful to Dr. Frank Fronczek and Dr. Gregory T. McCandless for their crystallographic expertise and willingness to explain how things work. I am very thankful to Dr. Dale Treleaven for his many helpful discussions, for introducing me to NMR, and for all the suggestions regarding this dissertation. Thank you to Dr. Thomas Weldegheorghis for his NMR expertise and for all his help.

I am forever thankful to Stanley group for helpful suggestions, fruitful discussions and friendships.

Table of Contents

Acknowledgements	ii
List of Tables	vi
List of Figures	vii
List of Schemes	xii
List of Abbreviations	xv
Abstract	xvi
Chapter 1: Introduction	1
1.1 Alkene Hydration	1
1.2 Mechanistic Aspects of Alkene Hydration Catalyzed by Late Transition Metal Complexes	8
1.3 Bimetallic Nickel Tetraphosphine Complexes as Possible Catalysts for Alkene Hydration/Oxidation	13
1.4 Alkene Oxidative Cleavage	17
1.5 References	21
Chapter 2: Investigations into Alkene Hydration/Oligomerization by Nickel Phosphine Complexes: The Unfortunate Role of Rubber Septa	26
2.1 Review of Prior Research	26
2.2 Results and Discussion: Further Investigation into Ni oligomerization Catalysis	30
2.3 Conclusions	35
2.4 References	35
Chapter 3: Nickel - Phosphine Mediated Oxidative Cleavage of Alkene C = C Bonds by O ₂	37
3.1 Background	37
3.2 Results and Discussion	37
3.2.1 Investigations into Alkene Oxidation in the Presence of Ni(II) Phosphine Complexes	37
3.2.2 Substrate Studies	41
3.2.3 Synthesis and Characterization of <i>meso</i> -Ni ₂ Br ₄ (<i>et</i> , <i>ph</i> -P ₄)	44
3.2.4 Other Systems Tested	47
3.2.5 Other Reaction Observations	48
Addition of AgBF ₄	48
Temperature	48
O ₂ Pressure	49
Water	49
Other Organic Solvents Tested	50
H ₂ O ₂ as Primary Oxidant	50

3.2.6	Proposed Mechanism	51
3.2.7	NMR Studies	53
	Investigations into the Nature of the Active Species	53
	Variable Temperature NMR	57
	Low Temperature NMR.....	60
	NMR Studies of the et, ph-P4 Ligand in Solution in the Presence of Oxygen.....	62
3.2.8	Oxidative Cleavage of Alkene in the Presence of Phosphine Ligands ..	65
3.3	Conclusions.....	73
3.4	References.....	73
Chapter 4: New Tetraphosphine Ligand Synthesis, Separation, Transition Metal Coordination, and Characterization.....		
		76
4.1	Introduction	76
4.2	Results and Discussion	82
4.2.1	Preparation of Cl(Ph)PCH ₂ P(Ph)Cl, 2	82
4.2.2	Preparation of 1-(Diethylphosphino)-2-Iodobenzene, 3(I)	91
4.2.3	Preparation of <i>rac,meso</i> -et,ph-P4-Ph.....	95
4.2.4	Separation of <i>rac</i> and <i>meso</i> -Diastereomers of et,ph-P4-Ph.....	101
4.2.5	Improved Preparation of et,ph-P4-Ph Ligand via Grignard Mediated P-C Coupling	107
4.2.6	Synthesis of Pt ₂ Cl ₄ (<i>rac</i> -et,pt-P4-Ph), 4R	113
4.2.7	Synthesis of PtNiCl ₄ (<i>rac</i> -et,pt-P4-Ph), 5R	117
4.2.8	Synthesis of [<i>rac</i> -Rh ₂ (nbd) ₂ (et,ph-P4-Ph)](BF ₄) ₂ , 6R	124
4.3	Conclusions and Future Directions	128
4.4	References.....	130
Chapter 5: Experimental Procedures and Additional Spectroscopic Data.....		
		134
5.1	General Considerations	134
5.2	General Procedure Used to Study Alkene Oligomerization Catalysis	134
5.3	General Procedure Used to Test for Alkene Hydration	135
	Method A.....	136
	Method B.....	136
5.4	Synthesis and Characterization of <i>meso</i> -Ni ₂ Cl ₄ (et,ph-P4)	136
5.5	General Procedure Used to Study Alkene Oxidative Cleavage Catalysis ...	137
5.6	Reaction of <i>meso</i> -Ni ₂ Cl ₄ (et,ph-P4) and 1-Hexene Monitored by Variable Temperature NMR	138
5.7	Variable Temperature NMR of the “final” Species.....	138
5.8	Synthesis of Methylenebis (Chlorophenylphosphine).....	138
	Method A.....	138
	Method B.....	139
	Method C.....	139
	Method D.....	139
	Method E.....	140
	Method F	140
5.9	Synthesis of 1-(Diethylphosphino)-2-Iodobenzene, 3(I)	140
5.10	Synthesis of 1-(Diethylphosphino)-2-Bromobenzene, 3(Br)	141

5.11 Synthesis of <i>rac,meso</i> -et,ph-P4-Ph Ligand	142
Method A.....	142
Method B.....	143
Method C.....	143
5.12 Separation <i>rac</i> and <i>meso</i> -et,ph-P4-Ph via Column Chromatography	145
5.13 Synthesis of Pt ₂ Cl ₄ (<i>rac</i> -et,ph-P4-Ph), 4R	145
5.14 Synthesis of PtNiCl ₄ (<i>rac</i> -et,ph-P4-Ph), 5R	146
5.15 Synthesis of [Rh ₂ (nbd) ₂ (<i>rac</i> -et,ph-P4-Ph)](BF ₄) ₂ , 4R	147
5.16 Additional Spectroscopic Data	148
5.17 References.....	155
Vita	156

List of Tables

Table 3.2.1	Crystallographic Data for <i>meso</i> -Ni ₂ Br ₄ (<i>et</i> , <i>ph</i> -P4)•2(CH ₃ CN).....	46
Table 3.2.2	Selected Bond Distances (Å) and Angles (°) for <i>meso</i> -Ni ₂ Br ₄ (<i>et</i> , <i>ph</i> -P4)•2(CH ₃ CN).....	47
Table 4.2.1	Chlorination of primary and secondary phosphines with C ₂ Cl ₆ and PCl ₅ as reported by Weferling.....	84
Table 4.2.2	Results from the chlorination of 2 with C ₂ Cl ₆ and PCl ₅	86
Table 4.2.3	Preparation of arylphosphines via magnesium-halide exchange reaction of aryl halides with <i>i</i> PrMgBr, followed by reaction with PEt ₂ Cl reported by Monteil.....	94
Table 4.2.4	Selected Bond Distances (Å) and Angles (deg) for one molecule of <i>rac</i> Pt ₂ Cl ₄ (<i>et</i> , <i>ph</i> -P4-Ph).....	117
Table 4.2.5	Selected Bond Distances (Å) and Angles (deg) for <i>rac</i> -NiPtCl ₄ (<i>et</i> , <i>ph</i> -P4-Ph)•CH ₂ Cl ₂	124
Table 4.2.6	Selected Bond Distances (Å) and Angles (°) for [Rh ₂ (<i>nbd</i>) ₂ (<i>rac</i> - <i>et</i> , <i>ph</i> -P4 Ph)](BF ₄) ₂ •2C ₃ H ₆ O	127

List of Figures

Figure 1.1.1	Shvo's catalyst.....	7
Figure 1.3.1	Binucleating tetraphosphine ligands <i>rac</i> - and <i>meso</i> -et,ph-P4.....	13
Figure 1.3.2	<i>Rac</i> -Ni ₂ Cl ₄ (et,Ph-P4) and <i>meso</i> -Ni ₂ Cl ₄ (et,Ph-P4).....	15
Figure 1.3.3	Binucleating tetraphosphine ligands <i>rac</i> - and <i>meso</i> -et,ph-P4-Ph	15
Figure 1.3.4	ORTEP plot of [Ni ₂ Cl ₂ (μ-OH)(<i>meso</i> -et,ph-P4-Ph)] ⁺ . Ni··Ni distance of 3.371 Å.....	17
Figure 2.1	Gel permeation chromatography of the white solid produced from three reactions of 1-hexene, 1-octene, and a mixture of 1- hexene/1-octene and Ni ₂ Cl ₄ (<i>meso</i> -et,ph-P4) in a H ₂ O/acetone solvent mixture (70°C)	26
Figure 2.2	FT-IR of the white solid produced from 1-hexene and Ni ₂ Cl ₄ (<i>meso</i> -et,ph-P4) in a H ₂ O/acetone solvent mixture (70°C) compared to a C ₃₆ H ₇₄ reference	27
Figure 2.3	(a) Nickel catalyst used by Keim to oligomerize ethylene to produce 1-alkenes of various chain lengths. ¹ (b) Ni(II) complexes used by Brookhart <i>et al.</i> in the presence of MAO (methylaluminoxane) as co-catalyst for ethylene polymerization. R = i-Pr, R' = H, Me, or 1,8-naphthdiyl	28
Figure 2.4	400 MHz ¹ H NMR of white powder in CDCl ₃ from the reaction of 1-hexene in the presence of <i>meso</i> -Ni ₂ Cl ₄ (et,ph-P4)	32
Figure 2.5	400 MHz ¹ H NMR of white powder in CDCl ₃ Top: from the reaction of vinyl acetate in the presence of <i>meso</i> -Ni ₂ Cl ₄ (et,ph-P4) catalyst. Bottom: from the reaction of 1-hexene in the presence of <i>meso</i> -Ni ₂ Cl ₄ (et,ph-P4) catalyst	34
Figure 3.2.1	The 5-11 ppm region of the ¹ H NMR spectrum of the sample from the reaction of <i>meso</i> -Ni ₂ Cl ₄ (et,ph-P4) with 1-hexene in acetone-d ₆ /D ₂ O (15% by volume). Resonances between 7.0 and 8.5 ppm are due to the phenyl-ring hydrogens on the et-ph-P4 ligand	39
Figure 3.2.2	³¹ P{ ¹ H} spectrum of <i>meso</i> -Ni ₂ Br ₄ (et,ph-P4) in CD ₃ CN.....	44
Figure 3.2.3	ORTEP (50% ellipsoids) of <i>meso</i> -Ni ₂ Br ₄ (et,ph-P4)•2(CH ₃ CN). Solvent molecules and hydrogen atoms omitted for clarity	45

Figure 3.2.4	ORTEP plot of $[\text{Ni}_2(\mu\text{-OH})\text{Cl}_2(\text{et,ph-P4-Ph})]^+$, 2 . Ellipsoids are shown at the 50% probability level. Hydrogens on the carbon atoms and the $[\text{NiCl}_4]^{2-}$ counter-anion are omitted for clarity 51
Figure 3.2.5	(Black spectrum) The 6-9.7 ppm region of the ^1H NMR spectra: <i>meso</i> - $\text{Ni}_2\text{Cl}_4(\text{et,ph-P4})$ in acetone- d_6 ; (red spectrum) D_2O added, after 3 days under O_2 54
Figure 3.2.6	$^{31}\text{P}\{^1\text{H}\}$ spectra of <i>meso</i> - $\text{Ni}_2\text{Cl}_4(\text{et,ph-P4})$ in CD_2Cl_2 (red line). $^{31}\text{P}\{^1\text{H}\}$ spectra of <i>meso</i> - $\text{Ni}_2\text{Cl}_4(\text{et,ph-P4})$ in acetone- $\text{d}_6/\text{D}_2\text{O}$ recorded 20 minutes after addition of D_2O (green line). $^{31}\text{P}\{^1\text{H}\}$ spectra of <i>meso</i> - $\text{Ni}_2\text{Cl}_4(\text{et,ph-P4})$ in acetone- $\text{d}_6/\text{D}_2\text{O}$ recorded 24 hours after addition of D_2O (black line). $^{31}\text{P}\{^1\text{H}\}$ spectra of <i>meso</i> - $\text{Ni}_2\text{Cl}_4(\text{et,ph-P4})$ in acetone- $\text{d}_6/\text{D}_2\text{O}$ recorded 2 days after addition of D_2O (blue line) ... 55
Figure 3.2.7	$^{31}\text{P}\{^1\text{H}\}$ spectra of the sample taken from reaction with 1-hexene in the presence of <i>meso</i> - $\text{Ni}_2\text{Br}_4(\text{et,ph-P4})$ in in acetone- $\text{d}_6/\text{D}_2\text{O}$ recorded 24 hours after the start of the reaction 56
Figure 3.2.8	ORTEP plot of $[\text{Ni}_2(\mu\text{-Cl})(\text{meso-et,ph-P4})_2]^{3+}$, (50% probability ellipsoids, hydrogen atoms omitted for clarity) 57
Figure 3.2.9	$^{31}\text{P}\{^1\text{H}\}$ spectra of <i>meso</i> - $\text{Ni}_2\text{Cl}_4(\text{et,ph-P4})$ with 1-hexene in acetone- $\text{d}_6/\text{D}_2\text{O}$ recorded at -15°C (light blue), -10°C (dark blue), 25°C (black), 50°C (orange), 80°C (purple), and 100°C (red). For higher temperatures the NMR tube was tube pressurized to 90 psi with O_2 59
Figure 3.2.10	^1H spectra of <i>meso</i> - $\text{Ni}_2\text{Cl}_4(\text{et,ph-P4})$ with 1-hexene in acetone- $\text{d}_6/\text{D}_2\text{O}$ solution recorded at 100°C , tube pressurized 90 psi of O_2 59
Figure 3.2.11	$^{31}\text{P}\{^1\text{H}\}$ NMR spectra of <i>meso</i> - $\text{Ni}_2\text{Cl}_4(\text{et,ph-P4})$ in acetone- $\text{d}_6/\text{D}_2\text{O}$ solution: a) at -20° , b) -20° , 1-hexene added, c) 5°C , d) 25°C 60
Figure 3.2.12	^1H spectra of <i>meso</i> - $\text{Ni}_2\text{Cl}_4(\text{et,ph-P4})$ in acetone- $\text{d}_6/\text{D}_2\text{O}$ solution: a) at -20° , b) -20° , 1-hexene added, c) 5°C , d) 25°C 61
Figure 3.2.13	$^{31}\text{P}\{^1\text{H}\}$ NMR spectra of <i>meso</i> -et,ph-P4 in acetone- d_6 exposed to air..... 63
Figure 3.2.14	$^{31}\text{P}\{^1\text{H}\}$ NMR spectra of <i>meso</i> -et,ph-P4 in acetone- d_6 under 90 psi O_2 . Recorded 1 day after pressurizing with O_2 (black line), 14 days (blue line), 35 days (red line) 64
Figure 3.2.15	The 6-10.5 ppm region of the ^1H NMR spectra: sample taken from the reaction with of <i>trans</i> - β -methylstyrene and <i>meso</i> -(et,ph-P4) in acetone- $\text{d}_6/\text{D}_2\text{O}$ exposed to air after 2 hours 66

Figure 3.2.16	$^{31}\text{P}\{^1\text{H}\}$ NMR spectra of the sample from the reaction with 1-hexene, <i>meso</i> -et,ph-P4 in acetone- $\text{d}_6/\text{D}_2\text{O}$ under N_2 recorded after 24 hrs (blue line), after 3 days (orange line), recorded 1.5 hours upon exposure to air (black line).....	67
Figure 3.2.17	The 6-10.5 ppm region of the ^1H NMR spectra: sample from reaction with 1-hexene, <i>meso</i> -(et,ph-P4) in acetone- $\text{d}_6/\text{D}_2\text{O}$ under N_2 , 24 hours (blue spectrum), same as above recorded 1.5 hours after exposure to O_2 (red spectrum).....	68
Figure 3.2.18	$^{31}\text{P}\{^1\text{H}\}$ NMR spectra of the sample from the reaction with 1-hexene, <i>meso</i> -et,ph-P4 in acetone- $\text{d}_6/\text{D}_2\text{O}$ at 45°C exposed to O_2 after 1.5 hours (black line), after 24 hours (red line)	69
Figure 4.1.1	Binucleating tetraphosphine ligands <i>rac</i> - and <i>meso</i> -et,ph-P4.....	76
Figure 4.1.2	New stronger binucleating tetraphosphine ligands <i>rac</i> - and <i>meso</i> -et,ph-P4-Ph.....	78
Figure 4.1.3	New P4-Ph ligand type with para substituted internal phenyl rings.....	81
Figure 4.2.1	$^{31}\text{P}\{^1\text{H}\}$ spectrum in CDCl_3 of the final product mixture from the reaction of 2 and C_2Cl_6 in Et_2O	85
Figure 4.2.2	$^{31}\text{P}\{^1\text{H}\}$ spectrum in CD_2Cl_2 of the final product mixture from the reaction with 1 eq $\text{H}(\text{Ph})\text{PCH}_2\text{P}(\text{Ph})\text{H}$ and 1.5 eq of C_2Cl_6 in Et_2O ..	87
Figure 4.2.3	(Bottom spectrum) $^{31}\text{P}\{^1\text{H}\}$ NMR spectrum of the crude reaction mixture with 1 and C_2Cl_6 in toluene and (top spectrum) isolated final product in C_6D_6	89
Figure 4.2.4	(Bottom spectrum) $^{31}\text{P}\{^1\text{H}\}$ NMR spectrum of 2 in C_6D_6 before dilution and (top spectrum) after dilution (top) in C_6D_6	90
Figure 4.2.5	$^{31}\text{P}\{^1\text{H}\}$ NMR of the final product mixture in C_6D_6 obtained after work up from the reaction of <i>o</i> -diiodobenzene with <i>i</i> PrMgBr, followed by addition of PEt_2Cl	95
Figure 4.2.6	$^{31}\text{P}\{^1\text{H}\}$ NMR spectrum of the crude product mixture obtained from reaction of 3(l) with <i>i</i> PrMgBr, followed by addition of 2.....	98
Figure 4.2.7	$^{31}\text{P}\{^1\text{H}\}$ NMR spectrum of the final product mixture in C_6D_6 purified via column chromatography on neutral alumina.....	100
Figure 4.2.8	^1H NMR spectra of 2.4-3.5 ppm region of the <i>meso</i> -et,ph-P4-Ph and unidentified phosphine impurities (red spectrum), mixture of	

	<i>meso</i> and <i>rac</i> -et,ph-P4-Ph (black spectrum), and <i>rac</i> -et,ph-P4-Ph (orange spectrum)	102
Figure 4.2.9	³¹ P { ¹ H} NMR spectra of first set of fractions containing unreacted 3(I) and other phosphine impurities (blue spectrum), second set containing <i>meso</i> -et,ph-P4-Ph and unidentified phosphine impurities (red spectrum), third set mixture of <i>meso</i> and <i>rac</i> -et,ph-P4-Ph (black spectrum), and forth set <i>rac</i> -et,ph-P4-Ph (orange spectrum).....	103
Figure 4.2.10	³¹ P { ¹ H} NMR recorded on the sample taken from reaction with 3(I) and <i>i</i> PrMgBr (bottom) after 6h at 0°C and (top) after 24h.....	105
Figure 4.2.11	Final product mixture after 24 hours Mg-I exchange at 0°C in C ₆ D ₆	106
Figure 4.2.12	³¹ P { ¹ H} NMR of the crude sample obtained from reaction of 1-bromo-2 iodobenzene with <i>i</i> PrMgBr (bottom) and final product obtained via distillation under reduced pressure (top spectrum)....	108
Figure 4.2.13	³¹ P { ¹ H} NMR spectrum recorded on the sample taken from reaction of 3(Br) with Mg turnings to generate arylphosphine magnesium reagent.....	109
Figure 4.2.14	(Bottom spectrum) ³¹ P { ¹ H} NMR crude product mixture and (top spectrum) final product mixture purified via column chromatography containing <i>meso</i> et,ph-P4-Ph in 96% purity	110
Figure 4.2.15	(Black spectrum) ³¹ P { ¹ H} NMR of 1:1 mixture of <i>rac</i> and <i>meso</i> -et,ph-P4-Ph, (purple spectrum) <i>meso</i> -et,ph-P4-Ph, and (red spectrum) <i>rac</i> -et,ph-P4-Ph	111
Figure 4.2.16	(Purple spectrum) ¹ H NMR of <i>meso</i> -et,ph-P4-Ph, (red spectrum) <i>rac</i> -et,ph-P4-Ph	112
Figure 4.2.17	The ³¹ P{ ¹ H} NMR of the reaction of PtCl ₂ (cod) and <i>rac</i> -et,ph-P4-Ph in CDCl ₃ after 2 hours	114
Figure 4.2.18	³¹ P{ ¹ H} NMR of the crude reaction mixture of PtCl ₂ (cod) and <i>rac</i> -et,ph-P4-Ph after 6 hrs of reaction (bottom spectrum) and purified Pt ₂ Cl ₂ (<i>rac</i> -et,ph-P4-Ph), 5R in CDCl ₃ (top spectrum)	115
Figure 4.2.19	ORTEP (50% ellipsoids) of one molecule of Pt ₂ Cl ₄ (<i>rac</i> -et,ph-P4-Ph), 5R, in the asymmetric unit. Hydrogen atoms are omitted for clarity	116
Figure 4.2.20	(Top spectrum) ³¹ P{ ¹ H} NMR of NiPtCl ₄ (<i>rac</i> -et,ph-P4-Ph) in C ₆ D ₆ , (middle) <i>rac</i> -Pt ₂ Cl ₄ (et,ph-P4-Ph), and (bottom) <i>rac</i> -Ni ₂ Cl ₄ (et,ph-P4-Ph)	120

Figure 4.2.21	^1H NMR of methylene bridge region for <i>rac</i> -NiPtCl ₄ (et, ph-P4-Ph) in CDCl ₃ 121
Figure 4.2.22	^1H NMR of methylene bridge region for <i>rac</i> -Ni ₂ Cl ₄ (et,ph-P4-Ph) in CD ₂ Cl ₂ 121
Figure 4.2.23	The $^{31}\text{P}\{^1\text{H}\}$ NMR of orange powder in C ₆ D ₆ obtained upon concentration of the filtrate <i>in vacuo</i> . Signals due to 6R are colored in red..... 122
Figure 4.2.24	ORTEP representation (50% ellipsoids) of NiPtCl ₄ (<i>rac</i> -et,ph-P4-Ph), 6R. Hydrogen atoms omitted for clarity..... 123
Figure 4.2.25	The $^{31}\text{P}\{^1\text{H}\}$ NMR of [<i>rac</i> -Rh ₂ (nbd) ₂ (et,ph-P4-Ph)](BF ₄) ₂ in CD ₂ Cl ₂ 125
Figure 4.2.26	The ^1H NMR of [<i>rac</i> -Rh ₂ (nbd) ₂ (et,ph-P4-Ph)](BF ₄) ₂ in CD ₂ Cl ₂ 126
Figure 4.2.27	ORTEP plot (50% ellipsoids) of [Rh ₂ (nbd) ₂ (<i>rac</i> -et,ph-P4-Ph)] ⁺² (hydrogens omitted for clarity) 126
Figure 5.1	$^{31}\text{P}\{^1\text{H}\}$ NMR (experimental and simulated) <i>rac</i> and <i>meso</i> -et,ph-P4-Ph 148
Figure 5.2	$^{31}\text{P}\{^1\text{H}\}$ NMR (experimental and simulated) <i>meso</i> -et,ph-P4-Ph 149
Figure 5.3	$^{31}\text{P}\{^1\text{H}\}$ NMR (experimental and simulated) <i>rac</i> -et,ph-P4-Ph 150
Figure 5.4	^1H NMR of <i>rac</i> and <i>meso</i> -et,ph-P4-Ph..... 151
Figure 5.5	^1H NMR of <i>meso</i> -et,ph-P4-Ph in C ₆ D ₆ showing 7.80-6.80 ppm and 1.60-0.70 ppm regions 152
Figure 5.6	^1H NMR of <i>rac</i> -et,ph-P4-Ph in C ₆ D ₆ showing 7.80-6.80 ppm and 1.60-0.70ppm regions 153
Figure 5.7	The ^1H NMR of <i>rac</i> -Pt ₂ Cl ₂ (et,ph-P4-Ph), 5R in CD ₂ Cl ₂ . Asterisked peaks are due to unremoved PtCl ₂ (cod) and solvent impurities 154
Figure 5.8	^1H NMR of <i>rac</i> -NiPtCl ₄ (et,ph-P4-Ph) in CDCl ₃ . Asterisked peaks are due to PtCl ₂ (cod) and solvent impurities 154

List of Schemes

Scheme 1.1.1	Synthesis of secondary and primary alcohols from alkenes.....	1
Scheme 1.1.2	Commercial methods used for manufacture of primary alcohols.....	2
Scheme 1.1.3	Commercial methods used for manufacture of primary alcohols: Alfol-Ziegler process	3
Scheme 1.1.4	Hydration of diethyl maleate catalyzed by $[\text{Pd}(\mu\text{-OH})(\text{L-L})]_2^{2+}$ or by a mixture of PdCl_4^{2-} and CuCl_2 . L-L = dppe, dcpe	4
Scheme 1.1.5	Hydration of Maleic acid to Malic acid catalyzed by monometallic cationic Pt(II) and Pd(II) complexes of tetra(o-aniliny)bis(phosphine) ligands.....	5
Scheme 1.1.6	Three sequence step to convert terminal alkenes to primary alcohols developed by Campbell <i>et al.</i>	6
Scheme 1.1.7	Reaction scheme for alkene hydration designed by Grubbs <i>et al.</i>	7
Scheme 1.2.1	Generic mechanism for direct hydration of alkenes catalyzed by a late transition metal complex.....	8
Scheme 1.2.2	Wacker Process and a Proposed Mechanism.....	10
Scheme 1.2.3	Migratory insertion and external attack pathways	11
Scheme 1.2.4	Reaction of dimethyl maleate with <i>cis</i> -Pt(OH)(Me)L ₂	11
Scheme 1.2.5	Reaction of ethylene with Cp*(PMe ₃)Ir(Ph)(OH) in the presence of 5 mol% Cp*(PMe ₃)Ir(Ph)(OTf).....	12
Scheme 1.2.6	Binuclear mechanism for insertion of ethylene into Ir-OH bond proposed by Bergman <i>et al.</i>	12
Scheme 1.2.7	1,2 and 2,1 addition products for insertion of alkene into Rh-OH Bond.....	13
Scheme 1.3.1	Aldehyde-water shift reaction.	14
Scheme 1.3.2	Proposed mechanism for direct hydration of alkenes catalyzed by bimetallic Ni complex.....	16
Scheme 1.4.1	Ozonolysis-mechanism	18
Scheme 1.4.2	Oxidative cleavage of alkene using OsO ₄ /NaIO ₄	19

Scheme 1.4.3	Oxidative cleavage of isoeugenol to vanillin and acetaldehyde with O ₂ catalyzed by Co(CMDPT) complex.....	20
Scheme 2.1	Cosse-Arlman type migratory insertion mechanism	29
Scheme 2.2	Proposed mechanism to produce Ni(H)(Cl)(P ₂) active catalyst for alkene oligomerization	29
Scheme 2.3	Chain-walking mechanism proposed by Brookhart	30
Scheme 3.1.1	Initial proposed mechanism to produce hexanal from 1-hexene	37
Scheme 3.2.1	Oxidative cleavage of 1-hexene	38
Scheme 3.2.2	Typical reaction scheme for uncatalyzed autoxidation of olefins.....	40
Scheme 3.2.3	Alkene substrates studied. Experiments with norbornene and norbornadiene did not show any products based on GC/MS analysis	42
Scheme 3.2.4	Proposed Reaction of <i>meso</i> -Ni ₂ Cl ₄ (<i>et</i> , <i>ph</i> -P ₄) with water and O ₂	52
Scheme 3.2.5	Mechanism for Oxidative Cleavage of an Alkene.....	53
Scheme 3.2.6	“Metathesis” Mechanism for Alkene Oxidative Cleavage	53
Scheme 3.2.7	Mechanism for autoxidation of trialkyl phosphines proposed by Buckler	71
Scheme 4.1.1	Proposed fragmentation pathway for the dirhodium catalyst based on NMR Studies	77
Scheme 4.1.2	Synthetic scheme for the <i>et</i> , <i>ph</i> -P ₄ -Ph ligand	80
Scheme 4.2.1	Synthetic scheme for preparation of Cl(Ph)PCH ₂ P(Ph)Cl, as reported (a) by Stelzer <i>et al.</i> , and (b) by Schmidbaur and Schnatterer.....	83
Scheme 4.2.2	Synthesis of Cl(Ph)PCH ₂ P(Ph)Cl, 2	83
Scheme 4.2.3	Preparation of 1-(Et ₂ P)-2-bromobenzene via low temperature halogen lithium exchange.....	91
Scheme 4.2.4	Synthetic procedure for preparation of 1-(Et ₂ P)-2-chlorobenzene via Grignard intermediate developed by Hart.....	91
Scheme 4.2.5	Synthetic procedure for preparation of 1-(Et ₂ P)-2-bromobenzene developed by Bennett	92

Scheme 4.2.6	Synthetic procedure for preparation of 1-(Cl ₂ P)-2-bromobenzene from <i>o</i> -bromoaniline	92
Scheme 4.2.7	First example of magnesium-halogen exchange	93
Scheme 4.2.8	Preparation of highly functionalized Grignard reagents by an iodine-magnesium exchange reaction.....	94
Scheme 4.2.9	Preparation of <i>o</i> -phenylenebisdiethylphosphine via lithium-halogen exchange, followed by treatment with PEt ₂ Cl.....	96
Scheme 4.2.10	Attempted preparation of <i>rac,meso</i> -et,ph-P4-Ph via lithium-mediated P-C coupling reaction	97
Scheme 4.2.11	Preparation of <i>rac,meso</i> -et,ph-P4-Ph via Grignard-mediated P-C coupling reaction	97
Scheme 4.2.12	Reaction scheme for synthesis of <i>rac,meso</i> -et,ph-P4-Ph	108
Scheme 4.2.13	Preparation of Pt ₂ Cl ₄ (<i>rac</i> -et,pt-P4-Ph), 4R	113
Scheme 4.2.14	Preparation of NiPtCl ₄ (<i>rac</i> -et,ph-P4-Ph), 5R	119
Scheme 4.2.15	Synthesis of [<i>rac</i> -Rh ₂ (nbd) ₂ (et,ph-P4-Ph)](BF ₄) ₂ , 6R	124

List of Abbreviations

Å	Angstrom
bp	boiling point
Bu	butyl
ca.	approximately
cod	1,5-cyclooctadiene
Cy	cyclohexyl
dcpe	1,2 Bis(dicyclohexyl-phosphino)ethane
DFT	density function theory
DMF	<i>N,N</i> -dimethylformamide
DMSO	dimethylsulfoxide
dppe	1,2-bis(diphenylphosphino)ethane
dppety	1,2-bis(diphenylphosphino)ethylene
dppp	1,3- <i>bis</i> (diphenylphosphino)propane
equiv.	equivalent(s)
Et	ethyl
g	gram(s)
GC	gas chromatography
h	hour(s)
¹ H NMR	proton nuclear magnetic resonance
Hz	hertz
L	liter
LAH	lithium aluminum hydride
M	molar (mol.L ⁻¹)
Me	methyl
MHz	megahertz
min	minute(s)
mL	milliliter(s)
mM	millimolar (mmol.L ⁻¹)
mmol	millimole(s)
mol	mole(s)
nbd	norbornadiene or bicyclo[2.2.1]hepta-2,5-diene
NMR	nuclear magnetic resonance
<i>o</i>	<i>ortho</i>
OAc	acetate
ORTEP	Oak Ridge thermal ellipsoid plot program
³¹ P{ ¹ H} NMR	proton-decoupled phosphorus-31 nuclear magnetic resonance
Ph	phenyl
<i>rac</i>	<i>racemic</i>
<i>t</i> or <i>tert</i>	<i>tertiary</i>
THF	tetrahydrofuran
TLC	thin layer chromatography
TOF	turnover frequency
TON	turnover number
tpp	triphenylphosphine

Abstract

The first chapter of this dissertation involves discussion of alkene hydration and oxidative cleavage reactions catalyzed by late transition metal complexes. Previously reported results are summarized here. Mechanistic aspects of alkene hydration catalyzed by late transition metal complexes are also explained. The second part of Chapter 1 focuses on motivation for using bimetallic nickel phosphine complexes as possible catalytic precursors for alkene hydration.

Chapter 2 describes studies into alkene hydration in the presence of catalytic amounts of dinickel phosphine complexes based on linear tetraphosphine ligand, $\text{PEt}_2\text{CH}_2\text{CH}_2(\text{Ph})\text{PCH}_2\text{P}(\text{Ph})\text{CH}_2\text{CH}_2\text{PEt}_2$, et,ph-P4. Under conditions tested no alcohol products were detected. However we have observed formation of a small amount of oxidative cleavage products. Results from studies of oxidative cleavage reactions are described in Chapter 3. It was established that only a substoichiometric conversion to corresponding aldehydes can be achieved in the presence of catalytic amounts of bimetallic nickel complexes or free et,ph-P4 ligand. Extensive NMR studies indicated that in the presence of water dinickel tetraphosphine complexes, *rac*- and *meso*- $\text{Ni}_2\text{X}_4(\text{et,ph-P4})$ ($\text{X} = \text{Br}, \text{Cl}$) are not stable and readily fall apart via phosphine arm dissociation. To address this problem new stronger chelating tetraphosphine ligand, $\text{PEt}_2(o\text{-C}_6\text{H}_4)\text{P}(\text{Ph})\text{CH}_2(\text{Ph})\text{P}(o\text{-C}_6\text{H}_4)\text{PEt}_2$, et,ph-P4-Ph has been designed by Stanley group. Chapter 4 describes improved synthesis of et,ph-P4-Ph and chromatographic procedure developed for separation of *rac*- and *meso*-diastereomers. The racemic form of et,ph-P4-Ph reacts with 2 equiv of $\text{PtCl}_2(\text{cod})$ or $[\text{Rh}(\text{nbd})_2](\text{BF}_4)$ to give bimetallic $\text{Pt}_2\text{Cl}_4(\text{rac-et,pt-P4-Ph})$, 4R and $[\text{rac-Rh}_2(\text{nbd})_2(\text{et,ph-P4})](\text{BF}_4)_2$, 6R, in which et,ph-P4-

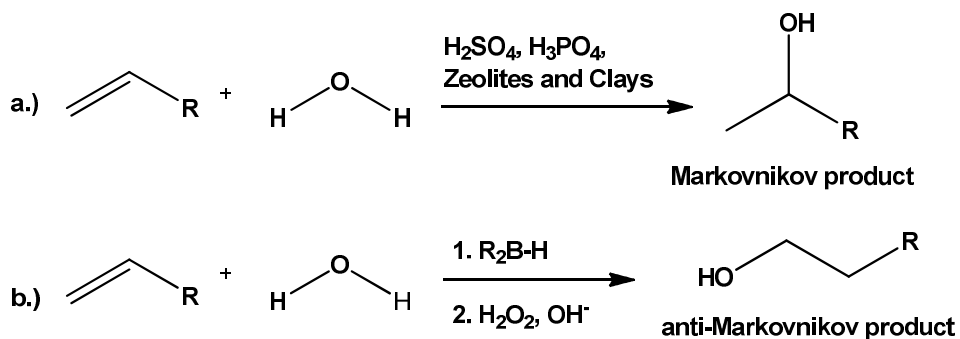
Ph acts as a bridging and chelating ligand. Heterobimetallic complex, $\text{NiPtCl}_4(\text{rac-et,pt-P4-Ph})$, 5R has been prepared by reaction of *rac-et,ph-P4-Ph* with 1 equiv of $\text{Ni}_2\text{Cl}_4 \cdot 6\text{H}_2\text{O}$, followed by dropwise addition of 1 equiv of $\text{PtCl}_2(\text{cod})$. Complexes 4R, 5R, and 6R have been characterized by $^{31}\text{P}\{^1\text{H}\}$ NMR spectroscopy and single-crystal X-ray diffraction studies.

Chapter 1: Introduction

1.1 Alkene Hydration

Alcohols are among the most important industrial chemicals and millions of tons are produced annually worldwide.¹ Methanol, ethanol, isopropanol, and the butanols have the highest production volume in the USA. Amyl alcohols (C₅) are used as solvents for fats, oils and resins. Higher alcohols in the C₆-C₁₈ range are mainly used in plasticizers (for polyvinylchloride), detergents, and surfactants. Alkene hydration, the addition of H₂O to a carbon-carbon double bond is one of the most useful methods for the synthesis of alcohols. This reaction does not occur in the absence of added catalyst, but can be easily catalyzed by acids, zeolites, and clays.² Generally acid-catalyzed direct hydration of alkenes does not yield primary alcohols, because it follows Markovnikov's rule, which states that an electrophile will add to the most substituted carbon to form the more stable carbocation intermediate.³ Consequently, linear α -olefins yield only secondary alcohols with the exception of ethanol (Scheme 1.1.1a).

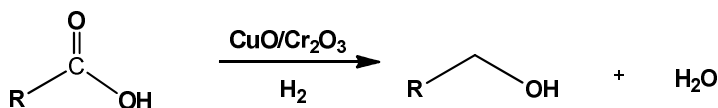
Scheme 1.1.1 Synthesis of secondary and primary alcohols from alkenes. R = alkyl or aryl group.²⁻³



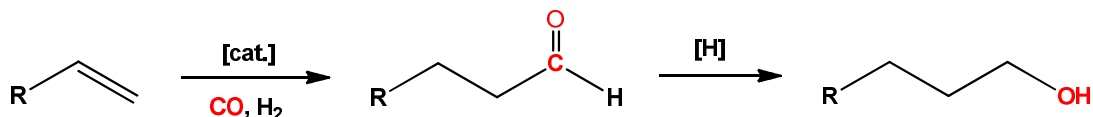
Primary alcohols are important and have a variety of uses including detergent precursors, plasticizers, and surfactants.¹ Currently there is no catalyst that catalyzes the direct hydration of unactivated alkenes to produce primary alcohols. This transformation can, however, be accomplished by indirect methods. Hydroboration-oxidation is widely used method for synthesis of primary alcohols (Scheme 1.1.1b).³ Although very effective, this method requires stoichiometric amounts of borane reagents and the peroxides used in the second step are of a major safety concern preventing large-scale applications. Current methods for the manufacture of primary alcohols in the industry include: hydrogenation of fatty acids or their esters catalyzed by CuO/Cr₂O₃ at 200-300 bar and 250-300°C to produce C₈ or greater unbranched primary alcohols, hydroformylation of α -olefins followed by hydrogenation to produce an alcohol with one extra carbon atom than the starting olefin (for example: 1-butanol from propene, 1-pentanol from 1-butene) (Scheme 1.1.2) and the Ziegler process which leads to linear even-numbered primary alcohols (Scheme 1.1.3).¹

Scheme 1.1.2 Commercial methods used for manufacture of primary alcohols.¹

1. Pressure hydrogenation of fatty acids catalyzed by CuO/Cr₂O₃



2. Hydroformylation/hydrogenation



Sasol operates the Ziegler process in their Lake Charles chemical plant that consists of three steps. AlEt_3 is reacted with ethylene at about 100°C and 100 atm to insert ethylene into the Al-Et groups producing longer-chain $\text{Al}(\text{R})^1(\text{R})^2(\text{R})^3$ compounds with even numbered alkyl groups that can vary in chain length. This is followed by oxidation with O_2 and hydrolysis with H_2O to produce alcohols and $\text{Al}(\text{OH})_3$, which is converted to extremely pure Al_2O_3 on heating. The different length alcohols are then separated by fractional distillation. Sometimes the ethylene chain growth reaction is coupled with a trans-alkylation step during which AlEt_3 compounds react with $\text{C}_{12}\text{-C}_{16}$ primary alkenes to produce alcohols of a more similar length.

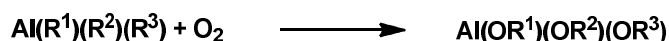
Scheme 1.1.3 Commercial methods used for manufacture of primary alcohols: Ziegler process.¹

Alfol-Ziegler process:

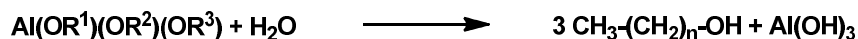
Step 1: Chain-growth reaction



Step 2: Oxidation to the corresponding alkoxydes



Step 3: Hydrolysis

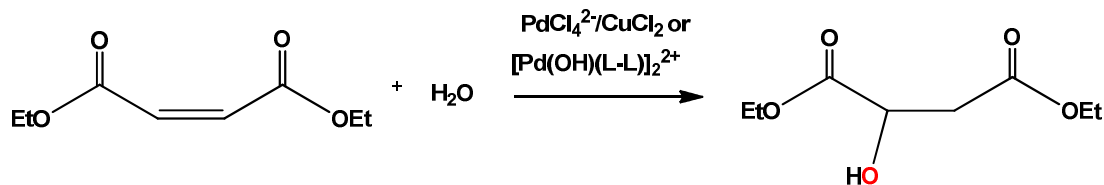


The currently used methods to make longer chain primary alcohols are far from perfect and typically require high pressures and temperatures. Consequently, development of transition-metal catalysts capable of direct hydration of terminal alkenes to primary alcohols under mild conditions has been of very high industrial interest and

could greatly improve current methods for producing primary alcohols. James F. Roth, retired chief scientist at Air Products & Chemicals has placed anti-Markovnikov addition of water to alkenes on the list of the top ten challenges for industrial catalysis.⁴

The only report on direct hydration of unactivated alkenes to produce primary alcohols mediated by a transition-metal catalyst was in 1986 by Trogler and coworkers.⁵ They reported that *trans*-Pt(H)(Cl)(PMe₃)₂ in the presence of NaOH and a phase-transfer catalyst catalyzes hydration of terminal alkene to primary alcohol (1-hexene to *n*-hexanol at 60°C and of 1-dodecene to *n*-dodecanol at 100°C) with only traces of branched alcohols detected in both examples. However, these results were later proven to be non-reproducible.⁶ There are no other reports on direct hydration of unactivated alkenes in the literature, but there are a few reports on hydration of activated alkenes (alkenes with electron withdrawing groups) catalyzed by late transition metal complexes. Ganguly and Roundhill reported that hydroxy-bridged bimetallic Pd(II) complexes containing bidentate phosphine ligands, [Pd(μ-OH)(L-L)]₂(BF₄)₂ (L-L = dppe, dcpe) catalyze hydration of diethyl maleate to diethyl malate at 120°C (Scheme 1.1.4).⁷

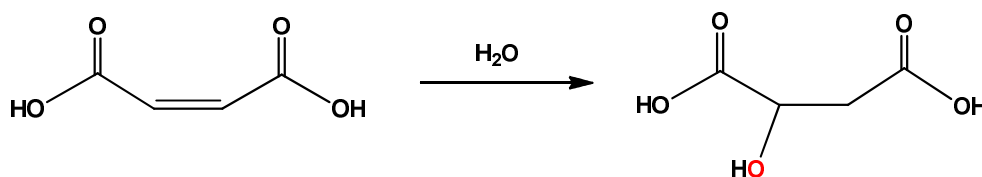
Scheme 1.1.4 Hydration of diethyl maleate catalyzed by [Pd(μ-OH)(L-L)]₂²⁺ or by a mixture of PdCl₄²⁻ and CuCl₂. L-L = dppe, dcpe.⁷



A mixture of PdCl₄²⁻ and CuCl₂ in aqueous THF solution also catalyzes the addition of water to diethyl maleate, although at higher temperatures (140°C rather than 120°C). These catalysts are not very active and reactions require high temperatures.

For example, the highest reported yield is 2.6 moles of diethyl malate/mol catalyst after 30 hours at 120°C in the presence of $[\text{Pd}(\mu\text{-OH})(\text{dppe})]_2^{2+}$. Hydration of 1-octene in the presence of the same catalysts and did not yield the corresponding alcohol. Only isomerization to internal isomers was observed. Jones *et al.* tested monometallic cationic Pt(II) and Pd(II) complexes of tetra(*o*-aniliny) bis(phosphine) for hydration of maleic acid to malic acid in water at 100°C (Scheme 1.1.5).⁸ These are also very poor catalysts with low turn-over numbers.

Scheme 1.1.5 Hydration of Maleic acid to Malic acid catalyzed by monometallic cationic Pt(II) and Pd(II) complexes of tetra(*o*-aniliny)bis(phosphine) ligands.⁸

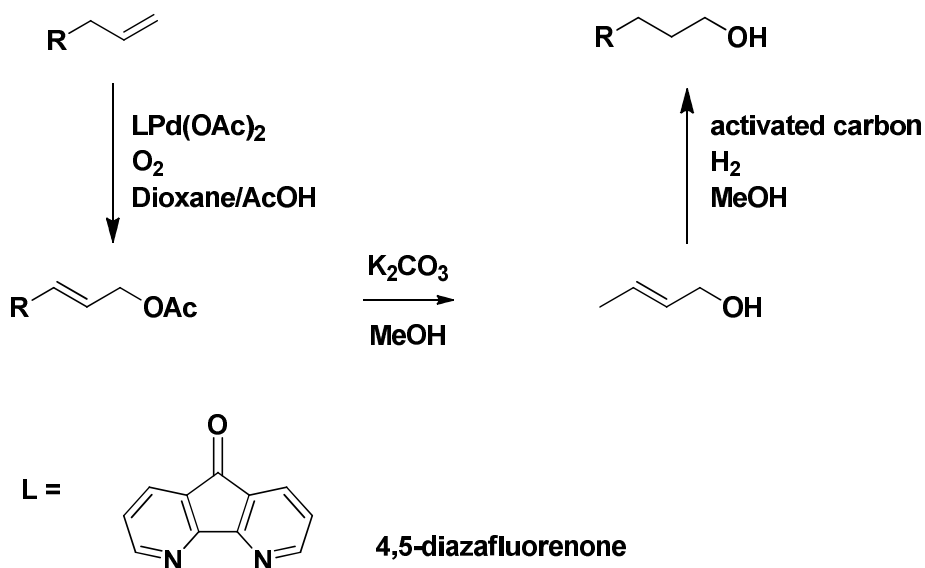


Interestingly Stewart *et al.* discovered that trialkylphosphines are active catalysts for hydration of activated alkenes in the absence of any metal catalyst.⁹ Metal-free alkyl phosphines are slightly better catalysts than Pt(II) or Pd(II) complexes described above. For example they report 77% conversion of 4-hexen-3-one catalyzed by $\text{P}(\text{CH}_3)_3$ after running reaction for 20 hours at room temperature.⁹ Although 77% conversion may seem good, industrial chemists are interested in the number of turnovers (TON) defined as the moles of the starting materials divided by moles of the catalyst used times the percent yield of the product. The TON for this reaction is 15.4 in 20 hours and represents a very poor catalyst from an activity viewpoint.

In addition to the direct hydration of alkenes some research groups have focused on multi-step approaches for this transformation. Campbell *et al.* developed an

interesting one-pot, three-step approach to convert terminal alkenes to primary alcohols.¹⁰ The three-step process includes: Pd-catalyzed allylic acetoxylation, followed by removal of acetate under basic conditions, and finally hydrogenation to the alcohol product (Scheme 1.1.6). The first step in this process is selective for terminal olefins, as β -methylstyrene, cyclohexene, methyl crotonate and methylenecyclohexane did not give desired products. Hydrogenation takes place under 1 atm H_2 in the presence of activated carbon and the Pd from the acetoxylation reaction, thus no additional catalyst is required. Although, good yields (71-78%) for conversion of terminal alkenes to primary alcohols were observed it is a three step process not really suitable for industrial applications.

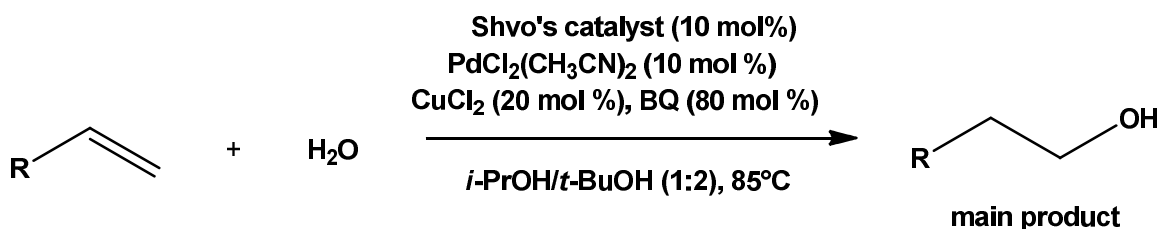
Scheme 1.1.6. Three sequence step to convert terminal alkenes to primary alcohols developed by Campbell *et al.*¹⁰



Robert H. Grubbs *et al.* also developed a new multi-step approach by combining a two-catalyst system: Wacker type palladium-catalyzed oxidation of terminal olefins with

ruthenium-catalyzed reduction through a hydride transfer (Scheme 1.1.7).¹¹ To favor aldehyde selectivity in the first cycle they used $\text{PdCl}_2(\text{CH}_3\text{CN})_2$ and in the reduction cycle a combination of *i*-PrOH and di-ruthenium Shvo's complex, a known catalyst for transfer hydrogenation of carbonyl compounds (Figure 1.1.1).¹²

Scheme 1.1.7. Reaction scheme for alkene hydration designed by Grubbs *et al.* R = aryl.¹¹



High regioselectivities ($\geq 20:1$, $1^\circ\text{OH} : 2^\circ\text{OH}$) for aryl-substituted terminal olefins were reported, but the selectivity for conversion of aliphatic substrates is rather low (1:1.4 for the hydration of 1-octene). This triple relay catalysis requires high catalysts loading and stoichiometric amounts of benzoquinone and is unacceptable for large scale industrial applications.

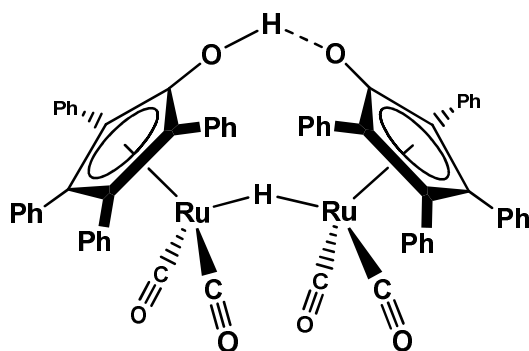


Figure 1.1.1. Shvo's catalyst.

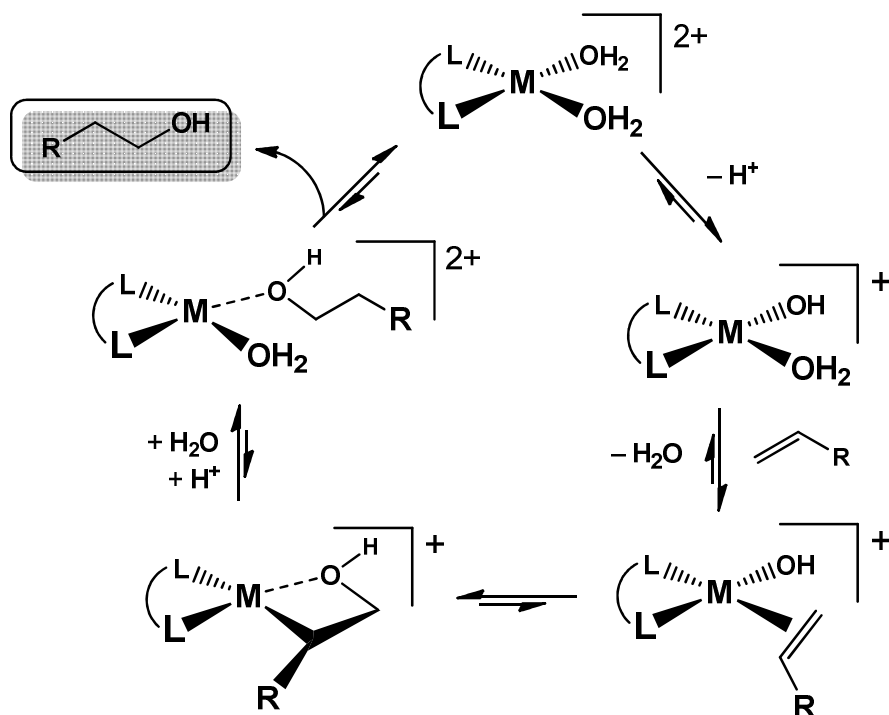
To summarize, direct hydration of unactivated alkenes is a difficult catalytic reaction and little success has been achieved only with activated alkenes. Newly

designed multistep transformations still require high catalyst loadings and are only selective towards specific classes of substrates.

1.2 Mechanistic Aspects of Alkene Hydration Catalyzed by Late Transition Metal Complexes

Mechanistic aspects play an important role in designing a new catalyst. In reference to direct alkene hydration catalyzed by late transition metal complexes the most likely mechanism involves metal-hydroxide complexes that can coordinate alkene and promote the migratory insertion of hydroxide with alkene as shown in Scheme 1.2.1. In the next step the alkyl-hydroxo complex can be protonated to produce an alcohol and a cationic metal complex which hydrolyzes water to regenerate the active species.

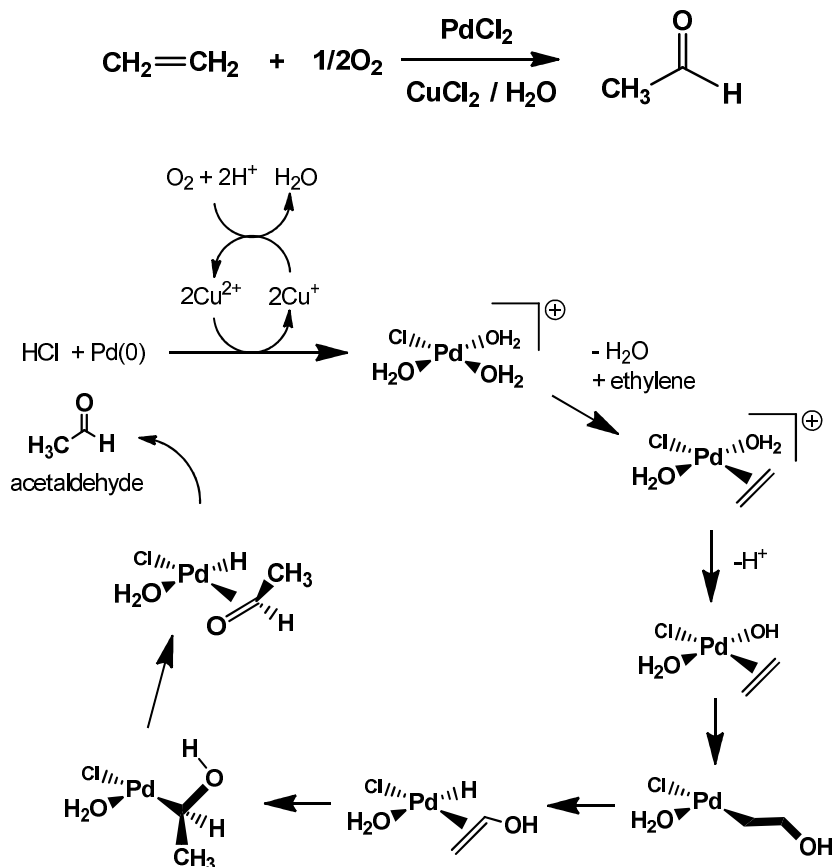
Scheme 1.2.1. Generic mechanism for direct hydration of alkenes catalyzed by a late transition metal complex. R = alkyl.



Later transition metals, especially Group 8, are believed to be important for this reaction since they do not have strong M-OH bonds, unlike early transition metals. Migratory insertion of the anionic ligand and alkene on the metal complex is the most difficult step in the proposed mechanism. Although migratory insertions of an alkene with a hydride or alkyl are well-studied and occur in many processes catalyzed by transition metal complexes (for example: different types of polymerizations of alkenes, hydrogenation, and hydroarylation of alkenes).^{12d,13} However, migratory insertions of alkene with metal-heteroatoms such as nitrogen, oxygen are much less common, but have been proposed in several catalytic reactions.¹⁴ Such examples include: Wacker oxidation, hydroamination, and carboaminations of alkenes.^{13d,15,16}

Intermolecular attacks by nucleophiles on coordinated olefins are much more common and well documented.¹⁷ The PdCl₂/CuCl₂ catalyzed oxidation of ethylene by O₂ to acetaldehyde in water is an important industrial reaction called the Wacker Process (Scheme 1.2.2).¹⁸ Because of its industrial importance the mechanism has been well studied, but there is still disagreement if it involves migratory insertion of Pd-OH species with an alkene or an external attack on the coordinated ethylene by water (Scheme 1.2.3).^{17,19} Both of these mechanistic steps are relevant to olefin hydration. Experimental and theoretical evidence supporting both of these pathways have appeared in the literature.^{17b,19-20} The latest studies showed that both alkene-M-OH migratory insertion or external nucleophilic attack of OH⁻ (or H₂O) on a coordinated alkene can take place depending on the electronic properties of alkenes, ligands and solvents used in the reactions.^{17b}

Scheme 1.2.2. Wacker Process and a Proposed Mechanism.

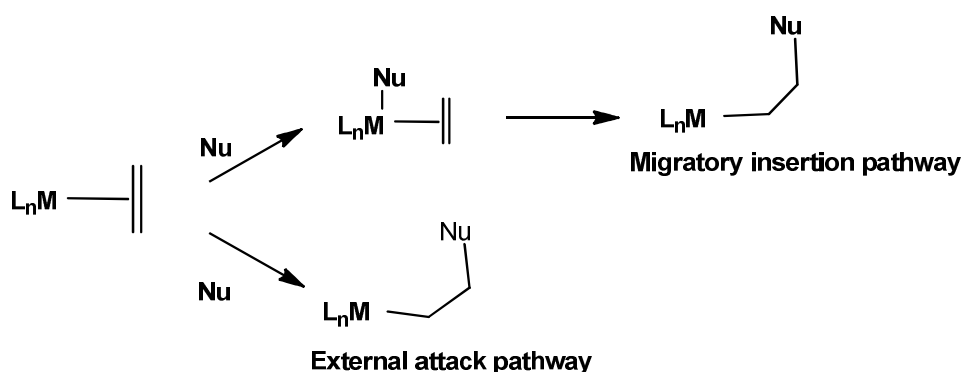


There are a few studies that provided strong evidence for migratory insertion of activated alkenes into a Pt(II)-OR bond. The migratory insertion of the activated alkene (C_2F_4) into the Pt-OMe bond of $\text{Pt}(\text{OMe})(\text{Me})(\text{dppe})$ to give $\text{Pt}(\text{CF}_2\text{CF}_2\text{OMe})(\text{Me})(\text{dppe})$ was reported by Bryndza *et al.*²¹ The final product was fully characterized by ^1H and ^{19}F NMR spectroscopy, by single crystal X-ray analysis, along with spectroscopic evidence for coordination of C_2F_4 to $\text{Pt}(\text{OMe})(\text{Me})(\text{dppe})$ prior to insertion.

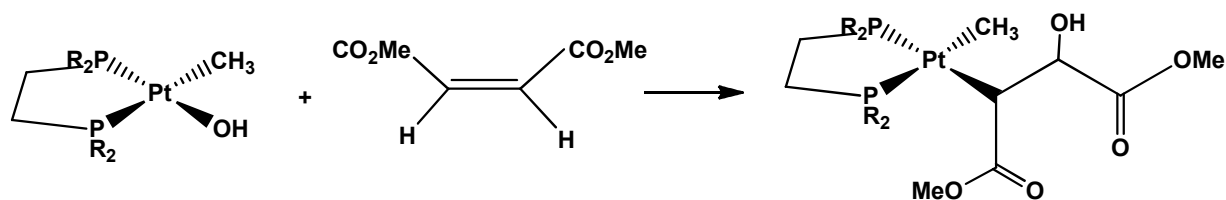
Bennett *et al.* observed insertion of dimethyl maleate into Pt-OH bonds of *cis*- $\text{Pt}(\text{OH})(\text{Me})\text{L}_2$ ($\text{L}_2 = 2\text{PPh}_3$, dppe, pdmp) as shown in Scheme 1.2.4.²² Addition of aqueous acids to a solution of *cis*- PtMeL_2 ($\text{L} = 2\text{PPh}_3$, dppe) gives $[\text{PtMe}(\text{H}_2\text{O})\text{L}_2]^+$ and

dimethyl malate. Although no insertion products with unactivated alkenes like ethylene, 1-hexene and cyclohexene were observed, this reaction models proposed steps in the catalytic alkene hydration cycle. In agreement with studies performed by Brynza experimental evidence certainly exists for the migratory insertion of M-OH with a coordinated olefin.

Scheme 1.2.3. Migratory insertion and external attack pathways.



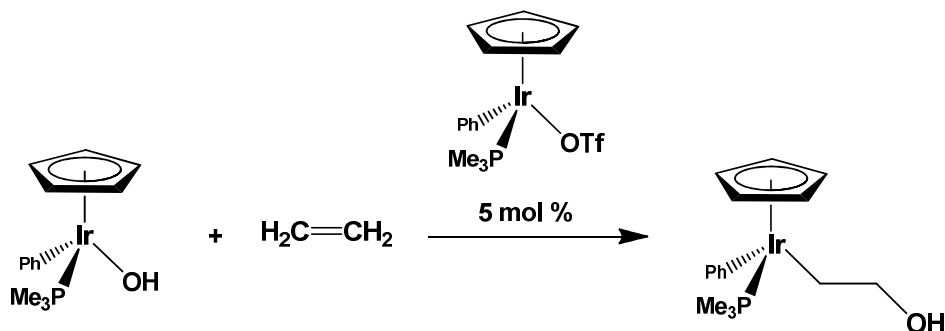
Scheme 1.2.4. Reaction of dimethyl maleate with *cis*-Pt(OH)(Me)L₂



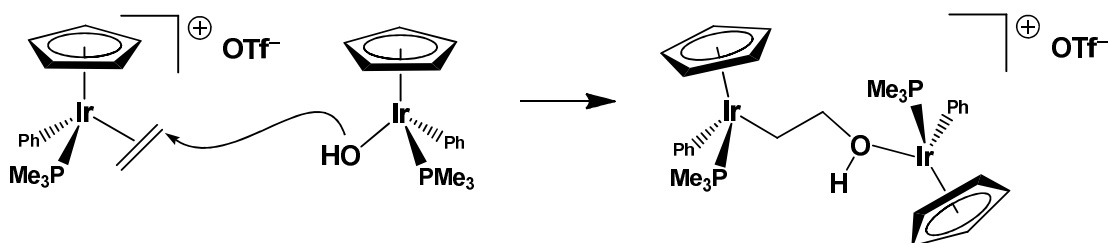
Bergman *et al.* observed that reaction of ethylene with Ir-OH complex, Cp*(PMe₃)Ir(Ph)-(OH) produced Cp*(PMe₃)Ir(Ph)(CH₂CH₂OH) as shown in Scheme 1.2.5.²³ However, this hydroxyethyl complex does not release a primary alcohol but instead goes on to produce the formyl methyl complex Cp*(PMe₃)Ir(Ph)(CH₂CHO). Based on experimental results it was proposed that the reaction of ethylene with the

metal-oxygen bond is catalyzed by cooperative participation of two Ir complexes, $\text{Cp}^*(\text{PMe}_3)\text{Ir}(\text{Ph})\text{OH}$ and $\text{Cp}^*(\text{PMe}_3)\text{Ir}(\text{Ph})\text{C}_2\text{H}_2(\text{OTf})$ as shown in Scheme 1.2.6.

Scheme 1.2.5. Reaction of ethylene with $\text{Cp}^*(\text{PMe}_3)\text{Ir}(\text{Ph})(\text{OH})$ in the presence of 5 mol% $\text{Cp}^*(\text{PMe}_3)\text{Ir}(\text{Ph})(\text{OTf})$.²³

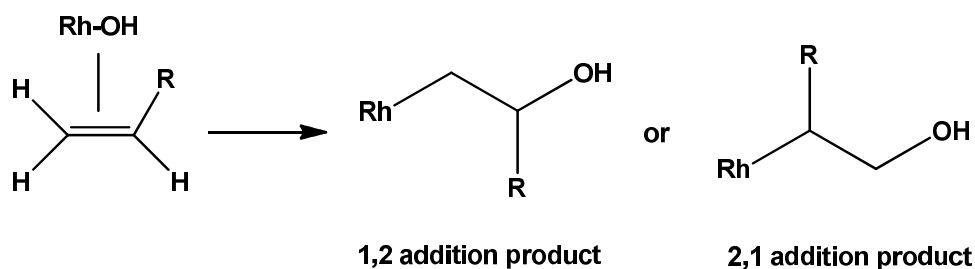


Scheme 1.2.6. Binuclear mechanism for insertion of ethylene into Ir-OH bond proposed by Bergman *et al.*²³



Results of computational studies that compared mechanism, rate and selectivity for insertions of olefins into metal-carbon, -nitrogen, and -oxygen bonds of rhodium-hydroxo complexes showed that the energy barrier for insertion of ethylene or propene into the Rh-OH bond of $(\text{PMe}_3)_2\text{Rh}(\eta^2\text{-CH}_2=\text{CHR})(\text{OH})$ ($\text{R}=\text{H}, \text{Me}$) is lower than those for insertion into a Rh-CH₃ bond.²⁴ However, calculated free energy barriers for migratory insertion of propene into a Rh-OH bond are lower for 1,2 addition which would result in formation of a secondary alcohol than 2,1 addition to produce primary alcohol (Scheme 1.2.7).

Scheme 1.2.7. 1,2 and 2,1 addition products for insertion of alkene into Rh-OH bond.



1.3 Bimetallic Nickel Tetraphosphine Complexes as Possible Catalysts for Alkene Hydration/Oxidation

Previous research in the Stanley group on rhodium hydroformylation has demonstrated that due to bimetallic cooperativity dirhodium complexes based on *rac*-et,ph-P4 are more active and more selective for hydroformylation than similar monometallic catalysts.²⁵ The tetraphosphine ligands, *rac*- and *meso*-et,ph-P4 designed by Stanley are perfectly suited for formation of bimetallic complexes and possesses both bridging and chelating functions (Figure 1.3.1).

Upon coordination to a metal center each pair of internal and external phosphine ligands forms a five-membered chelate ring with each metal center and the two metals are held together by a single rotationally flexible methylene bridge. Flexibility of methylene bridge allows bimetallic complexes to exist in *open*- or *closed*-modes where the metal centers are separated by 5-7 Å or by less than 3 Å.²⁶

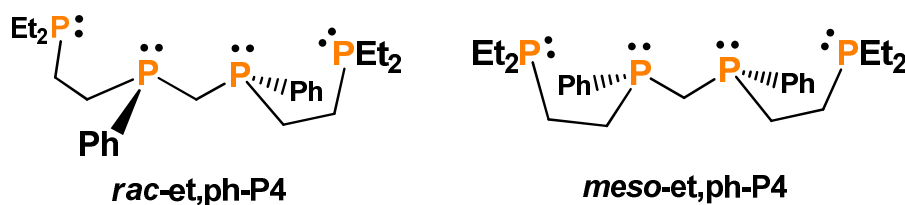
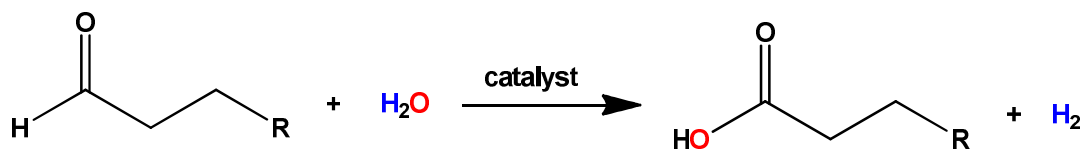


Figure 1.3.1. Binucleating tetraphosphine ligands *rac*- and *meso*-et,ph-P4.

In the process of investigations into the mechanism of hydroformylation it was accidentally discovered that our dirhodium tetraphosphine complex catalyzes reaction between aldehyde and water to produce carboxylic acids and H_2 as shown in Scheme 1.3.1.²⁷ This newly discovered catalytic reaction called the aldehyde-water shift reaction is related to the well-known water-gas shift catalysis ($CO + H_2O \rightarrow CO_2 + H_2$). The proposed catalyst for this catalytic reaction is $[Rh_2(\mu-CO)_2(CO)_2(rac\text{-}et,ph\text{-}P_4)]^{2+}$.

Scheme 1.3.1. Aldehyde-water shift reaction.



The ability of the proposed dicationic dirhodium complex to catalyze addition of water to aldehyde indicates the possibility that an analogous bimetallic complex might be able to perform alkene hydration. Stanley proposed to study the catalytic hydration of alkenes to produce terminal alcohols or other oxygen-containing products (e.g., aldehydes, ketones) using dinickel tetraphosphine complexes. Nickel has some advantages over previously studied Pd and Pt. It is the least expensive metal making it very attractive for industrial scale processes and the higher electronegativity of Ni compared to a second row Pd or a third row Pt center should assist in alkene activation for nucleophilic attack by either hydroxide or water.

Dinickel complexes based on *rac,meso*-*et,ph*-P4 can be easily prepared in nearly quantitative yields by reaction of *rac*-, or *meso*-*et,ph*-P4 with two equivalence of $NiCl_2 \cdot 6H_2O$.^{26a} Both *rac*- $Ni_2Cl_4(et,Ph-P_4)$ and *meso*- $Ni_2Cl_4(et,Ph-P_4)$ have been fully characterized. Coordination geometry of *et,ph*-P4 is shown in Figure 1.3.2.

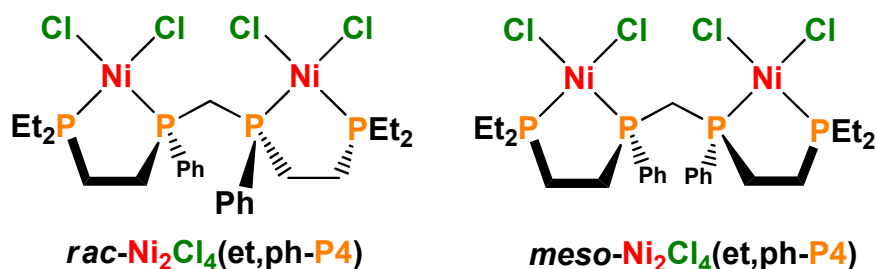


Figure 1.3.2. *Rac*-Ni₂Cl₄(et,Ph-P4) and *meso*-Ni₂Cl₄(et,Ph-P4).

Based on *rac*- and *meso*-et,ph-P4 ligand a new more rigid and stronger chelating tetraphosphine ligand, *rac*, *meso*-PEt₂(*o*-C₆H₄)P(Ph)CH₂(Ph)P(*o*-C₆H₄)PEt₂, (et,ph-P4-Ph) has been designed by Stanley group (Figure 1.3.3). This ligand has the same features as et,ph-P4, but flexible ethylene linkages have been replaced by more rigid *ortho*-substituted phenylene linkages. Synthesis of et,ph-P4-Ph was pioneered by Monteil.²⁸ Optimization of the synthesis and separation of *rac*- and *meso*- diastereomers of et,ph-P4-Ph are reported in Chapter 4.

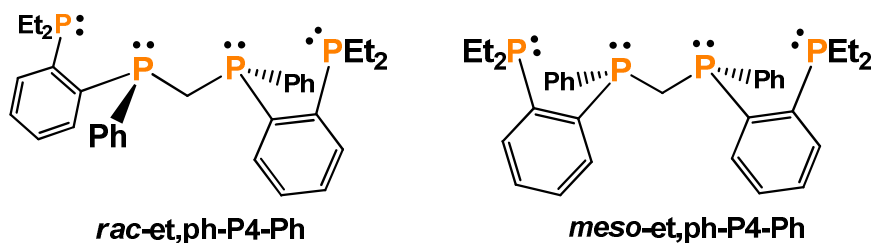
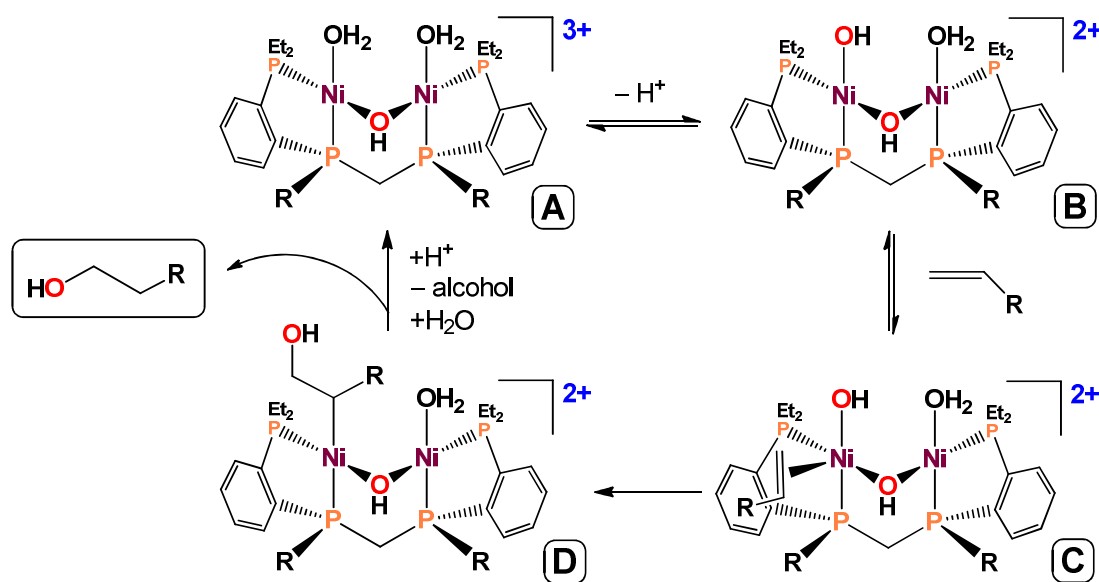


Figure 1.3.3. Binucleating tetraphosphine ligands *rac*- and *meso*-et,ph-P4-Ph.

One mechanistic possibility for direct hydration of alkene catalyzed by bimetallic Ni tetraphosphine complexes proposed by Prof. Stanley is shown in Scheme 1.3.2. The proposed mechanism involves a bridging hydroxide complex. Hydroxy-nickel complexes are known and have been previously reported in the literature.²⁹ Most of the reported structures are bridged complexes, but a few monometallic complexes have been

reported. A bimetallic nickel bridging hydroxide complex, $[\text{Ni}_2\text{Cl}_2(\mu\text{-OH})(\text{meso-et,ph-P4-Ph})]^+$ has also been characterized by Stanley group (Figure 1.3.4), indicating the possibility for formation of A from hydrolysis of water.³⁰ Loss of a proton from tricationic A produces dicationic B, which is an unsaturated 16 electron complex and could coordinate alkene to form C.

Scheme 1.3.2. Proposed mechanism for direct hydration of alkenes catalyzed by bimetallic Ni complex.



Nickel complexes in the +2 oxidation state are known to coordinate alkenes and a number of cationic $[\text{Ni(II)}]^+$ alkene complexes have been crystallographically characterized.³¹ The next step in the proposed mechanism is the migratory insertion of the hydroxide with coordinated alkene in complex C to form an OH-substituted alkyl ligand. As described earlier, migratory insertions of alkene into M-OH are rare, but have been proposed to occur in a few catalytic processes.^{19a,19b} Nucleophilic attack by water on coordinated alkene is also a possibility. There are two possibilities for migratory

insertion, first is to make primary OH product as shown in the Scheme 1.3.2, and second to make the branched OH product (not shown). Hydroxyalkyl complex D can be protonated off to produce primary alcohol as shown or β -hydride eliminate to produce an aldehyde. Coordination of water in the last step regenerates complex A.

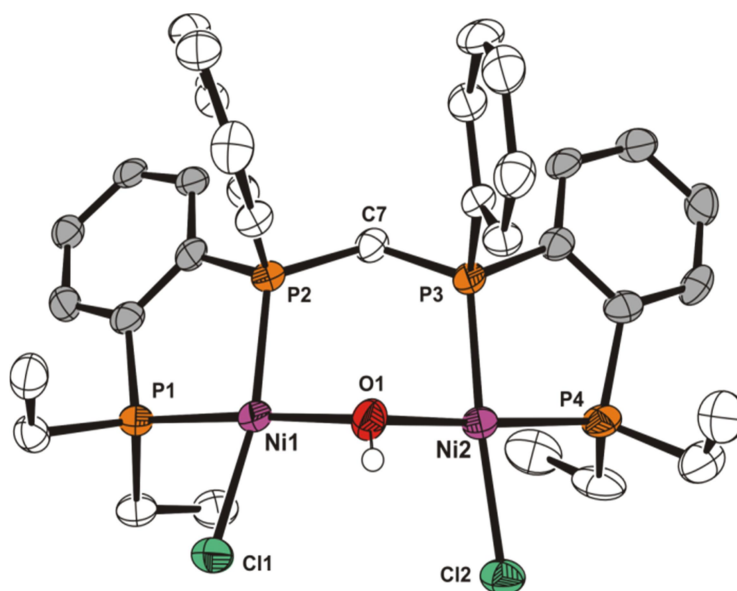


Figure 1.3.4. ORTEP plot of $[\text{Ni}_2\text{Cl}_2(\mu\text{-OH})(\text{meso-et,ph-P4-Ph})]^+$. Ni··Ni distance of 3.371 Å.³⁰

Although we have not isolated dinickel bridging hydroxide complex based on the et,ph-P4 ligand, Dr. William Schreiter has proposed that it forms readily from reaction with water.³² Results of research towards catalytic alkene hydration using dinickel complexes based on et,ph-P4 and et,ph-P4-Ph ligands and relevant monometallic phosphine complexes are described here.

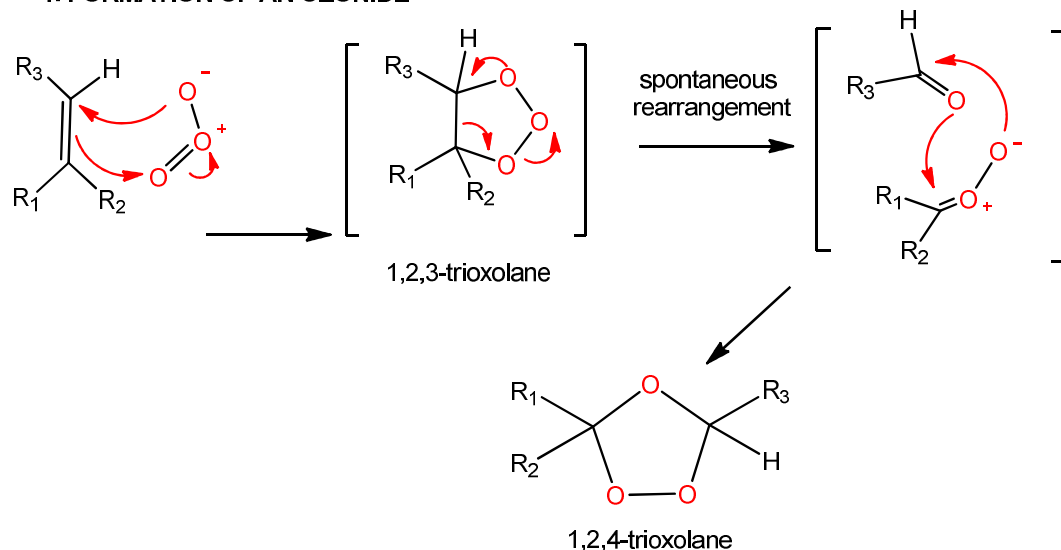
1.4 Alkene Oxidative Cleavage

The oxidative cleavage of a C=C double is a synthetically important reaction to introduce oxygen functionality into molecules.³ One of the well-known and frequently

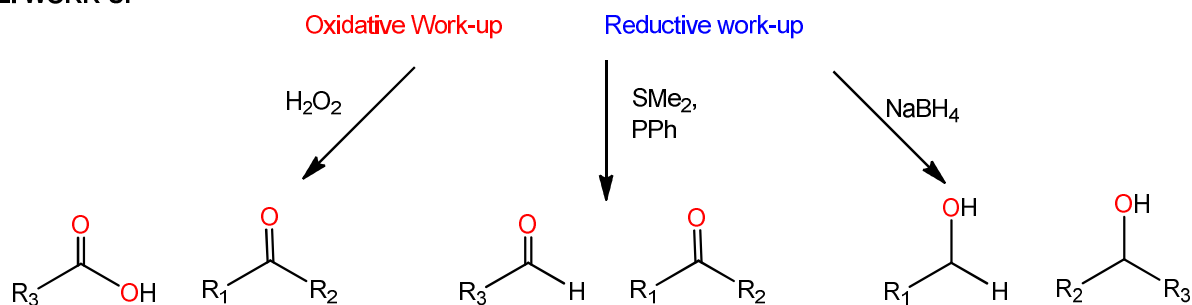
used methods for oxidative cleavage of a C=C double bond is ozonolysis, which is a two-step process shown in Scheme 1.4.1.

Scheme 1.4.1. Ozonolysis-mechanism.³

1. FORMATION OF AN OZONIDE



2. WORK-UP

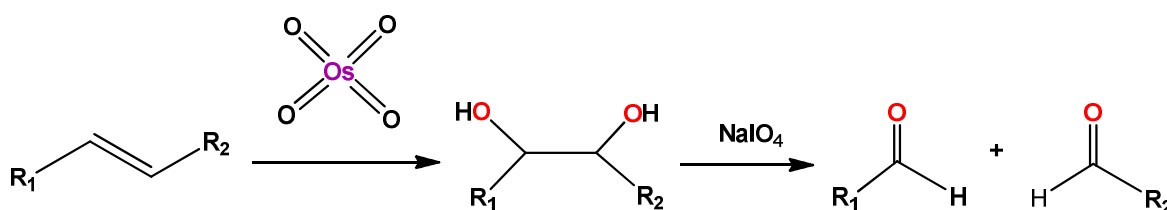


In the first step ozone reacts with an alkene to form a primary ozonide intermediate (1,2,3-trioxolane), which quickly rearranges to form a secondary ozonide (1,2,4-trioxolane). In the second step, work-up of the ozonide under reductive conditions with $(\text{CH}_3)_2\text{S}$ or PPh_3 yields ketones and aldehydes, with NaBH_4 alcohols can be isolated. Carboxylic acids and ketones are isolated after oxidative work-up in the presence of H_2O_2 . Although ozonolysis is a relatively clean reaction with good yields,

the ozonide intermediate is unstable and due to the safety concerns this process can not be used on a large industrial scale. Oxidative cleavage can also be performed with Lemieux-Johnson reagent, $\text{OsO}_4/\text{NaIO}_4$ as shown in Scheme 1.4.2.³³

For environmental and economic reasons many efforts have been directed at developing a transition-metal catalyst for selective cleavage of $\text{C}=\text{C}$ double bonds. The use of molecular oxygen as a primary oxidant to cleave the $\text{C}=\text{C}$ double bond is the most economical and environmentally friendly method to produce oxygenated products.

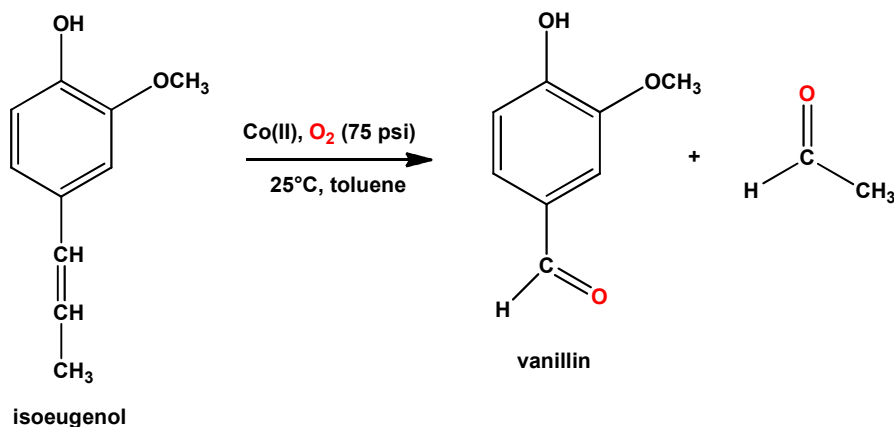
Scheme 1.4.2. Oxidative cleavage of alkene using $\text{OsO}_4/\text{NaIO}_4$.³³



They are only a few examples cited in the literature of transition-metal catalyzed oxidative cleavage of olefins that use oxygen. The most active catalyst was reported by Drago *et al.* in 1986.³⁴ They reported that $\text{Co}(\text{CMDPT})$ complex can effectively cleave isoegenol to give vanillin and acetaldehyde under relatively mild conditions (25°C and 75 psi. of O_2) (Scheme 1.4.3). However there are no follow up reports on this system aside from the original publication.

Baucharel *et al.* reported on manganese complexes that catalyze oxidative cleavage of variety of aliphatic and aromatic olefins in the presence of excess amount of thiophenol.³⁵ Simple metal salts such as: MnCl_2 , VCl_3 or CoCl_2 are also active in the presence of thiophenol. Up to 94% conversion to corresponding aldehydes and ketones at room temperature and under 75 psi. of O_2 was reported.

Scheme 1.4.3. Oxidative cleavage of isoeugenol to vanillin and acetaldehyde with O₂ catalyzed by Co(CMDPT) complex.³⁴



Wang *et al.* reported that Pd(OAc)₂ in the presence of a strong acid catalyzes oxidative cleavage of various terminal and internal olefins.³⁶ Although, high yields up to 89% were reported, this system operates at high temperature (100°C) and pressure (117 psi of O₂).

Tokunaga *et al.* investigated catalytic activities of Cu(II), Pd(II), Ru(II) towards oxidative cleavage of aromatic enol ethers.³⁷ They found that CuCl₂ catalyst was the most effective (up to 86% conversion to ketones). However, this catalyst is limited to enol ethers. Kaneda *et al.* found that RuO₂, in the presence of an excess amount of acetaldehyde, is active for oxidative cleavage of C=C double bond of terminal alkenes to produced aldehydes, which are further oxidized to carboxylic acids under conditions tested.³⁸

Although effective, all of these systems have serious disadvantages and are not commercially viable. With regard to Ni complexes they are no reports in the literature on Ni catalyzed oxidative cleavage of olefins using molecular oxygen. There is one report in the literature on oxidation of styrene with H₂O₂ catalyzed by NiCl₂(P₂) (P =

dppe, dppp, dppety).³⁹ The major product reported was benzaldehyde (up to 86.6% with $\text{NiCl}_2(\text{dppety})$) with styrene oxide (13.4%) as the only other product in that run, however very low catalytic activities were observed. Stability of these complexes in the presence of H_2O_2 is also questionable, as phosphines can be readily oxidized by H_2O_2 .

1.5 References

1. Weissermel, K.; Apre, H. J., *Industrial Organic Chemistry* 2nd rev. ed.; Weinheim-VCH, New York: 1993.
2. Wiseman, P., *An Introduction to Industrial Organic Chemistry*. Applied Science, London 1979.
3. M. B. Smith, J. M., *March's Advanced Organic Chemistry*. 5 ed.; Wiley, New York: 2001.
4. Roth, J. F., Evolving nature of industrial catalysis. *Applied Catalysis A: General* **1994**, 113 (2), 131-140.
5. Jensen, C. M.; Trogler, W. C., Catalytic Hydration of Terminal Alkenes to Primary Alcohols. *Science* **1986**, 233 (4768), 1069-1071.
6. Ramprasad, D.; Yue, H. J.; Marsella, J. A., Synthesis and characterization of trans-chlorohydridobis(trimethylphosphine)platinum and an investigation of its role in olefin hydration catalysis. *Inorganic Chemistry* **1988**, 27 (18), 3151-3155.
7. Ganguly, S.; Roundhill, D. M., Catalytic hydration of diethyl maleate to diethyl malate using divalent complexes of palladium(II) as catalysts. *Organometallics* **1993**, 12 (12), 4825-4832.
8. Jones, N. D.; Meessen, P.; Losehand, U.; Patrick, B. O.; James, B. R., Platinum(II) and Palladium(II) Complexes of Bisphosphine Ligands Bearing o-N,N-Dimethylaniliny Substituents: A Hint of Catalytic Olefin Hydration. *Inorganic Chemistry* **2005**, 44 (9), 3290-3298.
9. Stewart, I. C.; Bergman, R. G.; Toste, F. D., Phosphine-Catalyzed Hydration and Hydroalkoxylation of Activated Olefins: Use of a Strong Nucleophile to Generate a Strong Base. *Journal of the American Chemical Society* **2003**, 125 (29), 8696-8697.
10. Campbell, A. N.; White, P. B.; Guzei, I. A.; Stahl, S. S., Allylic C-H Acetoxylation with a 4,5-Diazafluorenone-Ligated Palladium Catalyst: A Ligand-Based Strategy To Achieve Aerobic Catalytic Turnover. *Journal of the American Chemical Society* **2010**, 132 (43), 15116-15119.

11. Dong, G.; Teo, P.; Wickens, Z. K.; Grubbs, R. H., Primary Alcohols from Terminal Olefins: Formal Anti-Markovnikov Hydration via Triple Relay Catalysis. *Science* **2011**, 333 (6049), 1609-1612.
12. (a) Muzart, J., Aldehydes from Pd-catalysed oxidation of terminal olefins. *Tetrahedron* **2007**, 63 (32), 7505-7521; (b) Shvo, Y.; Czarkie, D., Catalysis with tricarbonyl-tetrahapto-cyclopentadienone-ruthenium(O) complexes. a water-gas type reaction. *Journal of Organometallic Chemistry* **1986**, 315 (1), C25-C28; (c) Itami, K.; Palmgren, A.; Thorarensen, A.; Bäckvall, J.E., Chiral Benzoquinones as a New Class of Ligands for Asymmetric Catalysis: Synthesis and Application to the Palladium(II)-Catalyzed 1,4-Dialkoxylation of 1,3-Dienes. *The Journal of Organic Chemistry* **1998**, 63 (19), 6466-6471; (d) Krische, M. J.; Sun, Y., Hydrogenation and Transfer Hydrogenation. *Accounts of Chemical Research* **2007**, 40 (12), 1237-1237.
13. (a) Ittel, S. D.; Johnson, L. K.; Brookhart, M., Late-Metal Catalysts for Ethylene Homo- and Copolymerization. *Chemical Reviews* **2000**, 100 (4), 1169-1204; (b) Gibson, V. C.; Spitzmesser, S. K., Advances in Non-Metallocene Olefin Polymerization Catalysis. *Chemical Reviews* **2002**, 103 (1), 283-316; (c) Oxgaard, J.; Periana, R. A.; Goddard, W. A., Mechanistic Analysis of Hydroarylation Catalysts. *Journal of the American Chemical Society* **2004**, 126 (37), 11658-11665; (d) Gragor, N.; Henry, P. M., Evidence for a second mode of hydroxypalladation in aqueous solution. *Journal of the American Chemical Society* **1981**, 103 (3), 681-682.
14. (a) Hauger, B. E.; Huffman, J. C.; Caulton, K. G., Alkoxide Attack on Coordinated Olefin Can Be Reversible. *Organometallics* **1996**, 15 (7), 1856-1864; (b) Li, J. J.; Li, W.; James, A. J.; Holbert, T.; Sharp, T. P.; Sharp, P. R., Phosphine-Based Dinuclear Platinum(II) Diamido, Amido-Hydroxo, Oxo-Amido, Oxo-Imido, Diimido, and Dihydrazido Complexes. *Inorganic Chemistry* **1999**, 38 (7), 1563-1572; (c) Casalnuovo, A. L.; Calabrese, J. C.; Milstein, D., Rational design in homogeneous catalysis. Iridium(I)-catalyzed addition of aniline to norbornylene via nitrogen-hydrogen activation. *Journal of the American Chemical Society* **1988**, 110 (20), 6738-6744; (d) Zhou, J.; Hartwig, J. F., Intermolecular, Catalytic Asymmetric Hydroamination of Bicyclic Alkenes and Dienes in High Yield and Enantioselectivity. *Journal of the American Chemical Society* **2008**, 130 (37), 12220-12221; (e) El-Qisairi, A. K.; Qaseer, H. A.; Henry, P. M., Oxidation of olefins by palladium(II). Effect of reaction conditions, substrate structure and chiral ligand on the bimetallic palladium(II) catalyzed asymmetric chlorohydrin synthesis. *Journal of Organometallic Chemistry* **2002**, 656 (1-2), 168-176.
15. Gol, F. H., G.; Knüppel, P. C.; Stelzer, O., *Z. Naturforsch., B: Chem. Sci.* **1988**, 43 (1), 31-34.
16. Nakhla, J. S.; Kampf, J. W.; Wolfe, J. P., Intramolecular Pd-Catalyzed Carboetherification and Carboamination. Influence of Catalyst Structure on Reaction Mechanism and Product Stereochemistry. *Journal of the American Chemical Society* **2006**, 128 (9), 2893-2901.

17. (a) Stille, J. K.; James, D. E.; Hines, L. F., Stereochemistry of methoxypalladation of 2-butenes. *Journal of the American Chemical Society* **1973**, 95 (15), 5062-5064; (b) Baeckvall, J. E.; Akermark, B.; Ljunggren, S. O., Stereochemistry and mechanism for the palladium(II)-catalyzed oxidation of ethene in water (the Wacker process). *Journal of the American Chemical Society* **1979**, 101 (9), 2411-2416.
18. Takacs, J. M.; Xun-tian Jiang, J. M., The Wacker Reaction and Related Alkene Oxidation Reactions. *Current Organic Chemistry* **2003**, 7 (4), 369.
19. (a) Zaw, K.; Henry, P. M., Oxidation of olefins by palladium(II). Product distribution and kinetics of the oxidation of 2-cyclohexenol and 2-cyclohexenol-1-d by PdCl₄²⁻ in aqueous solution. *Organometallics* **1992**, 11 (6), 2008-2015; (b) Francis, J. W.; Henry, P. M., Palladium(II)-catalyzed exchange and isomerization reactions. Kinetics and stereochemistry of the isomerization of 2-(methyl-d₃)-4-methyl-1,1,1,5,5,5-hexafluoro-3-penten-2-ol in aqueous solution catalyzed by PdCl₄²⁻ at high chloride concentrations. *Organometallics* **1992**, 11 (8), 2832-2836.
20. Senn, H. M.; Blöchl, P. E.; Togni, A., Toward an Alkene Hydroamination Catalyst: Static and Dynamic ab Initio DFT Studies. *Journal of the American Chemical Society* **2000**, 122 (17), 4098-4107.
21. (a) Bryndza, H. E., Mechanism of olefin insertion into metal-oxygen bonds. Reaction of [(C₆H₅)₂PCH₂P(C₆H₅)₂]Pt(CH₃)(OCH₃) with tetrafluoroethylene. *Organometallics* **1985**, 4 (2), 406-408; (b) Bryndza, H. E.; Calabrese, J. C.; Wreford, S. S., Reaction of (DPPE)Pt(CH₃)(OCH₃) with tetrafluoroethylene. Synthesis and structural characterization of (DPPE)Pt(CH₃)(CF₂OCH₃). *Organometallics* **1984**, 3 (10), 1603-1604.
22. Bennett, M. A.; Jin, H.; Li, S.; Rendina, L. M.; Willis, A. C., cis-Hydroxyplatination of Dimethyl Maleate: Modeling the Intermediates in a Catalytic Alkene-Hydration Cycle with Organoplatinum(II)-Hydroxo Complexes. *Journal of the American Chemical Society* **1995**, 117 (32), 8335-8340.
23. Ritter, J. C. M.; Bergman, R. G., The Mechanism of Addition of an Ir-OH bond to Ethylene. Catalytic Tandem Activation by Two [η⁵-Cp*(Ph)IrPMe₃]⁺ Complex Fragments. *Journal of the American Chemical Society* **1997**, 119 (10), 2580-2581.
24. Tye, J. W.; Hartwig, J. F., Computational Studies of the Relative Rates for Migratory Insertions of Alkenes into Square-Planar, Methyl, Amido, and Hydroxo Complexes of Rhodium. *Journal of the American Chemical Society* **2009**, 131 (41), 14703-14712.
25. Broussard, M. E.; Juma, B.; Train, S. G.; Peng, W. J.; Laneman, S. A.; Stanley, G. G., A Bimetallic Hydroformylation Catalyst: High Regioselectivity and Reactivity Through Homobimetallic Cooperativity. *Science* **1993**, 260 (5115), 1784-1788.

26. (a) Laneman, S. A.; Fronczek, F. R.; Stanley, G. G., Synthesis of binucleating tetratertiary phosphine ligand system and the structural characterization of both meso and racemic diastereomers of {bis[(diethylphosphinoethyl)phenylphosphino]methane}tetrachlorodinickel. *Inorganic Chemistry* **1989**, 28 (10), 1872-1878; (b) Laneman, S. A.; Fronczek, F. R.; Stanley, G. G., A ligand-imposed cradle geometry for a dicobalt tetracarbonyl tetratertiary phosphine complex. *Inorganic Chemistry* **1989**, 28 (7), 1206-1207.
27. (a) Bridges, N. N. Kinetic and Mechanistic Studies of a Bimetallic Hydroformylation Catalyst. Louisiana State University, BatonRouge, 2000; (b) Aubry, D. A. Synthesis, Separation, and Reactivities of a Tetrphosphine Ligand and Investigations into its Applicability Towards Rhodium-Catalyzed Hydroformylation and Hydrocarboxylation. Louisiana State University, 2004.
28. Monteil, A. R. Investigation into the Dirhodium-Catalyzed Hydroformylation of 1-Alkenes and Preparation of a Novel Tetrphosphine Ligand. Ph.D. Disseretation, Louisisana State University, 2006.
29. (a) Carmona, E.; Marin, J. M.; Paneque, M.; Poveda, M. L., New nickel o-methylbenzyl complexes. Crystal and molecular structures of $\text{Ni}(\eta^3\text{-CH}_2\text{C}_6\text{H}_4\text{-o-Me})\text{Cl}(\text{PMe}_3)$ and $\text{Ni}_3(\eta^1\text{-CH}_2\text{C}_6\text{H}_4\text{-o-Me})_4(\text{PMe}_3)_2(\mu_3\text{-OH})_2$. *Organometallics* **1987**, 6 (8), 1757-1765; (b) Lopez, G.; Garcia, G.; Ruiz, J.; Sanchez, G.; Garcia, J.; Vicente, C., Synthesis of hydroxo-organo-complexes of the nickel group elements. *Journal of the Chemical Society, Chemical Communications* **1989**, (15), 1045-1046; (c) Carmona, E.; Marin, J. M.; Palma, P.; Paneque, M.; Poveda, M. L., Pyrrolyl, hydroxo, and carbonate organometallic derivatives of nickel(II). Crystal and molecular structure of $[\text{Ni}(\text{CH}_2\text{C}_6\text{H}_4\text{-o-Me})(\text{PMe}_3)(\mu\text{-OH})]_2 \cdot 2,5\text{-HNC}_4\text{H}_2\text{Me}_2$. *Inorganic Chemistry* **1989**, 28 (10), 1895-1900; (d) Lopez, G.; Garcia, G.; Sanchez, G.; Garcia, J.; Ruiz, J.; Hermoso, J. A.; Vegas, A.; Martinez-Ripoll, M., Hydroxo and azolate derivatives of pentafluorophenyl-nickel(II) complexes. Crystal structure of $[\text{NBu}_4]_2[\{\text{Ni}(\text{C}_6\text{F}_5)_2(\mu\text{-OH})\}_2]$ and $[\text{NBu}_4]_2[\{\text{Ni}(\text{C}_6\text{F}_5)_2\}_2(\mu\text{-OH})(\mu\text{-pyrazolato})]$. *Inorganic Chemistry* **1992**, 31 (8), 1518-1523; (e) Cámpora, J.; Matas, I.; Palma, P.; Graiff, C.; Tiripicchio, A., Fluoride Displacement by Lithium Reagents. An Improved Method for the Synthesis of Nickel Hydroxo, Alkoxo, and Amido Complexes. *Organometallics* **2005**, 24 (12), 2827-2830.
30. Monteil, A. R., Investigation into the Dirhodium-Catalyzed Hydroformylation of 1-Alkenes and Preparation of a Novel Tetrphosphine Ligand. *Ph.D. Dissertation, Louisiana State University* **2006**.
31. (a) Autissier, V.; Brockman, E.; Clegg, W.; Harrington, R. W.; Henderson, R. A., Synthesis of $[\text{Ni}(\eta^2\text{-CH}_2\text{C}_6\text{H}_4\text{R-4})\{\text{PPh}(\text{CH}_2\text{CH}_2\text{PPh}_2)_2\}]^+$ (R = H, Me or MeO) and protonation reactions with HCl. *Journal of Organometallic Chemistry* **2005**, 690 (7), 1763-1771; (b) Gareau, D.; Sui-Seng, C.; Groux, L. F.; Brisse, F.; Zargarian, D., Indenyl-Nickel Complexes Bearing a Pendant, Hemilabile Olefin Ligand: Preparation, Characterization, and Catalytic Activities. *Organometallics* **2005**, 24 (16), 4003-4013;

- (c) Zwecker, J.; Kuhlmann, T.; Pritzkow, H.; Siebert, W.; Zenneck, U., Electronic structures and reactivities of η^5 -2,3,5-tricarbahexaboranylnickel sandwich complexes. A combined electrochemical, preparative, and NMR spectroscopic approach. *Organometallics* **1988**, 7 (11), 2316-2324.
32. Schreiter, W. J. Investigations into Alkene Hydration and Oxidation Catalysis Louisiana State University, Baton Rouge, 2013.
33. Pappo, R.; Allen, J. D. S.; Lemieux, R. U.; Johnson, W. S., Notes Osmium Tetroxide-Catalyzed Periodate Oxidation of Olefinic Bonds. *The Journal of Organic Chemistry* **1956**, 21 (4), 478-479.
34. Drago, R. S.; Corden, B. B.; Barnes, C. W., Novel cobalt(II)-catalyzed oxidative cleavage of a carbon-carbon double bond. *Journal of the American Chemical Society* **1986**, 108 (9), 2453-2454.
35. Liu, S. T.; Reddy, K. V.; Lai, R. Y., Oxidative cleavage of alkenes catalyzed by a water/organic soluble manganese porphyrin complex. *Tetrahedron* **2007**, 63 (8), 1821-1825.
36. Wang, A.; Jiang, H., Palladium-Catalyzed Direct Oxidation of Alkenes with Molecular Oxygen: General and Practical Methods for the Preparation of 1,2-Diols, Aldehydes, and Ketones. *The Journal of Organic Chemistry* **2010**, 75 (7), 2321-2326.
37. Tokunaga, M.; Shirogane, Y.; Aoyama, H.; Obora, Y.; Tsuji, Y., Copper-catalyzed oxidative cleavage of carbon-carbon double bond of enol ethers with molecular oxygen. *Journal of Organometallic Chemistry* **2005**, 690 (23), 5378-5382.
38. Kaneda, K.; Haruna, S.; Imanaka, T.; Kawamoto, K., Ruthenium-catalysed oxidative cleavage reaction of carbon-carbon double bonds using molecular oxygen. *Journal of the Chemical Society, Chemical Communications* **1990**, (21), 1467-1468.
39. Cho, Y. J.; Lee, D. C.; Lee, H. J.; Kim, K.C.; Park, Y.C., Catalytic activities of Pt(II), Pd(II) and Ni(II)-diphosphine complexes for styrene oxidation. *Bull. Korean Chem. Soc.* **1997**, (18), 334-336.

Chapter 2: Investigations into Alkene Hydration/Oligomerization by Nickel Phosphine Complexes: The Unfortunate Role of Rubber Septa

2.1 Review of Prior Research

Initial investigations into alkene hydration catalysis using *meso*-Ni₂Cl₄(et,ph-P4) and *rac*-Ni₂Cl₄(et,ph-P4) with 1-hexene as a substrate in the presence of water showed no activity towards production of alcohols. However, reactions carried out at 70°C-80°C produced a white solid, which was identified via ¹H, ¹³C NMR, gel permeation chromatography (Figure 2.1), FT-IR (Figure 2.2.), and mass spectroscopy as a mixture of linear alkanes of a higher molecular weight ranging from a 5-mer to 326-mer of 1-hexene.¹

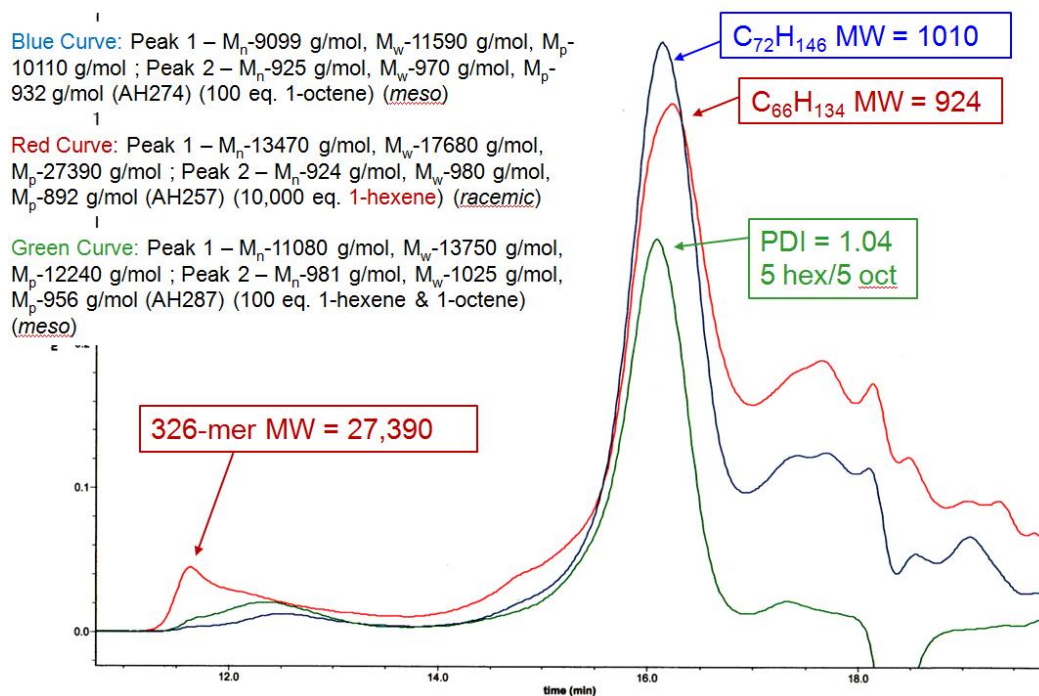


Figure 2.1. Gel permeation chromatography of the white solid produced from three different reactions of 1-hexene, 1-octene, and a mixture of 1-hexene/1-octene and Ni₂Cl₄(*meso*-et,ph-P4) in a water/acetone solvent mixture (70°C).¹

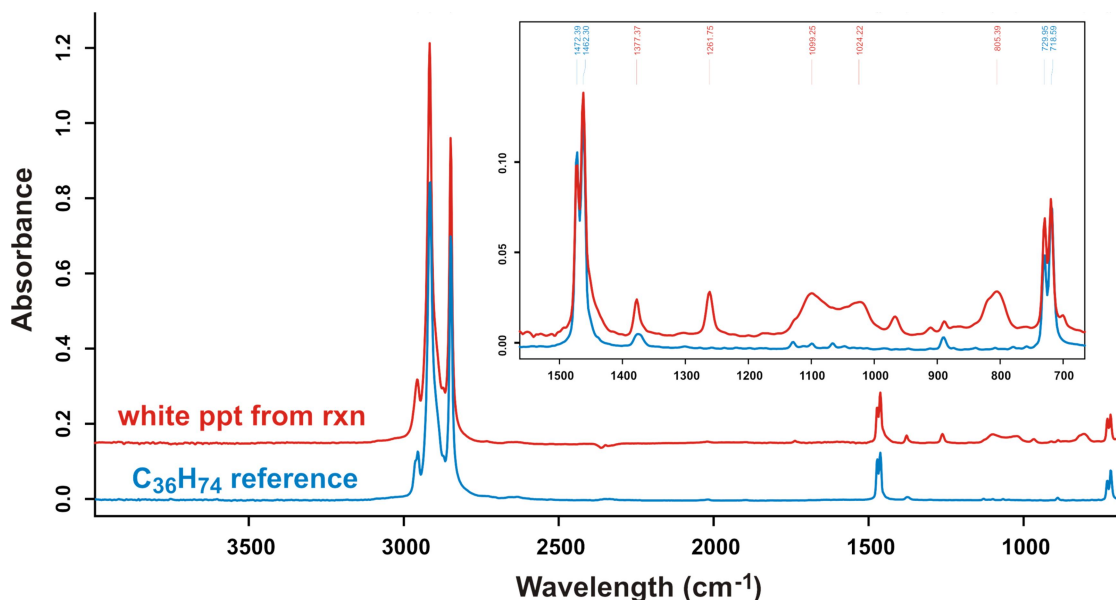


Figure 2.2. FT-IR of the white solid produced from 1-hexene and $\text{Ni}_2\text{Cl}_4(\text{meso-et,ph-P4})$ in a water/actone solvent mixture (70°C) compared to a $\text{C}_{36}\text{H}_{74}$ reference.¹

Based on the initial available data and analysis the following main features have been discovered about this reaction: water was necessary to obtain alkane products (typically used 30% water by volume), reactions run in acetone, THF, acetonitrile, toluene, DMSO, CH_2Cl_2 in the presence of water all worked for this reaction, reactions appeared initially not to be affected by exposure to O_2 , reactions carried out in the presence of monometallic $\text{NiCl}_2(\text{P}_2)$ ($\text{P} = \text{PPh}_3, \text{PCy}_3$) precursors also produced linear alkanes, all of the $\text{Ni}(\text{II})$ complexes tested showed high selectivity towards linear alkane products with less than 0.5% internal alkene based on ^1H and ^{13}C NMR analysis.¹

The initial conclusion was that in the presence of catalytic amounts of $\text{Ni}(\text{II})$ phosphine complexes 1-hexene is oligomerized to produce mostly linear alkanes. Nickel complexes are well known to catalyze oligomerization and polymerization of alkenes to produce linear or branched alkenes, but not alkanes. Shell higher olefins process (SHOP), well known industrial process, discovered by Keim utilizes Ni -catalysts of the

type shown in Figure 2.3a to produce 1-alkenes of various lengths (C_6 - C_{20}).² Brookhart *et al.* have described Ni(II) complexes based on α -diimines that are highly active for ethylene polymerization (Figure 1.2.3b).³

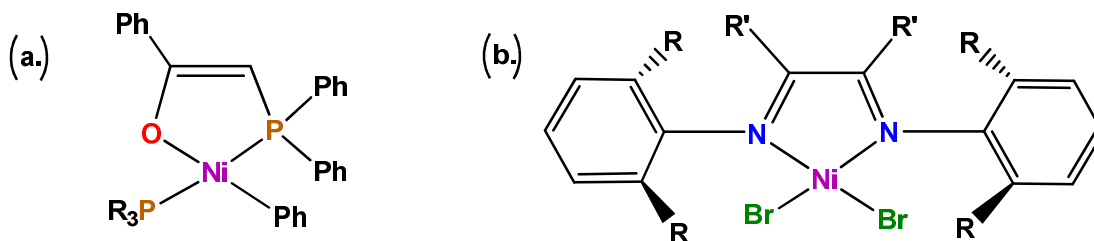
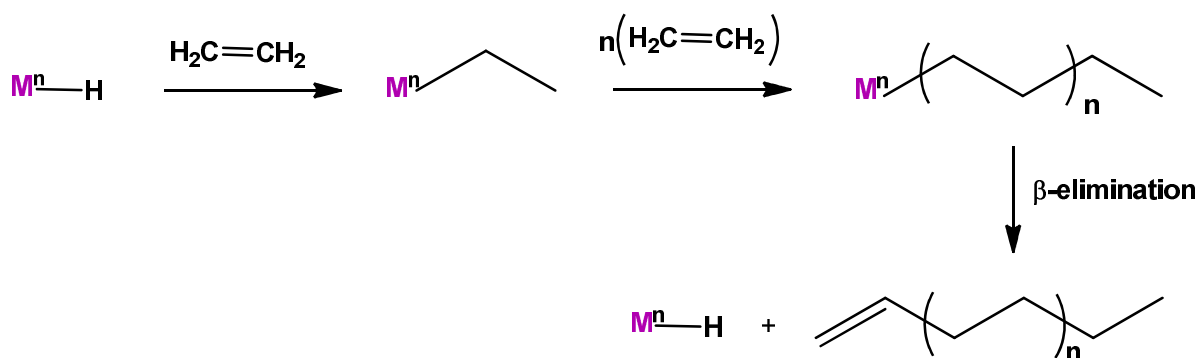


Figure 2.3. (a) Nickel catalyst used by Keim to oligomerize ethylene to produce 1-alkenes of various chain lengths.^{2a} (b) Ni(II) complexes used by Brookhart *et al.* in the presence of MAO (methylaluminoxane) as cocatalyst for ethylene polymerization. $R=i\text{-Pr}$, $R'=H, Me$, or 1,8-naphth-diyl.^{3b}

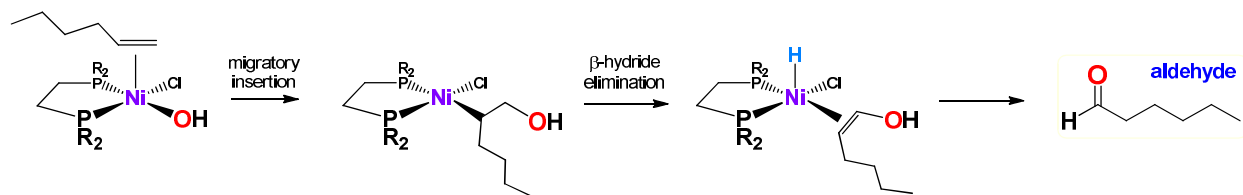
Bisphosphine complexes of the type $Ar_2PCH_2PAR_2$ and $1,2\text{-}Ar_2PC_6H_4PAR_2$ (Ar = ortho-substituted phenyl) of Ni(II) are also known as efficient catalysts for polymerization and oligomerization of alkenes (ethylene).⁴ It is generally accepted that oligomerization of olefins occurs by a Cosse-Arlman type migratory insertion mechanism shown in Scheme 2.1.⁵ This mechanism involves migratory insertion of olefin into a metal hydride (or alkyl) bond, followed by repeated insertions into the resulting metal alkyl bond. Chain termination occurs through β -hydride elimination to yield an α -olefin. In general the catalysts for oligomerization or polymerization require excess of aluminum alkyl (such as MAO, $AlEtCl_2$, $AlEt_3$, *etc.*) or hydride sources in order to initiate alkene oligomerization or polymerization by substituting one or more halides with an alkyl or hydride. Our starting $Ni_2Cl_4(eti,ph\text{-}P_4)$ complexes do not have any Ni-R (R = alkyl or hydride) bonds to start migratory insertion. No chloride insertions to make C-Cl bonds were observed (or expected). We initially believed that the reaction could be initiated by

a Ni-OH bond formed from Ni-Cl/H₂O exchange/deprotonation. The resulting Ni(OH)(Cl)(P₂) complex was proposed by Prof. Stanley to perform migratory insertion of the Ni-OH bond with a coordinated alkene to produce a Ni hydroxyalkyl complex as shown in Scheme 2.2.

Scheme 2.1. Cosse-Arlman type migratory insertion mechanism.⁵

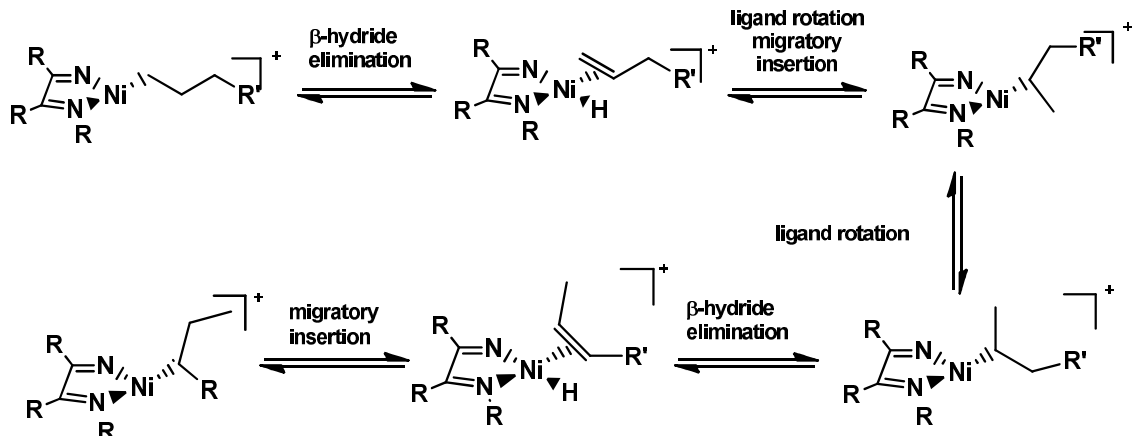


Scheme 2.2. Proposed mechanism to produce Ni(H)(Cl)(P₂) active catalyst for alkene oligomerization.



The hydroxylalkyl complex can do a β -hydride elimination to produce active Ni(H)(Cl)(P₂) catalyst and an aldehyde (or ketone if a secondary alcohol is produced). In agreement with the proposed mechanism ¹H NMR spectra of the samples taken from the reaction mixtures on some occasions showed a small singlet in aldehyde region at 9.73 ppm.¹ The observed selectivity for linear alkanes was explained by extensive isomerization, which Brookhart referred to as “chain walking”, shown in Scheme 2.3.^{3c,3d,6}

Scheme 2.3. Chain-walking mechanism proposed by Brookhart.^{3b}



Chain walking involves repeated alkyl β -hydride eliminations and reinsertions that move the metal center along the alkyl chain. Chain walking led to branching of the polymer chain, which was controllable by the ethylene pressure. Higher pressures of ethylene led to faster coordination to the catalyst and more linear polyethylene, while lower pressures allowed more chain walking and more branching in the polymer produced. This system, therefore, was highly tunable for the amount of branching via simple adjustment of the ethylene pressure. The main question for our system was how mostly saturated alkanes were produced without H₂ present could not be answered at that point. More detailed studies of the system were clearly needed.

2.2 Results and Discussion: Further Investigation into Ni Oligomerization Catalysis

To further study production of the white solid, reactions of 1-hexene in the presence of catalytic amounts of Ni₂Cl₄(et,ph-P4) were examined. For a typical experimental procedure 1 equivalent of *meso*-Ni₂Cl₄(et,ph-P4) was loaded into a round bottom flask followed by addition of acetone/water (15-30% water by volume). Next the

mixture was gently heated in a warm water bath for a short period of time (approximately 10 min) to form a homogeneous solution, followed by the addition of 100 equivalents of 1-hexene. The flask was then attached to a condenser and placed in a 70-80°C oil-bath for 24 hours. Final products were extracted with hexanes and after removal of the solvents *in vacuo*, a small amount (100-150 mg) of the off-white powder was obtained. Typically reactions were carried out in the presence of oxygen/air, but reactions under N₂ atmosphere were also examined. When temperature of reactions was lowered to 25°C a small amount of the white solid was still produced, but required a much longer reaction time (2-3 weeks).

In agreement with the initial studies, reactions of 1-hexene in the presence of water and catalytic amounts of *meso*-Ni₂Cl₄(et,ph-P4) always produced a small amount of the off-white powder. Samples from the reaction in progress taken at different time intervals (1 hour, 3 hours, 6 hours, 12 hours, and 24-hours) all contained a small amount of the white powder that clearly increased up to a point with longer reaction times. This white powder had a good solubility in non-polar organic solvents like CHCl₃ and hexane and ¹H NMR analysis showed signals in characteristic alkane region (0.5-1.8 ppm) (Figure 2.4). No signals in the alkene region (5-6 ppm) were observed. All attempts to analyze final products via GC/MS have failed, presumably due to a too-high molecular weight. Based on GC/MS analysis 1-hexene was completely consumed at the end of these reactions. In only a few cases left over 1-hexene was detected via GC/MS at the end of the reaction. Total amount of the white solid produced varied slightly for different experiments and was equal to 100-150 mg on average. Since amount of the 1-

hexene used in the reactions equals to 1.68 g on average only about 10% of 1-hexene was converted to the white solid and it was realized that we had a leakage problem.

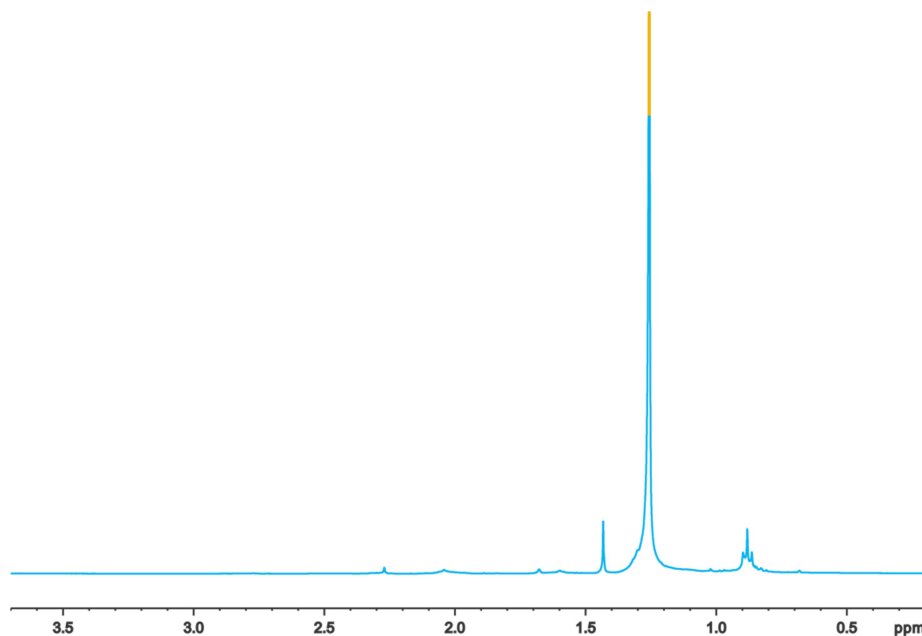


Figure 2.4. 400 MHz ¹H NMR of white powder in CDCl₃ from the reaction of 1-hexene in the presence of *meso*-Ni₂Cl₄(et,ph-P4) catalyst.

Based on the experimental data it was determined that the total mass loss of 1-hexene plus solvent from the reaction mixture was anywhere between 1.5 to 4 grams. Since all of the reactions were carried out in two or three neck round bottom flasks attached to a condenser with the remaining arms sealed with Suba seal septa, we tried to prevent the leak by using Teflon sealing rings on the condenser to flask joint. In these experiments the total amount of the mass lost was reduced down to 0.3-0.7g.

The leakage problem was finally solved by running reactions in a Teflon-sealed pressure vessel or by using a condenser on a one neck round bottom flask without any septa. Unexpectedly these reactions did not produce any detectable amounts of linear

alkane white precipitate. A similar effect was seen in Teflon-sealed NMR tube experiments where no linear alkanes were formed. Because no white solid was produced in the leak free reactions, we believed that some other undetected side product could be forming and when unable to escape was acting as an inhibitor. We speculated that this undetected side product had a low boiling (below 70°C) point and was able to escape along with the 1-hexene and solvents from the reaction vessel.

Numerous attempts to detect this second product via GC/MS and ^1H NMR were unsuccessful. In order to help identify the proposed second product and to test the scope of this reaction other substrates such as cyclohexene, norbornadiene, allyl alcohol, and vinyl acetate were also tested. Reaction conditions were exactly the same as described previously for the 1-hexene substrate. No products in the reactions run in a leak free setup were detected via GC/MS. Reactions, however, carried out in a round bottom flask sealed with rubber septa all produced a small amount of the white solid mixture of linear alkanes. Furthermore, each ^1H NMR spectrum of the final linear alkane product from the reactions of norbornadiene, allyl alcohol, and vinyl acetate in rubber septa-sealed reaction flasks looked nearly identical to each other with signals only in the characteristic alkane region. For comparison ^1H NMR of the final products from the reaction of vinyl acetate and from the reaction of 1-hexene are shown in Figure 2.5. No signals at higher frequency for protons on oxygen atoms, α -protons to the oxygen atom, or olefinic protons were present. Based on these results it was clear that the white solid produced was not related to the starting substrate.

Further proof that this reaction was not oligomerization was obtained after running a set of experiments with increasing catalyst concentration (from 10 mM up to

30 mM), while holding amount of the 1-hexene constant. As no expected increase in amount of the white solid produced was observed. Finally three blank reactions containing 1-hexene, acetone/water, and no catalyst carried out in the presence of septa conclusively demonstrated that the linear alkanes were not produced in a catalytic reaction, but simply extracted by the acetone/1-hexene mixture from the rubber Suba seal septa. These septa are made from natural red rubber, an elastic hydrocarbon polymer and are not heat resistant. Suba seal septa are no longer used to study the reactivity of our nickel complexes.

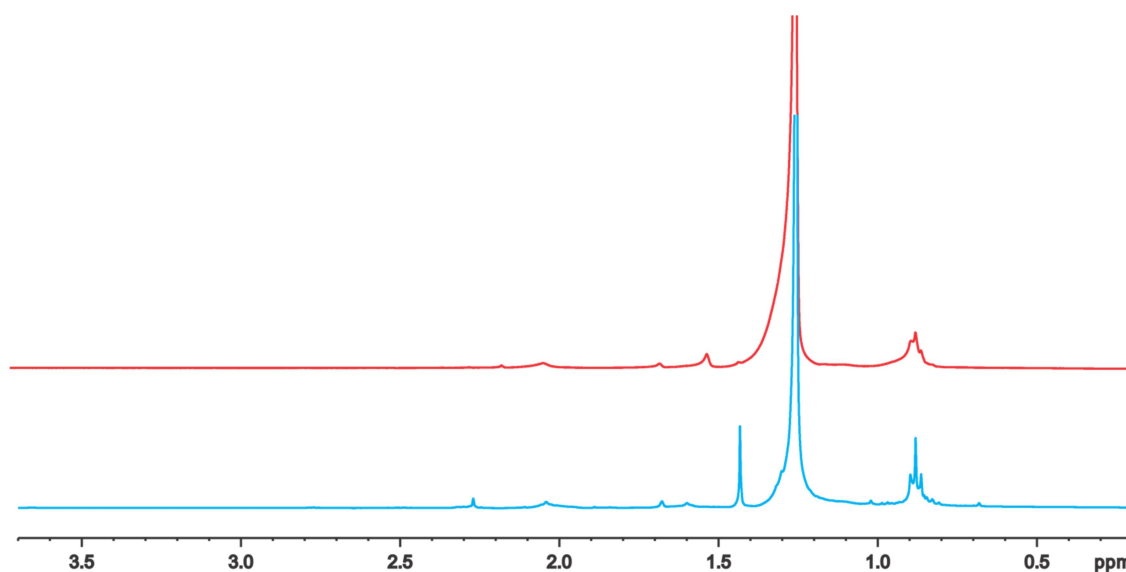


Figure 2.5. 400 MHz ¹H NMR of white powder in CDCl₃ Top: from the reaction of vinyl acetate in the presence of *meso*-Ni₂Cl₄(et,ph-P4) catalyst. Bottom: from the reaction of 1-hexene in the presence of *meso*-Ni₂Cl₄(et,ph-P4) catalyst.

Once the rubber septa were removed from our experimental set-up multiple hydration experiments of 1-hexene in the presence of water and catalytic amounts of *meso*-Ni₂Cl₄(et,ph-P4) or a mixture of *rac,meso*-Ni₂Cl₄(et,ph-P4) were reexamined.

Unfortunately there was no sign of activity. All attempts to achieve hydration of 1-hexene by changing reaction parameters such as temperature (increasing temperature up to 100°C), organic solvent fraction (acetone, THF, acetonitrile, toluene, DMSO, CH₂Cl₂), amount of water (increasing amounts for 5% up to 30%), addition of halide abstractor (1-4 equivalents of AgBF₄) did not yield any observable alcohol based on GC/MS.

2.3 Conclusions

Alkene hydration catalyzed by bimetallic Ni(II) species containing *rac,meso*-et,ph-P4 has been proven extremely difficult to achieve. Reactions carried out under mild conditions and without addition of strong bases or acids did not produce any detectable amount of alcohols. As described in Section 2.1 previous work in our group had shown that reactions of *meso*-NiCl₄(et,ph-P4) with 1-hexene in the presence of water at high temperatures and also at room temperature although at a much slower rate produced a small amount of alkane white solid. However, further testing with increasing catalyst concentrations, with various alkene substrates, as well as, mass balance analysis all pointed out that linear alkenes were not produced in reactions of *rac, meso*-Ni₂Cl₄(et,ph-P4) with alkene substrate, but simply extracted by the organic solvent/alkene substrate mixture from the rubber Suba seal septa.

2.4 References

1. Schreiter, W. J. Investigations into Alkene Hydration and Oxidation Catalysis Louisiana State University, Baton Rouge, 2013.
2. (a) Peuckert, M.; Keim, W., A new nickel complex for the oligomerization of ethylene. *Organometallics* **1983**, 2 (5), 594-597; (b) Hirose, K.; Keim, W., Olefin oligomerization with nickel PO chelate complexes. *Journal of Molecular Catalysis* **1992**, 73 (3), 271-276.

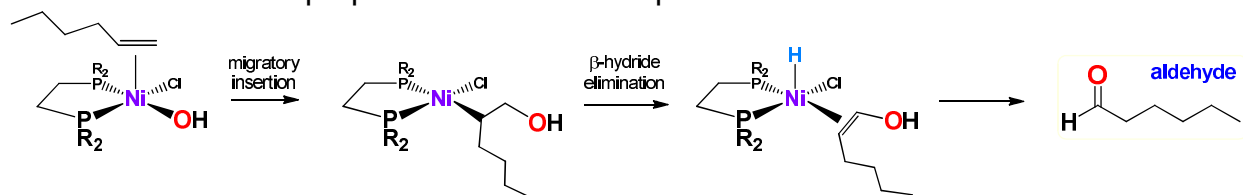
3. (a) Schmidt, G. F.; Brookhart, M., Implications of three-center, two-electron M-H-C bonding for related alkyl migration reactions: design and study of an ethylene polymerization catalyst. *Journal of the American Chemical Society* **1985**, *107* (5), 1443-1444; (b) Johnson, L. K.; Killian, C. M.; Brookhart, M., New Pd(II) and Ni(II) Based Catalysts for Polymerization of Ethylene and α -Olefins. *Journal of the American Chemical Society* **1995**, *117* (23), 6414-6415; (c) Killian, C. M.; Tempel, D. J.; Johnson, L. K.; Brookhart, M., Living Polymerization of α -Olefins Using Ni(II) α -Diimine Catalysts. Synthesis of New Block Polymers Based on α -Olefins. *Journal of the American Chemical Society* **1996**, *118* (46), 11664-11665; (d) Killian, C. M.; Johnson, L. K.; Brookhart, M., Preparation of Linear α -Olefins Using Cationic Nickel(II) α -Diimine Catalysts. *Organometallics* **1997**, *16* (10), 2005-2007.
4. Dennett, J. N. L.; Gillon, A. L.; Heslop, K.; Hyett, D. J.; Fleming, J. S.; Lloyd-Jones, C. E.; Orpen, A. G.; Pringle, P. G.; Wass, D. F.; Scutt, J. N.; Weatherhead, R. H., Diphosphine Complexes of Nickel(II) Are Efficient Catalysts for the Polymerization and Oligomerization of Ethylene: Steric Activation and Ligand Backbone Effects. *Organometallics* **2004**, *23* (26), 6077-6079.
5. (a) Cossee, P., Ziegler-Natta catalysis I. Mechanism of polymerization of α -olefins with Ziegler-Natta catalysts. *Journal of Catalysis* **1964**, *3* (1), 80-88; (b) Arlman, E. J.; Cossee, P., Ziegler-Natta catalysis III. Stereospecific polymerization of propene with the catalyst system $\text{TiCl}_3/\text{AlEt}_3$. *Journal of Catalysis* **1964**, *3* (1), 99-104.
6. Guan, Z.; Cotts, P. M.; McCord, E. F.; McLain, S. J., Chain Walking: A New Strategy to Control Polymer Topology. *Science* **1999**, *283* (5410), 2059-2062.

Chapter 3: Nickel-Phosphine Mediated Oxidative Cleavage of Alkene C=C Bonds by O₂

3.1 Background

In studying alkene hydration it was observed that in a number of reactions with *meso*-Ni₂Cl₄(et,ph-P4) and 1-hexene a small amount of aldehyde was produced.¹ As described previously during the initial testing ¹H NMR spectra of the samples from the reaction mixtures on some occasions showed a small singlet at 9.73 ppm (see Chapter 2, section 2.1). It was initially proposed that the aldehyde could have resulted from the β-hydride elimination of a nickel hydroxylalkyl species resulting from (alkene)-Ni-OH migratory insertion (Scheme 3.1.1).

Scheme 3.1.1. Initial proposed mechanism to produce hexanal from 1-hexene.



After a series of experiments it was determined that a small amount of aldehyde was produced from the reaction of 1-hexene in acetone/water in the presence of catalytic amounts of *meso*-Ni₂Cl₄(et,ph-P4), but only if the reaction was carried out in the presence of oxygen/air.¹

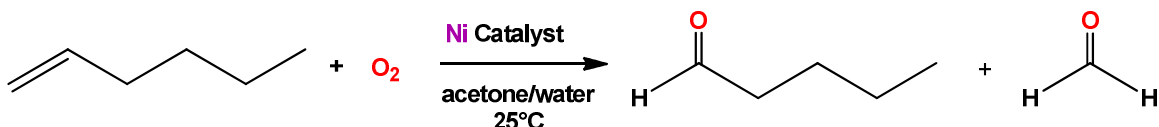
3.2 Results and Discussion

3.2.1 Investigations into Alkene Oxidation in the Presence of Ni(II) Phosphine Complexes

We have established that in the presence of dinickel complexes based on et,ph-P4 ligands 1-hexene is oxidized in the presence of O₂ in acetone/water solution to form

pentanal and formaldehyde as shown in Scheme 3.2.1. Although formaldehyde has not been detected, we believe it is being formed based on stoichiometry and the products formed from reactions of cyclic alkenes and unsymmetrical alkenes (see section 3.2.2).

Scheme 3.2.1. Oxidative cleavage of 1-hexene.



Typical reaction conditions consisted of catalytic amount (1 equivalent) of Ni₂Cl₄(et,ph-P4) in water/acetone solution, 1-hexene (30-100 equivalents), exposed to air/O₂ atmosphere and at room temperature. This reaction is not catalytic and only small amount of 1-hexene is oxidized to pentanal. Formation of the aldehyde is fast and pentanal can be observed in less than an hour from the start of the reaction by ¹H NMR and by GC/MS analysis. The ¹H NMR spectrum shown in Figure 3.2.1, shows a small singlet at 9.73 ppm, which was assigned to an aldehydic proton. A slight increase in the aldehyde peak has been observed by ¹H NMR over time, but stops after about two days from the start of the reaction.

Control experiments performed in the absence of the catalyst did not yield any detectable amounts of aldehyde. Because on some occasions the aqueous layer contained NiCl₂ (identified by the greenish color of the aqueous layer), control experiments with NiCl₂·6H₂O in the absence of any phosphine ligand were also tested and showed no detectable aldehydes.

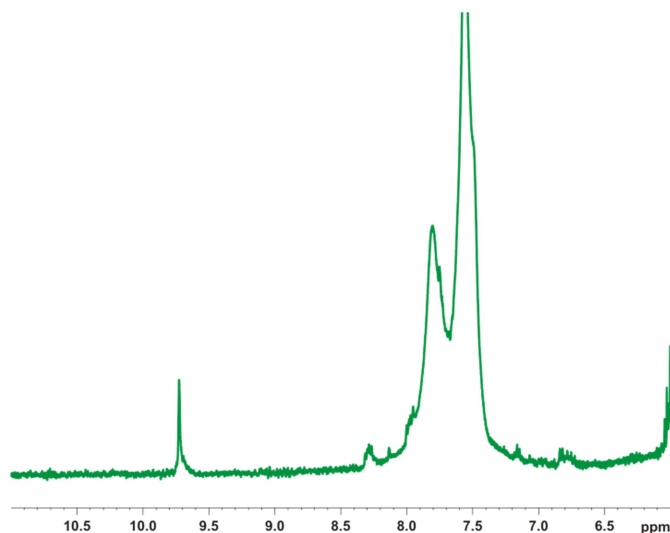


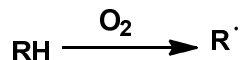
Figure 3.2.1. The 5-11 ppm region of the ^1H NMR spectrum of the sample from the reaction of *meso*- $\text{Ni}_2\text{Cl}_4(\text{et,ph-P4})$ with 1-hexene in acetone- $\text{d}_6/\text{D}_2\text{O}$ (15% by volume). Resonances between 7.0 and 8.5 ppm are due to the phenyl-ring hydrogens on the et-ph-P4 ligand.

It is well known that alkenes in the presence of oxygen from the air can undergo autoxidation under relatively mild conditions.² Hydrocarbon autoxidation can be initiated by light, heat, metallic ions, or by any molecule which decomposes to give free radicals. On the other hand, antioxidants, molecules that have resonance stabilized radicals can be used to suppress autoxidation. Autoxidations of alkenes proceed by a free-radical initiated chain reaction mechanism, which involves peroxide intermediates as shown in Scheme 3.2.2.^{2a} In the first phase of the reaction free radicals are formed by interaction of the oxygen with the hydrocarbon. In the chain propagation phase the radicals react with oxygen to generate peroxy radicals, which can further react with hydrocarbons to produce hydroperoxides. Most hydroperoxides can readily decompose into radicals as shown in chain branching step. Radicals formed this way can further react with the hydrocarbon to generate more radicals or combine with another radical to form nonradical products. Chain termination occurs by recombination of two radicals to

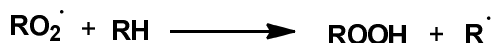
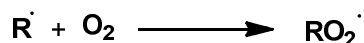
produce variety of products such as: epoxides, alcohols, ketones, polymeric peroxides, etc. Due to the lack of selectivity uncontrolled autoxidation processes are of a limited synthetic value.

Scheme 3.2.2. Typical reaction scheme for uncatalyzed autoxidation of olefins.^{2a}

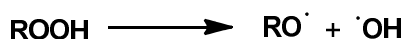
Chain initiation



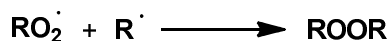
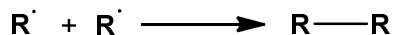
Chain propagation



Chain branching



Chain termination



Because the cleavage reactions of 1-hexene in the presence of oxygen could occur through a very common radical initiated auto-oxidation mechanism, our initial goal was to rule out the possibility of autoxidation mechanism. Reactions of *meso*-Ni₂Cl₄(et,ph-P4) with 1-hexene in the presence of radical inhibitors such as butylated hydroxy toluene and hydroquinone monomethyl ether were investigated.¹ It was observed that in the presence of radical inhibitors pentanal was still produced from 1-hexene, however reactions were slowed down.

We did not observe long induction periods as would be expected for a free radical initiated process. Formation of aldehyde was detected by ^1H NMR and GC/MS after 20 minutes from the start of the reaction. Lastly, if this reaction was catalyzed by a radical initiated auto-oxidation than a variety of products would be produced. Our reactions appear to be extremely clean and it is, therefore, highly unlikely that formation of the aldehyde is caused by autoxidation. However, if other products are formed, then it could be difficult to detect due to their very low overall concentration. Based on the available data we have concluded that this reaction proceeds by a mechanism other than autoxidation.

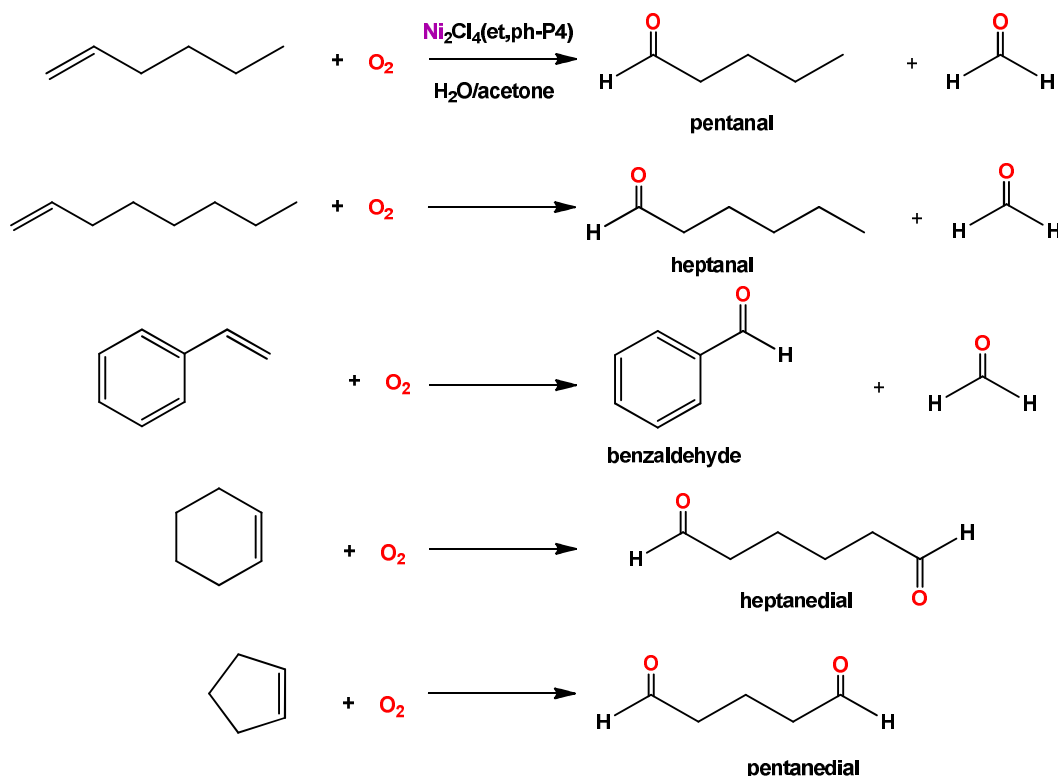
Our observations on oxidative cleavage of 1-hexene with O_2 in the presence of $\text{Ni}_2\text{Cl}_4(\text{et,ph-P4})$ to produce aldehydes could be a great improvement in this area of transition-metal catalysis if high catalytic activities were achieved.

3.2.2 Substrate Studies

To determine the scope of this reaction we tested a variety of alkene substrates including 1-octene, styrene, cyclohexene, cyclopentene, norbornene, and norbornodiene. As shown in Scheme 3.2.6 this reaction is not limited to aliphatic alkenes, reactions with aromatic and cyclic alkenes showed that corresponding aldehydes and dialdehydes are produced in small amounts. Based on the results obtained in all cases oxidative cleavage of the C-C double bond is observed. In cases when terminal alkenes were used, each time during the reaction the C-C double bond of alkene is broken and new C=O double bonds are formed producing two aldehyde products, one of them being formaldehyde. When cyclic alkenes were used the products are dialdehydes. No products were detected via GC/MS from reactions with

norbornene and norbornadiene. Samples from the reactions with these substrates were not analyzed by ^1H NMR.

Scheme 3.2.3. Alkene substrates studied. Experiments with norbornene and norbornadiene did not show any products based on GC/MS analysis.



Because the products produced from the reactions with cyclohexene and cyclopentane are 1,6-hexanedial and 1,5-pentenedial we firmly believe that the second product from reactions of terminal alkenes must be formaldehyde. However we were not able to detect formaldehyde via GC/MS because it comes out of the column prior to the solvent delay. All of the heavier aldehydes and dialdehydes produced were characterized by GC/MS and ^1H NMR analysis. Molecular ion peak is not generally seen for aliphatic aldehydes, due to the ease of fragmentation of a bond next to an oxygen atom. However, we do see the molecular ion peak for aromatic benzaldehyde.

A co-injection experiment showed single, sharp peak on a GC-chromatogram when a small amount of pentanal (authentic sample) was added to the sample taken from the reaction with 1-hexene. The ^1H NMR spectra recorded on the samples taken from the reactions carried out in deuterated solvents always showed a small singlet in the aldehyde region (9.2-10.2 ppm). The exact frequency of the aldehyde peak varies depending on the aldehyde produced in the reaction. Because only a small amount of the aldehyde was formed in our reactions, we were not able to isolate it for comparison with authentic samples via NMR spectroscopy. However, spiking the NMR tube sample taken from the reaction with 1-hexene with pentanal resulted in a large increase in the intensity of the singlet at 9.7 ppm. The ^1H NMR data plus the GC/MS data firmly identify the production of aldehydes.

To quantify the amount of the aldehyde produced in our reactions via GC/MS we have chosen styrene as a substrate. Toluene was used as an internal standard. The concentration of benzaldehyde was calculated from a calibration curve and on average was equal to 3 mM. Based on these results our reactions are sub stoichiometric because the catalyst concentration was always 10 mM. Aldehydes produced in reactions with other substrates were not quantified via GC/MS due to a smaller peak area (in some cases below the quantification limit). Nevertheless it is apparent from GC/MS and ^1H NMR analysis that the amount of the aldehyde formed in reactions with other substrates studied is extremely small and cannot be much different from the amount of benzaldehyde produced in reactions with styrene.

3.2.3 Synthesis and Characterization of *meso*-Ni₂Br₄(et,ph-P4)

To study effects of halide ligands we synthesized the *meso*-Ni₂Br₄(et,ph-P4) complex. The *meso*-Ni₂Br₄(et,ph-P4) was synthesized in high yield (96 %) by reaction of two equiv. of NiBr₂ with one equiv. of *meso*-et,ph-P4 (minor *rac*-et,ph-P4 impurity about 3%). The brown-orange powder obtained by vacuum filtration appears air-stable in solution and in the solid state. The ³¹P{¹H} spectrum of *meso*-Ni₂Br₄(et,ph-P4) in CD₃CN is shown in Figure 3.2.2. The spectral data is very similar to previously reported *meso*-Ni₂Cl₄(et,ph-P4), and exhibits two sets of signals due to inequivalent internal and external phosphorus atoms.¹²

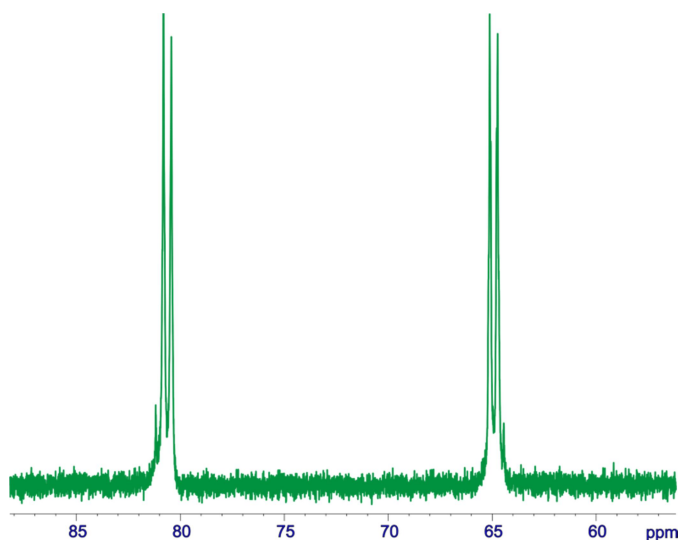


Figure 3.2.2. ³¹P{¹H} spectrum of *meso*-Ni₂Br₄(et,ph-P4) in CD₃CN.

For *meso*-Ni₂Br₄(et,ph-P4) the two pseudo-doublets of triplets 80.62 ppm (P external, J_{P-P} = 61.8 Hz) and 64.93 ppm (P internal, J_{P-P} = 61.6 Hz) are slightly shifted downfield compared to *meso*-Ni₂Cl₄(et,ph-P4) (two pseudo-doublets of triplets at 74.28 ppm (P external, J_{P-P} = 78.2 Hz) and 58.32 ppm (P internal, J_{P-P} = 72.8.0 Hz). The doublet splitting is due to a two bond coupling of internal to external phosphorous atoms

through the nickel center ($^2J_{\text{p}_{\text{ext}}-\text{p}_{\text{int}}}$). Additional three bond coupling through the ethylene in between P external to P internal ($^3J_{\text{p}_{\text{int}}-\text{p}_{\text{ext}}}$) and the four bond coupling in between P external in one half of the molecule with P internal in the other half of the molecule ($^4J_{\text{p}_{\text{ext}}-\text{p}_{\text{int}}}$) generates a pseudo-triplet pattern. Orange crystals of *meso*-Ni₂Br₄(et,ph-P4) suitable for X-ray diffraction were obtained by slow evaporation of an CH₃CN solution at room temperature. Some crystallographic data is shown in Table 3.2.1. Crystal structure of the *meso*-Ni₂Br₄(et,ph-P4) is shown in Figure 3.2.3, and selected bond distances and angles are given in Table 3.2.2.

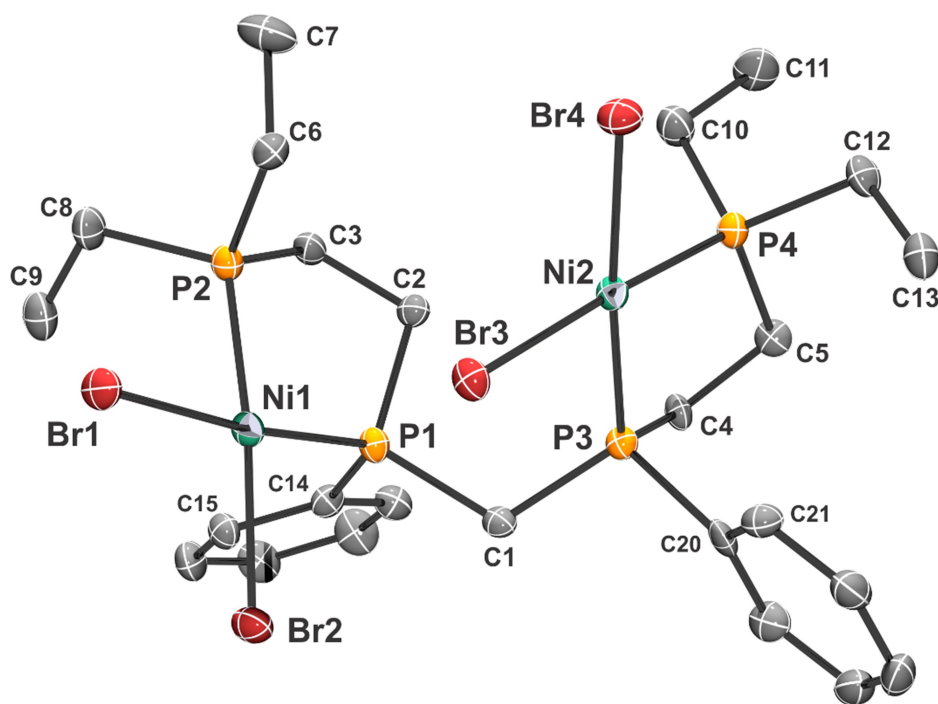


Figure 3.2.3. ORTEP (50% ellipsoids) of *meso*-Ni₂Br₄(et,ph-P4) 2(CH₃CN). Solvent molecules and hydrogen atoms omitted for clarity.

The structure is very similar to previously reported *meso*-Ni₂Cl₄(et,ph-P4).^{12a} The Ni atoms are in +2 oxidation state with a d⁸ electron configuration. The coordination of

each Ni center is slightly distorted square-planar and the et,ph-P4 ligand is coordinated in the typical bridging and chelating manner. As expected, the Br-Ni-Br angle is somewhat expanded (95.7° average) and the P-Ni-P chelate angle is reduced to 87.2° (same for each side). It is important to note that the Br(3), which is coordinated to Ni(2) is close to Ni(1) with a distance of 3.2021(9) Å. This weak interaction brings the two metal centers closer to each other resulting in a much shorter Ni···Ni distance of 4.6539(9) Å compared to 6.272(1) Å for *meso*-Ni₂Cl₄(et,ph-P4).^{12a} Such a bridging interaction was not observed for the *meso*-Ni₂Cl₄(et,ph-P4) complex because bromide is a better bridging ligand due to the larger size and better polarizability compared to chloride. Experimental results showed that *meso*-Ni₂Br₄(et,ph-P4) is also active for oxidative cleavage, but no noticeable improvement in the amount of aldehydes produced was observed.

Table 3.2.1. Crystallographic Data for *meso*-Ni₂Br₄(et,ph-P4) 2(CH₃CN)

Formula	Ni ₂ Br ₄ P ₄ C ₂₅ H ₄₀ , 2(CH ₃ CN)
fw	938.62
space group	Monoclinic, <i>P</i> 2/ <i>c</i>
<i>a</i> , Å	8.9086(10)
<i>b</i> , Å	26.670(4)
<i>c</i> , Å	15.812(2)
β, deg	100.392(1)
<i>V</i> , Å ³	3695.2(8)
<i>Z</i>	4
<i>d</i> _{calc} , Mg m ⁻³	1.768
temp, K	90
radiation, (Mo Kα), λ, Å	0.71073
R(<i>F</i> ₀)	0.052
R _w (<i>F</i> ₀)	0.114

Table 3.2.2. Selected Bond Distances (Å) and Angles (°) for *meso*-Ni₂Br₄(et,ph-P4), 2(CH₃CN)

Ni1...Ni2	4.6539(9)	Br1-Ni1-P2	86.94(4)
Ni1-Br1	2.3519(7)	Br2-Ni1-P1	90.60(4)
Ni1-Br2	2.3609(8)	Br2-Ni1-P2	169.50(5)
Ni-P1	2.1524(13)	P1-Ni1-P2	87.20(5)
Ni1-P2	2.1553(7)	Br3-Ni2-Br4	95.96(3)
Ni2-Br3	2.3472(7)	Br3-Ni2-P4	174.89(5)
Ni2-Br4	2.3485(8)	Br3-Ni2-P3	88.97(4)
Ni2-P3	2.1491(14)	Br4-Ni2-P3	174.44(5)
Ni2-P4	2.1571(14)	Br4-Ni2-P4	89.07(4)
P1-C1	1.852(5)	P3-Ni2-P4	87.20(5)
P3-C3	1.823(5)	Ni1-P1-C1	118.31(15)
Br1-Ni1-Br2	95.51(3)	Ni2-P3-C1	120.48(16)
Br1-Ni1-P1	173.83(5)	P1-C1-P3	117.0(3)

3.2.4 Other Systems Tested

In addition to the et,ph-P4 ligand, other monodentate and bidentate chelating phosphine ligands were also tested such as: tpp, dppe, dppp and dcpe. The nickel phosphine complexes were synthesized according to the literature methods.¹³ 1-hexene and styrene were the only alkenes tested for oxidative cleavage under the previously described reaction conditions, which consisted of 100 equivalents of an alkene substrate, 1 equivalent of nickel complex in acetone/water (15% water by volume) solution, room temperature, and exposed to air. Samples taken from the reaction

mixtures were analyzed via GC/MS. These reactions were not studied by NMR spectroscopy. $\text{NiCl}_2(\text{dppe})$, $\text{NiCl}_2(\text{dppp})$ and $\text{NiCl}_2(\text{dcpe})$ are all active for oxidative cleavage, producing small amount of corresponding aldehydes. However, $\text{NiCl}_2(\text{PPh}_3)_2$ was not active under conditions tested, indicating that triaryl phosphines are not suited for this reaction.

3.2.5 Other Reaction Observations

In order to achieve catalytic turnovers different reaction parameters were varied. In this studies 1-hexene was used as a substrate in the presence of catalytic amounts of *meso*- $\text{Ni}_2\text{Cl}_4(\text{et,ph-P4})$. Reactions were carried out under standard reaction conditions unless otherwise stated.

Addition of AgBF_4

For many reactions catalyzed by transition metal complexes it has been found that the catalytic activity can be enhanced by going from neutral to cationic complexes.¹⁴ A common method to generate a cationic metal complex is halide ligand abstraction by an appropriate reagent. Chloride abstraction with AgBF_4 from $\text{Ni}_2\text{Cl}_4(\text{et,ph-P4})$ should result in a more active cationic or multi-cationic complexes. In these complexes electrophilicity of the nickel center is expected to increase and could assist in the activation of alkene substrate. Addition of 1, 2, and 4 equivalents of AgBF_4 to $\text{Ni}_2\text{Cl}_4(\text{et,ph-P4})$ did not result in any increase in the amount of the pentanal produced.

Temperature

Increasing temperature from 25°C to up to 90°C did not result in any apparent increase in the amount of the pentanal produced. However, at higher temperatures faster production of the pentanal was observed. Approximately the same amount of the

pentanal was produced in less than 3 hours as compared to the amount of pentanal produced in 24 hours at 25°C. Reactions at higher temperatures were carried out in a high-pressure NMR tubes in acetone-d₆/D₂O and were purged with O₂.

O₂ Pressure

As described in Section 2.2.1 it was established that oxidative cleavage of alkenes occurred only when reactions were carried out exposed to oxygen/air. Reactions under N₂ atmosphere, as expected, did not produce any detectable amount of oxidative cleavage products. To determine if increasing oxygen pressure will result in higher conversions reactions under balloon pressure and under 100 psi of O₂ were investigated. Unfortunately, no apparent improvement in the amount of the pentanal produced was observed. However formation of the pentanal was faster at increased pressures of O₂, but not as fast as in reactions carried out at higher temperatures. Reactions pressurized to 100 psi of were carried out in a high-pressure NMR tubes in acetone-d₆/D₂O.

Water

After running a series of experiments with varying water content from 3-30% by volume it was determined that at least 5% water (by volume) is necessary for this reaction, as no pentanal was detected in the samples taken from the reactions carried out in water/acetone (3% water by volume) or in pure acetone. Increasing amounts of water up to 30% by volume (miscibility of the organic substrates limited us to 30% water) does not affect the amount of aldehyde produced.

Other Organic Solvents Tested

In addition to the acetone-water system, other solvent systems were also studied. Reactions carried out in acetonitrile/water (15% water by volume), THF/water (15% water) and DMSO/water (15% volume) also produced pentanal. The amount of pentanal produced from 1-hexene was not noticeably affected by the various organic solvents tested.

H₂O₂ as Primary Oxidant

The use of hydrogen peroxide as a primary oxidant can also be considered as environmentally friendly process because water is formed as a byproduct. It is well known that phosphines can be easily oxidized in the presence of strong oxidizers like H₂O₂. Therefore, transition metal complexes based on nitrogen ligands are generally used to study oxidation reactions in the presence of strong oxidizing agents like H₂O₂ that readily oxidize metal-coordinated phosphine ligands. Interestingly, Cho *et al.* reported on oxidation of styrene with H₂O₂ catalyzed by Pt(II), Pd(II), and Ni(II) complexes based on phosphine ligands.¹⁰ No comments with regard to oxidation of phosphine ligands under conditions tested were made by the authors, although a large excess (50 equivalents based on the catalyst) of H₂O₂ was used.

We have found that addition of four equivalents of aqueous H₂O₂ to a solution of *meso*-Ni₂Cl₄(et,ph-P4) in water/acetone (15% water) resulted in immediate formation of white precipitate indicating complete phosphine oxidation. No other reactions with H₂O₂ as a primary oxidant were studied.

3.2.6 Proposed Mechanism

The ^{31}P NMR studies (Section 3.2.7) showed that the starting *meso*- $\text{Ni}_2\text{X}_4(\text{et,ph-P4})$ ($\text{X}=\text{Cl}, \text{Br}$) complex in the presence of both water and oxygen reacts almost immediately to form a mixture of different species. We believed that one of this newly formed species is active for oxidative cleavage. As shown in Scheme 2.2.4 *meso*- $\text{Ni}_2\text{X}_4(\text{et,ph-P4})$ could react with water to form the cationic bridging hydroxide complex, 2. Although complex 2 was not observed via NMR, its formation was proposed based on the previously characterized hydroxide bridged complex, $[\text{Ni}_2\text{Cl}_2(\mu\text{-OH})(\text{meso-et,ph-P4-Ph})]^+$ (Figure 3.2.4).

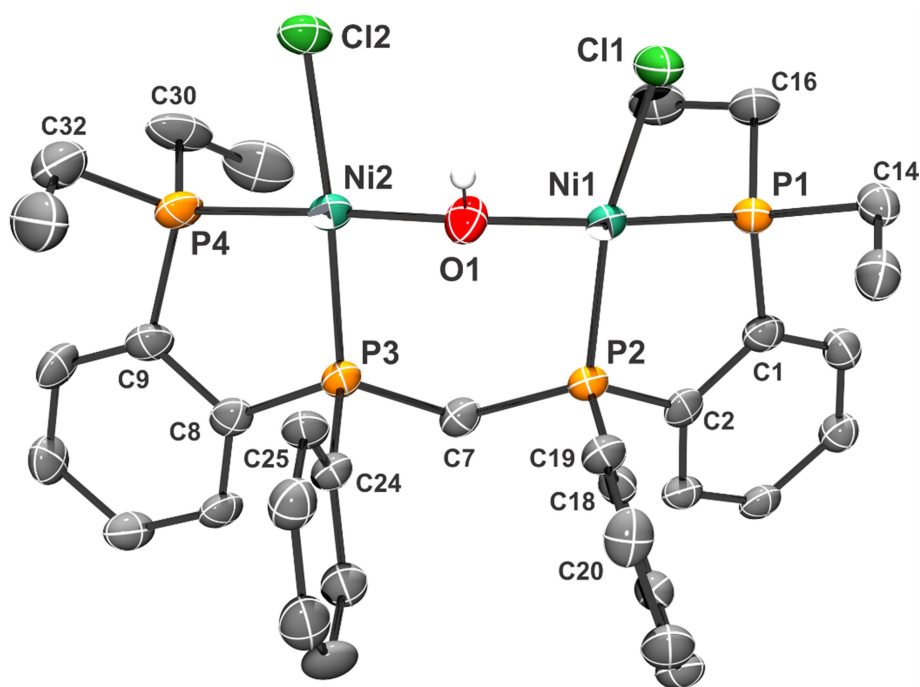
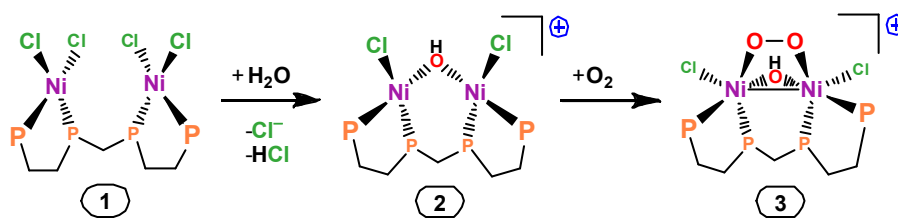


Figure 3.2.4. ORTEP plot of $[\text{Ni}_2(\mu\text{-OH})\text{Cl}_2(\text{et,ph-P4-Ph})]^+$, 2. Ellipsoids are shown at the 50% probability level. Hydrogens on the carbon atoms and the $[\text{NiCl}_4]^{2-}$ counter-anion are omitted for clarity.

Complex 2 can react with oxygen to form 3, which could initiate the oxidative cleavage reaction with alkene. There are no reports in the literature on bridging OH, O_2

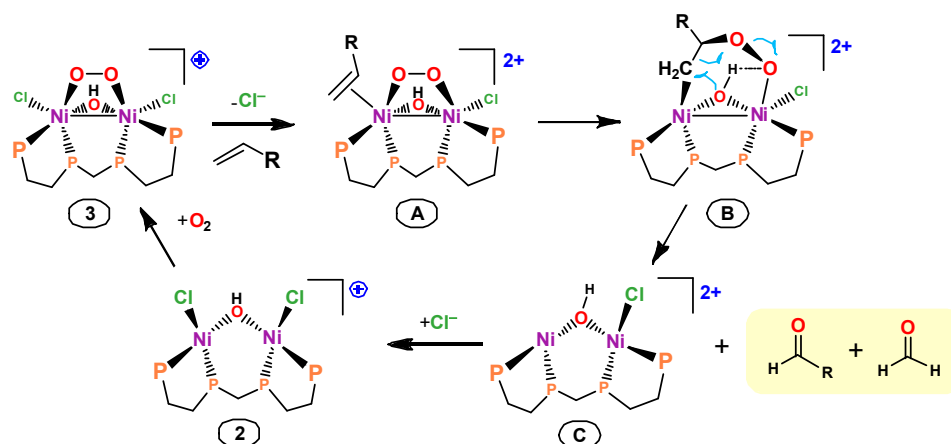
structures for nickel, but these systems have been characterized for bimetallic complexes of Co, Fe and Rh.¹⁵ All of the previously characterized structures, however, have *trans* orientations of the OH and O₂ ligands. Due to the *cis*-chelating design of our ligand in complex 3 the O₂ and OH are *cis* to one another. Based on the DFT calculations performed by Professor Stanley there is a prediction for a Ni-Ni bond (Ni-Ni = 2.485 Å) in the DFT optimized structure for 3. Each nickel center has been assigned +3 oxidation state (d⁷ electron configuration) with bridging peroxide (O₂²⁻) and OH⁻ ligands.

Scheme 3.2.4. Proposed Reaction of meso-Ni₂Cl₄(et,ph-P4) with water and O₂.



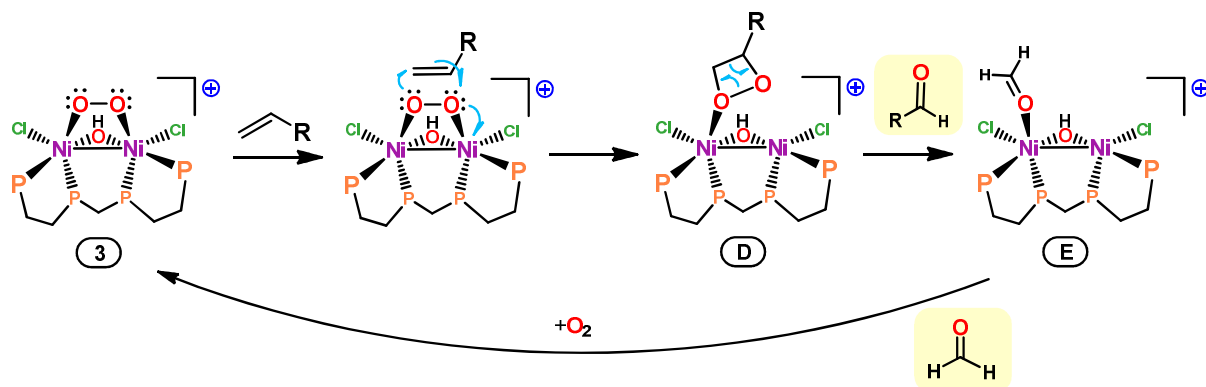
Based on the proposed active species 3 two likely mechanisms for oxidative cleavage had been put forward by Prof. Stanley. The first mechanism is shown in Scheme 3.2.5 and involves chloride ligand dissociation followed by alkene coordination in the first step to form A. Next migratory insertion of alkene and peroxide ligand results in formation of complex B. In the next step proton transfer from the bridging hydroxide to the peroxide initiates a reductive elimination of the hydroxide oxygen and Ni-CH₂ group. Cleavage of the CH₂-CHR and O-O bonds yields two aldehydes and complex C. Coordination of chloride, followed by reaction with O₂ regenerates starting complex 3. Based on this mechanism one oxygen atom from O₂ and one from the bridging hydroxide is incorporated into the two aldehydes.

Scheme 3.2.5. Mechanism for Oxidative Cleavage of an Alkene.



A second proposed mechanism is shown in Scheme 3.2.6. This mechanism does not involve coordination of alkene to the Ni center. As shown in Scheme 3.2.6 alkene directly reacts with bridging peroxide to form a dioxetane ring system which falls apart to produce two aldehydes. Based on this mechanism both oxygen atoms in the two aldehyde products come from O_2 .

Scheme 3.2.6. “Methathesis” Mechanism for Alkene Oxidative Cleavage.



3.2.7 NMR Studies

Investigations into the Nature of the Active Species

The ^1H NMR spectrum of a sample taken from reaction of 1-hexene in D_2O /acetone- d_6 with *meso*- $\text{Ni}_2\text{Cl}_4(\text{et},\text{ph-P4})$ (standard reaction conditions) large

changes in the aromatic region were observed (Figure 3.2.5) in addition to the formation of the 9.73 ppm resonance assigned to aldehyde product. Since, *meso*-Ni₂Cl₄(et,ph-P4) is the only species in solution (aside from traces of the *rac*-complex) that will give signals in the aromatic region, the changes observed are due to modifications of the structure of *meso*-Ni₂Cl₄(et,ph-P4) during oxidative cleavage reaction. Careful ¹H NMR analysis of the reactions run in the absence of O₂, in the absence of 1-hexene, and in the absence of water indicated that the changes are definitely caused by water. The initial ¹H NMR spectrum of *meso*-Ni₂Cl₄(et,ph-P4) in acetone-d₆ shows two sets of resonances in the aromatic region centered around 7.6 and 8.8 ppm (Figure 3.2.5, black spectrum). After addition of water the two main resonances decrease in intensity and several new multiplets are present. Newly formed multiplets gradually increase in intensity, but after a few days remain unchanged (Figure 3.2.5, red spectrum).

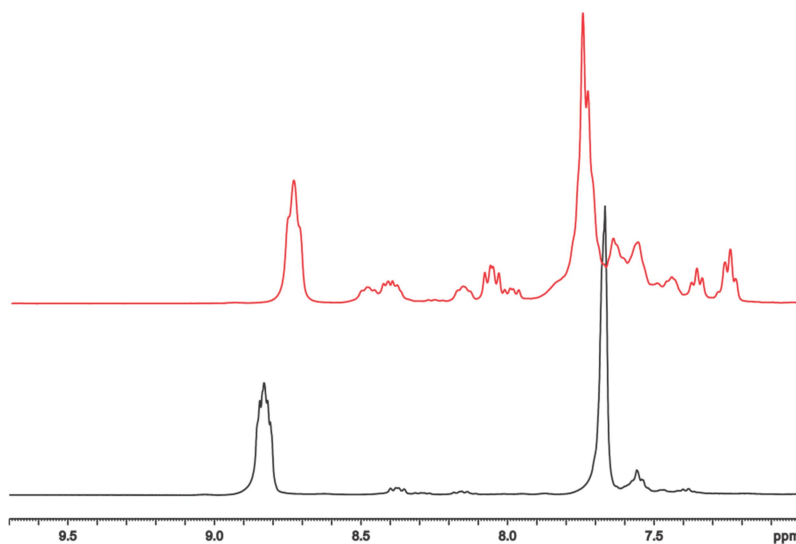


Figure 3.2.5. (Black spectrum) The 6-9.7ppm region of the ¹H NMR spectra: *meso*-Ni₂Cl₄(et,ph-P4) in acetone-d₆; (red spectrum) D₂O added, after 3 days under O₂.

The $^{31}\text{P}\{^1\text{H}\}$ NMR analysis confirms that the addition of water cause major changes in the the structure of *meso*- $\text{Ni}_2\text{Cl}_4(\text{et,ph-P4})$. The initial $^{31}\text{P}\{^1\text{H}\}$ spectrum of *meso*- $\text{Ni}_2\text{Cl}_4(\text{et,ph-P4})$ in acetone- d_6 shows two doublet of pseudo-triplets at 73.9 and 58.1 ppm (Figure 3.2.6, red line).

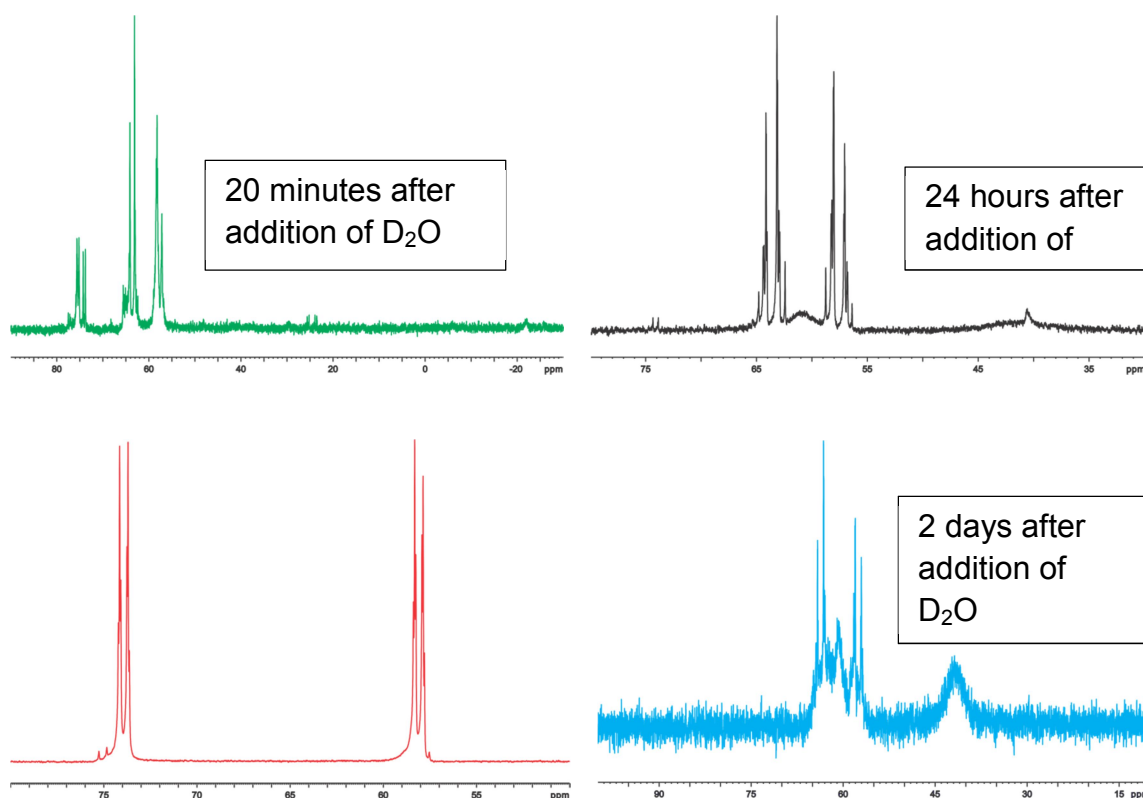


Figure 3.2.6. (Red spectrum) $^{31}\text{P}\{^1\text{H}\}$ spectra of *meso*- $\text{Ni}_2\text{Cl}_4(\text{et,ph-P4})$ in CD_2Cl_2 ; (green spectrum) $^{31}\text{P}\{^1\text{H}\}$ spectra of *meso*- $\text{Ni}_2\text{Cl}_4(\text{et,ph-P4})$ in in acetone- $\text{d}_6/\text{D}_2\text{O}$ recorded 20 minutes after addition of D_2O ; (black spectrum) $^{31}\text{P}\{^1\text{H}\}$ spectra of *meso*- $\text{Ni}_2\text{Cl}_4(\text{et,ph-P4})$ in in acetone- $\text{d}_6/\text{D}_2\text{O}$ recorded 24 hours after addition of D_2O ; (blue spectrum) $^{31}\text{P}\{^1\text{H}\}$ spectra of *meso*- $\text{Ni}_2\text{Cl}_4(\text{et,ph-P4})$ in in acetone- $\text{d}_6/\text{D}_2\text{O}$ recorded 2 days after addition of D_2O .

After the initial addition of water the $^{31}\text{P}\{^1\text{H}\}$ NMR spectrum becomes very complex, with several new resonances due to at least three new Ni-phosphine species formed (Figure 3.2.6, green line). Low intensity signal at around -22 ppm could be due

to a partially uncoordinated phosphine ligand present in solution. In agreement with the ^1H NMR data, new signals change over time and after about 24 hours $^{31}\text{P}\{^1\text{H}\}$ NMR spectrum shows two broad resonances centered at about 40 and 60 ppm overlapping with two complex multiplets centered at 58 and 64 ppm (Figure 3.2.6, black spectrum). Over the next few days intensity of the multiplets decreased as the broad resonances increase in intensity (Figure 3.2.6, blue spectrum).

The same behavior was observed via ^1H NMR and ^{31}P NMR analysis of samples taken from reactions with 1-hexene in the presence of *meso*- $\text{Ni}_2\text{Br}_4(\text{et,ph-P4})$ complex in acetone- $\text{d}_6/\text{D}_2\text{O}$. However, the newly formed signals had a slightly different chemical shift indicating the presence of one or more bromide ligands (Figure 3.2.7).

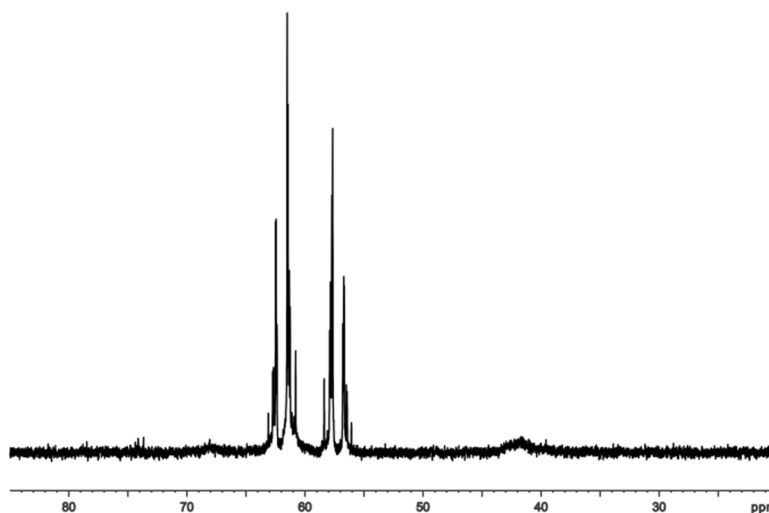


Figure 3.2.7. $^{31}\text{P}\{^1\text{H}\}$ spectra of the sample taken from reaction with 1-hexene in the presence of *meso*- $\text{Ni}_2\text{Br}_4(\text{et,ph-P4})$ in acetone- $\text{d}_6/\text{D}_2\text{O}$ recorded 24 hours after the start of the reaction.

Dr. William Schreiter established that the new species formed in our reactions is $[\text{Ni}_2(\mu\text{-Cl})(\text{meso-et,ph-P4})_2]^{3+}$, a dinickel double-et,ph-P4 complex (Figure 3.2.8).¹

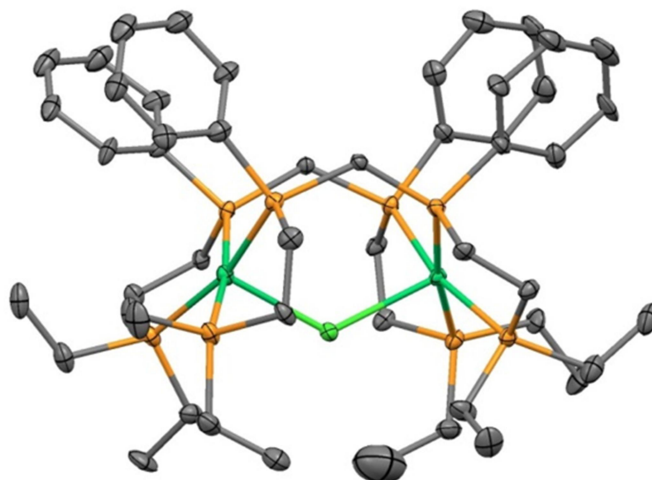


Figure 3.2.8. ORTEP plot of $[\text{Ni}_2(\mu\text{-Cl})(\text{meso-et,ph-P4})_2]^{3+}$, (50% probability ellipsoids, hydrogen atoms omitted for clarity).¹

Anderson *et al.* characterized similar diplatinum complex using the phenylated version of our et,ph-P4 ligand, $[\text{Pt}_2(\mu\text{-Cl})(\text{meso-ph,ph-P4})_2]^{3+}$.¹⁶ Reactions with 1-hexene in the presence of the $[\text{Ni}_2(\mu\text{-Cl})(\text{meso-et,ph-P4})_2][\text{BF}_4]_3$ complex did not show any activity for oxidative cleavage.¹

Variable Temperature NMR

Broadened resonances observed in $^{31}\text{P}\{^1\text{H}\}$ NMR spectra could indicate either some dynamic exchange process or the presence of paramagnetic nickel species.¹⁷ To test if formation of the broad resonances observed is caused by some exchange process we decided to study the behavior of *meso*- $\text{Ni}_2\text{Cl}_4(\text{et,ph-P4})$ in the presence of 1-hexene in acetone- $\text{d}_6/\text{D}_2\text{O}$ solution as a function of temperature via $^{31}\text{P}\{^1\text{H}\}$ NMR (Figure 3.2.9). The $^{31}\text{P}\{^1\text{H}\}$ NMR spectrum recorded at 25°C is shown in Figure 3.2.9, black line. The only resonances observed after two days from the start of the reaction are two broad signals centered at 60 and 40 ppm.

At lower temperatures the rate of exchange slows down and two resolved multiplet signals centered 60 and 40 ppm are observed (Figure 3.2.9, dark blue spectrum (-10°C) and light blue spectrum (-15°C)). At higher temperatures (50°C) the peaks broaden and become invisible at 80°C (Figure 3.2.9, orange and purple spectra). This phenomenon is reversible within minutes. No coalescence was observed up to 100°C (Figure 3.2.9, red spectrum). Observations described above were very confusing at that time because in dynamic exchange process the exchange rate increases at higher temperature and eventually equals the frequency difference between the different environments and the signals should coalesce.¹⁷ Since our reaction was carried out in $\text{D}_2\text{O}/\text{acetone-d}_6$ we did not attempt to collect NMR data at temperatures higher than 100°C . Our observations at lower temperatures were completely consistent with a dynamic exchange process. One possible explanation proposed at that time was a combination of exchange and interconversion between diamagnetic and paramagnetic centers. The paramagnetic character increases at higher temperatures and eventually the peaks become invisible.

The ^1H NMR spectrum recorded on the same sample also showed broadened resonances at room temperature, raising temperature to 100°C did not cause any changes in the spectrum (Figure 3.2.10). This could be due to the fact that phosphorus nuclei are directly bonded to a paramagnetic Ni center and therefore the $^{31}\text{P}\{^1\text{H}\}$ NMR spectra are more influenced compared to the ^1H NMR spectra. To determine if paramagnetic Ni(III) complexes were formed in our reactions the samples were analyzed via EPR (Electron Paramagnetic Resonance) spectroscopy. No signals due to paramagnetic species were observed. Based on the $^{31}\text{P}\{^1\text{H}\}$ NMR data, however, the

line broadening is most clearly observed at higher temperatures, but the EPR data was measured at room temperatures. Therefore, the EPR analysis did not provide definite proof on the absence of paramagnetic Ni(III) in our samples.

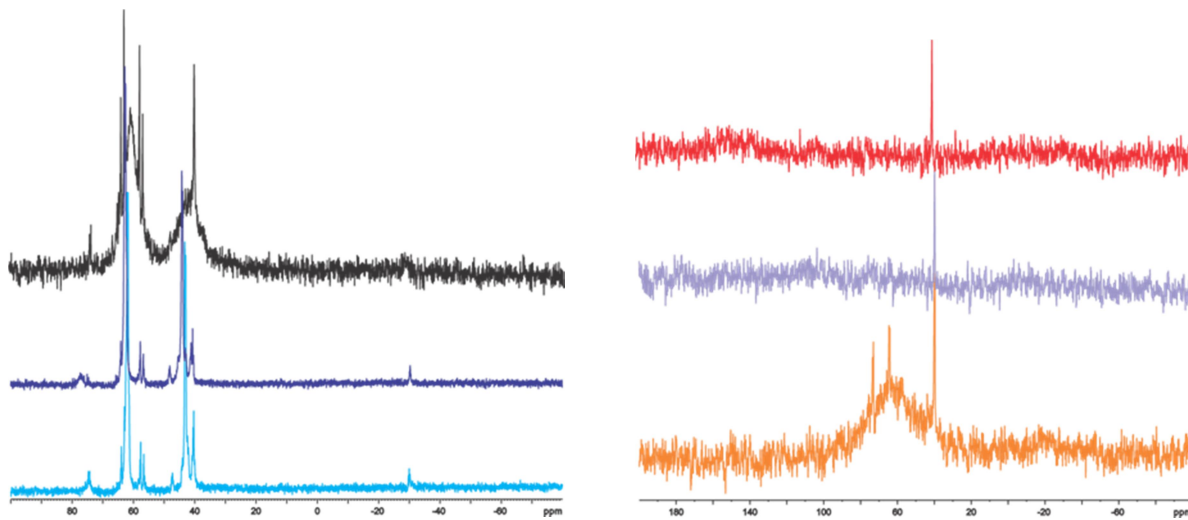


Figure 3.2.9. (Light blue spectrum) $^{31}\text{P}\{^1\text{H}\}$ spectra of *meso*- $\text{Ni}_2\text{Cl}_4(\text{et,ph-P4})$ with 1-hexene in acetone- $\text{d}_6/\text{D}_2\text{O}$ recorded at -15°C (light blue); (dark blue spectrum) -10°C ; (black spectrum) 25°C ; (orange spectrum) 50°C ; (purple spectrum) 80°C , and (red spectrum) 100°C . For higher temperatures the NMR tube was tube pressurized to 90 psi with O_2 .

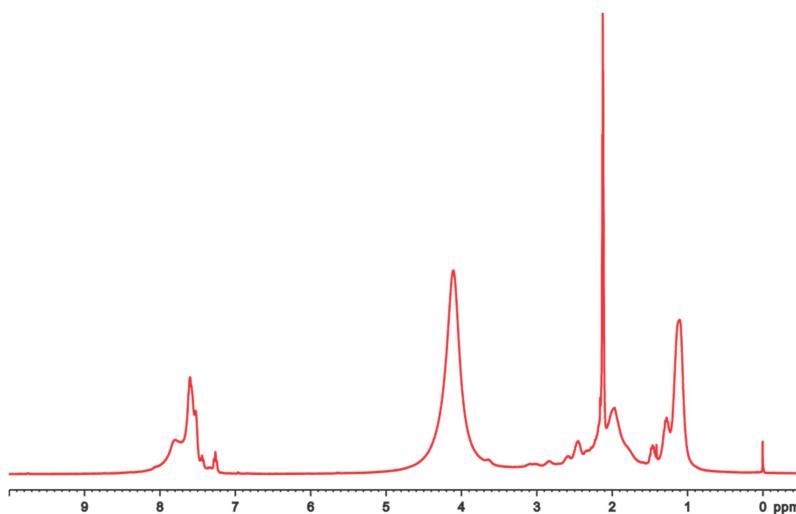


Figure 3.2.10. ^1H spectra of *meso*- $\text{Ni}_2\text{Cl}_4(\text{et,ph-P4})$ with 1-hexene in acetone- $\text{d}_6/\text{D}_2\text{O}$ solution recorded at 100°C , tube pressurized 90psi of O_2 .

Low Temperature NMR

The ^1H and $^{31}\text{P}\{^1\text{H}\}$ NMR analyses showed that addition of water to a solution of *meso*- $\text{Ni}_2\text{Cl}_4(\text{et,ph-P4})$ causes the formation of several different species that are only present for a relatively short period of time before converting to the broad resonances and a symmetrical species identified as $[\text{Ni}_2(\mu\text{-Cl})(\text{meso-et,ph-P4})_2]^{3+}$. We believed that one of the intermediate species formed after addition of water is active for the alkene oxidation, but does not last long enough to do any catalysis resulting in a very small amount of the aldehyde formed. To try and observe intermediate species that are present during the time of aldehyde formation reactions were monitored by ^1H and $^{31}\text{P}\{^1\text{H}\}$ NMR as a function of temperature. The $^{31}\text{P}\{^1\text{H}\}$ NMR spectra recorded are shown in Figure 3.2.11.

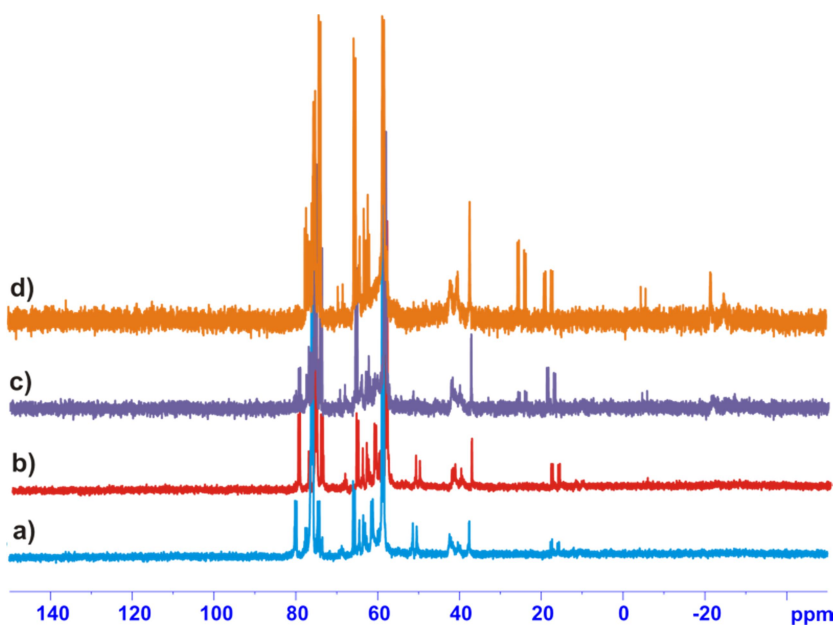


Figure 3.2.11. $^{31}\text{P}\{^1\text{H}\}$ NMR spectra of *meso*- $\text{Ni}_2\text{Cl}_4(\text{et,ph-P4})$ in acetone- $\text{d}_6/\text{D}_2\text{O}$ solution: a) at -20° , b) -20° , 1-hexene added, c) 5°C , d) 25°C .

First, a solution of *meso*-Ni₂Cl₄(et,ph-P4) in acetone-d₆ and D₂O (5% by volume) was cooled to –20 °C and ³¹P{¹H} and ¹H NMR spectra were recorded (Figure 3.2.11 a and 3.2.12a).

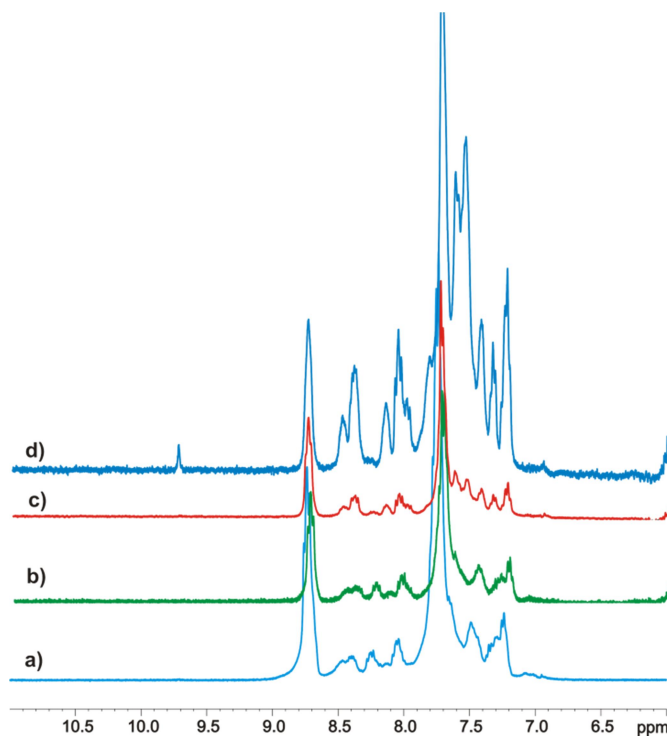


Figure 3.2.12. ¹H spectra of *meso*-Ni₂Cl₄(et,ph-P4) in acetone-d₆/D₂O solution: a) at –20°, b) –20°, 1-hexene added, c) 5°C, d) 25°C.

After addition of excess 1-hexene at –20°C no significant changes were observed (Figure 3.2.11,b and 3.2.12,b). The temperature was then raised to 5°C and ¹H NMR and then ³¹P{¹H} spectra were recorded (Figure 3.2.11,c and 3.2.12,c). No aldehyde peak was observed at 5°C by ¹H NMR. The sample was next warmed to 25°C and the corresponding ¹H NMR spectrum showed a singlet at 9.73 ppm corresponding to the aldehyde proton (Figure 3.2.12,d). At the same temperature formation of the broad resonances were observed via ³¹P{¹H} NMR (Figure 3.2.11,d). Based on these

observations pentanal is only produced in the presence of the broad resonances. Intensity of the aldehyde peak only increases slightly once the broad resonances are observed via $^{31}\text{P}\{^1\text{H}\}$ NMR. During the experiment a Ni-alkene complex was not detected, as resonances corresponding to the vinylic protons of 1-hexene remained the same. However because only very small amount of 1-hexene is converted to pentanal any changes in resonances due to vinylic protons could be difficult to observe.

NMR Studies of the et,ph-P4 Ligand in Solution in the Presence of Oxygen.

Due to the ease of phosphine oxidation in the presence of air/ O_2 transition metal phosphine complexes are not generally used in oxidation catalysis. We did not observe formation of phosphine oxides or any changes in the $^{31}\text{P}\{^1\text{H}\}$ NMR spectrum of *meso*- $\text{Ni}_2\text{Cl}_4(\text{et,ph-P4})$ in acetone- d_6 after exposure to air when no water was present. Based on the NMR studies in the presence of both O_2/air and water $\text{Ni}_2\text{X}_4(\text{et,ph-P4})$ ($\text{X}=\text{Cl}, \text{Br}$) converts to a mixture different species, but no formation of phosphine oxide was observed except for two very low intensity resonances at 23.7 and 25.4 ppm that are present for a short time before conversion to broad resonances.(Figure 3.2.9). Generally phosphine oxides have very sharp resonances and chemical shifts between 30 and 60 ppm, which were not observed.

Because we did not observe any evidence for formation of significant amounts of phosphine oxide in our reactions we decided to study reactions of et,ph-P4 ligand with air/ O_2 (no D_2O present) in acetone- d_6 via $^{31}\text{P}\{^1\text{H}\}$ NMR. The ^{31}P NMR spectra were recorded 1 day, 3 days, 8 days and 29 days after solution of *meso*-et,ph-P4 in acetone- d_6 was exposed to air (Figure 2.2.13). One day after exposure to air, in addition to characteristic signals for *meso*-et,ph-P4 at $-16.8(\text{t})$ and $-24.3(\text{t})$ ppm, two new low

intensity signals at 49 and 38 ppm were observed. After the next several days a mixture of the new signals in 56 to 14 ppm range appeared and their intensity slowly increased over time. However signals due to the *meso*-et,ph-P4 were still high in intensity. For example, even after 8 days upon exposure to air the signals due to the *meso*-et,ph-P4 ligand were around 68% by integration. Even after 29 days signals due to the *meso*-et,ph-P4 ligand were still present with integration indicating that 32% of the mixture was unreacted P4 ligand.

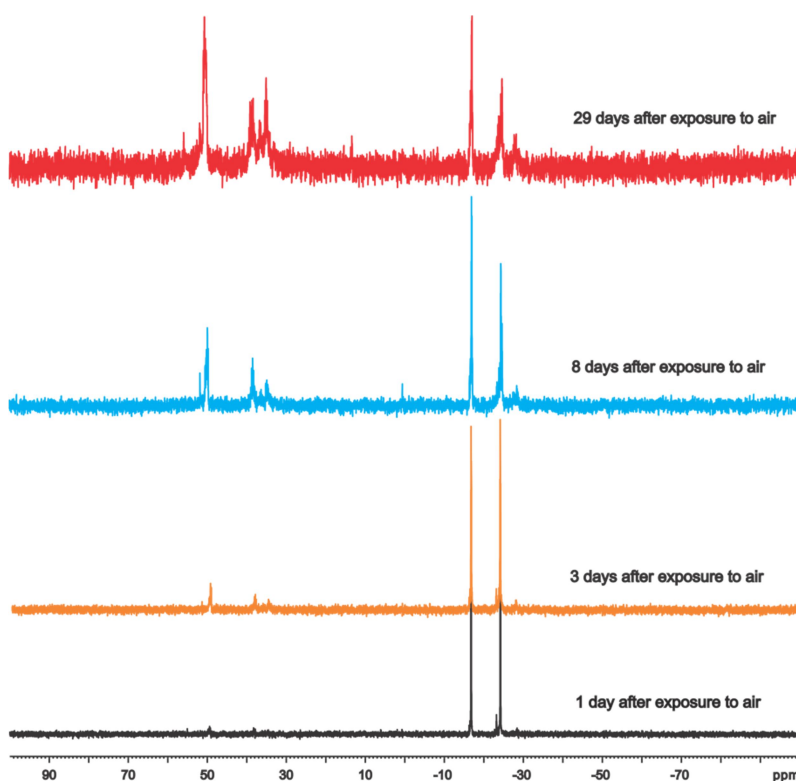


Figure 3.2.13. $^{31}\text{P}\{^1\text{H}\}$ NMR spectra of *meso*-et,ph-P4 in acetone- d_6 exposed to air.

These results were completely unexpected because our group had always assumed that the et,ph-P4 ligand is oxygen sensitive due to the presence of alkylated external phosphines which can be compared to PET_3 , which easily oxidizes upon exposure to air. Completely surprised by these results we repeated this experiment

using high-pressure NMR tube pressurized to 90psi with pure O₂. The ³¹P NMR spectra collected are shown in Figure 3.2.14.

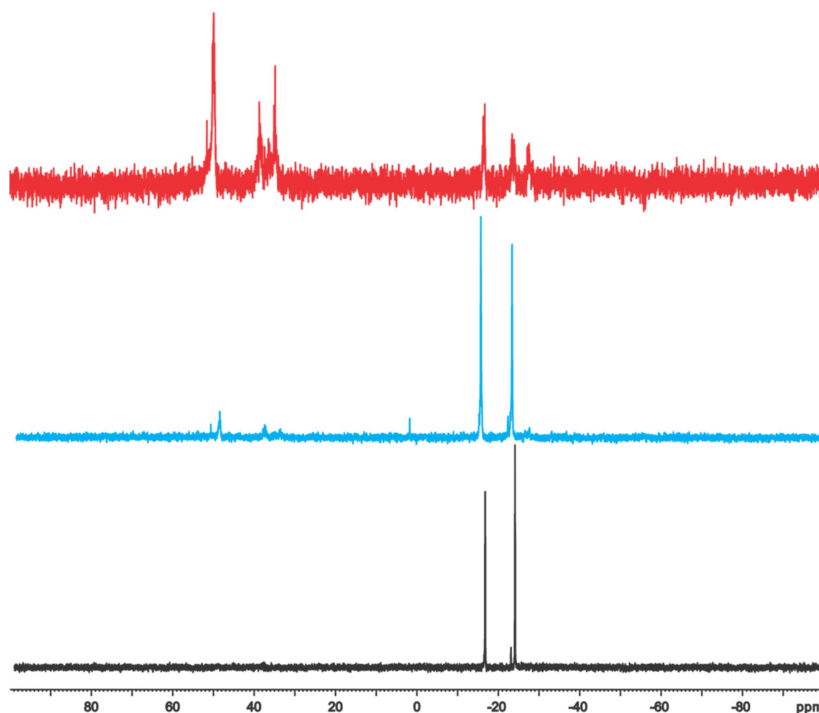


Figure 3.2.14. (Black spectrum) ³¹P{¹H} NMR spectra of *meso*-et,ph-P4 in acetone-d₆ under 90 psi O₂, recorded 1 day after pressurizing with O₂; (blue spectrum) after 14 days; (red spectrum) after 35 days.

Only after 14 days formation of a mixture of new signals in the oxidized phosphine region were observed. After 35 days signals due to the *meso*-et-ph-P4 were still present, although in low intensity. Based on the observations described above et-ph-P4 ligand is not particularly sensitive to oxygen.

New ³¹P NMR signals in Figures 3.2.14 (red line) are due to the oxidized or partially oxidized *meso*-et,ph-P4 centered at 37 and 50ppm have a similar chemical shift as the broad resonances centered at 40 and 60 ppm observed for the sample of *meso*-Ni₂Cl₄(et,ph-P4) in acetone-d₆/D₂O solution 2 days after addition of D₂O (Figure 3.2.6, blue line). Later Dr. William Schreiter demonstrated that addition of aqueous H₂O₂

to a solution of *rac,meso*-et,ph-P4 acetone-d₆/D₂O resulted in formation of new resonances centered at 40 and 60ppm. Addition of solid NiCl₂·6H₂O results in broadening of the signals. Therefore, it was concluded that the process of phosphine oxidation via a nickel species and the O₂/alkene oxidative cleavage process take place at the same time and the two are coupled together.

3.2.8 Oxidative Cleavage of Alkene in the Presence of Phosphine Ligands

The dinickel double-et,ph-P4 complex, [Ni₂(μ-Cl)(*meso*-et,ph-P4)₂][NiCl₄]₂ could only form as a result of complete dissociation of *meso*-et,ph-P4 ligand from the Ni center. Therefore, reactions of 1-hexene in the presence of free *meso*-et,ph-P4 in water/acetone solvent system were investigated. Unexpectedly reactions carried out exposed to O₂/air at 25°C produced a small amount of pentanal. However, reactions of 1-hexene in the presence of free *meso*-et,ph-P4 carried out under inert atmosphere did not produce any detectable amount of pentanal.

In addition to 1-hexene, reactions of styrene and *trans*-β-methylstyrene were also studied under the same reaction conditions exposed to air/O₂. The only product detected via GC/MS was benzaldehyde. Production of acetaldehyde as the second product from the oxidative cleavage of *trans*-β-methylstyrene was established by ¹H NMR. The ¹H NMR spectrum recorded on the sample taken from the reaction with *trans*-β-methylstyrene in acetone-d₆/ D₂O solution showed two resonances in the aldehyde region, one singlet from benzaldehyde, and one quartet for acetaldehyde (Figure 3.2.15).

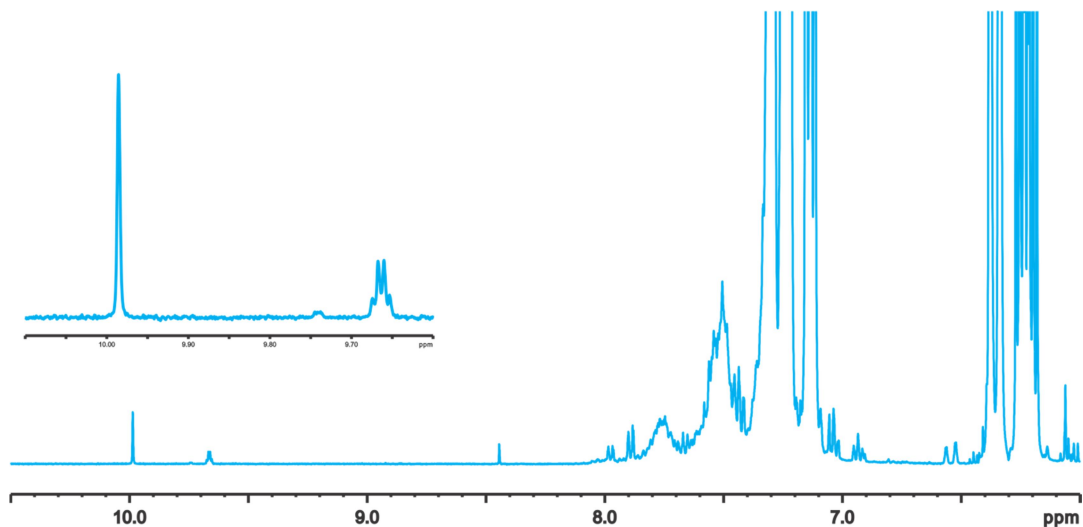


Figure 3.2.15. The 6-10.5 ppm region of the ^1H NMR spectra: sample taken from the reaction with of *trans*- β -methylstyrene, *meso*-(*et*,*ph*-P4) in acetone- $\text{d}_6/\text{D}_2\text{O}$ exposed to air after 2 hours.

Intensity of the singlet peak was considerably increased after spiking the sample with an authentic sample of benzaldehyde. Based on spiking experiment and on the broadened quartet resonance, which is expected for acetaldehyde due to the splitting from the neighboring methyl group, the two products in the O_2 reaction with *trans*- β -methylstyrene are benzaldehyde and acetaldehyde.

To further study reactions of alkenes and O_2 in the presence of *meso*-*et*,*ph*-P4, reactions of 1-hexene in the presence of *meso*-*et*,*ph*-P4 in acetone- $\text{d}_6/\text{D}_2\text{O}$ *under N₂ atmosphere* carried out at 25°C and at 45°C were analyzed via ^1H and ^{31}P NMR spectroscopy. As expected in the absence of O_2 no changes to the structure of *meso*-*et*,*ph*-P4 were observed via ^{31}P NMR. The ^{31}P NMR spectra of the samples taken from the reaction in progress after 24 hours and after 3 days looked identical to each other and showed resonances characteristic to *meso*-*et*,*ph*-P4 ligand (Figure 3.2.16, blue and orange lines).

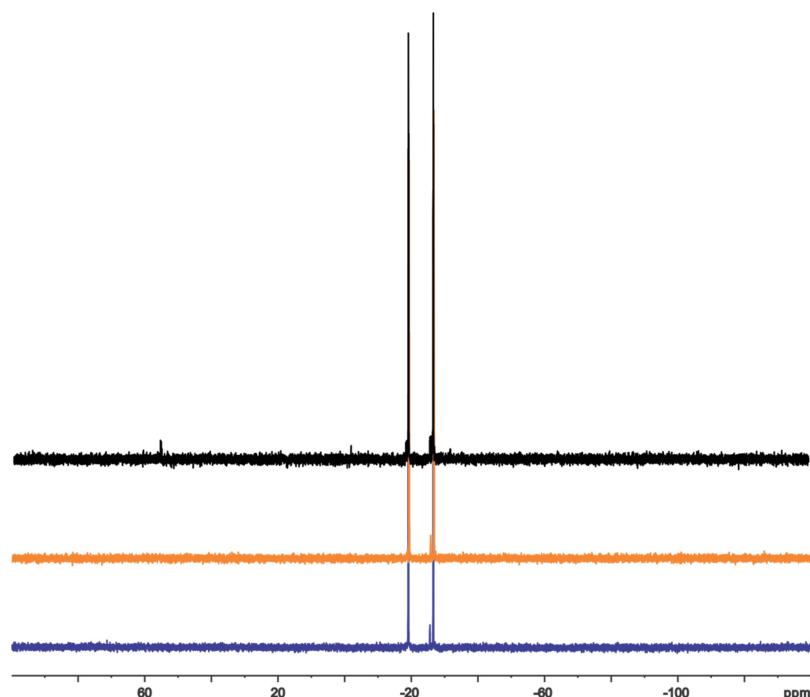


Figure 3.2.16. $^{31}\text{P}\{^1\text{H}\}$ NMR spectra of the sample from the reaction with 1-hexene, *meso*-et,ph-P4 in acetone- $\text{d}_6/\text{D}_2\text{O}$ under N_2 recorded after 24 hours (blue line), after 3 days (orange line), recorded 1.5 hours upon exposure to air (black line).

The ^1H NMR spectrum recorded on the same sample did not show any resonances in the aldehyde region (Figure 3.2.17, blue line). Reactions carried out at 45°C under N_2 also did not show any changes via ^1H NMR and ^{31}P NMR.

Next the NMR tubes containing reaction samples were open to air for a period of 5 minutes and after 1.5 hours ^1H NMR and ^{31}P NMR spectra were recorded. The ^1H NMR spectra recorded on the both samples showed a small singlet in the aldehyde region (^1H NMR spectrum recorded on the sample from the reaction at 25°C is shown in Figure 3.2.17, red line). The ^{31}P spectrum recorded on the sample that was exposed to air and kept at room temperature showed a mixture of very low intensity signals centered at 55 ppm (Figure 3.2.16, black line).

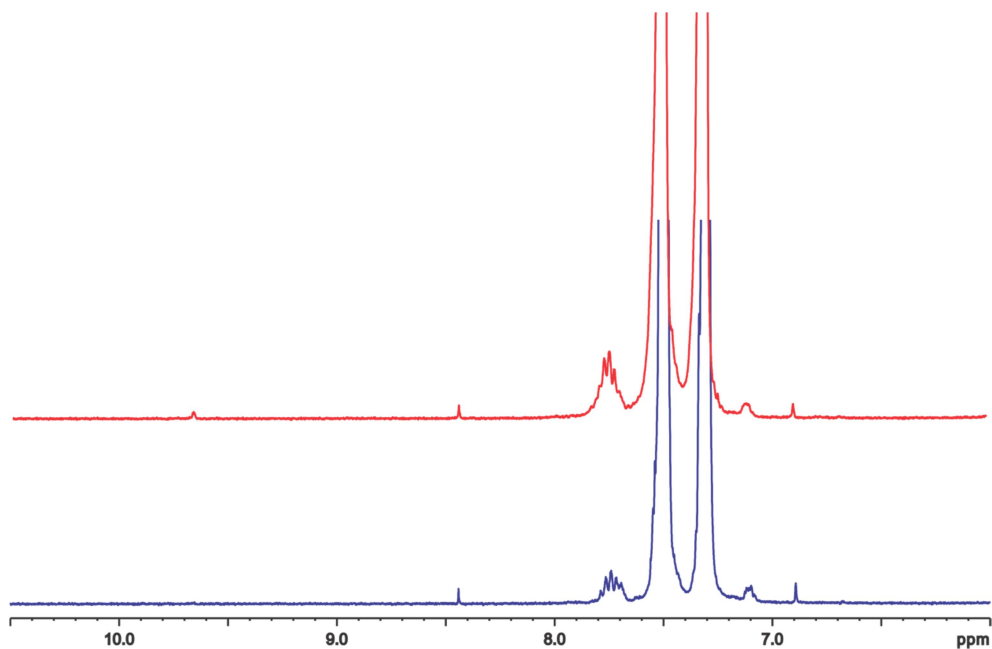


Figure 3.2.17. The 6-10.5 ppm region of the ^1H NMR spectra: (blue spectrum) sample from reaction with 1-hexene, *meso*-(et,ph-P4) in acetone- d_6 / D_2O under N_2 , 24 hours, (red spectrum) same as above recorded 1.5 hours after exposure to O_2 .

Phosphine oxides have chemical shifts of about +30 to +60 ppm and new signals observed via ^{31}P NMR at around 55 ppm after exposure of the samples to air are most likely due to a small amount of oxidized or partially oxidized *meso*-et,ph-P4. It is important to note that despite the fact that new resonances observed on ^{31}P NMR spectrum were very small in intensity formation of the aldehyde was already detected by ^1H NMR. In the ^{31}P NMR spectrum recorded on the sample that was exposed to air and kept for 1.5 hours at 45°C the signals characteristic to *meso*-et,ph-P4 were no longer present and a mixture of new signals from 36.7 to 57.33 ppm and from -31.50 to -18.41 ppm were observed (Figure 3.2.18, black line). The ^{31}P spectrum of the same sample recorded after a period of 24 hours at 45°C showed resonances only in the oxidized phosphine region (Figure 3.2.18, red line). These signals are clearly due to

more than one newly formed species such as: fully oxidized *meso*-(et,ph-P4) ligand and several different partially oxidized P4 ligand species.

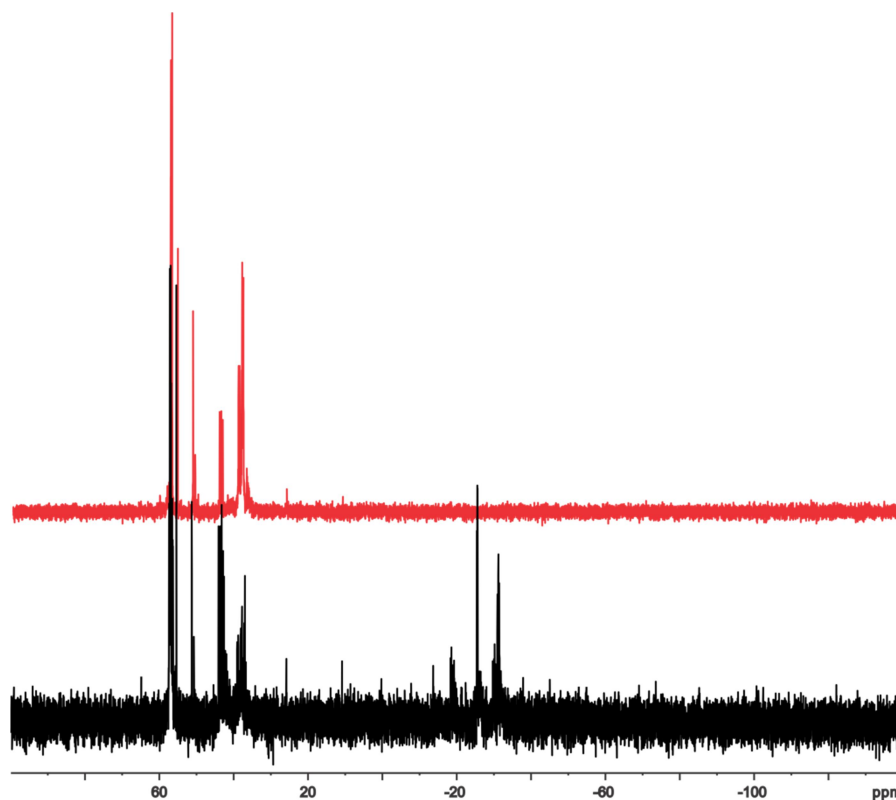


Figure 3.2.18. (Black spectrum) $^{31}\text{P}\{^1\text{H}\}$ NMR spectra of the sample from the reaction with 1-hexene, *meso*-et,ph-P4 in acetone- $\text{d}_6/\text{D}_2\text{O}$ at 45°C exposed to O_2 after 1.5 hours, (red spectrum) after 24 hours.

To quantify the amount of the aldehyde produced in reactions with alkene and *meso*-(et,ph-P4) via GC/MS we have chosen styrene as a substrate. Toluene was added as an internal standard. The concentration of benzaldehyde was calculated from a calibration curve and is equal to 1.6 mM for reactions carried out at 25°C for 24 hours (this number is an average of 3 runs). We have also observed that the amount of the aldehyde produced after the first two to three hours does not increase. For example: amount of the benzaldehyde present in a sample taken from the reaction in progress

after 2.5 hours was equal to 1.5 mM and after 24 hours amount of benzaldehyde hadn't changed.

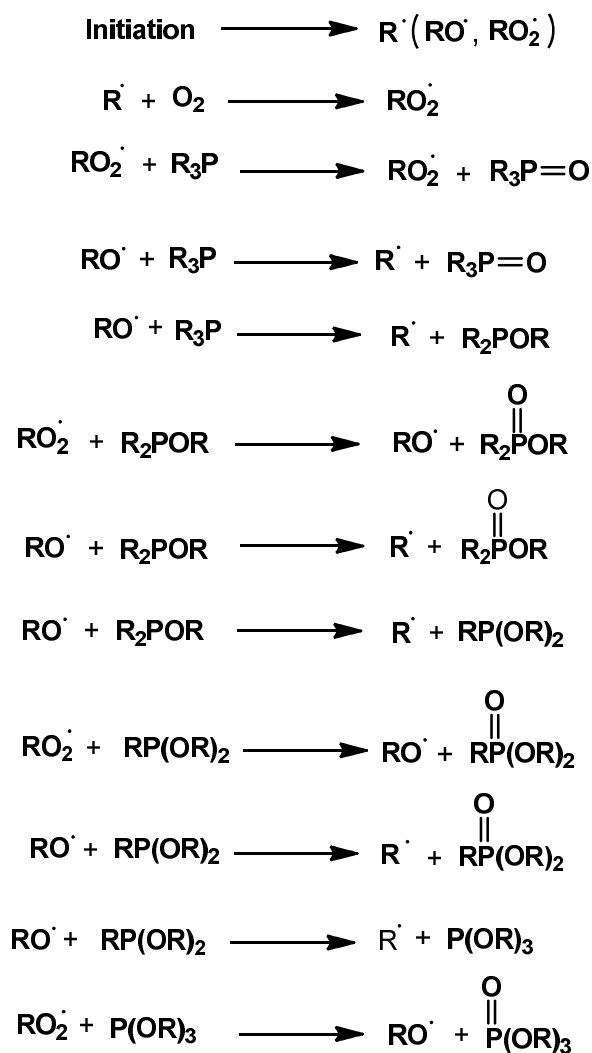
It is important to note that reactions carried out in the presence of *meso*-Ni₂Cl₄(et,ph-P4) produce slightly higher amounts of the aldehyde. For example it was determined that amount of the aldehyde in the sample taken from a reaction with styrene and *meso*-Ni₂Cl₄(et,ph-P4) after 3 hours was 2.3 mM (based only on 1 experiment). We believe that this supports coordination of the O₂ to the Ni centers, which assists in the reaction with phosphine and alkene. But phosphine clearly plays a key role in this sub-stoichiometric reaction.

Based on the results described above oxidative cleavage in our reactions occurs as a result of phosphine oxidation. Reactivity of the phosphines with oxygen is known to be in the following order benzyl > alkyl > aryl phosphines.¹⁸ Based on the NMR studies described in Section 3.2.7 *meso*-et,ph-P4 is not especially air/O₂ sensitive in the absence of H₂O. Extremely small amounts of oxidized phosphine were observed via ³¹P NMR days after being exposed to air/O₂. However in the presence of both O₂/air and water free *meso*-et,ph-P4 ligand and *meso*-Ni₂Cl₄(et,ph-P4) complex both react with O₂ much more quickly to form significant amount of phosphine oxides.

Similar to the autoxidation of alkenes, autoxidation of phosphines is a rapid free-radical chain reaction.¹⁸ Autoxidation of alkenes are characterized by a long induction periods, but this is not the case in autoxidation of phosphines.^{2a,18} Sheldon Buckler studied the autoxidation of trialkylphosphines and observed that reactions of PBu₃ and PCy₃ with air (solutions containing phosphines were blown with air) were very fast and went almost to completion in less than one hour at 26°C.¹⁸ The major products from

autoxidation of PBU_3 and PCy_3 were corresponding tertiary phosphine oxides and phosphonic acid esters. In addition, small amounts of phosphonate and phosphate esters were also detected. Buckler reported induction period of only four minutes at -20°C , no induction period at 26°C , and extremely slow reaction at -80°C . Based on the experimental data the mechanism for autoxidation of alkylphosphines was proposed (Scheme 3.2.7).¹⁸ This mechanism accounts for a variety of products detected in the reactions of trialkylphosphines with oxygen.

Scheme 3.2.7. Mechanism for autoxidation of trialkyl phosphines proposed by Buckler.¹⁸



Based on the data presented, in reactions with alkene and O₂ in the presence of free *meso*-et,ph-P4, phosphine oxidation and alkene cleavage are coupled together. Therefore, one possibility is that radicals formed during phosphine oxidation could initiate the autoxidation of alkene to produce the products of oxidative cleavage. However no other oxygen containing products were detected via GC/MS analysis in our reaction mixtures.

In addition there are some significant differences between Buckler's study and our system. Buckler, for example, studied the influence of styrene on the autoxidation of PBu₃ and reported no effect on the rate or the product distribution were observed and at the end of the reaction styrene was recovered unchanged in nearly 90% yield at the end of the reaction.¹⁸ We clearly see the formation of benzaldehyde in our system, although it could be that Buckler missed the small amount if it was produced in his reaction. The other difference is that we require at least 5% water to observe the oxidative cleavage of alkene to aldehyde. So water clearly plays an important role in our reaction chemistry. Finally, GC/MS analysis should be able to pick up the other oxygen-containing organic products expected from a simple free-radical process. Yet, we have only found aldehyde in the GC/MS analysis of the alkene oxidative cleavage reaction. Questions about our chemistry still remain.

3.3 Conclusions

Reactions of alkene in the presence of water and catalytic amounts of nickel phosphine complexes to produce the products of oxidative cleavage were investigated. Studies have shown that these reactions are not catalytic and produce only a small

amount of aldehydes. All attempts to make these reactions catalytic have failed. To gain insight into the mechanism reactions were studied via NMR spectroscopy. Based on these studies we have established that in the presence of water Ni complexes based on *et*,*ph*-P4 ligand fall apart, followed by oxidation of phosphine ligand. It was further established that reactions of alkene in the presence of free phosphine ligand also produce a small amount of aldehydes. The $^{31}\text{P}\{^1\text{H}\}$ and ^1H NMR analysis clearly demonstrated that phosphine oxidation and alkene cleavage reactions are coupled together. All of the data presented in this chapter suggests that mechanism other than simple autoxidation is responsible for oxidative cleavage in our reactions.

To the best of our knowledge oxidative cleavage of alkene substrates in the presence of small amount of phosphine ligands reported here is the first such report. Farther studies into the mechanism of this transformation could help improve production of aldehydes making this reaction of potential synthetic interest.

3.4 References

1. Schreiter, W. J. Investigations into Alkene Hydration and Oxidation Catalysis Louisiana State University, Baton Rouge, 2013.
2. (a) Frank, C. E., Hydrocarbon autoxidation. *Chem. Rev. (Washington, DC, U. S.)* **1950**, *46*, 155-69; (b) Van Sickle, D. E.; Mayo, F. R.; Arluck, R. M.; Syz, M. G., Oxidations of Acyclic Alkenes. *Journal of the American Chemical Society* **1967**, *89* (4), 967-977; (c) Farmer, E. H.; Bloomfield, G. F.; Sundralingam, A.; Sutton, D. A., The course and mechanism of autoxidation reactions in olefinic and polyolefinic substances, including rubber. *Rubber Chem. Technol.* **1942**, *15*, 756-64; (d) Bateman, L., Olefin oxidation. *Quart. Revs. (London)* **1954**, *8*, 147-67.
3. M. B. Smith, J. M., *March's Advanced Organic Chemistry*. 5 ed.; Wiley, New York: 2001.
4. Pappo, R.; Allen, J. D. S.; Lemieux, R. U.; Johnson, W. S., Notes-Osmium Tetroxide-Catalyzed Periodate Oxidation of Olefinic Bonds. *The Journal of Organic Chemistry* **1956**, *21* (4), 478-479.

5. Drago, R. S.; Corden, B. B.; Barnes, C. W., Novel cobalt(II)-catalyzed oxidative cleavage of a carbon-carbon double bond. *Journal of the American Chemical Society* **1986**, *108* (9), 2453-2454.
6. Liu, S.-T.; Reddy, K. V.; Lai, R.-Y., Oxidative cleavage of alkenes catalyzed by a water/organic soluble manganese porphyrin complex. *Tetrahedron* **2007**, *63* (8), 1821-1825.
7. Wang, A.; Jiang, H., Palladium-Catalyzed Direct Oxidation of Alkenes with Molecular Oxygen: General and Practical Methods for the Preparation of 1,2-Diols, Aldehydes, and Ketones. *The Journal of Organic Chemistry* **2010**, *75* (7), 2321-2326.
8. Tokunaga, M.; Shirogane, Y.; Aoyama, H.; Obora, Y.; Tsuji, Y., Copper-catalyzed oxidative cleavage of carbon-carbon double bond of enol ethers with molecular oxygen. *Journal of Organometallic Chemistry* **2005**, *690* (23), 5378-5382.
9. Kaneda, K.; Haruna, S.; Imanaka, T.; Kawamoto, K., Ruthenium-catalysed oxidative cleavage reaction of carbon-carbon double bonds using molecular oxygen. *Journal of the Chemical Society, Chemical Communications* **1990**, (21), 1467-1468.
10. Cho, Y.J.; Lee, D.C.; Lee, H.J.; Kim, K.C.; Park, Y.C., Catalytic activities of Pt(II), Pd(II) and Ni(II)-diphosphine complexes for styrene oxidation. *Bull. Korean Chem. Soc.* **1997**, (18), 334-336.
11. Weissmehl, K. A., *Industrial Organic Chemistry* 2nd rev. ed.; Weinheim-VCH, New York: 1993.
12. (a) Laneman, S. A.; Fronczek, F. R.; Stanley, G. G., Synthesis of binucleating tetratertiary phosphine ligand system and the structural characterization of both meso and racemic diastereomers of {bis[(diethylphosphinoethyl)phenylphosphino]methane}tetrachlorodinickel. *Inorganic Chemistry* **1989**, *28* (10), 1872-1878; (b) Aubry, D. A.; Laneman, S. A.; Fronczek, F. R.; Stanley, G. G., Separating the Racemic and Meso Diastereomers of a Binucleating Tetrachlorophosphine Ligand System through the Use of Nickel Chloride. *Inorganic Chemistry* **2001**, *40* (19), 5036-5041.
13. (a) Booth, G.; Chatt, J., Some complexes of ditertiary phosphines with nickel(II) and nickel(III). *J. Chem. Soc.* **1965**, 3238-41; (b) Venanzi, L. M., Tetrahedral nickel(II) complexes and the factors determining their formation. I. Bistriphenylphosphine nickel(II) compounds. *J. Chem. Soc.* **1958**, 719-24.
14. Hahn, C., Enhancing Electrophilic Alkene Activation by Increasing the Positive Net Charge in Transition-Metal Complexes and Application in Homogeneous Catalysis. *Chemistry A European Journal* **2004**, *10* (23), 5888-5899.
15. (a) Albert Cotton, F.; Daniels, L. M.; Jordan IV, G. T.; Murillo, C. A., The exceptional structural versatility of 2,2'-dipyridylamine (Hdpa) and its ions [dpa]⁻ and [H₂dpa]⁺. *Polyhedron* **1998**, *17* (4), 589-597; (b) Zhang, X.; Furutachi, H.; Fujinami, S.;

- Nagatomo, S.; Maeda, Y.; Watanabe, Y.; Kitagawa, T.; Suzuki, M., Structural and Spectroscopic Characterization of (μ -Hydroxo or μ -Oxo)(μ -peroxo)diiron(III) Complexes: Models for Peroxo Intermediates of Non-Heme Diiron Proteins. *Journal of the American Chemical Society* **2004**, 127 (3), 826-827; (c) Baranovskii, I. B. Z., A. N.; Dikareva, L.M.; Rotov, A. V., Reaction of rhodium(II) pyridine sulfate complexes with molecular oxygen. *Neorganicheskoi Khimii* **1986**, 31, 10.
16. Nair, P.; Anderson, G. K.; Rath, N. P., Palladium and Platinum Complexes Containing the Linear Tetrphosphine Bis[[(diphenylphosphino)ethyl]phenylphosphino]methane. *Organometallics* **2003**, 22 (7), 1494-1502.
17. Crabtree, R. H., *The organometallic chemistry of the transition metals*. 4th ed.; John Wiley: Hoboken, N.J., 2005; p xiii, 546 p.
18. Buckler, S. A., Autoxidation of Trialkylphosphines. *Journal of the American Chemical Society* **1962**, 84 (16), 3093-3097.

Chapter 4: New Tetraphosphine Ligand Synthesis, Separation, Transition Metal Coordination, and Characterization

4.1 Introduction

Research in Stanley group into bimetallic cooperativity in homogeneous catalysis has been focused on the binucleating tetraphosphine ligand, *rac*- and *meso*-et,ph-P4, shown in Figure 4.1.1

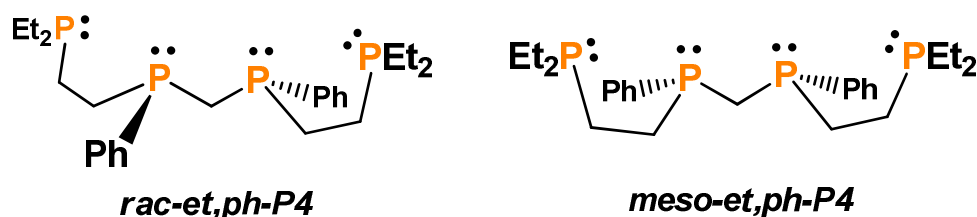


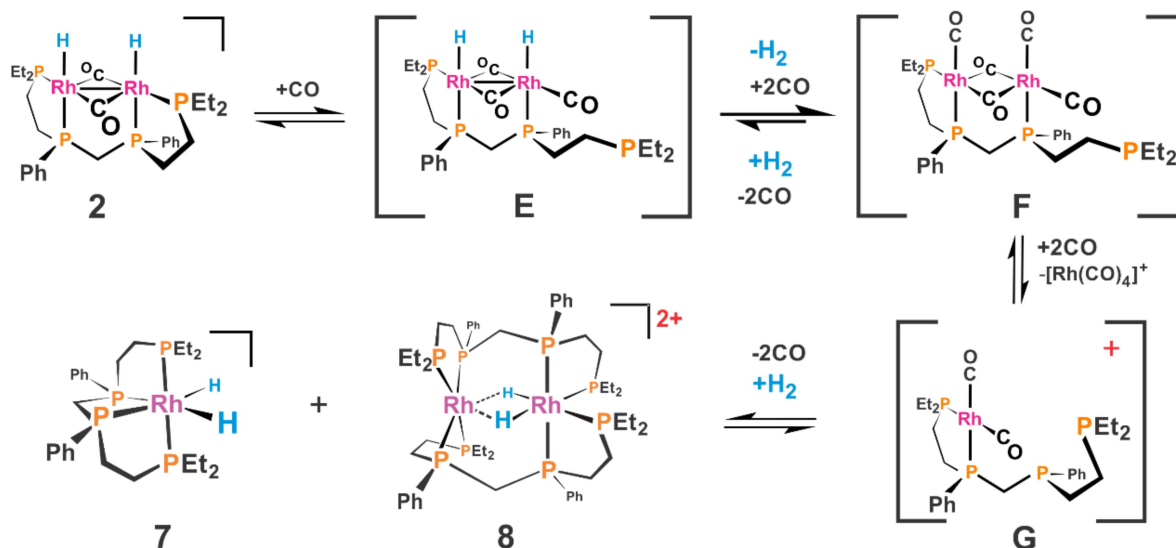
Figure 4.1.1 Binucleating tetraphosphine ligands *rac*- and *meso*-et,ph-P4.

These ligands are capable of both bridging and chelating to allow for bimetallic cooperativity while maintaining a *cis* orientation of the non-bridging ligands coordinated to the metal centers.¹ The dicationic dirhodium complex based on the *rac*-et,ph-P4 ligand has been shown to be far more active and regioselective for hydroformylation catalysts compared to monometallic analogues and is one of the best examples of bimetallic cooperativity in homogeneous catalysis.²

The et,ph-P4 ligand was designed to coordinate strongly to two metal centers with mainly alkylated strong donor phosphines and the chelate effect. However *in situ* high-pressure NMR studies with the proposed dicationic bimetallic Rh-tetraphosphine catalyst, $[\text{Rh}_2\text{H}_2(\mu\text{-CO})_2(\text{CO})_{2-x}(\text{rac-et,ph-P4})]^{2+}$ ($x = 0\text{-}2$), in acetone- d_6 revealed that et,ph-P4 ligand does not coordinate strongly enough to the cationic Rh centers.^{2c, 3}

Based on the *in situ* NMR spectroscopic studies a mechanism of catalyst decomposition has been proposed (Scheme 4.1.1).

Scheme 4.1.1 Proposed fragmentation pathway for the dirhodium catalyst based on NMR studies.³



The flexible ethylene linkage between internal and external phosphines allows for phosphine arm dissociation from one of the Rh centers in complex **2**. Coordination of CO produces complex **E**. Complex **E** is more electron deficient because the σ -donating PR₃ group has been replaced with a π -back bonding CO ligand that favors reductive elimination of hydrogen to form **F**. Complex **F** can lose a rhodium center to form **G**, which can react with another molecule of **G** and with H₂ to form species **8** or the tetraphosphine ligand can wrap around single Rh center following reaction with H₂ to form monometallic complex **7**. The chloride analog of **7** has been crystallographically characterized.⁴ Double P4-ligand dirhodium complexes have also been crystallographically characterized, but not proposed complex **8**.⁴⁻⁵ Based on the *in situ* NMR studies complex **8** is favored under high concentration of catalyst (30mM), while **7**

is favored at lower concentrations (1mM).^{3b} Neither 7 or 8 are hydroformylation catalysts. Formation of 7 and 8 indicates that the et,ph-P4 ligand dissociates too easily even though it was designed to coordinate two metals strongly.

Similar problems have been observed with dinickel complexes based on the et,ph-P4 ligand, $\text{Ni}_2\text{X}_4(\text{et,ph-P4})$ ($\text{X}=\text{Cl}, \text{Br}$), during oxidative cleavage studies. As described in Section 3.2.7 addition of water causes large changes in the structures of dinickel phosphine complexes as observed via ^1H and $^{31}\text{P}\{^1\text{H}\}$ NMR spectroscopy. Bimetallic Ni-phosphine complexes react with water immediately to form at least three new Ni-phosphine species including a small amount of partially uncoordinated phosphine as indicated by a low intensity signal at -22 ppm (see Chapter 3, Figure 3.2.6, green spectrum).

After 24 hours the main species in solution is $[\text{Ni}_2(\mu\text{-Cl})(\text{meso-et,ph-P4})_2]^{3+}$, dinickel double-et,ph-P4 species that has been crystallographically characterized (Figure 3.2.8).⁶ Formation of large amounts of $[\text{Ni}_2(\mu\text{-Cl})(\text{meso-et,ph-P4})_2]^{3+}$ clearly indicates that et,ph-P4 dissociates far too easily in solution. To address phosphine arm dissociation problem a new more rigid and stronger chelating tetraphosphine ligand, et,ph-P4-Ph has been designed (Figure 4.1.2).

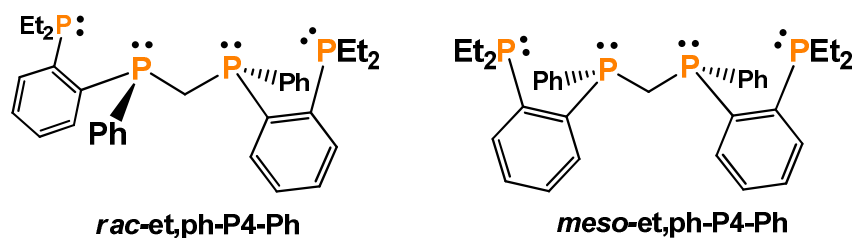


Figure 4.1.2 New stronger binucleating tetraphosphine ligands *rac*- and *meso*-et,ph-P4-Ph.

The et,ph-P4-Ph ligand has the same basic features as et,ph-P4 including a flexible methylene bridge that connects two internal phosphine atoms, but the flexible ethylene linkages between internal and external phosphines has been replaced by a more rigid and spatially defined *ortho*-substituted phenylene linkage. The rigid 1,2-disubstituted phenylene linkages should result in a much stronger chelating bisphosphine unit. Similar to et,ph-P4, the internal phosphorus atoms in et,ph-P4-Ph have three different substituents making them chiral and generating a pair of diastereomers *racemic* (*R,R* and *S,S*) and *meso* (*R,S*). Ortho-phenylenebis (dialkylphosphine) ligands have been previously studied and transition metal complexes containing this ligand type have been prepared.⁷

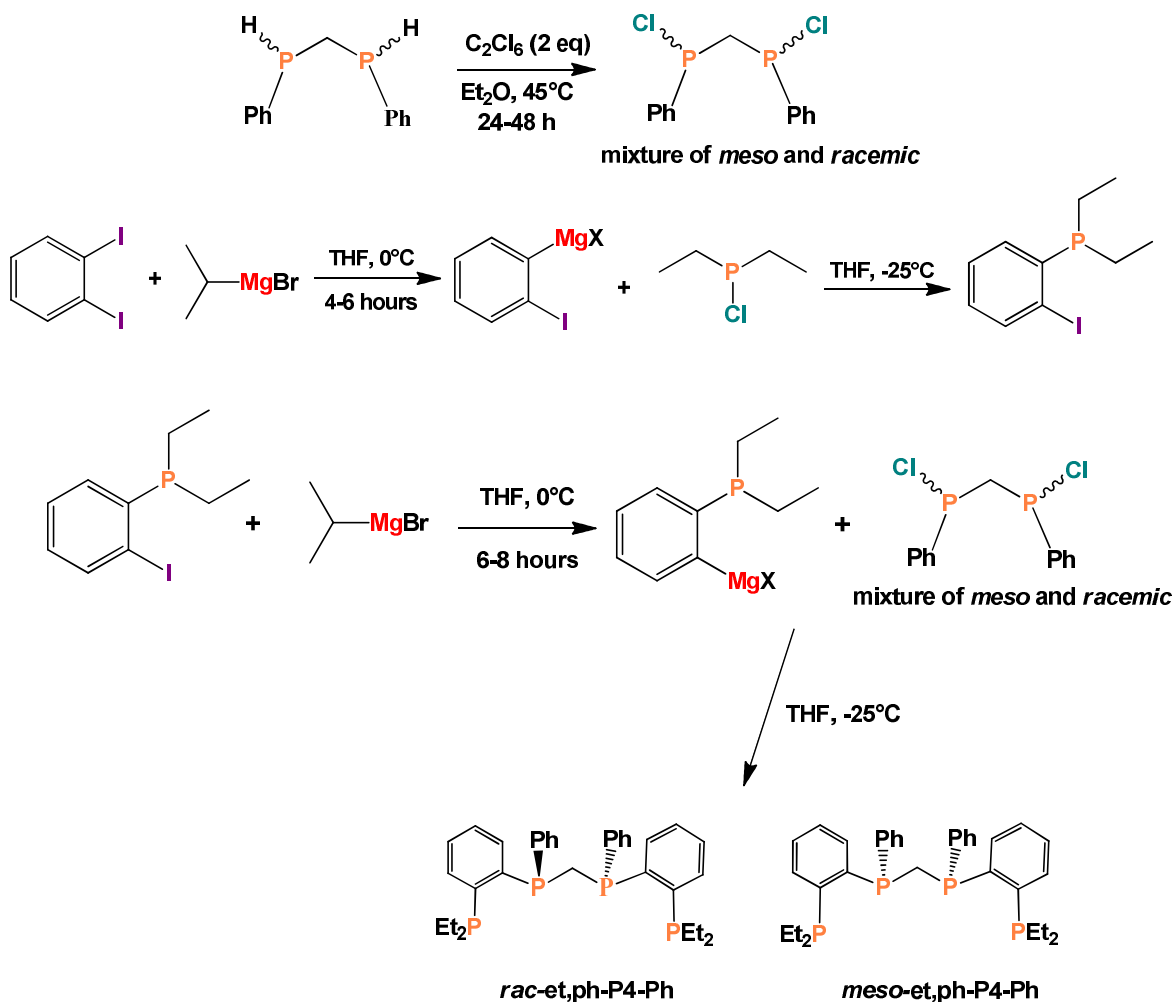
The synthesis of et,ph-P4-Ph was pioneered by Alexandre Monteil.⁸ The synthetic procedure for the et,ph-P4-Ph ligand is shown in Scheme 4.1.2 and features Mg-I exchange reactions. However, at the time of the initial synthesis no procedure for the separation of diastereomers was developed and some of the synthetic procedures required optimization.

Separation of the diastereomers is essential because for dirhodium catalyzed hydroformylation the *rac*-et,ph-P4 ligand forms the active and regioselective catalyst.^{2a} The *meso*-diastereomer is not desirable for the use in hydroformylation because it forms a far less active catalyst with poor chemoselectivity.

Following the work of Monteil, Mark Peterson has worked on improving the synthesis of this new ligand and on the separation of the *rac*- and *meso*-diastereomers.⁹ However, all attempts to separate *rac*- and *meso*-et,ph-P4-Ph had been unsuccessful.

For the separation of the *rac*- and *meso*-diastereomers of the old et,ph-P4 ligand two strategies have been developed.¹⁰ The first strategy is by partial crystallization from hexane at low temperatures. The *meso*-diastereomer crystallizes at -30°C after several hours and *racemic* ligand stays in solution. The two are easily separated by cannula or filtration. This process is repeated until the mixture is at least 90% *racemic*. The $[\text{Rh}_2(\text{nbd})_2(\text{rac-et,ph-P4})](\text{BF}_4)_2$ catalyst precursor crystallizes from acetone allowing us to obtain pure *rac*-catalyst even though we only start with 90% *rac-et,ph-P4* ligand.

Scheme 4.1.2. Synthetic scheme for the et,ph-P4-Ph ligand.



The second strategy with the old et,ph-P-4 ligand involves the high-yield synthesis of dinickel tetrachloride complexes, *rac*- and *meso*-Ni₂Cl₄(et,ph-P4), which can be conveniently separated due to the different solubility of the *rac*- and *meso*-diastereomers in ethanol. The *meso*-Ni₂Cl₄(et,ph-P4) forms a precipitate while *rac*-Ni₂Cl₄(et,ph-P4) stays in solution and can be easily separated by a simple filtration. Addition of a large excess of NaCN displaces the pure *meso*- and *rac*- et,ph-P4 ligands from the metal centers and results in formation of the water-soluble [Ni(CN)₄]²⁻ complex. Although good yields and high purities of diastereomers have been previously reported, we have found that this procedure is difficult to reproduce and the use of excess cyanide is not environmentally friendly.

The et,ph-P4-Ph ligand, unfortunately, is a gunky paste and has been proven impossible to separate via partial crystallization. After numerous attempts to crystallize the new P4 ligand using a variety of organic solvents (EtOH, CH₂Cl₂, THF, toluene, acetone, hexane) failed, the next strategy was to synthesize derivatives of this ligand by functionalizing the terminal phenyl rings with *t*-butyl or NMe₂ groups to allow for easier separation of the *rac*- and *meso*-diastereomers (Figure 4.1.3). These synthetic modification efforts have also failed.

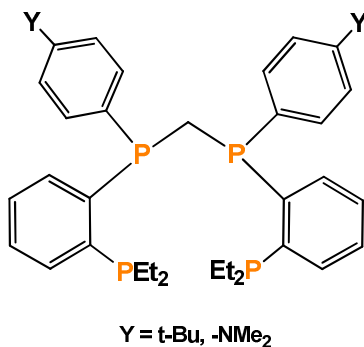


Figure 4.1.3. New P4-Ph ligand type with para substituted internal phenyl rings.

Recently William Schreiter developed a modified version of the nickel chloride separation, however this method does not work well with et,ph-P4-Ph ligand because it coordinates much more strongly to the nickel centers than et,ph-P4.⁶ The cyanolysis procedure requires even larger excesses of NaCN (over 250 equivalents) to liberate the Ni centers, but with limited yield. Thus it is unsuitable for obtaining large amounts of pure *rac*- and *meso*-et,ph-P4-Ph ligands.

In the next section optimization of the new et,ph-P4-Ph ligand synthesis as well as procedure developed for the successful separation of this ligand will be described. Synthesis and characterization of homo and hetero bimetallic complexes based on this ligand will also be presented in the following chapter.

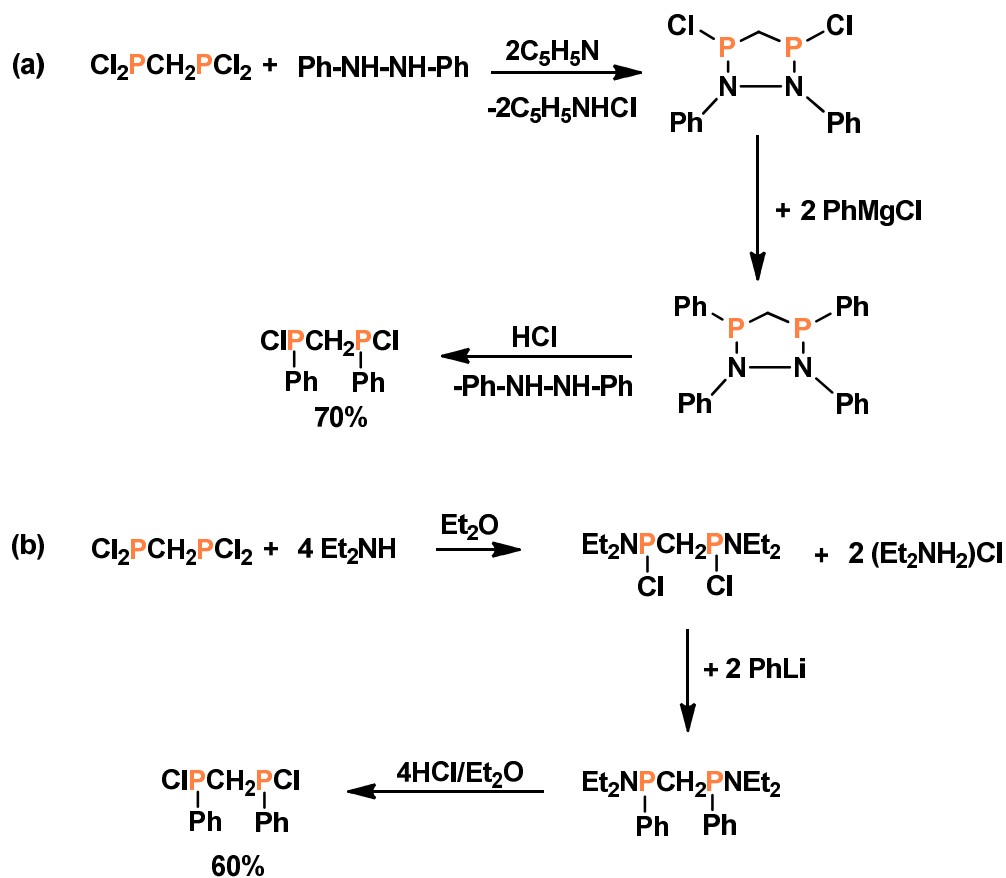
4.2. Results and Discussion

4.2.1 Preparation of Cl(Ph)PCH₂P(Ph)Cl, 2

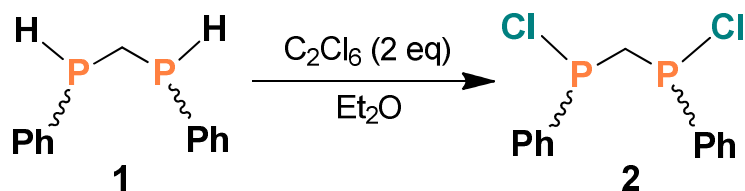
Two methods have been developed for the preparation of 2 and both use commercially available Cl₂PCH₂PCl₂, as a starting reagent as shown in Scheme 4.2.1.¹¹ Although good yields were reported, these are multistep procedures and require the preparation of too many intermediates.

In 1987 N. Weferling reported on chlorination of primary and secondary phosphines into the corresponding chlorophosphines in good to excellent yields by using C₂Cl₆ and PCl₅ as chlorinating agents (Table 4.2.1).¹² Alexandre Monteil successfully utilized C₂Cl₆ to convert of Ph(H)PCH₂P(H)Ph, 1, into the corresponding chlorophosphine, 2 (Scheme 4.2.2).⁸ Therefore, we first attempted the straight-forward synthesis of 2 via chlorination of 1 with C₂Cl₆ according to the procedure reported by Monteil. Results of the studies are presented in Table 4.2.2.

Scheme 4.2.1 Synthetic scheme for preparation of Cl(Ph)PCH₂P(Ph)Cl, as reported (a) by Stelzer *et al.*, and (b) by Schmidbaur and Schnatterer.¹¹

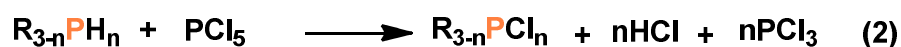
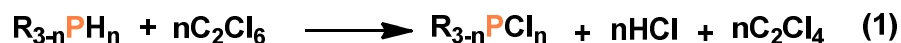


Scheme 4.2.2 Synthesis of Cl(Ph)PCH₂P(Ph)Cl, **2**.⁸



To synthesize **2** as described by Monteil, C₂Cl₆ solid was added at once to a solution of **1** in diethyl ether and the resulting mixture was heated with stirring at 35-39°C for 24 h (Table 4.2.2, entry 1). At the end of that period reaction mixture turned light pink in color and significant amount of a white solid was observed.

Table 4.2.1 Chlorination of primary and secondary phosphines with C₂Cl₆ and PCl₅ as reported by Weferling.¹²



n = 1,2

Phosphine	Chlorinating agent	Solvent/Temperature/Duration	Chlorophosphine % yield
C ₆ H ₁₁ PH ₂	C ₂ Cl ₆	Toluene/125°C/2 hours	96%
C ₆ H ₁₁ PH ₂	PCl ₅	Toluene/25-70°C/2 hours	95%
(<i>t</i> -Bu)PH ₂	C ₂ Cl ₆	Toluene/60-120°C/6 hours	48%
(<i>sec</i> -Bu)PH ₂	PCl ₅	Toluene/25-70°C/4 hours	94%
(<i>n</i> -Bu) ₂ PH	PCl ₅	Toluene/30°C/1 hour	71%
(C ₆ H ₁₁) ₂ PH	C ₂ Cl ₆	Toluene/90°C/2 hours	96%
PhPH ₂	C ₂ Cl ₆	Toluene/150°C/5 hours	74%
PhPH ₂	PCl ₅	Toluene/25-70°C/4 hours	94%

We first attempted to remove the solid byproduct from the final reaction mixture by filtration through the plug of Celite as previously described.⁸ However, after partial concentration of the filtrate *in vacuo* more solid crushed out of the solution. After a few additional filtrations we were still unable to completely remove the white solid byproduct from the desired 2. Additionally, repeated filtrations resulted in the loss of significant amounts of the desired product. The ³¹P{¹H} NMR spectrum of the final product mixture (Figure 4.2.1) showed a single resonance at 83.2 ppm (s) corresponding to 2 (lit. 81.8 ppm (s) and 81.6 ppm (s) in CDCl₃)^{11a} despite the presence of a 1:1 mixture of diastereomers (explained below) and a mixture of low intensity signals representing

approximately 10% of the phosphorus nuclei as determined by integration of the signals. The $^{31}\text{P}\{^1\text{H}\}$ NMR spectrum of the white solid byproduct did not show any signals corresponding to phosphorus nuclei. ^{13}C NMR spectroscopy established that the white solid is unreacted C_2Cl_6 .

The presence of significant amounts of unreacted C_2Cl_6 at the end of this reaction is not understood, because exactly two equivalents of C_2Cl_6 were used to convert two P-H groups into two P-Cl groups as required by the stoichiometry of reaction (eq 1).

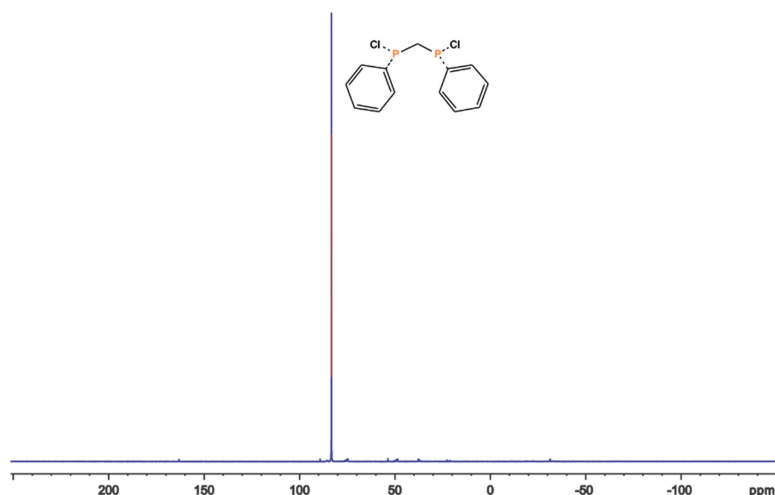


Figure 4.2.1 $^{31}\text{P}\{^1\text{H}\}$ spectrum in CDCl_3 of the final product mixture from the reaction of 2 and C_2Cl_6 in Et_2O .

Next, instead of combining the reactants at once prior to applying heat we attempted dropwise addition of 1 in Et_2O to concentrated solution of C_2Cl_6 in Et_2O heated at 35°C (Table 4.2.2, entry 2). Unreacted starting material, C_2Cl_6 , was also present at the end of this reaction. Reversing the order in which reactants were mixed also did not change the outcome of the reaction (Table 4.2.22, entry 3). Using only 1.5 equivalents of C_2Cl_6 per 1 equivalent of 1 (Table 4.2.22, entry 4) resulted in complete

consumption of **1** and formation of the desired chlorinated product in only 65% purity as estimated from $^{31}\text{P}\{^1\text{H}\}$ NMR spectrum of a final product mixture by integration of the signals (Figure 4.2.2). The major problem with the work up following reaction of **1** and C_2Cl_6 in diethyl ether is that the desired chlorinated product cannot be isolated by simple vacuum distillation because it is thermally unstable and decomposes at temperatures of above 100°C to produce PhPCl_2 and polymer residue.^{11a} Filtering through Celite does not remove the unreacted C_2Cl_6 , which is soluble to some degree in ether.

Table 4.2.2 Results from the chlorination of **2** with C_2Cl_6 and PCl_5 .

Entry	Chlorinating agent	Reaction conditions	Results
1	2 equiv C_2Cl_6	$\text{Et}_2\text{O}/35\text{-}39^\circ\text{C}/24$ hours ^a	Unreacted C_2Cl_6 , 2 not isolated
2	2 equiv C_2Cl_6	$\text{Et}_2\text{O}/35^\circ\text{C}/24$ hours ^b	Unreacted C_2Cl_6 , 2 not isolated
3	2 equiv C_2Cl_6	$\text{Et}_2\text{O}/35^\circ\text{C}/24$ hours ^c	Unreacted C_2Cl_6 , 2 not isolated
4	1.5 equiv C_2Cl_6	$\text{Et}_2\text{O}/35^\circ\text{C}/24$ hours ^d	2 not isolated 65% purity
5	2 equiv PCl_5	toluene/ $75\text{-}81^\circ\text{C}/$ 3 hours	2 not isolated 80% purity
6	2 equiv C_2Cl_6	toluene/ $70\text{-}74^\circ\text{C}/$ 3 hours	87 % yield 100% purity

^aAll reagents were mixed at once prior to applying heat. ^bSolution of **1** in Et_2O (1M) was added dropwise to a solution of C_2Cl_6 in Et_2O (1M). ^cSolution of C_2Cl_6 in Et_2O (1M) was added dropwise to a solution of **1** in Et_2O (1M). ^d1.5 equivalents of C_2Cl_6 was used per 1 equivalent of **1**. ^eSolution of **1** in toluene (1M) was added dropwise to a stirred solution of PCl_5 in toluene (0.5M) heated at 75°C . ^fSolution of **1** in toluene (10M) was added dropwise to a solution of C_2Cl_6 in toluene (2M).

Heating the final reaction mixture above 100°C (up to 115°C) for 10 min under reduced pressure resulted in sublimation of C₂Cl₆ followed by immediate crystallization to form a ring at the neck of the Schlenk flask. Pure product 2 can then be easily transferred via pipet under inert atmosphere. Sublimation of unreacted C₂Cl₆ from the final reaction mixture results in 83-87% yield of 2 with a 100% purity based on the ³¹P{¹H} NMR spectroscopy.

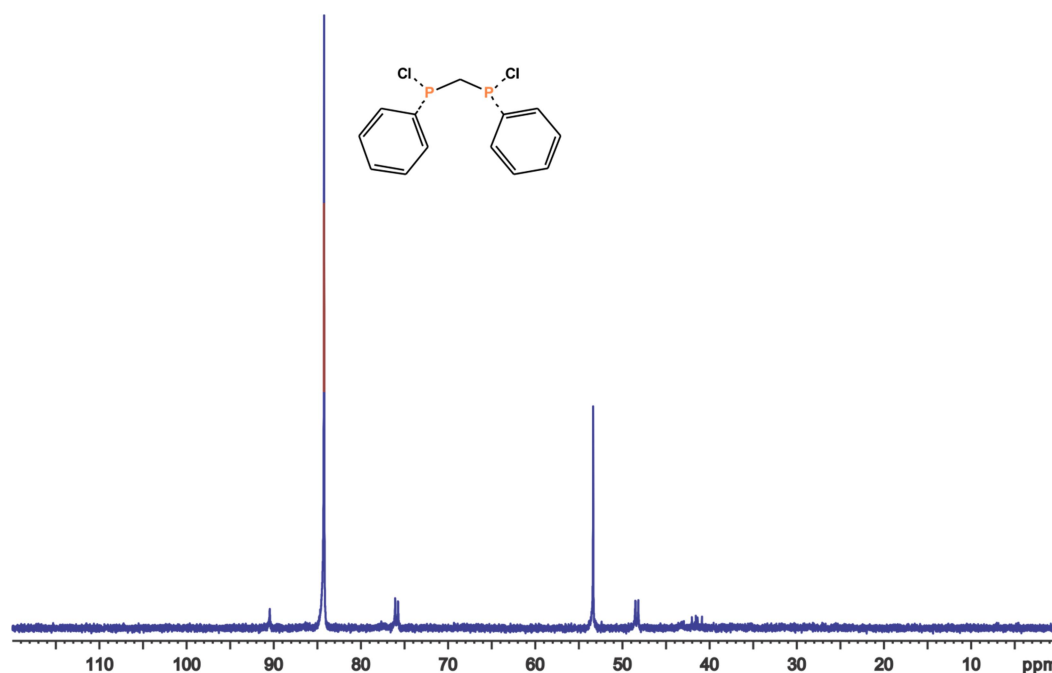


Figure 4.2.2. ³¹P{¹H} spectrum in CD₂Cl₂ of the final product mixture from the reaction with 1 eq H(Ph)PCH₂P(Ph)H and 1.5 eq of C₂Cl₆ in Et₂O.

Although very good yields of the desired chlorinated product can be obtained after sublimation work up, as was mentioned above, 2 is thermally unstable and heating at above 100°C can result in decomposition and lowering of the overall yield. Although we did not observe any decomposition after 15 min at temperatures of up to 115°C, heating for a longer period of time or at higher temperatures will result in the decomposition of 2.

Because good yields for conversion of simple primary and secondary phosphines to phosphine chlorides using PCl_5 was reported by Weferling, we have also attempted chlorination of **1** using PCl_5 .¹² Dropwise addition of concentrated (1 M) solution of **1** in toluene to a stirred solution of PCl_5 (0.5 M) in toluene resulted in exothermic reaction. The immediate formation of an orange powder was observed. Reaction was allowed to proceed with stirring at 74-81°C for two hours. At the end of this period $^{31}\text{P}\{^1\text{H}\}$ NMR spectrum of the crude reaction mixture showed four signals: 220 ppm (PCl_3), 162 ppm (PhPCl_2), 86.9 ppm (**2**), and 54.2 ppm (unidentified species). No signals corresponding to the starting materials were observed. Heating at 75°C for an additional 2 hours did not change the composition of the crude reaction mixture. To remove the orange solid byproduct the final mixture was filtered through Celite and the filtrate was concentrated *in vacuo* to yield colorless viscous oil. The ^{31}P NMR spectrum of the final product showed two signals at 89.1 ppm (s) due to the presence of desired **2** and at 51.9 ppm (s) due to unidentified phosphorus containing species with relative intensities of approximately 4:1. We were unable to separate **2** from the unwanted byproduct.

Because chlorination of **1** with C_2Cl_6 appeared far cleaner than chlorination of **1** with PCl_5 we decided to reexamine this reaction using other organic solvents. Monteil reported that reaction with **1** and C_2Cl_6 in toluene (heating at 140°C for 18 hours) resulted in decomposition of **2**.⁸ Because **2** is unstable at temperatures of above 100°C we reexamined this reaction at lower temperature. A concentrated solution of **1** (10 M) in toluene was added dropwise by cannula over 45 mins to a stirred solution of C_2Cl_6 (heated to about 75-80°C) in toluene (2 M). During addition formation of HCl gas was observed and the flask was occasionally purged with nitrogen to help remove HCl

released from the reaction. The reaction was allowed to stir for 2 hours at 75-80°C. At the end of this period the $^{31}\text{P}\{^1\text{H}\}$ NMR of the crude reaction mixture showed that 1 was completely consumed and 2 was the only product (Figure 4.2.3, bottom spectrum). After removal of the solvent *in vacuo* the desired chlorinated product was obtained in 87% isolated yield. The $^{31}\text{P}\{^1\text{H}\}$ NMR spectrum of the final product, once again, showed only one resonance at 86.9 ppm due to compound 2, which should exist as two diastereomers (Figure 4.2.3, top spectrum).

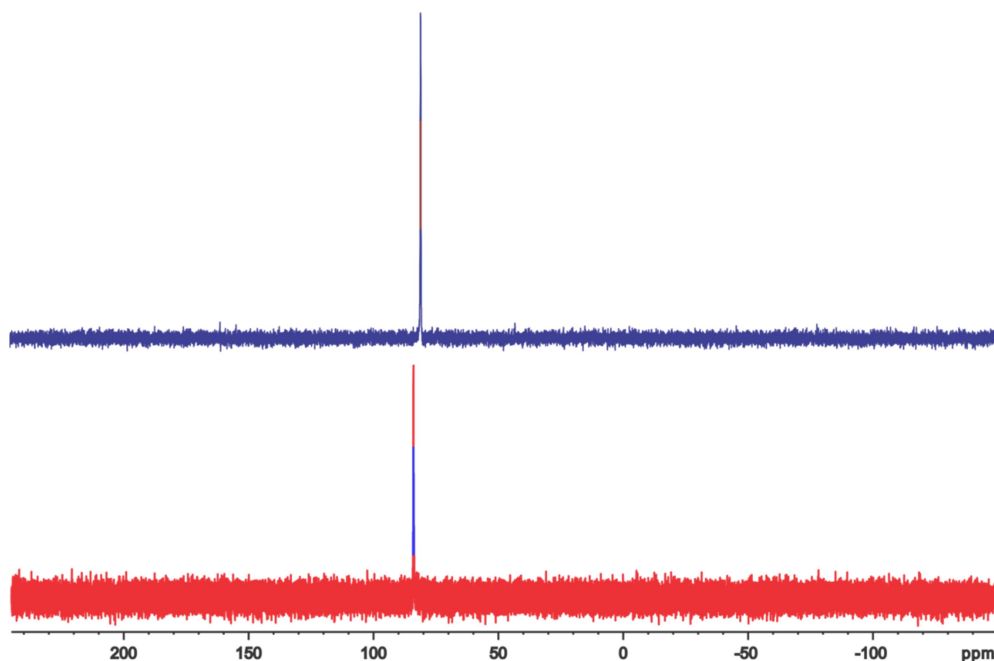


Figure 4.2.3. (Bottom spectrum) $^{31}\text{P}\{^1\text{H}\}$ NMR spectrum of the crude reaction mixture with 1 and C_2Cl_6 in toluene and (top spectrum) isolated final product in C_6D_6 .

Whether one or two resonances are observed depends on the solvent and concentration. For example, the $^{31}\text{P}\{^1\text{H}\}$ NMR spectrum of 2 in benzene- d_6 showed one singlet at 81.0 ppm, suggesting that only one of the diastereomers was formed. However, upon dilution of the NMR tube sample the $^{31}\text{P}\{^1\text{H}\}$ NMR spectrum now shows

two singlets at 81.3 ppm and 81.0 ppm due to the expected *rac*- and *meso*-diastereomers (Figure 4.2.4). In a non-aromatic solvent only one resonance is observed, e.g., the ^{31}P NMR spectrum of 2 in CD_2Cl_2 shows only one singlet at 83.2 ppm in CDCl_3 and one singlet at 84.2 ppm in CDCl_3 (see Figures 4.2.1 and 4.2.2). Based on these observations the chemical shift values of *rac*- and *meso*-2 are highly dependent on the concentration and on the solvent. The chemical shift values for *rac*- and *meso*-2 are, therefore, accidentally degenerate under high concentration conditions and in non-aromatic solvents.

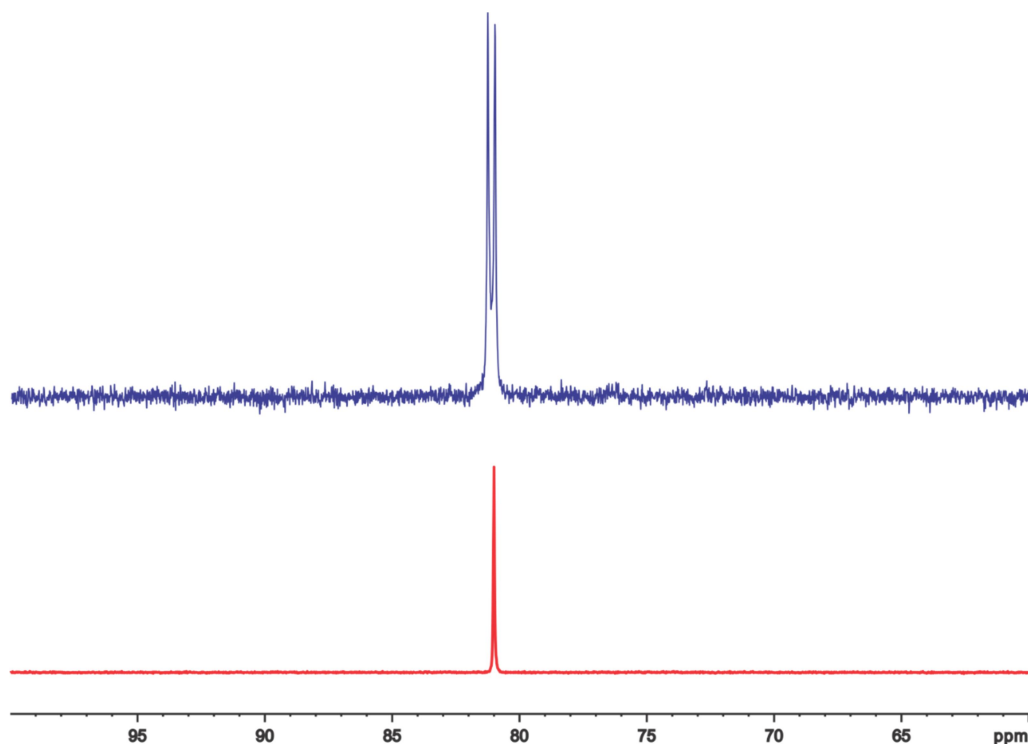


Figure 4.2.4. $^{31}\text{P}\{^1\text{H}\}$ NMR spectrum of 2 in C_6D_6 before dilution (bottom) and after dilution (top) in C_6D_6 .

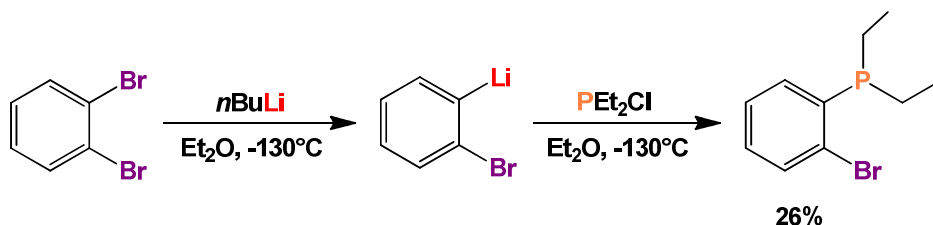
Overall improvement of this procedure was achieved by slow addition of a solution of 1 in toluene to a solution of C_2Cl_6 in toluene at $75\text{--}80^\circ\text{C}$, followed by heating

at this temperature for 2-3 hours. As a result the reaction time was optimized and the isolated yield of **2** was increased to 85-87%.

4.2.2 Preparation of 1-(diethylphosphino)-2-iodobenzene, **3(I)**

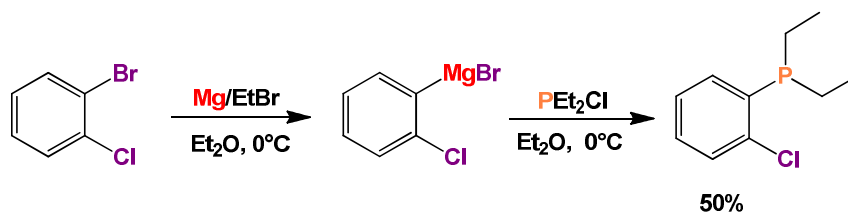
Two methods have been developed for preparation of compounds of the type $\text{o-X-C}_6\text{H}_4\text{P}(\text{Et})_2$ (X = halogen substituent) starting from o-halobenzene, however both suffer from low yields.¹³ The first method utilizes a low-temperature halogen-lithium exchange between o-dibromobenzene and *n*BuLi. Thus, reaction of o-dibromobenzene with *n*BuLi at -130°C , followed by addition of PEt_2Cl yielded 1-(Et_2P)-2-bromobenzene, **3(Br)** in 26% yield (Scheme 4.2.3).

Scheme 4.2.3. Preparation of **3(Br)** via low temperature halogen-lithium exchange.¹³



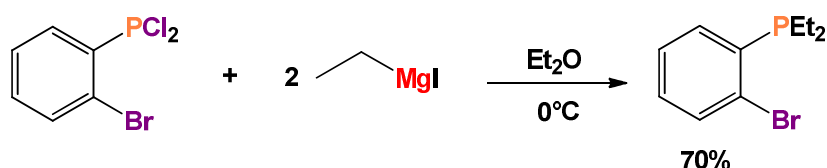
The second method involves synthesis of a Grignard reagent by reaction of o-bromo-chloro-benzene with one equivalent of magnesium in the presence of EtBr. The resulting mono-Grignard reagent upon reaction with PEt_2Cl yielded 1-(Et_2P)-2-chlorobenzene, **3(Cl)** in 50% yield (Scheme 4.2.4).

Scheme 4.2.4. Synthetic procedure for preparation of 1-(Et_2P)-2-chlorobenzene via Grignard intermediate developed by Hart.¹³

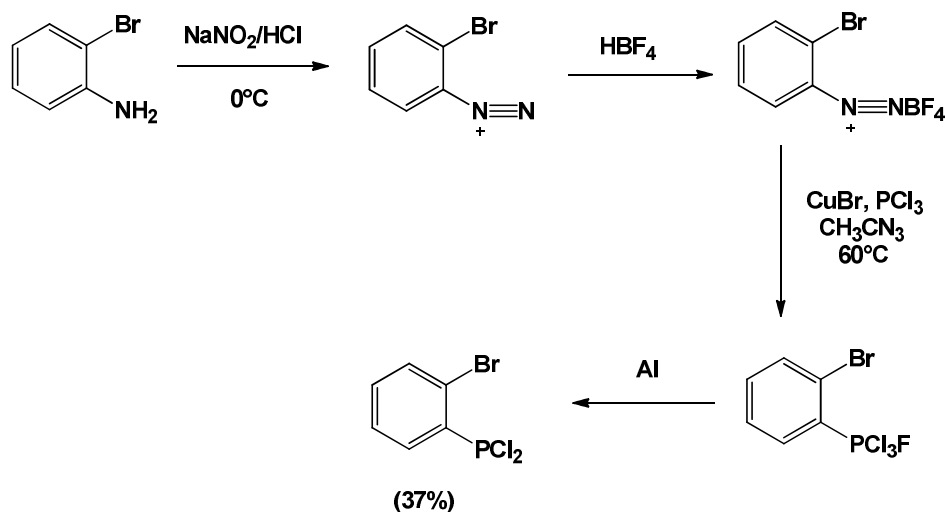


A higher yield alternative approach to synthesis of **3(Br)** by reaction of 1-(Cl₂P)-2-bromobenzene with EtMgI Grignard was developed by Bennett (Scheme 4.2.5).¹⁴ However, this approach requires the multi-step synthesis of 1-(Cl₂P)-2-bromobenzene from *o*-bromoaniline, which has been previously prepared in low (37%) yield (Scheme 4.2.6).¹⁵

Scheme 4.2.5. Synthetic procedure for preparation of 1-(Et₂P)-2-bromobenzene developed by Bennett.¹⁴



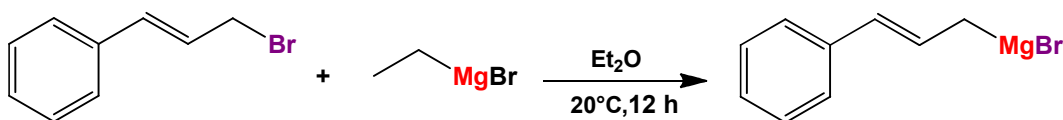
Scheme 4.2.6. Synthetic procedure for preparation of 1-(Cl₂P)-2 bromobenzene from *o*-bromoaniline.¹⁵



Monteil attempted the synthesis of **3(Br)** via preparation of an intermediate Grignard reagent by reaction of *o*-dibromobenzene with Mg metal in the presence of EtBr.⁸ He reported that the treatment of intermediate Grignard with PEt₂Cl produced the desired *o*-bromophenylphosphine in low yield (20% isolated yield using Mg powder and

10% yield using Mg turnings). Low isolated yields in these reactions were presumably due to a side reaction of Mg with EtBr to produce the corresponding alkyl Grignard. Formation of $o\text{-MgBrC}_6\text{H}_4\text{PEt}_2$ without the use of EtBr was not observed, due to low reactivity of Mg toward o -dibromobenzene. High yield (95%) synthesis of $\text{Br}(o\text{-C}_6\text{H}_4)\text{MgBr}$ through magnesium-iodine exchange reaction of 1-bromo-2-iodobenzene with $i\text{PrMgBr}$ was reported by Boymond *et al.*¹⁶ Preparation of Grignard reagents via metal-halogen exchange was first reported in 1931 by Prevost, who synthesized (cinnamyl) MgBr by reaction of cinnamyl bromide with EtMgBr . (Scheme 4.2.7).¹⁷

Scheme 4.2.7. First example of magnesium-halogen exchange.¹⁷



Recently it has been demonstrated that magnesium-halogen exchange reaction can be used to prepare a large variety of highly functionalized organomagnesium reagents if the exchange rate is fast enough at temperatures below 0°C .^{16, 18} Synthesis of aromatic organomagnesium reagents containing functional groups such as ester, amide, nitrile or a halogen substituent prepared via Mg-I exchange reactions in good yield have been reported (Scheme 4.2.8).¹⁶

Monteil successfully utilized magnesium-halogen exchange reaction to prepare Grignard reagents of the type, $\text{X}(o\text{-C}_6\text{H}_4)\text{MgBr}$ ($\text{X}=\text{I}, \text{Br}, \text{F}$), which upon reaction with an electrophile, PEt_2Cl produced corresponding o -halophenylphosphines (Table 4.2.3).⁸ The best results were obtained when desired o -disubstituted aryl halides were treated with $i\text{PrMgBr}$ at 0°C and allowed to react at this temperature for 6 hours, followed by addition of PEt_2Cl at -25°C

Scheme 4.2.8. Preparation of highly functionalized Grignard reagents by an iodine-magnesium exchange reaction.¹⁶

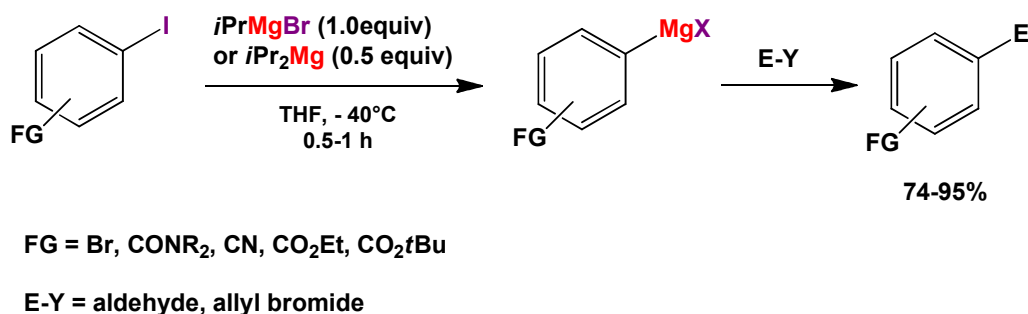
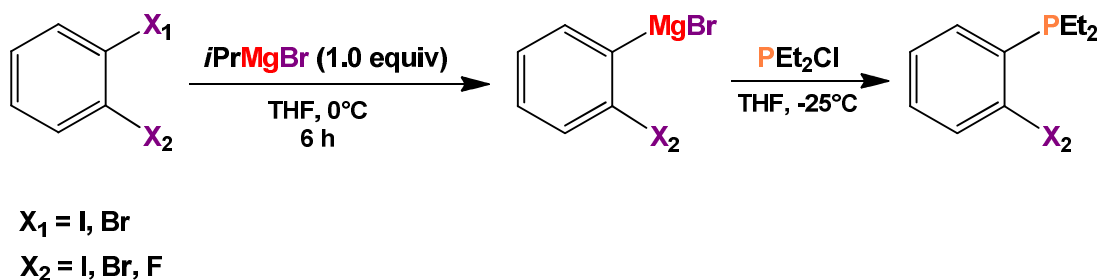


Table 4.2.3. Preparation of arylphosphines via magnesium-halide exchange reaction of aryl halides with *i*PrMgBr, followed by reaction with PEt_2Cl reported by Monteil.⁸



Substrate	Product	Yield (%)
1,2-dibromobenzene	1-(Et_2P)-2-bromobenzene	76
1,2-diiodobenzene	1-(Et_2P)-2-iodobenzene	75
1-Bromo-2-fluorobenzene	1-(Et_2P)-2-fluorobenzene	74

Initially we prepared 3(I) according to previously described procedure using magnesium-iodine exchange reaction (3(I) is the preferred reagent in the last step of the new et,ph-P4-Ph synthesis, see Section 4.2.3).

The only modification to this procedure was the time that was allowed for reaction of 1,2-diiodobenzene with *i*PrMgBr, as it was established that a time period of 6 hours is not necessary for complete conversion of 1,2-diiodobenzene to the corresponding mono

Grignard reagent. Based on GC/MS analyses of samples taken from the reaction in progress after quenching with water, complete conversion was observed after 1 hour. After work up, 3(I) was obtained by short path distillation *in vacuo* as an air- and light-sensitive colorless liquid in 77 % yield. Typical yields are 68-77%. The ^{31}P $\{^1\text{H}\}$ NMR spectrum of the final product showed a major resonance at 0.3 ppm (s) corresponding to the desired 3(I) and a mixture of additional low intensity resonances at -14.3 ppm (s), -26.2 ppm (s), -26.5 ppm (s) and -26.8 ppm (s) corresponding to less than 4% of the phosphorus nuclei as determined by integration (Figure 4.2.5). The singlet at -14.3 ppm is likely due to Et_2PPh formed by decomposition of 3(I).

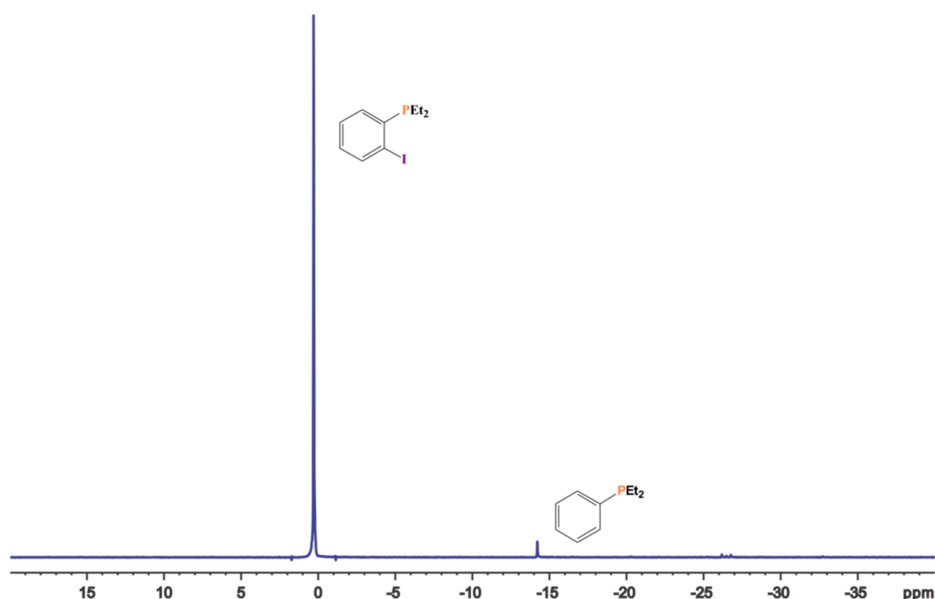


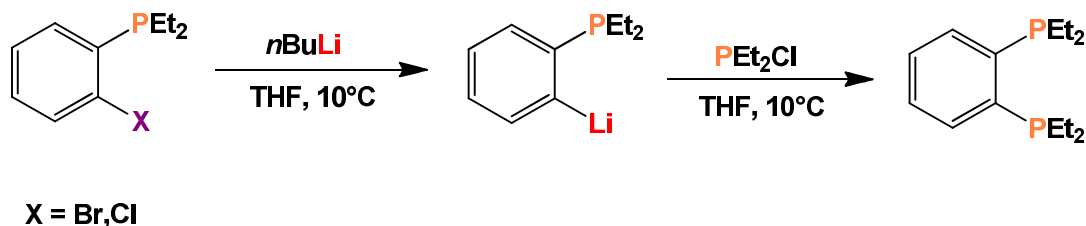
Figure 4.2.5. ^{31}P $\{^1\text{H}\}$ NMR of the final product mixture in C_6D_6 obtained after work up from the reaction of *o*-diiodobenzene with *i*PrMgBr, followed by addition of PEt_2Cl .

4.2.3 Preparation of *rac,meso-et,ph*-P4-Ph

Two strategies have been investigated for the preparation of *rac,meso-et,ph*-P4-Ph by reaction of 2 with 2 equiv of 3(X) (X = I, Br). The first strategy involves lithium-

mediated P-C coupling reaction of *o*-lithiophenylenediethylphosphine, *o*-LiC₆H₄PEt₂, with the chlorophosphine, 2.⁸ Previously acceptable 56% yield for the preparation of *o*-C₆H₄(PEt₂)₂ by reaction of *o*-BrC₆H₄PEt₂ with *n*BuLi, followed by treatment with PEt₂, was reported by Hart (Scheme 4.2.9).¹³ However, reaction of *o*-ClC₆H₄PEt₂ with *n*BuLi, followed by treatment with PEt₂ resulted in only 27% yield of the desired phosphine. Monteil reported that all his attempts at the preparation of *rac,meso*-et,ph-P₄-Ph via lithiation of 3(I) or 3(Br) followed by *in situ* reaction with 2 failed (Scheme 4.2.10).⁸

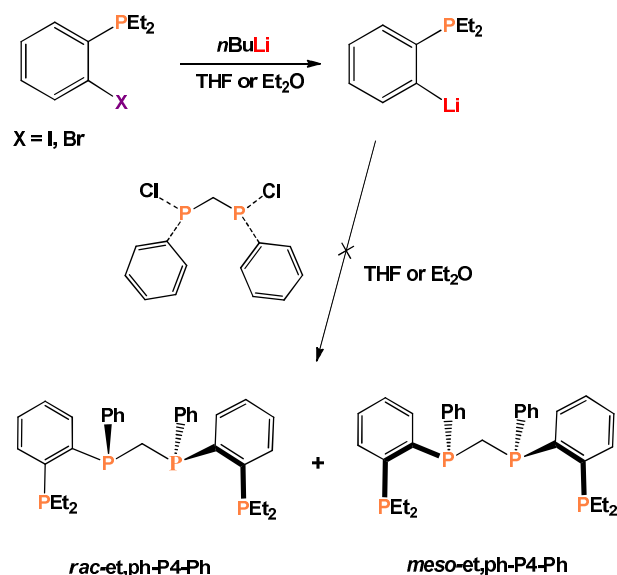
Scheme 4.2.9. Preparation of *o*-phenylenebisdiethylphosphine via lithium-halogen exchange, followed by treatment with PEt₂Cl.¹³



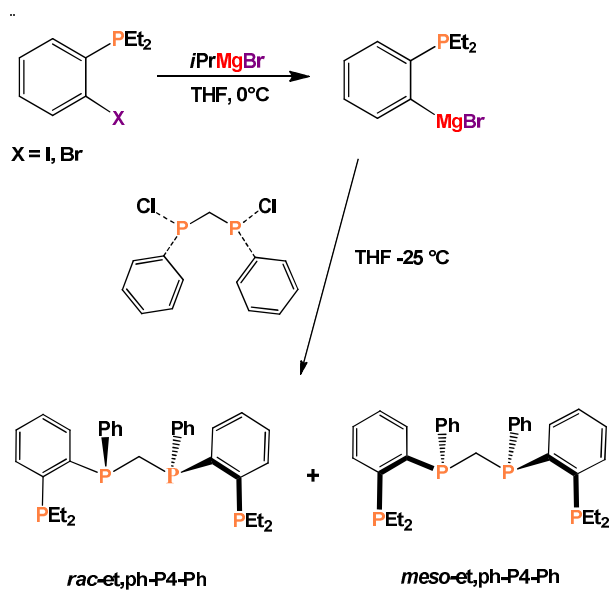
The second strategy involves Grignard mediated P-C coupling reaction (through I-Mg exchange) as shown in Scheme 4.2.11.⁸ Monteil reported that reaction of 3(Br) with *i*PrMgBr at 0°C, followed by addition of 2 did not result in formation of the desired product, instead the ³¹P {¹H} NMR showed formation of a byproduct, *rac,meso*-(*i*-Pr)(Ph)PCH₂P(Ph)(*i*-Pr), resulting from reaction of *i*PrMgBr with 2. However, under the same reaction conditions treatment of more reactive iodo analog, 3(I) with *i*PrMgBr, followed by addition of bisphosphine 2 gave the desired *rac,meso*-et,ph-P₄-Ph ligand.

Because the preparation of *rac,meso*-et,ph-P₄-Ph only worked using a Grignard-mediated P-C coupling reaction of 3(I) with chlorophosphine 2, we initially attempted to reproduce this procedure.

Scheme 4.2.10. Attempted preparation of *rac,meso-et,ph-P4-Ph* via lithium-mediated P-C coupling reaction.⁸



Scheme 4.2.11. Preparation of *rac,meso-et,ph-P4-Ph* via Grignard-mediated P-C coupling reaction.



The desired *rac,meso-et,ph-P4-Ph* ligand was synthesized by reaction of 3(I) with *i*PrMgBr at 0°C for 8 hours, followed by reaction with 2 at -25°C. The reaction was then allowed to slowly warm to 25°C and additional stirring continued for 18 hours. At

the end of this time period the reaction was quenched with water and the final products were extracted with diethyl ether and dried over Na₂SO₄. Removal of the solvents *in vacuo* gave the crude product mixture as a slightly yellow viscous paste.

The ³¹P{¹H} NMR spectrum (recorded unlocked in diethyl ether) showed a complex second order pattern at approximately –26.0 to –33.0 ppm due to the desired et,ph-P4-Ph ligand (mostly *meso* form as determined by ¹H NMR spectroscopy and explained below). The et,ph-P4-Ph resonances overlapped with signals likely due to the intermediate P3 species, along with additional signals in the negative and positive ppm regions due to unidentified phosphine impurities that include oxidized phosphines (Figure 4.2.6).

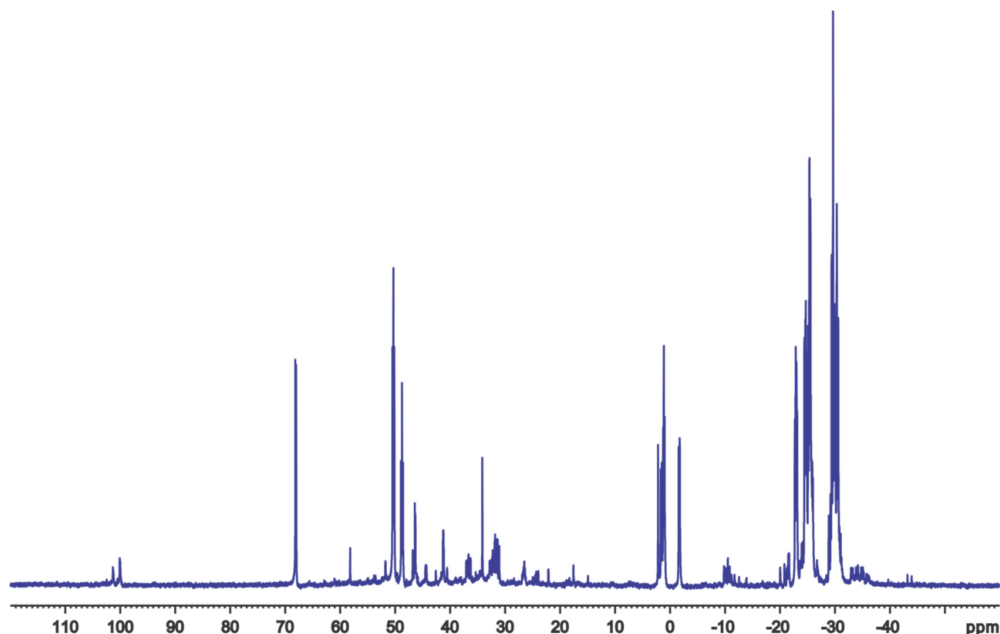


Figure 4.2.6. ³¹P {¹H} NMR spectrum of the crude product mixture obtained from reaction of 3(l) with *i*PrMgBr, followed by addition of 2.

Due to overlap of the resonances from *meso*-et,ph-P4-Ph with resonances due to phosphine impurities, the purity of the desired product cannot be determined from the ³¹P{¹H} NMR spectrum of the crude product mixture.

It is noteworthy that even though formation of a 1:1 mixture of *rac* and *meso*-diastereomers of et,ph-P4-Ph is expected from Grignard-mediated coupling of 3(I) with *rac,meso*-2, mostly *meso*-diastereomer forms with just traces of *rac*-et,ph,P-4,ph (established from ^1H NMR of the methylene bridge region). Currently we don't have any explanation for this unexpected diastereoselectivity. The *rac*-et,ph-P4-Ph can be obtained by epimerization of the final product mixture containing mostly *meso*-et,ph-P4-Ph by heating at 130°C for one to two hours.

We first attempted purification of the final product mixture by distillation *in vacuo*. However, unreacted 3(I) was the only fraction obtained in the collection flask leaving the rest of the byproducts and the desired final product in the distilling flask. It was previously reported that the crude reaction mixture can be purified by precipitation from ethanol at -30°C.⁸ We have found that this method is difficult to reproduce, all my attempts to obtain clean *rac,meso*-et,ph-P4-Ph by precipitation from a minimal amount of ethanol at low temperatures have failed. However, on some occasions a very small amount of the white precipitate was obtained upon cooling for days at -30°C, but the majority of the desired product remained in solution. Therefore in order to obtain any significant amount of the desired *rac,meso*-et,ph-P4-Ph precipitation from ethanol at low temperatures has to be repeated multiple times, but still with low yields.

After numerous attempts to purify the crude product mixture via recrystallization at low temperatures or by slow evaporation of the solvent I established that a relatively clean separation could be achieved by column chromatography on neutral alumina (4 × 12 cm) using CH₂Cl₂ as the eluent. The ^{31}P { ^1H } NMR spectrum of purified product mixture showed a complex second order pattern at -26.0 to -33.0 ppm due to the

presence of the *meso*-et,ph-P4-Ph (89%), a resonance at -0.8 ppm (s) due to a small amount of unreacted 3(I) (less than 2%), two signals at -15.4 ppm (s) and -16.6 ppm (s, 3%) with one of them possibly due to $\text{PhP}(\text{Et})_2$ formed by decomposition of 3(I) and two doublets centered at -7.2 ppm ($J_{\text{p-p}} = 10$ Hz) and -8.3 ppm ($J_{\text{p-p}} = 10$ Hz) due to unidentified phosphine impurities (less than 6 %, Figure 4.2.7).

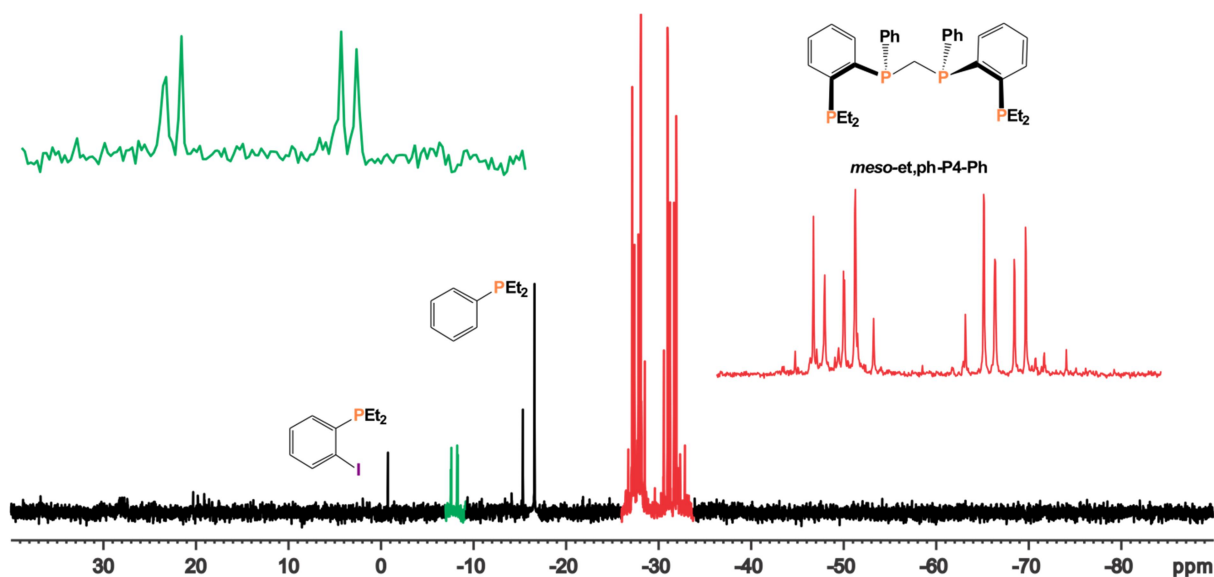


Figure 4.2.7. $^{31}\text{P} \{^1\text{H}\}$ NMR spectrum of the final product mixture in C_6D_6 purified via column chromatography on neutral alumina.

Although this column chromatography procedure removes most of the impurities including oxidized phosphines, 3(I) and some other small unidentified phosphine impurities cannot be removed via this method. The amount of unreacted 3(I) present in the crude product mixture tends to vary and, on average, is equal to 16%. As mentioned above, unreacted small arm can be easily removed by distillation under reduced pressure (bp = $130^\circ\text{C}/0.5$ Torr), however this process results in epimerization of et,ph-P4-Ph ligand.

4.2.4. Separation of *rac* and *meso*-diastereomers of et,ph-P4-Ph

After extensive experimentation it was established that the separation of *rac* and *meso* diastereomers of et,ph-P4-Ph (obtained by epimerization) can be achieved via column chromatography on neutral alumina (Grade IV) using a CH₂Cl₂/hexanes solvent system (1:4). Although the et,ph-P4-Ph ligand reacts slowly with O₂, all of the chromatography procedures described above were carried out in air using dry (as received from Sigma-Aldrich) N₂-degassed solvents.

Unreacted 3(l) and other impurities are easily recovered as the first set of fractions. The next set of fractions contains *meso*-et,ph-P4-Ph and a small amount of unidentified phosphine impurities, followed by a mixture of *meso* and *rac*-et,ph-P4-Ph. The last set of fractions contains *rac*-et,ph-P4-Ph in pure form.

The ¹H NMR spectra of separated fractions is shown in Figure. 4.2.8 and ³¹P {¹H} spectra of the four sets of fractions are shown in Figure 4.2.9. The ³¹P {¹H} NMR of each et,ph-P4-Ph diastereomer has a complex second order pattern and is not particularly useful in establishing the purity of the diastereomers. However, the purity of *meso* and *rac*- diastereomers can be easily established from their ¹H NMR spectra (Figure 4.2.8). The *meso*-et,ph-P4-Ph, diastereomer shows two sets of doublets of triplets in the methylene bridge region centered at 2.80 ppm and at 3.08 ppm due to the nonequivalent hydrogens of the central CH₂ group, while *rac* diastereomer shows a triplet at 2.99 ppm due to the magnetically equivalent CH₂ hydrogens.

The diastereomers can also be separated by eluting with a DCM/toluene/hexane (1:2:3) solvent system which gives a slightly better separation of *rac* and *meso*-et,ph-P4-Ph, however poorer separation between unwanted impurities and *meso*-et,ph-P4-

Ph. In addition, the high boiling point of toluene makes it harder to completely remove solvent from the desired products. Therefore, CH₂Cl₂/hexanes (1:4) is the preferred solvent system for separation of *rac* and *meso*-diastereomers of et,ph-P4-Ph ligand. No separation was observed when using neutral alumina Grades III and V.

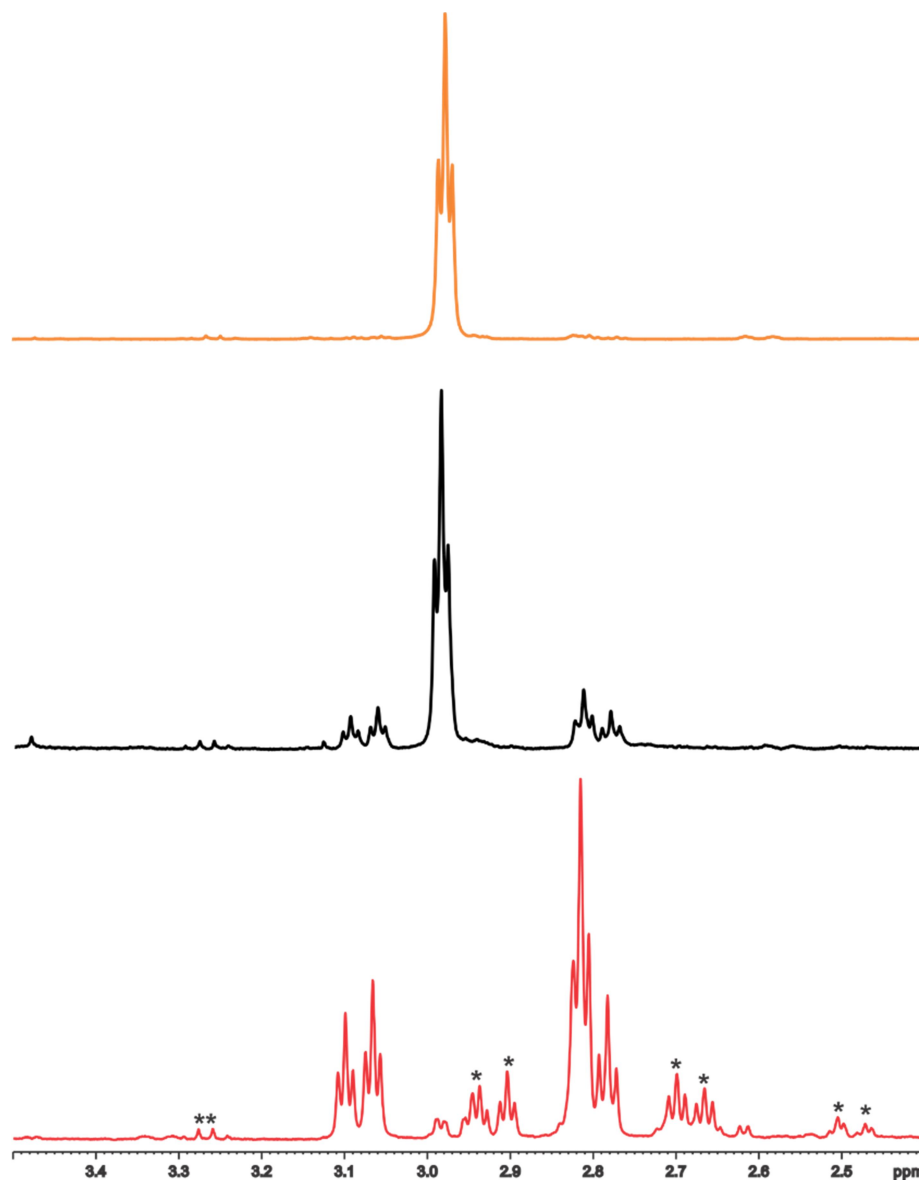


Figure 4.2.8. (Red spectrum) ¹H NMR spectra of 2.4-3.5 ppm region of the *meso*-et,ph-P4-Ph and unidentified phosphine impurities, (black spectrum) mixture of *meso* and *rac*-et,ph-P4-Ph, (orange spectrum) and *rac*-et,ph-P4-Ph.

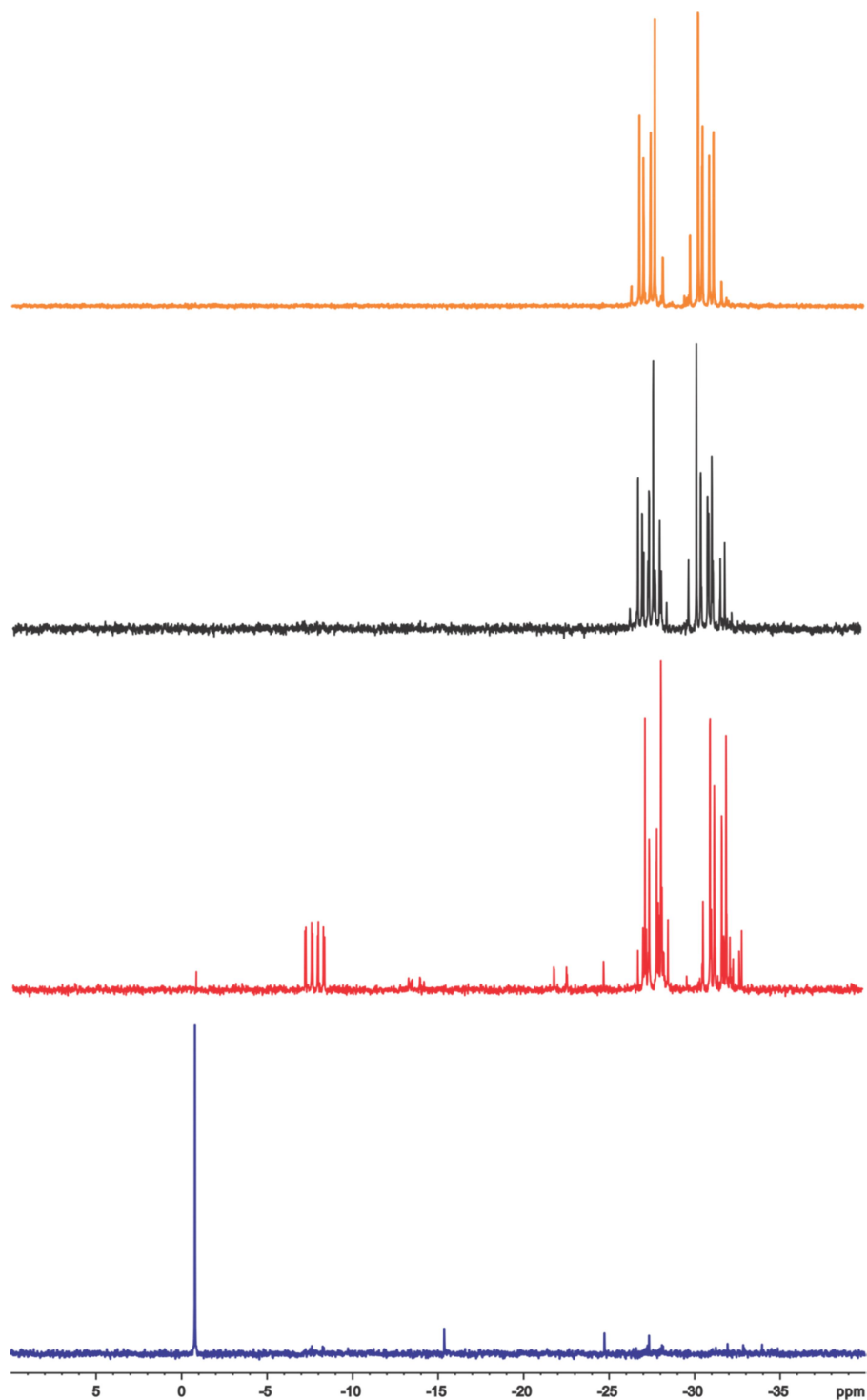


Figure 4.2.9. (Blue spectrum) ^{31}P $\{^1\text{H}\}$ NMR spectra of first set of fractions containing unreacted 3(I) and other phosphine impurities, (red spectrum) second set containing *meso*-et,ph-P4-Ph and unidentified phosphine impurities, (black spectrum) third set mixture of *meso* and *rac*-et,ph-P-4,ph, and (orange spectrum) fourth set *rac*-et,ph-P4- Ph.

The bimetallic rhodium complex based on the *rac*-et,ph-P4 ligand is a precursor to highly active and regioselective hydroformylation catalyst.^{2a} The *meso*-et,ph-P4 ligand forms a significantly less active catalyst with considerably higher side reactions and lower regioselectivity. Therefore, the *rac*-et,ph-P4,Ph is the desired diastereomer for rhodium catalyzed hydroformylation, however bimetallic rhodium complexes based on the *meso*-et,ph-P4-Ph also will be tested and hence it is essential to obtain both diastereomers in high purity. The presence of a large amount of phosphine impurities in the crude product mixture obtained via Grignard-mediated P-C coupling and our inability to purify the *meso*-diastereomer prompted us to reexamine the last two steps of the *rac*, *meso*-et,ph-P4,Ph synthesis.

In the Grignard mediated P-C coupling reaction with 3(I) and chlorophosphine 2 formation of the side products is very likely if conversion of 3(I) to the corresponding magnesium reagent via I/Mg exchange is not complete before the chlorophosphine is added to the reaction mixture. Therefore, the reaction mixture containing the intermediate magnesium reagent was analyzed via ³¹P{¹H} NMR. Reaction with 3(I) and *i*PrMgBr was allowed to proceed for 6 hours at 0°C (as previously described) and the resulting product mixture contained a high intensity ³¹P signal at –0.6 ppm due to unreacted 3(I) and a singlet at –16.0 ppm, presumably due to the arylphosphine Grignard (Figure 4.2.10).

The ³¹P{¹H} NMR analysis, therefore, clearly indicated that a large amount of 3(I) still remained in solution after stirring for 6 hours at 0°C. To allow the iodine-magnesium reaction to complete, the mixture was allowed to stir at 0°C for an additional 16 hours. At the end of this time period, based on ³¹P {¹H} NMR analysis, all of the 3(I)

has been converted to arylphosphine Grignard (Figure 4.2.10). Subsequent addition of 2 was carried out as previously described at -25°C . After removal of the solvents *in vacuo* the $^{31}\text{P}\{^1\text{H}\}$ NMR of the final product mixture showed that the amount of phosphine impurities was greatly reduced, as shown in Figure 4.2.11 (compare to Figure 4.2.6).

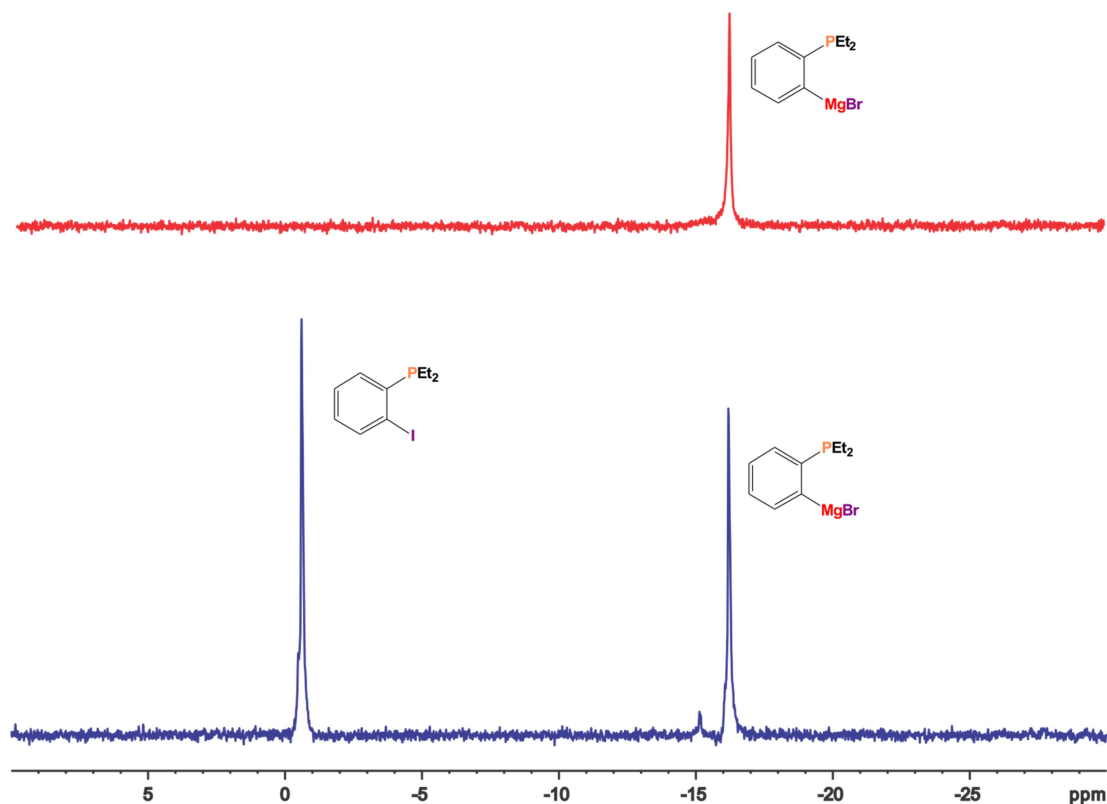


Figure 4.2.10. (Bottom spectrum) $^{31}\text{P}\{^1\text{H}\}$ NMR recorded on the sample taken from reaction with 3(I) and *i*PrMgBr after 6h at 0°C and (top spectrum) after 24h.

Overall the longer reaction time allowed for nearly complete conversion of 3(I) to the desired magnesium reagent prior to addition of chlorophosphine 2 and the amount of byproducts was greatly reduced in the final reaction mixture. However, the $^{31}\text{P}\{^1\text{H}\}$ NMR showed the presence of two doublets centered at -7.2 ppm ($J_{\text{p-p}} = 10$ Hz) and

–8.3 ppm ($J_{\text{p-p}} = 10$ Hz) due to unidentified phosphine impurities, which we were unable to separate from the desired *meso*-et,ph-P4-Ph ligand.

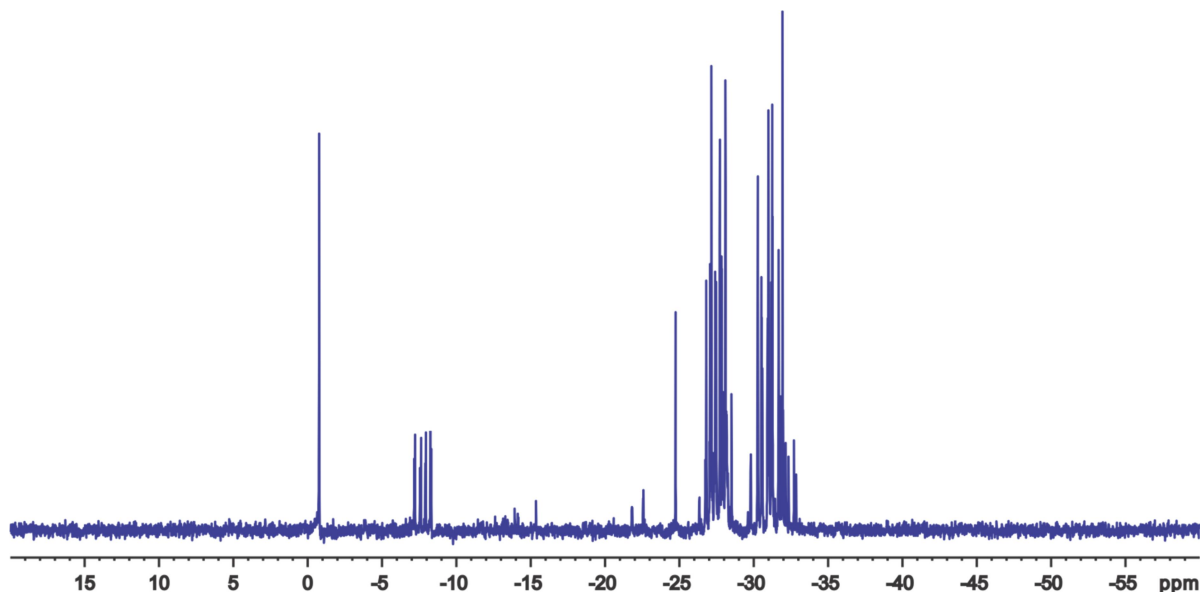


Figure 4.2.11. Final product mixture after 24 hours Mg-I exchange at 0°C in C₆D₆.

It is well known that the rate of Mg-I exchange is accelerated by electron withdrawing groups and reduced by electron donating groups.^{18b, 19} In 1986 Villieras *et al.* reported that CHBr₃ can be converted to the corresponding Grignard, HBr₂CMgCl by reaction with *i*PMgCl at –78°C.^{19a} Other published examples include full conversion of 1,4-dibromo-2,3,5,6-tetrafluorobenzene in 15 min into the corresponding dimagnesium species by reaction with EtMgBr at –78°C, conversion of 1-iodo-2,4-dinitrobenzene in 30 s by reaction with *i*PrMgBr at –40°C, and sufficiently fast (30 min) conversion of methyl 4-iodobenzoate upon reaction with *i*PrMgBr at –20°C.^{19b, 20} On the other hand, 1-iodo-4-methoxybenzene requires one hour at 25°C for a full conversion into the corresponding Grignard reagent.^{18a} Clearly, the electron-rich diethyl phosphine substituent slows down the rate of the Mg-I exchange as evidenced by the long (about

24 hours) time period required for a full conversion of 3(I) into the corresponding Grignard reagent. To increase the rate of this reaction we attempted the reaction with 3(I) and *i*PrMgBr at higher temperatures (25°C), however large amounts of the PhPEt₂ decomposition product of 3(I) were observed via ³¹P{¹H} NMR. Decomposition of the Grignard reagent could be due to the presence of the isopropyl iodide formed in the iodine-magnesium exchange reaction, it was reported by Boymond *et al.* that isopropyl iodide presumably eliminates hydroiodic acid.¹⁶

4.2.5 Improved Preparation of et,ph-P4-Ph Ligand via Grignard Mediated P-C Coupling

In attempt to reduce formation of unwanted side-products we attempted to prepare et,ph,P-4,Ph ligand via Grignard mediated P-C coupling using the more standard direct reaction of aryl halide with elemental Mg (Scheme 4.2.12).

Compound 3(Br) was synthesized by previously described procedures via reaction of 1-bromo-2-iodobenzene and *i*PrMgBr, followed by addition of Et₂PCl.⁸ The only modification introduced was the time period allowed for reaction of 1-bromo-2-iodobenzene with *i*PrMgBr. Based on GC/MS analysis only 1.5 hours at 0°C (not 6 hours as previously reported) were required for a complete conversion of 1-bromo-2-iodobenzene to the corresponding magnesium reagent. Exchange of the less reactive bromine was not detected under these conditions. Treatment of arylphosphine magnesium reagent with Et₂PCl gave 3(Br) in 87% yield. After work up 3(Br) was obtained by short path distillation under reduced pressure in 87% yield, with a purity greater than 98% based on ³¹P{¹H} NMR (Figure 4.2.12).

Scheme 4.2.12. Reaction scheme for synthesis of *rac,meso*-et,ph-P4-Ph

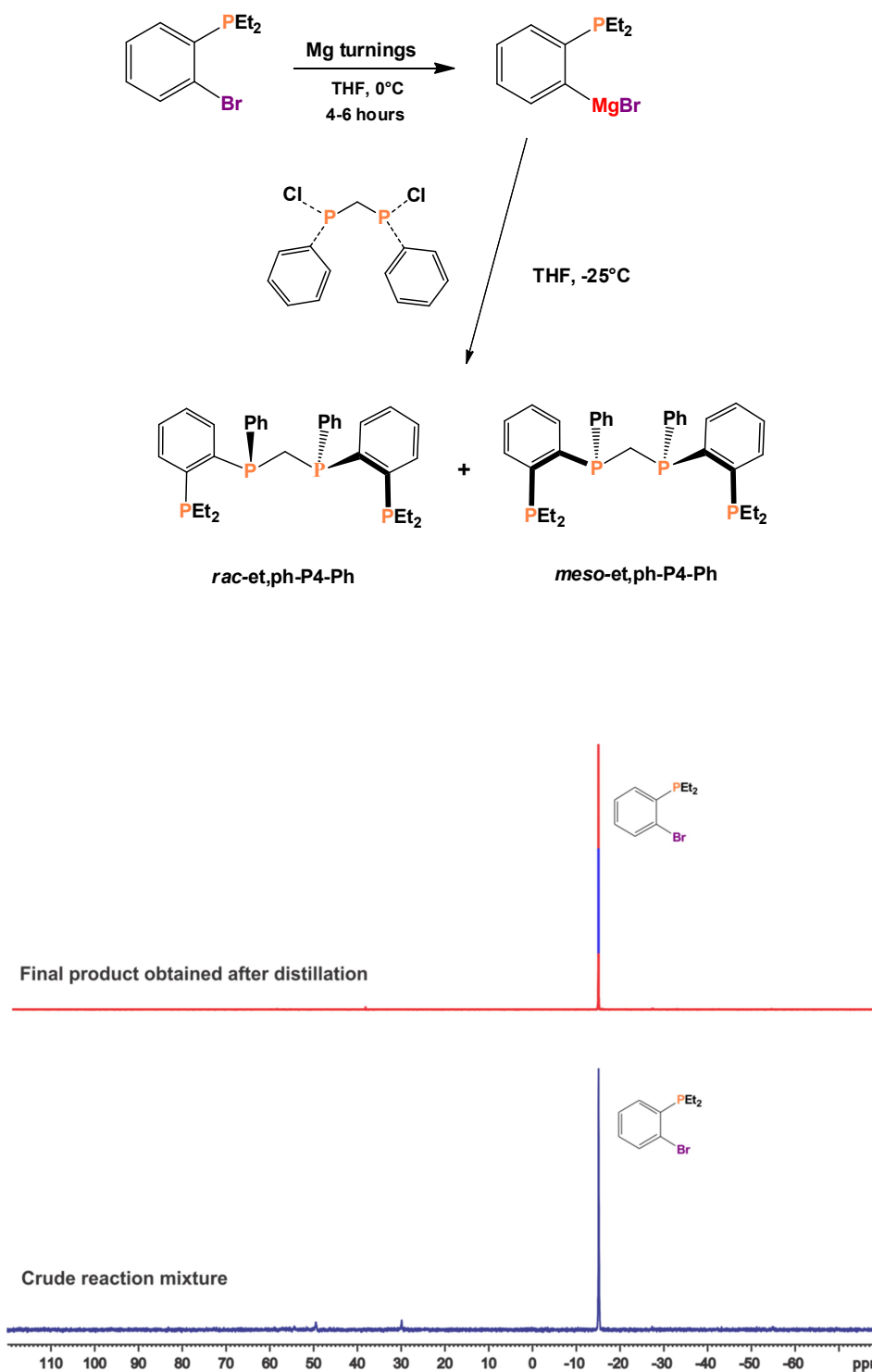


Figure 4.2.12. (Bottom spectrum) $^{31}\text{P}\{^1\text{H}\}$ NMR of the crude sample obtained from reaction of 1-bromo-2-iodobenzene with *i*PrMgBr and (top spectrum) final product obtained via distillation under reduced pressure.

To prepare the arylphosphine magnesium reagent, a solution of 3(Br) in THF was added to a flask containing 1.1 equiv of Mg turnings and the resulting mixture was gently heated. After one hour at 30°C no reaction was observed. Additional heating at 40°C also did not help to initiate the reaction. Reaction was initiated by heating at 65-75°C for 30 minutes and high temperatures (65-70°C) were required for the reaction to proceed. After heating at this temperature for three hours most of the Mg turnings were consumed and solution turned red-brown in color. The $^{31}\text{P}\{^1\text{H}\}$ NMR spectrum showed a single resonance at -16.2 ppm (s), presumably due to the desired arylphosphine Grignard (Figure 4.2.13).

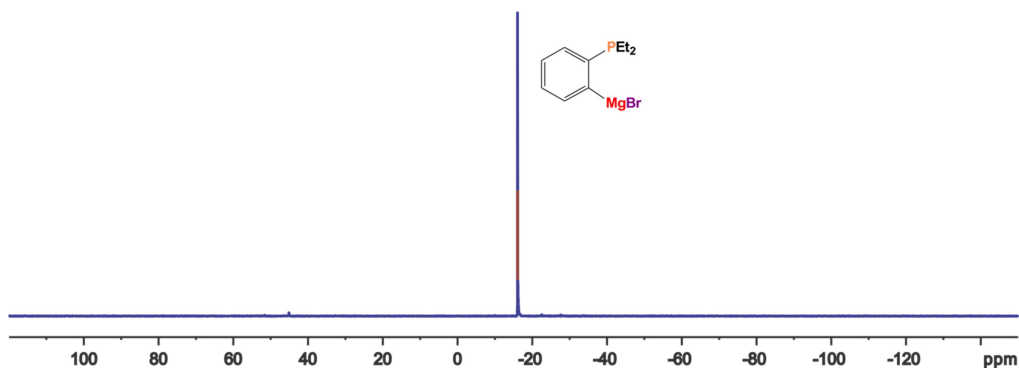


Figure 4.2.13. $^{31}\text{P}\{^1\text{H}\}$ NMR spectrum recorded on the sample taken from reaction of 3(Br) with Mg turnings to generate arylphosphine magnesium reagent.

Next the mixture containing arylphosphine Grignard was allowed to cool to 25°C, followed by addition to a solution of 2 cooled to -35°C. After stirring at this temperature for one hour, the mixture was slowly warmed to 25°C and stirring continued for an additional 16 hours. After work up the final product mixture was obtained as a yellowish thick paste containing 4% unreacted 3(Br), 77% *meso*-et,ph-P4-Ph (small traces of *rac*-diastereomer present) and 19% phosphine impurities that likely contain oxidized

phosphines and the P3 intermediate species (Figure 4.2.14). By comparison to Figure 4.2.11, the Grignard mediated reaction of 3(Br) with Cl(Ph)PCH₂P(Ph)Cl, via reaction of arylphosphine halide with Mg, generated far fewer impurities.

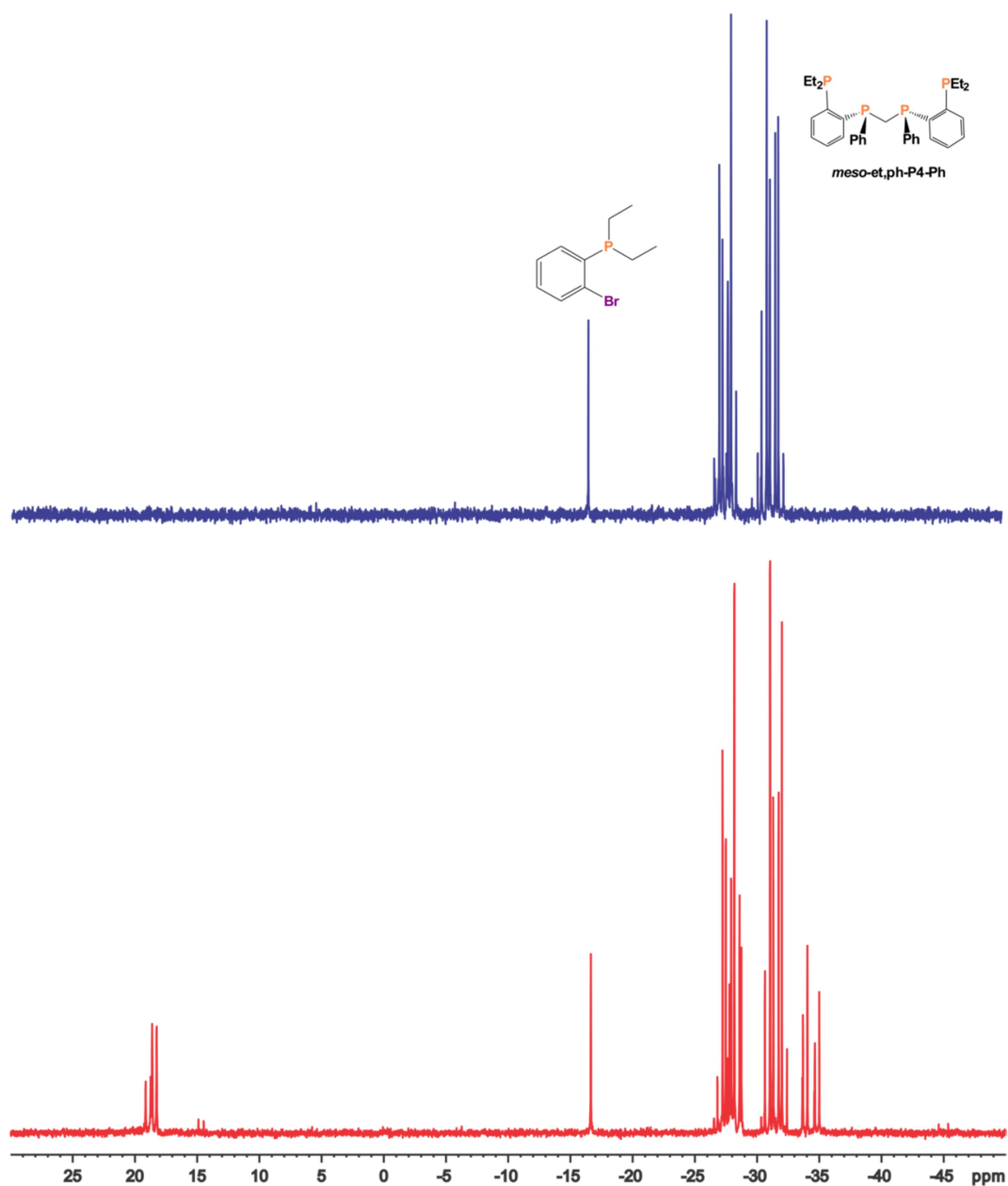


Figure 4.2.14. (Bottom spectrum) ³¹P {¹H} NMR crude product mixture and (top spectrum) final product mixture purified via column chromatography containing *meso*-et,ph-P4-Ph in 96% purity.

Purification via column chromatography on neutral alumina eluting with CH_2Cl_2 yielded the final product mixture as a white paste like solid that contained less than 4% of the unreacted small arm and over 96% *meso*-et,ph,P-4,Ph (small traces of *rac*-diastereomer present) as determined by integration of the NMR signals (Figure 4.2.14).

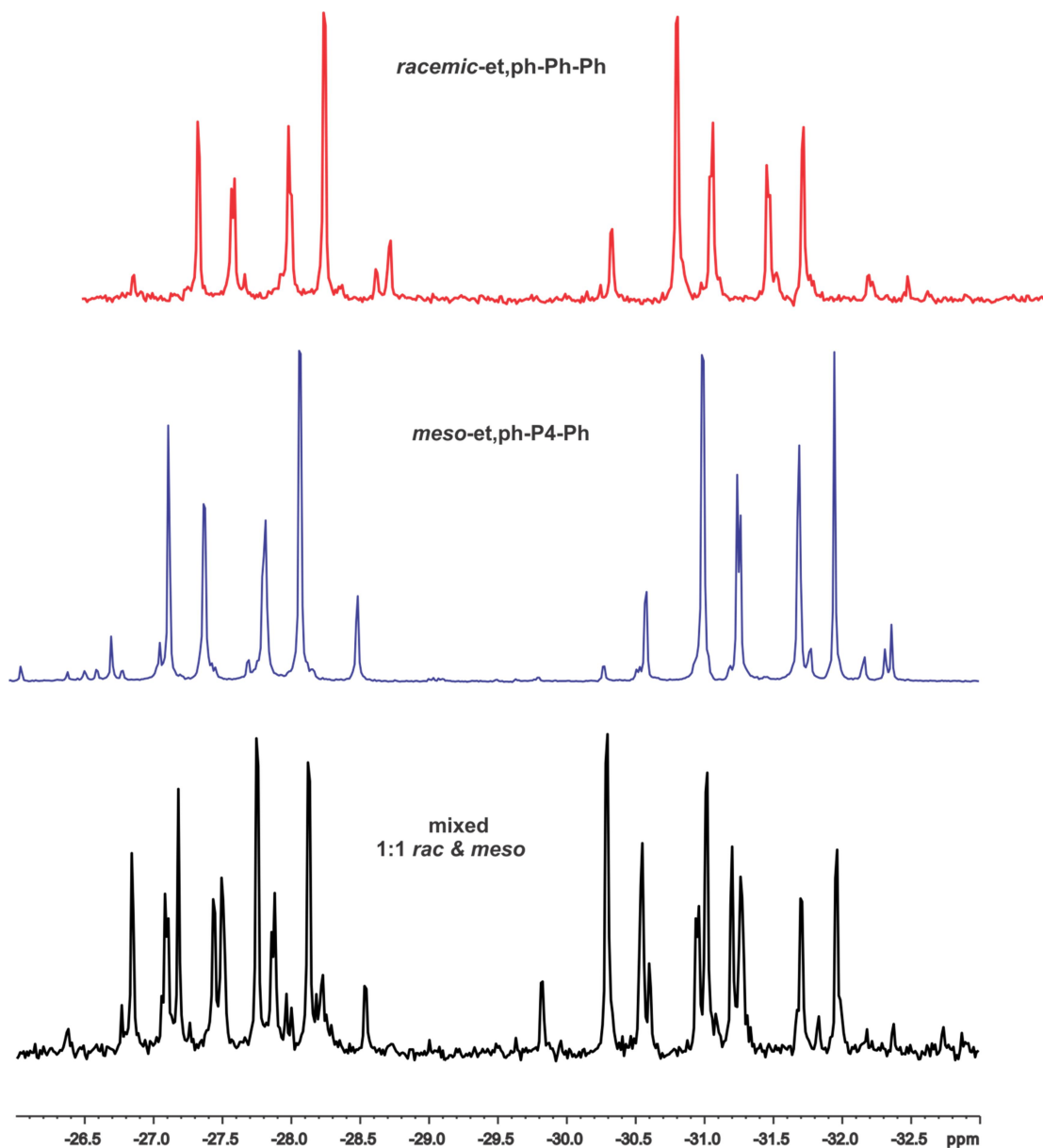


Figure 4.2.15. (Black spectrum) $^{31}\text{P} \{^1\text{H}\}$ NMR of 1:1 mixture of *rac* and *meso*-et,ph-P4-Ph, (purple spectrum) *meso*-et,ph-P4-Ph, (red spectrum) and *rac*-et,ph-P4-Ph.

The only impurity present after purification is the unreacted **3**(Br) which can be easily removed via distillation *in vacuo* (b.p. 84°C/0.5 Torr). Since the boiling point of **3**(Br) is below 100°C it can be removed without epimerization if pure *meso* form of the et,ph-P4-Ph is desired.

Separation of *rac* and *meso* diastereomers of et,ph-P4-Ph (obtained by epimerization) was carried out as previously described on neutral alumina (Grade IV) by eluting with CH₂Cl₂:hexanes (1:4). The ³¹P {¹H} NMR spectrum of each diastereomer is shown in Figure 4.2.15 and ¹H NMR of methylene bridge region is shown in Figure 4.2.16. The ³¹P NMR spectrum was successfully simulated using MestReNova (version 8.1.1) and manually optimized to fit the experimental spectrum of each diastereomer.

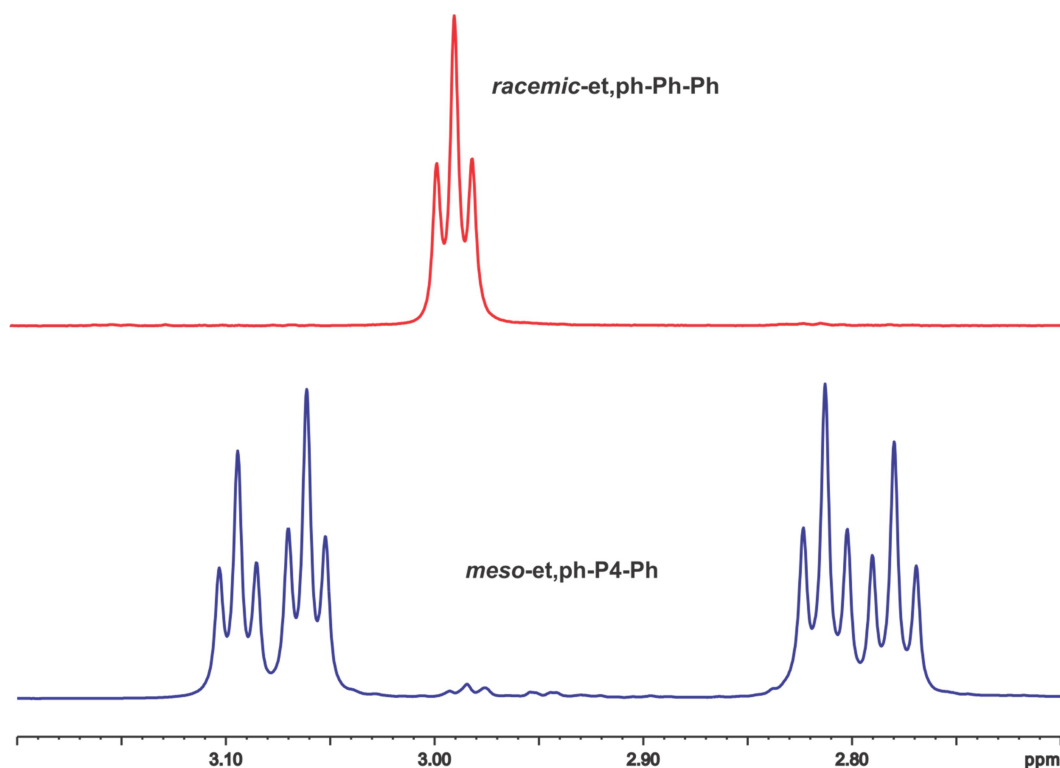


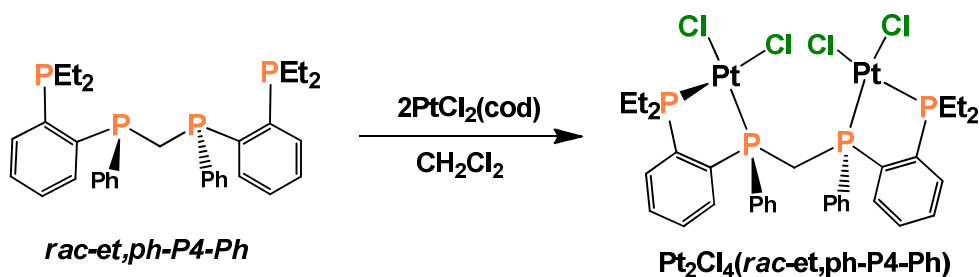
Figure 4.2.16. (Purple spectrum) ¹H NMR of *meso*-et,ph-P4-Ph, (red spectrum) *rac*-et,ph-P4-Ph.

Overall improvement of this procedure was achieved by preparation of intermediate Grignard reagent, $\text{Et}_2\text{P}(\text{o-C}_6\text{H}_4)\text{MgBr}$ via reaction of $\text{I}(\text{Br})$ with elemental Mg followed by addition of chlorophosphine 2. As a result the *meso* diastereomer was obtained in over 98% purity (after column chromatography) and the isolated yield was improved from 60-65% to 68%. The column chromatography procedure for the separation of *rac* and *meso*-diastereomers of *et,ph-P4-Ph* was developed and optimized.

4.2.6. Synthesis of $\text{Pt}_2\text{Cl}_4(\text{rac-et,pt-P4-Ph})$, 4R

The bimetallic platinum complex containing the *et,ph-P4-Ph* ligand, 4R has been prepared by the reaction of two equiv of $\text{PtCl}_2(\text{cod})$, (cod = 1,5-cyclooctadiene) with *rac-et-Ph-P4-Ph* in CH_2Cl_2 (Scheme 4.2.13).

Scheme 4.2.13. Preparation of $\text{Pt}_2\text{Cl}_4(\text{rac-et,pt-P4-Ph})$, 4R.



Nair *et al.* reported on the synthesis of the analogous Pt complex, $\text{Pt}_2\text{Cl}_4(\text{meso-DPPEPM})$, by reaction of DPPEPM with $\text{PtCl}_2(\text{cod})$ for 15 minutes at 25°C .²¹ However we have observed that much longer reaction times or higher temperatures are required for the preparation of 4R. This lower apparent reactivity is surprising because *et,ph-P4-Ph* is a stronger donating phosphine and less sterically hindered relative to DPPEPM, which is the phenylated version of our original *et,ph-P4* ligand.

The $^{31}\text{P}\{^1\text{H}\}$ NMR spectrum recorded on the crude sample taken from the reaction medium after two hours consisted of two sharp resonances at 49.8 ppm (s) and 31.2 ppm (s), presumably due to the 4R, and a mixture of signals in the positive and in the negative regions due to unidentified intermediate species (Figure 4.2.17). The resonances in the negative region of $^{31}\text{P}\{^1\text{H}\}$ NMR spectrum are characteristic for uncoordinated phosphines and are likely due to the intermediate monometallic platinum complex, $\text{PtCl}_2(\kappa^2\text{-rac-et,ph-P4-Ph})$. After stirring for an additional four hours at 35 - 39°C, the $^{31}\text{P}\{^1\text{H}\}$ NMR of a crude reaction mixture showed two resonances at 49.7 ppm (s) and 30.9 ppm (s) ppm corresponding to the desired 4R complex (Figure 4.2.18).

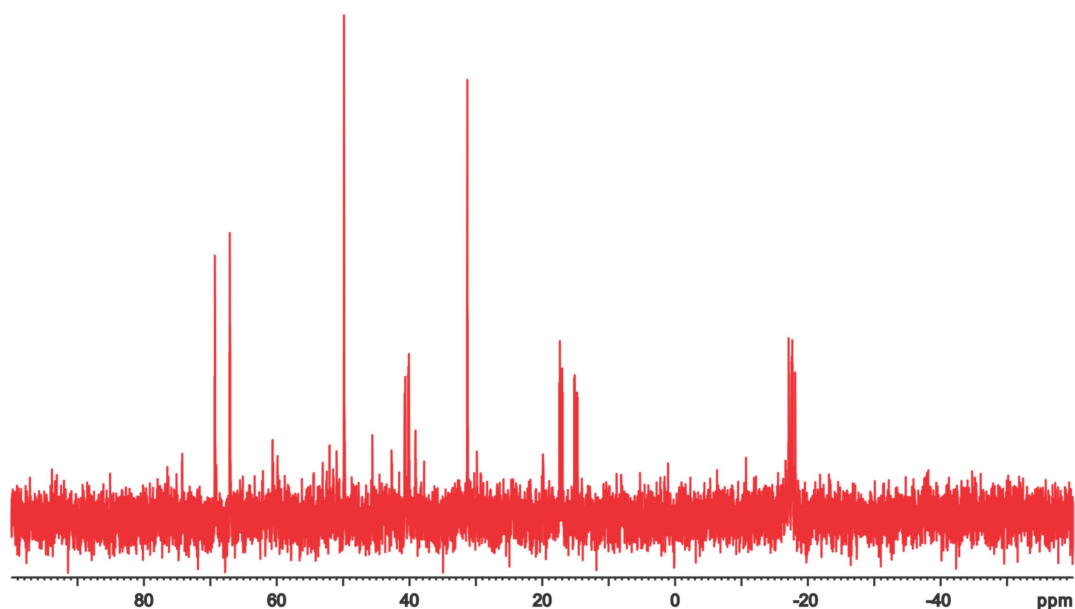


Figure 4.2.17. The $^{31}\text{P}\{^1\text{H}\}$ NMR of the sample taken from reaction of $\text{PtCl}_2(\text{cod})$ with *rac-et,ph-P4-Ph* in CDCl_3 after 2 hours.

Based on the $^{31}\text{P}\{^1\text{H}\}$ spectrum of the crude reaction mixture the desired Pt_2 complex 4R can be obtained in 100% purity after a 6 hr reaction (Figure 4.2.18, bottom spectrum). Removal of the solvent *in vacuo* followed by precipitation with diethyl ether from the minimal amount of CH_2Cl_2 yielded 4R as a light yellow solid (78%). The $^{31}\text{P}\{^1\text{H}\}$

NMR spectrum of 4R shows signals at 49.7 ppm ($^1J_{\text{Pt-P}} = 3483$ Hz) and 30.9 ($^1J_{\text{Pt-P}} = 3698$ Hz) due to terminal and internal P atoms (Figure 4.2.18, top spectrum).

Resonances due to the internal and external P atoms are tentatively assigned based on previous work with the old et-ph-P-4 ligand and metal complexes based on it.

Additional NMR work is needed to confirm the assignments for internal and external phosphines. The complex appears to be air stable in the solid state and in solution.

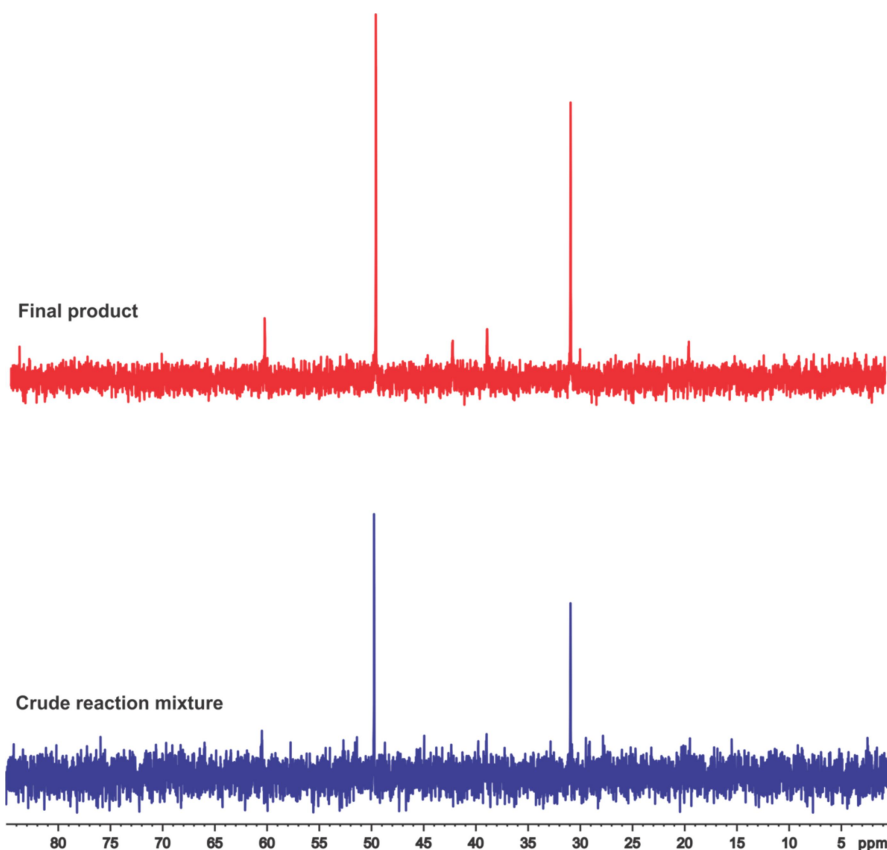


Figure 4.2.18. (Bottom spectrum) $^{31}\text{P}\{^1\text{H}\}$ NMR of the crude reaction mixture of $\text{PtCl}_2(\text{cod})$ and *rac*-et,ph-P4-Ph after 6 hrs of reaction and (top spectrum) purified $\text{Pt}_2\text{Cl}_2(\text{rac-et,ph-P4-Ph})$, 5R in CDCl_3 .

Colorless crystals of 4R suitable for X-ray diffraction were obtained by slow evaporation of an acetonitrile solution at room temperature. The crystals are in the P1 space group with two molecules of the Pt_2 complex in the asymmetric unit.

The ORTEP of one 4R molecule from the asymmetric unit together with the atomic numbering scheme is shown in Figure 4.2.19, selected bond distances and angles are given in Table 4.2.4. The structure confirms the bimetallic character and that each Pt center adopts a square planar geometry with the et,ph-P4-Ph ligand coordinating in the expected bridging and chelating manner.

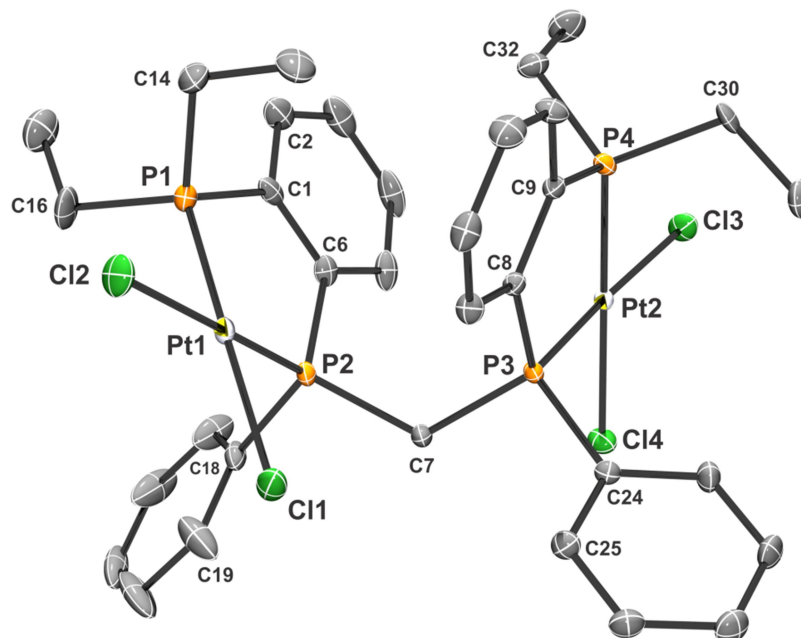


Figure 4.2.19. ORTEP (50% ellipsoids) of one molecule of $\text{Pt}_2\text{Cl}_4(\text{rac-et,ph-P4-Ph})$, 4R, in the asymmetric unit. Hydrogen atoms are omitted for clarity.

The two PtCl_2P_2 planes are rotated away from each other with a $\text{Pt}\cdots\text{Pt}$ separations of 5.920 Å (Pt1-Pt2) and 5.992 Å (Pt3-Pt4), which are comparable to $\text{PtMe}_2(\text{DPPEPM})\text{PtCl}_2$ (5.931 Å) and $\text{Pd}_2\text{Cl}_4(\text{DPPEPM})$ (6.08 Å).²¹⁻²² This metal-metal distance is slightly shorter than in $\text{Pt}_2\text{Cl}_4(\text{rac-1,2-DPPEPE})$, in which the two internal phosphines are connected by ethylene bridge.²³ The $\text{Pt-P}\cdots\text{P-Pt}$ torsional angles are 134.8° (Pt1/Pt2) and 138.4° (Pt3/Pt4). The Pt centers are approximately symmetrically rotated away from one another, which is typical for open-mode racemic bimetallic

complexes based on our old et,ph-P-4 ligand. The central P-C-P angles for 4R is 122.1° and 121.8° are slightly increased from the 121.1° in PtMe₂(DPPEPM)PtCl₂. The P-C-P angle in Ni₂Cl₄(*rac*-et,ph-P4-Ph) is 118.6°. ²²

Table 4.2.4. Selected Bond Distances (Å) and Angles (deg) for one molecule of *rac*-Pt₂Cl₄(et,ph-P4-Ph), 4R

Pt1-Cl1	2.3837(10)	Pt2-Cl3	2.3624(9)
Pt1-Cl2	2.3452(10)	Pt2-Cl4	2.3682(10)
Pt1-P1	2.2200(11)	Pt2-P3	2.2081(9)
Pt1-P2	2.1919(10)	Pt2-P4	2.2128(11)
P2-C7	1.820(4)	P3-C7	1.839(4)
P1-Pt1-P2	85.61(4)	P1-Pt1-Cl2	90.86(4)
P1-Pt1-Cl1	177.37(4)	P2-Pt1-Cl2	175.36(4)
P2-Pt1-Cl1	91.81(4)	Cl1-Pt1-Cl2	91.69(4)
P3-Pt2-P4	87.79(3)	P3-Pt2-Cl3	176.07(4)
P3-Pt2-Cl4	89.46(3)	P4-Pt2-Cl3	91.25(4)
P4-Pt2-Cl4	177.03(3)	Cl3-Pt2-Cl4	91.42(3)
Pt1-P2-C7	117.07(14)	Pt2-P3-C7	113.67(13)
P2-C7-P3	122.1(2)		

4.2.7. Synthesis of NiPtCl₄(*rac*-et,pt-P4-Ph), 5R

Heterobimetallic complexes are of significant interest, due to the catalytic potential of these systems. Complexes containing the bis(phosphino)methane group, P-CH₂-P, are of a special interest because such ligands are often used to favor the formation of a M-M bond. However, the preparation of mixed metal complexes is not

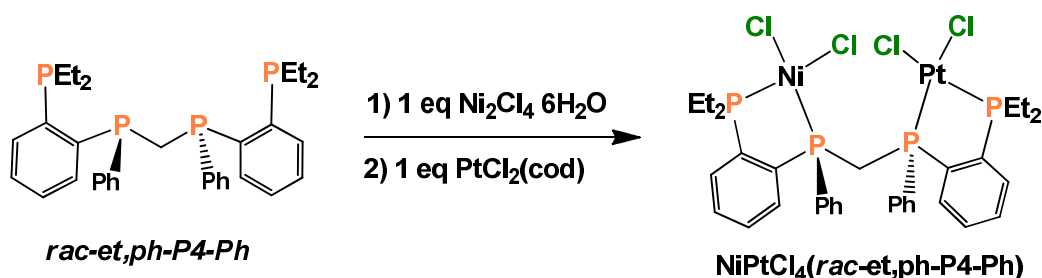
straight forward due to the possibility to produce a mixture of homo and heterobimetallic species. Heterobimetallic complexes based on the binucleating tetraphosphine ligand DPPEPM, which is a phenyl substituted derivative of our et,ph-P4 ligand have been reported.²⁴ Anderson *et al.* observed that addition of 1 mol equiv of metal precursor $\text{PtR}_2(\text{cod})$, $\text{R} = \text{Me}, \text{Ph}$, to a solution of DPPEPM, results in formation of monometallic complexes of the form $\text{PtR}_2(\kappa^2\text{-DPPEPM})$ are obtained with just traces of the bimetallic $\text{Pt}_2\text{R}_4(\text{DPPEPM})$ complex.^{24b} Reaction of these monometallic Pt complexes with $\text{PdCl}_2(\text{cod})$ results in formation of unsymmetrical ligated species in high yield, with just traces of the symmetrical complexes. However, if the addition is in reverse order, i.e., if DPPEPM is added to a solution of $\text{PtR}_2(\text{cod})$, mixtures of products are obtained.

Mixed metal complexes based on the P6 ligand, $(\text{Et}_2\text{PCH}_2\text{CH}_2)_2\text{PCH}_2\text{P-}(\text{CH}_2\text{CH}_2\text{Et}_2)_2$, eHTP, have been previously prepared in Stanley's lab.²⁵ It was found that reaction of one equivalent of K_2PtCl_4 with one equivalent of eHTP followed by addition of one equivalent of $\text{NiCl}_2 \cdot 6\text{H}_2\text{O}$ produces the mixed metal complex in 50% yield, which is the statistically expected yield. However, when addition is performed in the reverse order, i.e., if $\text{NiCl}_2 \cdot 6\text{H}_2\text{O}$ added to eHTP, followed by addition of K_2PtCl_4 , the mixed-metal complex is formed in higher yield (67%). The reason for increased yield is displacement of the more weakly bound Ni atoms by Pt from some of the $\text{Ni}_2\text{Cl}_2(\text{eHTP})^{+2}$ complex to produce the mixed Ni/Pt system.

With this chemistry in mind, we examined the possibility of preparing mixed metal complex containing et,ph-P4-Ph ligand by addition of 1 equiv of $\text{Ni}_2\text{Cl}_4 \cdot 6\text{H}_2\text{O}$ to a solution of *rac*-et,ph-P4-Ph, followed by dropwise addition of 1 equiv of $\text{PtCl}_2(\text{cod})$ (Scheme 4.2.14). After stirring for 16 hours, the solvent was removed *in vacuo* to yield

an orange solid, which upon precipitation with hexanes and a minimal amount of CH_2Cl_2 , yielded 5R as an orange powder. Because this reaction was carried out on a small scale the overall yield of 5R could not be determined.

Scheme 4.2.14. Preparation of $\text{NiPtCl}_4(\text{rac-et,ph-P4-Ph})$, 5R.



The $^{31}\text{P}\{^1\text{H}\}$ NMR spectrum of orange 6R shows four resonances, two doublets at 66.6 ($J_{\text{P-P}} = 75.1$ Hz) ppm and 47.7 ppm ($J_{\text{P-P}} = 75.1$ Hz) arising from the external and internal phosphorus atoms coordinated to the Ni center ($J_{\text{P-P}} = 75.1$ Hz), one unresolved doublet at 49.74 ppm ($J_{\text{Pt-P}} = 3493$ Hz) and one broad singlet at 31.84 ppm ($J_{\text{Pt-P}} = 3644$ Hz) arising from phosphorus atoms coordinated to the Pt center (Figure 4.2.20). The $^{31}\text{P}\{^1\text{H}\}$ NMR signals for each half of the molecule are similar to the $^{31}\text{P}\{^1\text{H}\}$ NMR signals previously found for the respective Ni_2 and Pt_2 homobimetallic complexes based on et,ph-P4-Ph.

The ^1H NMR spectrum of the methylene bridge region shows two unresolved multiplets at 5.01 ppm and 4.84 ppm due to the coupling of two non-equivalent protons of the central CH_2 group with each other and with the phosphorus atoms (Figure 4.2.22). Upon ^{31}P -decoupling the complicated methylene bridge set of resonances simplifies to a set of doublets with $^2J_{\text{H-H}} = 14.6$ Hz. Non-equivalence of these methylene protons confirms the presence of the heterobimetallic complex 5R and not a 1:1 mixture

of the two homobimetallic complexes. The symmetric bimetallic species, $\text{Pt}_2\text{Cl}_4(\text{rac-et,ph-P4-Ph})$ and $\text{Ni}_2\text{Cl}_4(\text{rac-et,ph-P4-Ph})$, have equivalent protons on the methylene group that produces a triplet pattern (see Figure 4.2.22). The ^1H NMR of methylene bridge region of $\text{Ni}_2\text{Cl}_4(\text{rac-et,ph-P4-Ph})$ shows one triplet due to the equivalent protons of the central CH_2 group.

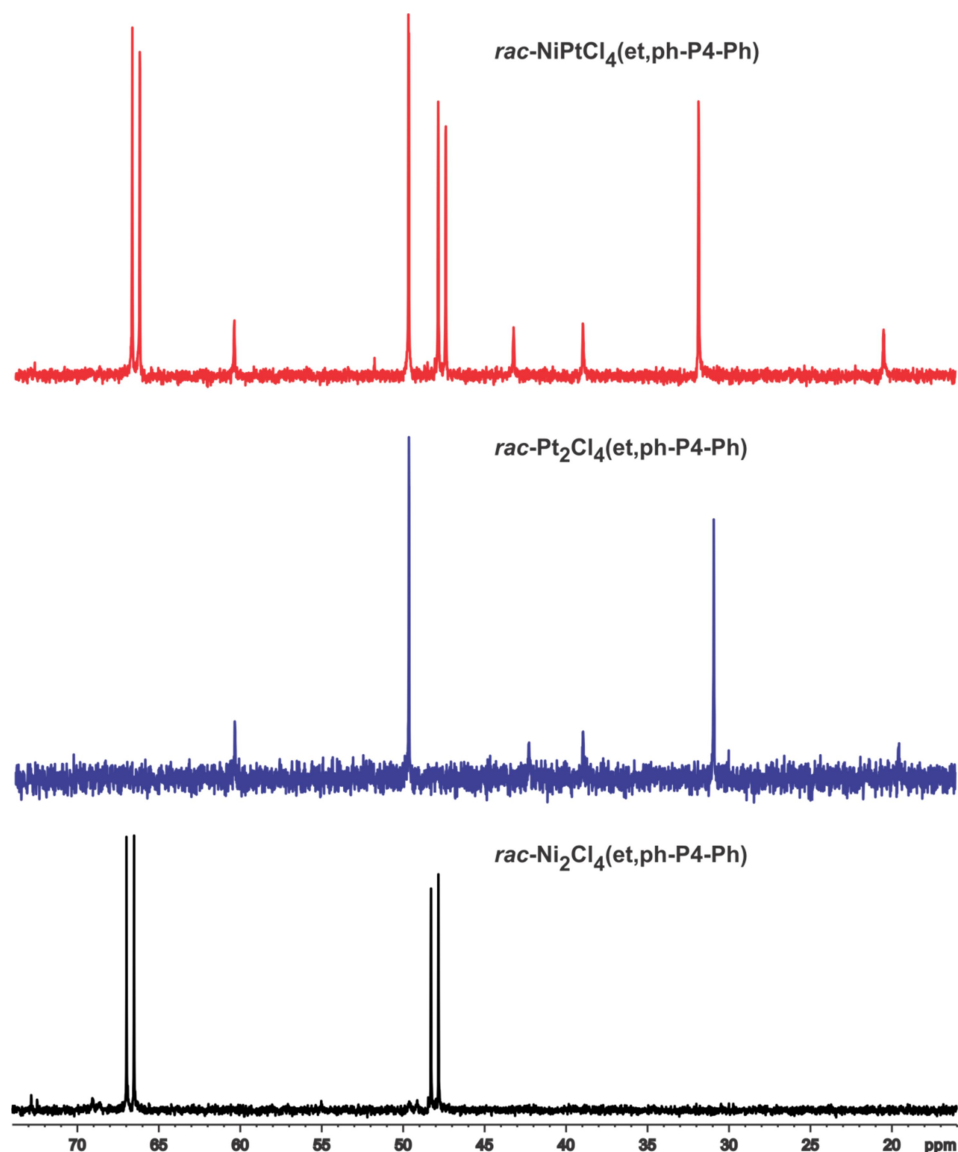


Figure 4.2.20. (Top spectrum) $^{31}\text{P}\{^1\text{H}\}$ NMR of 6R in C_6D_6 , (middle spectrum) 5R, and (bottom spectrum) $\text{rac-Ni}_2\text{Cl}_4(\text{et,ph-P4-Ph})$.

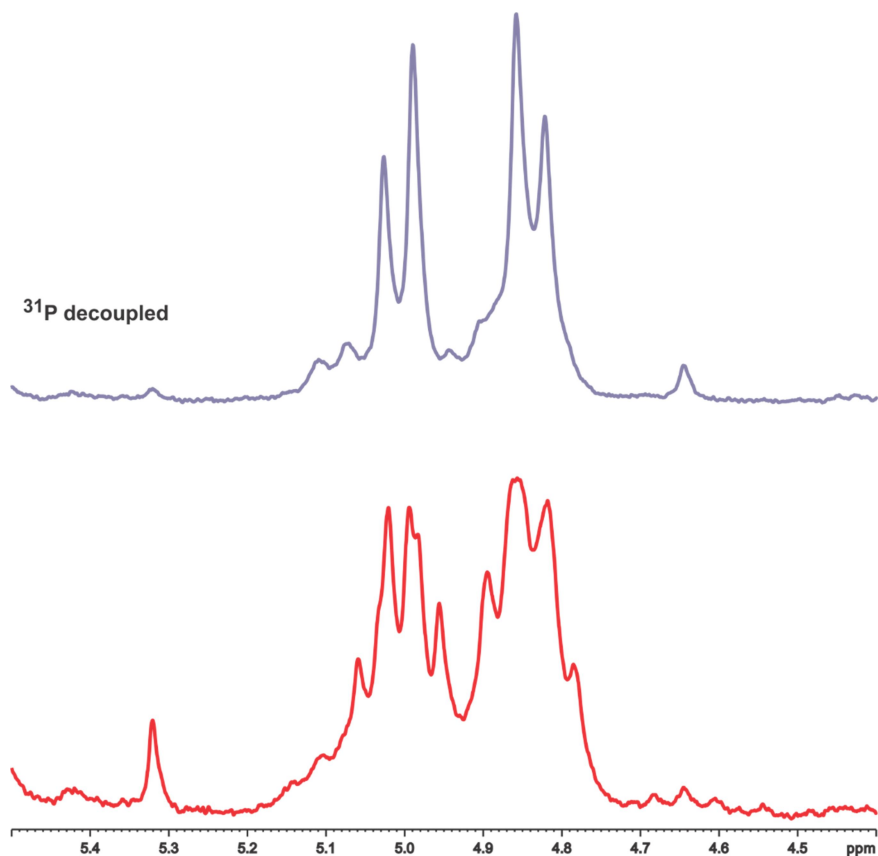


Figure 4.2.21. ^1H NMR of methylene bridge region for 6R in CDCl_3 .

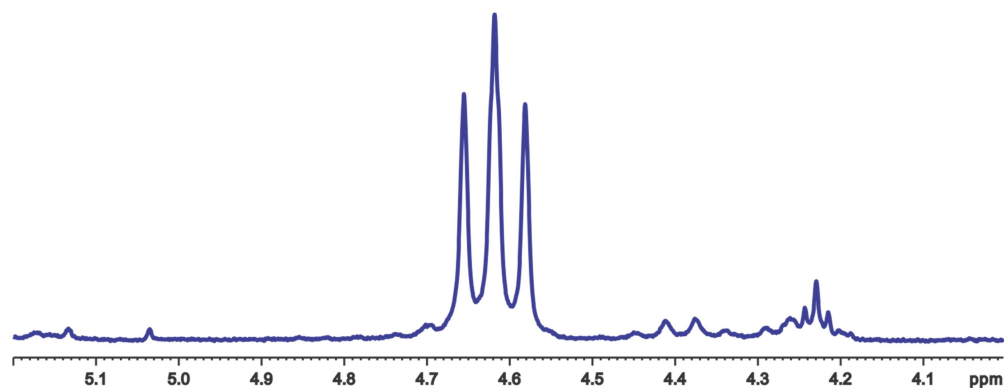


Figure 4.2.22. ^1H NMR of methylene bridge region for *rac*- $\text{Ni}_2\text{Cl}_4(\text{et,ph-P4-Ph})$ in CD_2Cl_2 .

The $^{31}\text{P}\{^1\text{H}\}$ NMR of orange powder obtained upon concentration of the filtrate *in vacuo* showed a mixture of signals including signals due to 5R (some amount remained dissolved in solution after precipitation with hexanes), and signals due to symmetrical

bimetallic species ($\text{Ni}_2\text{Cl}_4(\text{rac-et,ph-P4-Ph})$ and 5R) (Figure 4.2.23). However, based on the signal intensities in the $^{31}\text{P}\{^1\text{H}\}$ NMR spectrum the desired heterobimetallic 5R is the major product.

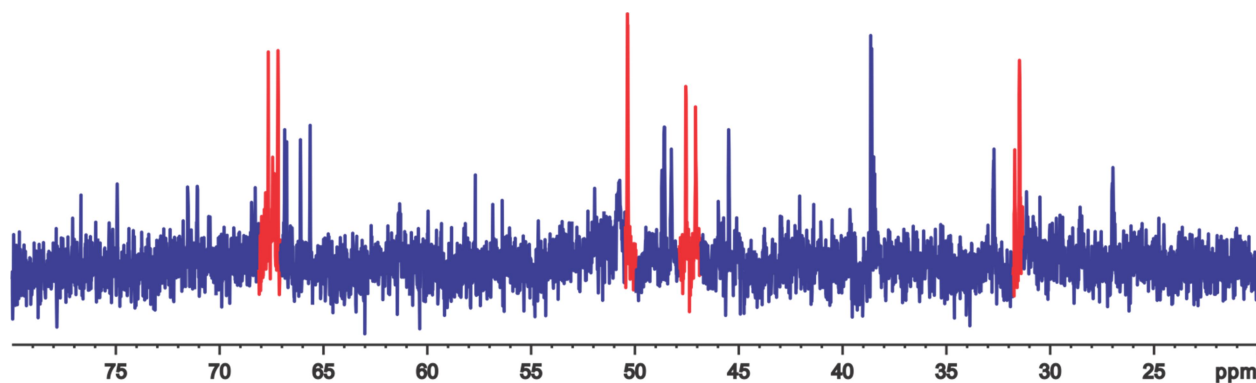


Figure 3.2.23. The $^{31}\text{P}\{^1\text{H}\}$ NMR of orange powder in C_6D_6 obtained upon concentration of the filtrate *in vacuo*. Signals due to 5R are colored in red.

When the tabular orange crystals of 5R grown by slow evaporation of CH_2Cl_2 were analyzed via X-ray crystallography, it was found that the structure is disordered over the metal-containing sites, with both metal sites being partially populated with Ni and Pt. Dr. Fronczek performed a number of careful refinements of the structure to model the disorder and establish the amounts of Ni and Pt at each site.

The first model refinement used a variable mix of Ni and Pt, where the fraction of Ni and Pt summed to one. The results were that at the Pt/Ni1 site, the mix refined to about 2/3 Pt and 1/3 Ni, while at the Pt/Ni2 site, it was the other way around. There was no constraint on the relationship between the mix at the Pt/Ni1 site and the mix at the Pt/Ni2 site; each was allowed to refine independent of the other. Nevertheless, this refinement got very close to the expected 1:1 ratio of Ni:Pt, namely 1.02:0.98.

Given the NMR data pointing to a true heterobimetallic complex, Dr. Fronczek added restraints to the refinement requiring that not only must each site sum to Ni + Pt

= 1, but the entire sample must have Ni = Pt. That model refined to 67% Pt and 33% Ni at the Pt/Ni1 site, and 33% Pt and 67% Ni at the Pt/Ni2 site with an R value of 3.6%.

Based on the X-ray data, the $^{31}\text{P}\{^1\text{H}\}$ and especially the ^1H NMR analysis described above, we believe that 5R is a true heterobimetallic Ni-Pt complex. The M2 metal site has the larger Pt percent composition and is labeled as Pt in the ORTEP plot shown in Figure 4.2.24, with selected bond distances and angle given in Table 4.2.5.

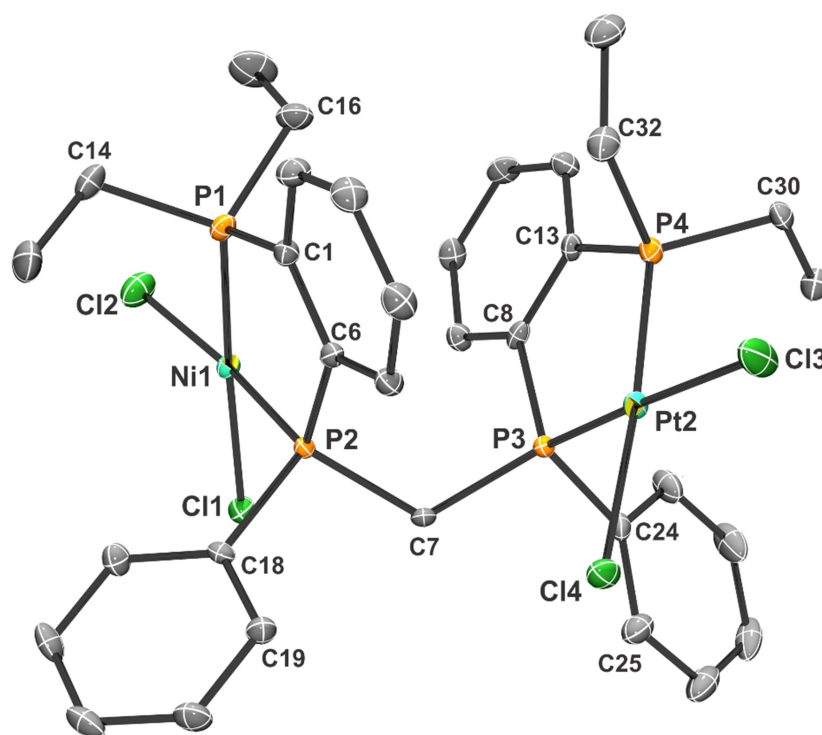


Figure 4.2.24. ORTEP representation (50% ellipsoids) of NiPtCl₄(rac-et,ph-P4-Ph), 5R. Hydrogen atoms omitted for clarity.

Both of the metal centers adopt the standard square planar geometry with a Ni...Pt distance of 5.898 Å and a Ni-P...P-Pt torsional angle of 134.1°. Each metal center is coordinated by two phosphorus atoms and two chlorides. The central P-C-P angle is 119.25(16)° and is similar to that found in Ni₂Cl₄(rac-et,ph-P4-Ph) (118.60(6)°) and in 4R (122.1(2)°).⁶

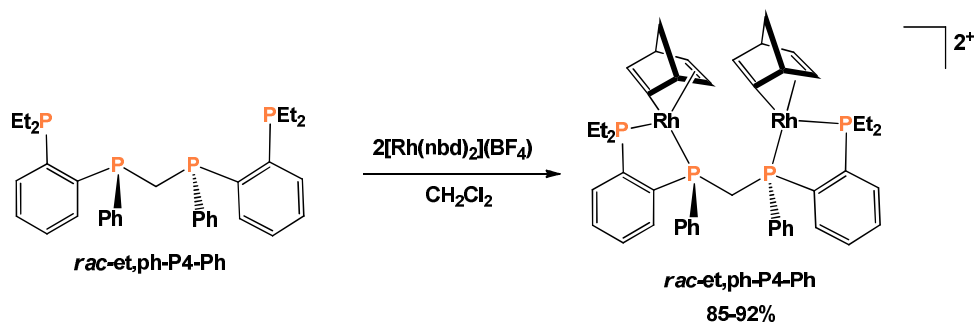
Table 4.2.5. Selected Bond Distances (Å) and Angles (deg) for *rac*-NiPtCl₄(*et*,*ph*-P4-Ph), CH₂Cl₂.

Pt-Cl1	2.3363(8)	Ni-Cl3	2.2234(9)
Pt-Cl2	2.2902(8)	Ni-Cl4	2.2740(8)
Pt-P1	2.1832(11)	Ni-P3	2.1485(8)
Pt-P2	2.1883(7)	Ni-P4	2.1493(8)
P2-C7	1.833(3)	P3-C7	1.820(3)
P1-Pt-P2	88.07(4)	P1-Pt-Cl2	90.64(3)
P1-Pt-Cl1	176.67(3)	P2-Pt-Cl2	173.48(4)
P2-Pt-Cl1	88.92(3)	Cl1-Pt-Cl2	92.51(3)
P3-Ni-P4	87.74(3)	P3-Ni-Cl3	172.28(4)
P3-Ni-Cl4	89.60(3)	P4-Ni-Cl3	89.42(3)
P4-Ni-Cl4	175.30(3)	Cl3-Ni-Cl4	93.70(3)
Pt-P2-C7	116.49(10)	Ni-P3-C7	118.15(10)
P2-C7-P3	119.25(16)		

4.2.8 Synthesis of [*rac*-Rh₂(*nbd*)₂(*et*,*ph*-P4-Ph)](BF₄)₂, 6R

The dirhodium norbornodiene complex based on the *rac*-*et*,*ph*-P4-Ph ligand, [*rac*-Rh₂(*nbd*)₂(*et*,*ph*-P4-Ph)](BF₄)₂, 6R has been synthesized by reaction of *rac*-*et*,*ph*-P4-Ph with a stoichiometric amount of [Rh(*nbd*)₂](BF₄) analogously to the previously described synthesis of [*rac*-Rh₂(*nbd*)₂(*et*,*ph*-P4)](BF₄)₂ (Scheme 4.2.15).^{2a}

Scheme 4.2.15. Synthesis of [*rac*-Rh₂(*nbd*)₂(*et*,*ph*-P4-Ph)](BF₄)₂, 6R.



After solvent removal and recrystallization in from acetone at -40°C , 6R was isolated as a red-brown solid in good yield (85-92%). The complex is soluble in CH_2Cl_2 , benzene, acetone, and MeOH; but is not soluble in THF, diethyl ether, or hexanes. The complex is stable under nitrogen atmosphere in the solid state and in solution. The $^{31}\text{P}\{^1\text{H}\}$ NMR spectrum of 6R shows two resonance due to the internal and terminal P atoms consistent with the formation of one diastereomer (Figure 4.2.25).

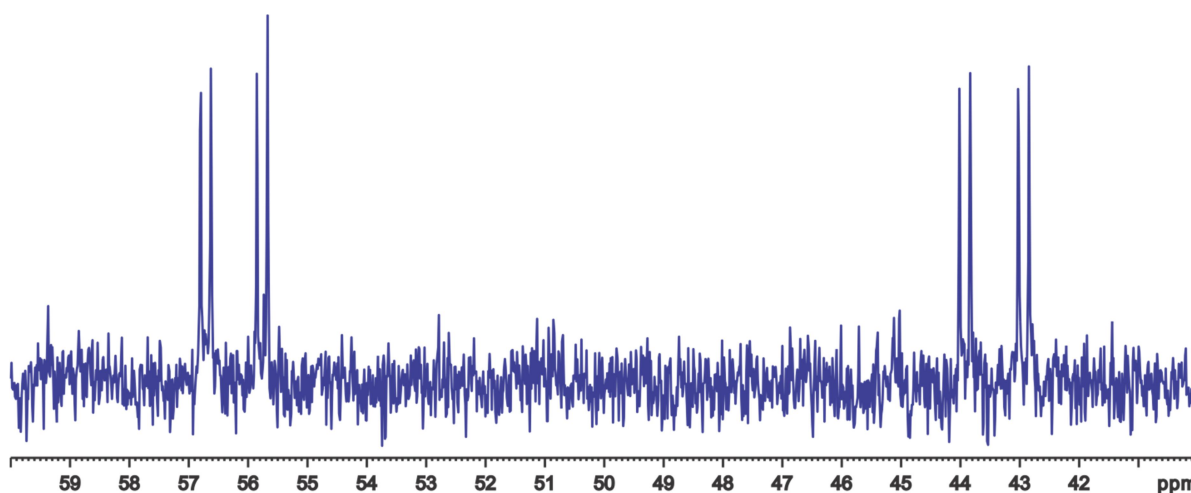


Figure 4.2.25. The $^{31}\text{P}\{^1\text{H}\}$ NMR of 4R in CD_2Cl_2 .

A pair of doublet doublets (dd) centered at 56.2 ppm ($J_{\text{Rh-P}} = 154.3 \text{ Hz}$, $J_{\text{Pint-Pext}} = 29.0 \text{ Hz}$) are assigned to the external phosphines and a pair of dd at 43.4 ppm ($J_{\text{Rh-P}} = 160.6 \text{ Hz}$, $J_{\text{Pint-Pext}} = 29.0 \text{ Hz}$) ppm are assigned to the internal phosphines. The ^1H NMR spectrum of 6R of the methylene bridge region exhibits a triplet at 3.80 ppm ($J_{\text{P-H}} = 9.5 \text{ Hz}$) due to magnetically equivalent hydrogens on the central CH_2 group (Figure 4.2.26).

The solid state structure of 6R has been determined by X-ray crystallography. The ORTEP plot and numbering scheme is shown in Figure 4.2.27. Selected bond distances and angles are given in Table 4.2.6.

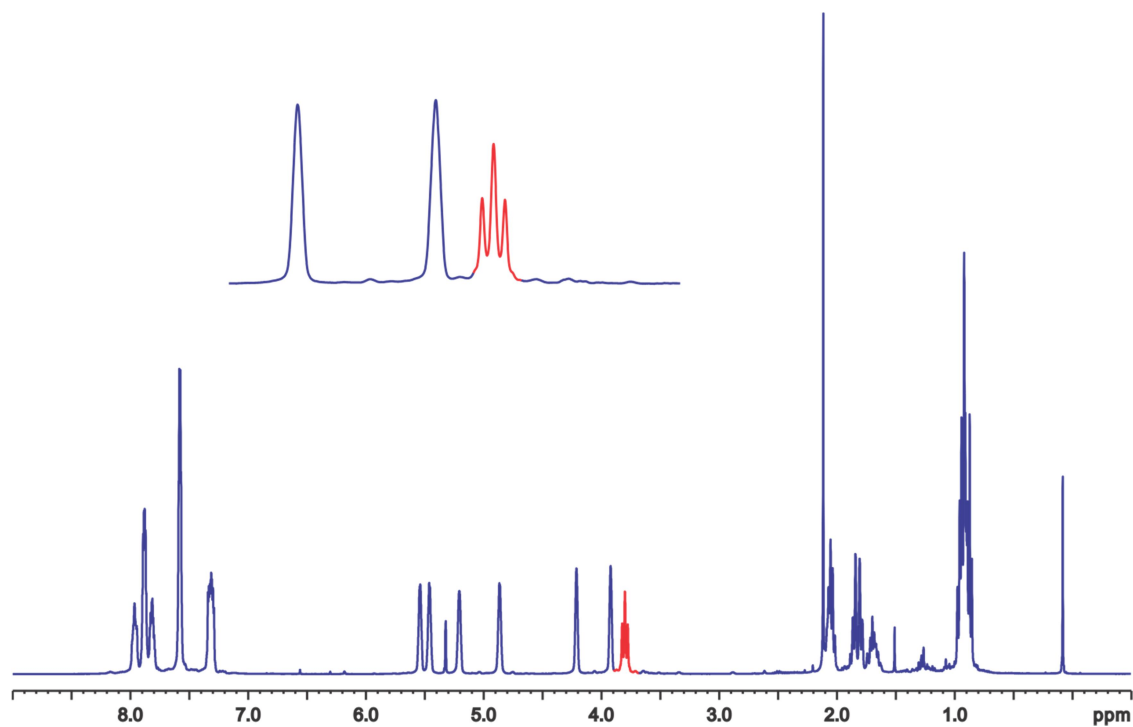


Figure 4.2.26. The ^1H NMR of $[\text{rac-Rh}_2(\text{nbd})_2(\text{et,ph-P4-Ph})](\text{BF}_4)_2$ in CD_2Cl_2 .

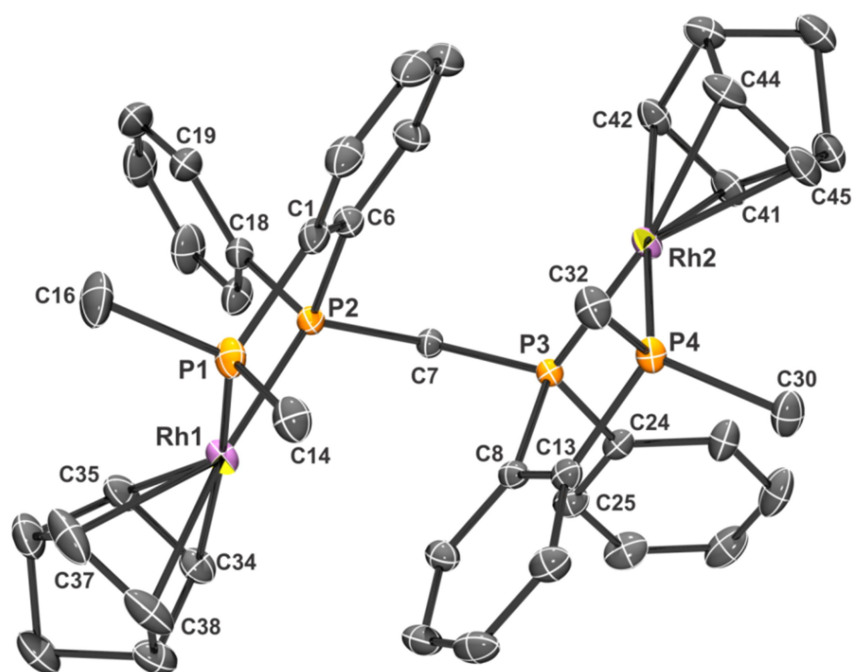


Figure 4.2.27. ORTEP plot (50% ellipsoids) of $[\text{Rh}_2(\text{nbd})_2(\text{rac-et,ph-P4-Ph})]^{+2}$ (hydrogens omitted for clarity).

Table 4.2.6. Selected Bond Distances (Å) and Angles (°) for [Rh₂(nbd)₂(*rac*-et,ph-P4-Ph)](BF₄)₂, 2C₃H₆O

Rh1-C34	2.257(2)	Rh2-C41	2.221(2)
Rh1-C35	2.229(2)	Rh2-C42	2.243(2)
Rh1-C37	2.207(2)	Rh2-C44	2.209(2)
Rh1-C38	2.227(2)	Rh2-C45	2.211(2)
Rh1-P1	2.2822(5)	Rh2-P3	2.2798(5)
Rh1-P2	2.2948(5)	Rh2-P4	2.2869(6)
P2-C7	1.839(2)	P3-C7	1.844(2)
P1-Rh1-P2	84.648(19)	P3-Rh2-P4	84.57(2)
P1-Rh1-C34	168.89(6)	P3-Rh2-C41	99.11
P1-Rh1-C35	147.02(6)	P3-Rh2-C42	105.62(6)
P1-Rh1-C37	95.06(6)	P3-Rh2-C44	169.46(8)
P1-Rh1-C38	104.05(6)	P3-Rh2-C45	150.65(9)
P2-Rh1-C34	168.89(6)	P4-Rh2-C41	142.95(7)
P2-Rh1-C35	99.50(6)	P4-Rh2-C42	169.76(6)
P2-Rh1-C37	151.02(7)	P4-Rh2-C44	104.56(7)
P2-Rh1-C38	169.07(6)	P4-Rh2-C45	93.67(7)
C37-Rh1-C38	36.39(9)	C44-Rh2-C45	35.93(12)
C37-Rh1-C35	65.79(8)	C44-Rh2-C41	76.88(9)
C38-Rh1-C35	76.89(8)	C45-Rh2-C41	65.43(10)
C37-Rh1-C34	76.95(8)	C44-Rh2-C42	65.38(9)
C38-Rh1-C34	64.94(8)	C45-Rh2-C42	77.01(9)
C35-Rh1-C34	35.55(9)	C41-Rh2-C42	35.93(9)
P2-C7-P3	118.60(10)		

The structure reveals that it is a dicationic bimetallic complex, each rhodium center is in +1 oxidation state (d⁸ electron configuration), and adopts the expected square planar coordination geometry. The *rac*-et,ph-P4-Ph ligand is coordinated in the anticipated bridging and chelating manner.

The structure is similar to previously described $[\text{Rh}_2(\text{nbd})_2(\text{rac-et,ph-P4})](\text{BF}_4)_2$.^{2a} The two rhodium centers are rotated away from each other such that Rh...Rh distance is 6.010 Å, somewhat longer than the Rh...Rh distance of 5.527 Å found in $[\text{rac-Rh}_2(\text{nbd})_2(\text{et,ph-P4})](\text{BF}_4)_2$. The dihedral Rh-P1...P2-Rh angle is 122.5°, which is quite a bit larger than the 110.7° value observed in $[\text{rac-Rh}_2(\text{nbd})_2(\text{et,ph-P4})](\text{BF}_4)_2$. The central P-C-P angle for 6R is 118.6°, also comparable to that found in $[\text{rac-Rh}_2(\text{nbd})_2(\text{et,ph-P4})](\text{BF}_4)_2$ (120.9°), $\text{Pt}_2\text{Cl}_4(\text{rac-et,ph-P4-Ph})$ (122.1°), and $\text{Ni}_2\text{Cl}_4(\text{rac-et,ph-P4-Ph})$ (118.6°).^{2a, 6} The Rh-P bond lengths Rh1-P1, Rh-P2, Rh2-P3, Rh2-P4 are 2.2822(5) Å, 2.2948(5) Å, 2.2798(5) Å, 2.2869(6) Å, respectively, and are practically the same as those found in $[\text{Rh}_2(\text{nbd})_2(\text{rac-et,ph-P4})](\text{BF}_4)_2$ (2.2929(6) Å, 2.2996(6) Å, 2.2850(6) Å, 2.3204(6) Å). The bond lengths and angles in the norbornodiene ligands are very similar to those previously reported.²⁶

4.3 Conclusions and Future Directions

The synthesis of the et,ph-P4-Ph ligand was revised and successful chromatographic procedure for separation and purification of the *rac*- and *meso*-diastereomers of et,ph-P4-Ph ligand were developed. The synthesis described here affords the desired tetraphosphine ligand in high yield and in 98% purity (after column chromatography). Iodine-magnesium exchange mechanism that we applied for the preparation of aryl phosphine Grignard reagent can be extended to other substituted phosphines. The most interesting feature of the synthesis is that *meso* form of et,ph-P4-Ph ligand is formed almost exclusively during the reaction, with just traces of the *rac*-et,ph-P4-Ph. Heating is required in order to obtain a 1:1 mixture of *rac*- and *meso*-et,ph-P4-Ph.

We have shown that *rac*-et,ph-P4-Ph ligand may be used to generate bimetallic Pt and Rh complexes, *rac*-Pt₂Cl₄(et,ph-P4-Ph), 4R and [*rac*-Rh₂(nbd)₂(et,ph-P4-Ph)](BF₄)₂, 6R. Both complexes have been characterized by ³¹P{¹H} NMR spectroscopy and single-crystal X-ray diffraction studies. In the solid-state the two metal centers metal are rotated away from each other such that Rh...Rh distance is 6.010 Å, and Pt...Pt distance is 5.920 Å (Pt1-Pt2) and 5.992 Å (Pt3-Pt4). Bimetallic Rh complex, [*rac*-Rh₂(nbd)₂(et,ph-P4-Ph)](BF₄)₂, 6R can be prepared in 85-92% yield and will be tested as a catalytic precursor for hydroformylation. Work is currently underway to synthesize the *meso* form of the bimetallic Rh complex, 6M, which will also be tested for hydroformylation. The use of *rac* and *meso* forms of the catalyst precursor should provide information into the mechanism of hydroformylation with this new stronger chelating ligand. We believe that the far stronger chelate effect of the et,ph-P4-Ph ligand will produce catalysts that will have the high activity and regioselectivity observed for the previously described et,ph-P4 ligand, but will be far more resistant to the deactivating fragmentation reactions.

Preparation of bimetallic Pt complex, *rac*-Pt₂Cl₄(et,ph-P4-Ph), 4R will be carried out on the larger scale and will also be tested for hydroformylation and other reactions. We have shown that heterobimetallic, NiPtCl₄(*rac*-et,ph-P4-Ph), 5R can be prepared by careful addition of 1 equiv of Ni₂Cl₄·6H₂O to a solution of *rac*-et,ph-P4-Ph, followed by the dropwise addition of 1 equiv of PtCl₂(cod). Heterobimetallic 5R has been characterized spectroscopically and by crystallography. Although the X-ray structure has a Pt/Ni disorder problem, the refinements strongly suggest that the system is heterobimetallic. The ¹H NMR data for the central P4 methylene bridge is the strongest

evidence for the heterobimetallic Ni-Pt complex, 5R. Heterobimetallic structures will be used in the future for hydroformylation and other reactions.

4.4 References

1. (a) Laneman, S. A.; Fronczek, F. R.; Stanley, G. G., A new class of binucleating tetratertiaryphosphine ligands. The synthesis and crystallographic characterization of the chiral diastereomer of a rhodium(I) dimer: $\text{Rh}_2\text{Cl}_2(\text{CO})_2(\text{eLTTP})$ ($\text{eLTTP} = (\text{Et}_2\text{PCH}_2\text{CH}_2)(\text{Ph})\text{PCH}_2\text{P}(\text{Ph})(\text{CH}_2\text{CH}_2\text{PEt}_2)$). *Journal of the American Chemical Society* **1988**, *110* (16), 5585-5586; (b) Laneman, S. A.; Fronczek, F. R.; Stanley, G. G., Synthesis of binucleating tetratertiary phosphine ligand system and the structural characterization of both meso and racemic diastereomers of {bis[(diethylphosphinoethyl)phenylphosphino]methane}tetrachlorodinickel. *Inorganic Chemistry* **1989**, *28* (10), 1872-1878.
2. (a) Broussard, M. E.; Juma, B.; Train, S. G.; Peng, W.-J.; Laneman, S. A.; Stanley, G. G., A Bimetallic Hydroformylation Catalyst: High Regioselectivity and Reactivity Through Homobimetallic Cooperativity. *Science* **1993**, *260* (5115), 1784-1788; (b) Aubry, D. A.; Bridges, N. N.; Ezell, K.; Stanley, G. G., Polar Phase Hydroformylation: The Dramatic Effect of Water on Mono- and Dirhodium Catalysts. *Journal of the American Chemical Society* **2003**, *125* (37), 11180-11181; (c) Matthews, R. C.; Howell, D. K.; Peng, W.-J.; Train, S. G.; Treleaven, W. D.; Stanley, G. G., Bimetallic Hydroformylation Catalysis: In Situ Characterization of a Dinuclear Rhodium(II) Dihydrido Complex with the Largest Rh-H NMR Coupling Constant. *Angewandte Chemie International Edition in English* **1996**, *35* (19), 2253-2256.
3. (a) Matthews, R. C. *In Situ Spectroscopic Studies of a Bimetallic Hydroformylation Catalyst*. Louisiana State University, 1999; (b) Gueorguieva, P. G. *Spectroscopic and Synthetic Studies Relating to a Dirhodium Hydroformylation Catalyst*. Louisiana State University, 2004; (c) Polakova, D. *Studies on a Dirhodium Tetrphosphine Hydroformylation Catalyst*. Louisiana State University, Baton Rouge, 2012.
4. Hunt, C.; Fronczek, F. R.; Billodeaux, D. R.; Stanley, G. G., A Monometallic Rh(III) Tetrphosphine Complex: Reductive Activation of CH_2Cl_2 and Selective Meso to Racemic Tetrphosphine Ligand Isomerization. *Inorganic Chemistry* **2001**, *40* (20), 5192-5198.
5. Hunt, C.; Nelson, B. D.; Harmon, E. G.; Fronczek, F. R.; Watkins, S. F.; Billodeaux, D. R.; Stanley, G. G., A binuclear rhodium(I) complex with two tetrphosphine ligands at 100 K. *Acta Crystallographica Section C* **2000**, *56* (5), 546-548.
6. Schreiter, W. J. *Investigations into Alkene Hydration and Oxidation Catalysis*. Louisiana State University, Baton Rouge, 2013.

7. (a) Warren, L. F.; Bennett, M. A., Stabilization of high formal oxidation states of the first-row transition metal series by o-phenylenebis(dimethylphosphine). *Journal of the American Chemical Society* **1974**, *96* (10), 3340-3341; (b) Warren, L. F.; Bennett, M. A., Comparative study of tertiary phosphine and arsine coordination to the transition metals. Stabilization of high formal oxidation states by o-phenylene-based chelate ligands. *Inorganic Chemistry* **1976**, *15* (12), 3126-3140; (c) Sethulakshmi, C. N.; Subramanian, S.; Bennett, M. A.; Manoharan, P. T., Electron paramagnetic resonance studies of two low-spin hexacoordinate di(tertiary phosphine) complexes of nickel(III). *Inorganic Chemistry* **1979**, *18* (9), 2520-2525; (d) Roberts, N. K.; Wild, S. B., Metal complexes containing diastereoisomers and enantiomers of o-phenylenebis(methylphenylarsine) and its phosphorus analog. 1. Stereochemistry and dynamic behavior of square-planar and square-pyramidal complexes of bivalent nickel. *Inorganic Chemistry* **1981**, *20* (6), 1892-1899; (e) Roberts, N. K.; Wild, S. B., Metal complexes containing Diastereoisomers and Enantiomers of o-Phenylenebis(methylphenylarsine) and its Phosphorous Analogue. 2. Stereochemistry and Dynamic Behaviour of Square-Planar and Square-Pyramidal Complexes of Bivalent Palladium and Platinum. *Inorganic Chemistry* **1981**, *20* (6), 1900-1910; (f) Mashima, K.; Komura, N.; Yamagata, T.; Tani, K.; Haga, M. A., Synthesis and Crystal Structure of a Cationic Trinuclear Ruthenium(II) Complex, $[\text{Ru}_3(\mu^2\text{-Cl})_3(\mu^3\text{-Cl})_2\{1,2\text{-bis(diphenylphosphino)benzene}\}_3]\text{PF}_6$. *Inorganic Chemistry* **1997**, *36* (13), 2908-2912; (g) McDonagh, A. M.; Humphrey, M. G.; Hockless, D. C. R., Selective preparation of cis-or trans-dichlorobis{(R,R)-1,2-phenylenebis(methylphenylphosphine-P)}osmium(II) from dimethylsulfoxide complex precursors. *Tetrahedron: Asymmetry* **1997**, *8* (21), 3579-3583.
8. Monteil, A. R. Investigation into the Dirhodium-Catalyzed Hydroformylation of 1-Alkenes and Preparation of a Novel Tetraphosphine Ligand. Ph.D. Dissertation, Louisiana State University, 2006.
9. Peterson, M. A. Toward the Advancement of Tetraphosphine Ligand Synthesis for Homogeneous Bimetallic Catalysis. Louisiana State University, Baton Rouge, 2013.
10. Aubry, D. A.; Laneman, S. A.; Fronczek, F. R.; Stanley, G. G., Separating the Racemic and Meso Diastereomers of a Binucleating Tetraphosphine Ligand System through the Use of Nickel Chloride. *Inorganic Chemistry* **2001**, *40* (19), 5036-5041.
11. (a) Schmidbaur, H.; Schnatterer, S., Synthese und Eigenschaften offenkettiger und cyclischer λ^3 , λ^3 -Diphosphaalkane $\text{RR}'\text{P-CH}_2\text{-PR}'\text{R}$. *Chemische Berichte* **1986**, *119* (9), 2832-2842; (b) Gol, F. H., G.; Knüppel, P. C.; Stelzer, O., *Z. Naturforsch., B: Chem. Sci.* **1988**, *43* (1), 31-34.
12. Weferling, N., Neue Methoden zur Chlorierung von Organophosphorverbindungen mit P-H-Funktionen. *Zeitschrift für anorganische und allgemeine Chemie* **1987**, *548* (5), 55-62.

13. Hart, F. A., 665. The preparation of o-phenylenedi(tertiary phosphines) and a tri(tertiary phosphine). *Journal of the Chemical Society (Resumed)* **1960**, (0), 3324-3328.
14. Bennett, M. A.; Bhargava, S. K.; Hockless, D. C. R.; Welling, L. L.; Willis, A. C., Dinuclear Cycloaurated Complexes Containing Bridging (2-Diphenylphosphino)phenylphosphine and (2-Diethylphosphino)phenylphosphine, $C_6H_4PR_2$ (R = Ph, Et). Carbon–Carbon Bond Formation by Reductive Elimination at a Gold(II)–Gold(II) Center. *Journal of the American Chemical Society* **1996**, 118 (43), 10469-10478.
15. Talay, R.; Rehder, D., *Z. Naturforsch., B: Chem.* **1981**, 36, 451-62.
16. Boymond, L.; Rottländer, M.; Cahiez, G.; Knochel, P., Preparation of Highly Functionalized Grignard Reagents by an Iodine–Magnesium Exchange Reaction and its Application in Solid-Phase Synthesis. *Angewandte Chemie International Edition* **1998**, 37 (12), 1701-1703.
17. Prevost, C., *Bull. Soc. Chim. Fr.* **1931**, 49.
18. (a) Jensen, A. E.; Dohle, W.; Sapountzis, I.; Lindsay, D. M.; Vu, V. A.; Knochel, P., Preparation and reactions of functionalized arylmagnesium reagents. *Synthesis-Stuttgart* **2002**, (4), 565-569; (b) Knochel, P.; Dohle, W.; Gommermann, N.; Kneisel, F. F.; Kopp, F.; Korn, T.; Sapountzis, I.; Vu, V. A., Highly Functionalized Organomagnesium Reagents Prepared through Halogen–Metal Exchange. *Angewandte Chemie International Edition* **2003**, 42 (36), 4302-4320.
19. (a) Villieras, J.; Kirschleger, B.; Tarhouni, R.; Rambaud, M., NUCLEOPHILIC PROPERTIES OF MONOHALOGENATED, NONFUNCTIONALIZED CARBENOIDs. *Bulletin De La Societe Chimique De France* **1986**, (3), 470-478; (b) Tamborsk.C; Moore, G. J., Synthesis Of Polyfluoroaromatic Magnesium Compounds Through Exchange Reaction. *Journal of Organometallic Chemistry* **1971**, 26 (2), 153-&.
20. Cali, P.; Begtrup, M., Synthesis of arylglycines by reaction of diethyl N-Boc-iminomalonate with organomagnesium reagents. *Synthesis-Stuttgart* **2002**, (1), 63-66.
21. Nair, P.; Anderson, G. K.; Rath, N. P., Palladium and Platinum Complexes Containing the Linear Tetrphosphine Bis[[(diphenylphosphino)ethyl]phenylphosphino]methane. *Organometallics* **2003**, 22 (7), 1494-1502.
22. Nair, P.; Anderson, G. K.; Rath, N. P., Bimetallic platinum complexes containing linear tetrphosphine ligands. *Inorganic Chemistry Communications* **2002**, 5 (9), 653-656.

23. Goller, H.; Brüggeller, P., Binuclear platinum(II) complexes containing 1,1,4,7,10,10-hexaphenyl-1,4,7,10-tetraphosphadecane (P4): first X-ray structure of a tetraphos dimer. *Inorganica Chimica Acta* **1992**, 197 (1), 75-81.
24. (a) Nair, P.; Anderson, G. K.; Rath, N. P., Approaches to bi- and trimetallic platinum and palladium complexes using the DPPEPM ligand. *Inorganic Chemistry Communications* **2003**, 6 (10), 1307-1310; (b) Nair, P.; White, C. P.; Anderson, G. K.; Rath, N. P., Unsymmetrical complexes containing the linear tetraphosphine ligand DPPEPM. *Journal of Organometallic Chemistry* **2006**, 691 (3), 529-537.
25. Saum, S. E.; Askham, F. R.; Laneman, S. A.; Stanley, G. G., The synthesis of heterobimetallic systems based on a hexatertiaryphosphine ligand system: cobalt-nickel and nickel-platinum complexes. *Polyhedron* **1990**, 9 (10), 1317-1321.
26. (a) Cano, M.; Heras, J. V.; Ovejero, P.; Pinilla, E.; Monge, A., Heterobimetallic group 6 rhodium complexes: I. Formation of tribridges derivatives $[(OC)_3M(\mu-Cl)(\mu-CO)(\mu-dppm)Rh(NBD)]$ (M = Mo, W) by ring opening of $[(CO)_4M(dppm-PP)]$. Crystal structure of $[(CO)_3Mo(\mu-Cl)(\mu-CO)(\mu-dppm)Rh(NBD)]$. *Journal of Organometallic Chemistry* **1991**, 410 (1), 101-110; (b) Robertson, J. J.; Kadziola, A.; Krause, R. A.; Larsen, S., Preparation and characterization of four- and five-coordinate rhodium(I) complexes. Crystal structures of chloro(2-phenylazo)pyridine)(norbornadiene)rhodium(I), (2,2'-bipyridyl)(norbornadiene)rhodium(I) chloride hydrate, and chloro(2,2'-bipyridyl)(norbornadiene)rhodium(I). *Inorganic Chemistry* **1989**, 28 (11), 2097-2102.

Chapter 5: Experimental Procedures and Additional Spectroscopic Data

5.1 General Considerations

Unless otherwise noted, all manipulations were carried out under a nitrogen atmosphere by using Schlenk and glove box techniques. Organic solvents and chemicals were from Sigma-Aldrich; Et_2Zn and $\text{NiCl}_2 \cdot 6\text{H}_2\text{O}$ were from Strem Chemicals. Neutral alumina was obtained from Fisher. The et,ph-P4 , $\text{Ni}_2\text{Cl}_4(\text{et,ph-P4})$ were prepared as previously described.¹ Monometallic Ni complexes, $\text{NiCl}_2(\text{dppe})$, $\text{NiCl}_2(\text{dcpe})$, $\text{NiCl}_2(\text{dppp})$ and $\text{NiCl}_2(\text{tpp})_2$ were made according to the literature procedures.² $(\text{H})(\text{Ph})\text{PCH}_2\text{P}(\text{Ph})(\text{H})$, Et_2PCl , $[\text{Rh}(\text{nbd})_2](\text{BF}_4)$ were prepared as previously described.³ Solvents were obtained dry and under N_2 or degassed with N_2 and were used without further purification. All NMR spectra were recorded on a Bruker Avance spectrometer (^1H at 400.0 MHz, ^{31}P at 161.9 MHz), a Bruker DPX 250 MHz spectrometer, or an Avance III 400 MHz spectrometer. NMR data was analyzed and simulated using MestReNova (v8.1.1).

^1H chemical shifts are reported relative to TMS. ^{31}P chemical shifts are reported relative to the signal of external 85% H_3PO_4 . The GC/MS data was obtained on Agilent Technologies 6890N Network GC system/5975 B VL MSD. Column = HP-5MS (30m x 0.25mm x 0.25 μm). High resolution MS data obtained from an Agilent 6210 LC electrospray system.

5.2 General Procedure Used to Study Alkene Oligomerization Catalysis

Typically reactions were carried out in the presence of oxygen/air, but a number of reactions were carried out under a nitrogen atmosphere.

A round bottom flask was charged with solid *meso*-Ni₂Cl₄(*et*,*ph*-P₄) (0.145 g, 0.2 mmol) and 20 ml of acetone/water (15-30% water by volume). The flask was placed in a warm water bath and allowed to stir for 10-15 min (or until homogeneous solution was formed). To this was added required alkene substrate (20 mmol, 100 equiv), the flask was then attached to the condenser and reaction mixture was stirred overnight at 70-80°C. Samples of the reaction mixture were taken from reaction in progress at the appropriate time interval and analyzed by GC-MS. The products were extracted with hexane (3 × 10 ml) and after removal of the solvents *in vacuo* a small amount of the off-white solid was obtained. Amount of the off-white solid obtained varied slightly for different experiments and was equal to 0.100-0.150 g.

For experiments with increasing catalyst concentration 20 mM and 30 mM solutions of mixed *rac,meso*-Ni₂Cl₄(*et*,*ph*-P₄) in 20 ml of acetone/water (water 30% by volume) were used. Concentration of the 1-hexene substrate was 1M.

Alkene substrates tested: 1-hexene, cyclohexene, norbornadiene, allyl alcohol, and vinyl acetate.

For ¹H and ³¹P{¹H} NMR analysis reactions were carried out on the small scale (3mL = total volume) in the deuterated organic solvents and D₂O.

5.3 General Procedure Used to Test for Alkene Hydration

Typically reactions were carried out in the presence of oxygen/air, but a number of reactions were carried out under a nitrogen atmosphere by using Schlenk and glove box techniques.

Reaction parameters such as organic solvent, amount of water, and temperature were varied in the study. Organic solvents tested: acetone, THF, acetonitrile, toluene,

DMSO, CH₂Cl₂. Amount of water: All reactions contained at least 5%, 10%, 15%, 20%, 25%, 30% water. Temperature: 25°C, 40-45°C, 70-75°C, 95-100°C

Method A

A round bottom flask was charged with solid *meso*-Ni₂Cl₄(*et*,*ph*-P4) or a mixture of *rac*, *meso*-Ni₂Cl₄(*et*,*ph*-P4) (0.145 g, 0.2 mmol) and 20 ml of organic solvent/water (5-30% water by volume). The flask was placed in a warm water bath and allowed to stir for 10-15 min (or until homogeneous solution was formed). To this was added the required alkene substrate (20 mmol, 100 equiv), the resulting mixture was stirred overnight at 25°C or with heating to the desired temperature. Samples of the reaction mixture were taken from reaction in progress at the appropriate time interval and analyzed by GC/MS.

Method B

Same as Method A, the only difference is that prior to addition of 1-hexene a desired amount (1, 2, or 4 equivalents to Ni complex) of AgBF₄ was added. The resulting mixture was stirred for 20 min and the white precipitate was removed by filtration. To a clear filtrate solution was added 1-hexene (20 mmol, 100 equiv to Ni complex) and the mixture was stirred overnight at 25°C or with heating to the desired temperature. Samples of the reaction mixture were taken from reaction in progress at the appropriate time interval and analyzed by GC/MS.

5.4 Synthesis and Characterization of *meso*-Ni₂Cl₄(*et*,*ph*-P4)

The *meso*-Ni₂Br₄(*et*,*ph*-P4) complex was made according to the literature procedures with modification for the desired halide.¹ Final product was obtained as a brown-orange powder in 96% yield.

$^{31}\text{P}\{^1\text{H}\}$ NMR (161.976 MHz, CD_2Cl_2): $P_{\text{ext}} = 80.6$ ppm (pseudo dt) ($J_{\text{P-P}} = 61.8$ Hz); $P_{\text{int}} = 64.9$ ppm (dd) ($J_{\text{P-P}} = 61.6$ Hz).

Assignments for internal and terminal phosphorus atoms have been made tentatively based on the previous assignments for the *rac*- and *meso*- $\text{Ni}_2\text{Cl}_4(\text{et,ph-P4})$ complexes.

Orange crystals of *meso*- $\text{Ni}_2\text{Br}_4(\text{et,ph-P4})$ suitable for X-ray diffraction were obtained by slow evaporation of an CH_3CN solution at room temperature.

5.5 General Procedure Used to Study Alkene Oxidative Cleavage Catalysis

Typically reactions were carried out in the presence of oxygen/air, or under balloon pressure of oxygen.

A round bottom flask equipped with a magnetic stir bar was charged with the appropriate Ni complex (10mM) and solvent (2 to 20 ml total volume). The mixture was allowed to stir for a few minutes to fully dissolve the metal complexes, followed by addition of substrate (5-100 eq. to Ni). The flask was purged with O_2 . After being stirred at room temperature for the desired length of time, samples were taken and analyzed by GC-MS. For ^1H and $^{31}\text{P}\{^1\text{H}\}$ NMR analysis reactions were carried out in the deuterated organic solvents and D_2O .

Alkene substrates tested: 1-hexene, 1-octene, styrene, cyclohexene, cyclopentene, norbornene, and norbornadiene.

Amount of benzaldehyde produced was quantified via GC-MS using internal standard and was equal to 3 mM on average.

5.6 Reaction of *meso*-Ni₂Cl₄(et,ph-P4) and 1-Hexene Monitored by Variable Temperature NMR

An aliquot of a freshly prepared acetone-d₆/D₂O solution of *meso*-Ni₂Cl₄(et,ph-P4) (10mM) was added to a 5-mm NMR tube. After determining the ¹H and ³¹P{¹H} NMR spectra at –20°C, one drop of 1-hexene was added. The ¹H and ³¹P{¹H} NMR spectra were recorded at –20, –5, +5 and + 25°C.

5.7 Variable Temperature NMR of the “final” Species

For this experiment, an aliquot from the reaction of *meso*-Ni₂Cl₄(et,ph-P4) (10mM) with 1-hexene (30 eq.) in acetone-d₆/D₂O solution was placed into a 5-mm NMR tube. The ¹H and ³¹P{¹H} NMR spectra were recorded at –5, +5 and + 25°C. The sample was then carefully transferred into a high pressure 5-mm NMR tube and pressurized with 90 psi of oxygen. The ¹H and ³¹P{¹H} NMR spectra were recorded at –5, 25, 50, 80 and 100°C.

5.8 Synthesis of Methylenebis(chlorophenylphosphine), 2

Method A (Table 3.2.2, entry 1)

This procedure has been previously reported.⁴ Round bottom flask was loaded with (H)(Ph)PCH₂P(Ph)(H), 1 (6.62 g, 28.5 mmol), C₂Cl₆ (13.50 g, 57.0 mmol) and diethyl ether (55 mL). The resulting mixture was heated to 35-39°C and allowed to stir for 24 h. At the end of this time period solution was light pink in color and a white solid (unreacted C₂Cl₆) was formed. The mixture was cooled to room temperature and filtered over a plug of Celite. After partial (about 5 mL) removal of the solvent *in vacuo* (with heating to 50-55°C) more of the white solid crashed of the solution and filtration over a plug of Celite was repeated at least three times. White solid could not be completely

separated from the final product. Final product mixture (3.60 g, 42%) was obtained as viscous pink oil (2 and a small amount of C₂Cl₆ that remained after repeated filtrations).

³¹P {¹H} NMR (161.976 MHz, CDCl₃): 83.2 ppm (s) [lit. 81.8 ppm (s) and 81.6 ppm (s)].

Method B (Table 3.2.2, entry 2)

This procedure is a modification of previously reported. To a solution of C₂Cl₆ (16.05 g, 67.8 mmol) in diethyl ether (70 mL) heated to 35°C solution of 1 (7.87 g, 33.9 mmol) in Et₂O (35 mL) was added dropwise over a period of 15 min. The reaction was allowed to proceed with stirring at 35°C for 24h. Same work up as described in Method A. Unfortunately % yield could not be determined due to the failure to separate compound 2 from unreacted C₂Cl₆. Total of 6.49 g (64%) was obtained as a final product mixture (2 and a small amount of C₂Cl₆ that remained after repeated filtrations).

Method C (Table 3.2.2, entry 3)

This procedure is modification of previously reported and is similar to Method B, but the addition was performed in reverse order. Solution of C₂Cl₆ (11.32 g, 47.8 mmol.) in Et₂O (50 mL) was added to 1 (5.55 g, 23.9 mmol) in diethyl ether (25 mL). The % yield was not be determined due to the failure to separate compound 2 from unreacted C₂Cl₆. Total of 2.74 g, (38%) was obtained as a final product mixture (2 and a small amount of C₂Cl₆ that remained after repeated filtrations).

Method D (Table 3.2.2, entry 4)

This procedure was exactly the same as Method A. The only difference was that a 1.5 equivalents of C₂Cl₆ was used per 1 equivalent of 1. Compound 2 was obtained in a 65% purity as estimated by ³¹P{¹H} NMR. The % yield could not be determined due to the failure to separate 2 from unwanted impurities.

Method E (Table 3.2.2, entry 5)

This procedure was adopted from the previously reported procedure.⁵ To a solution of 1 (2.00 g, 8.6 mmol) in toluene (9 mL) heated to 75°C solution of PCl_5 (3.60 g, 17.2 mmol) in toluene (34 mL) was added over a period of 30 minutes. The immediate formation of an orange precipitate was observed. The reaction was allowed to proceed with stirring at 75-81°C for 3 h. Solution was filtered through a plug of Celite to remove the orange precipitate. Clear filtrate solution was concentrated *in vacuo* to yield 2 (80% purity) and a mixture of phosphorus containing species including PCl_3 , PhPCl_2 . The % yield was not determined due to the failure to separate compound 2 from unwanted impurities.

Method F (Table 3.2.2, entry 6)

This procedure was adopted from the previously reported procedure.⁵ A solution of 1 (7.18 g, 30.9 mmol) in toluene (3 mL) was added dropwise within 40 min to a stirred solution of C_2Cl_6 (14.6 g, 61.8 mmol) in toluene (31 mL), heated to 75-80°C. During addition HCl gas was released from the reaction and the flask was occasionally purged with N_2 to help remove HCl released from the reaction. The mixture was allowed to stir for 2 hours at 72-82°C. Solvent was removed *in vacuo* (with heating to 75-80°C) to give 87% of 2 as a light pink oil. Yields are typically between 85-87% and purity is 98% or higher based on ^{31}P NMR.

^{31}P {1H} NMR (161.976 MHz, C_6D_6): 86.9 ppm (s) [lit. 81.8 ppm (s) and 81.6 ppm (s)].⁵

5.9 Synthesis of 1-(Diethylphosphino)-2-Iodobenzene, 3(I)

This procedure is an improvement of the previously reported procedure.⁴ The following procedure was carried out in a Schlenk flask covered with aluminum foil in

order to exclude light. Solution of 1,2-di-iodobenzene (46.03 g, 139.5 mmol) in THF (150.0 mL) cooled to 0°C was slowly treated with 2.9 M solution of *i*PrMgBr in THF (48.1 ml, 139.5 mmol). Reaction was allowed to proceed stirring at 0°C for 1 hour. At the end of this time period a sample from the crude reaction mixture was quenched with water and analyzed via GC-MS. Complete conversion is normally observed in 1 to 2 hours at 0°C. Next reaction mixture was cooled to -25°C and solution of Et₂PCl (17.37 g, 139.5 mmol) in THF (150 mL) cooled to -25°C was added drop-wise. Reaction was allowed stir for 4-6 hours and was allowed to warm to room temperature. Next 50 mL of degassed water was then added to the reaction mixture and stirring was continued for 15 minutes. The organic layer was removed by cannula and aqueous layer was extracted with diethyl ether (3 x 50 mL). The combined organic extracts were dried over Na₂SO₄ and concentrated *in vacuo*. Clean product was obtained by short-path distillation *in vacuo* to yield 29.66 g of air/light sensitive, colorless liquid: bp 130-135°C (0.5 Torr) Yield: 68 %

The yields are typically between 68-77%. The purity is 96% based on ³¹P{¹H} NMR.

³¹P {¹H} NMR (161.976 MHz, C₆D₆): 0.3 ppm (s) [lit. 0.3 ppm (s)].⁴

5.10 Synthesis of 1-(Diethylphosphino)-2-Bromobenzene, 3(Br)

This procedure is an improvement of the previously reported procedure.⁴ The following procedure is similar to the one described for synthesis of 3(I) and was carried out using 1-bromo-2-iodobenzene (13.78 g, 48.7 mmol) and 2.9 M solution of *i*PrMgBr in THF (16.7 ml, 48.7 mmol), and Et₂PCl (6.67 g, 53.6 mmol). Based on the GC-MS analysis of an aliquot taken from the crude reaction mixture after quenching with water complete conversion to the corresponding Grignard reagent was observed after 1.5

hours. Clean product was obtained by short-path distillation *in vacuo* to yield 12.5 g of air sensitive, colorless liquid: bp 84-86°C (0.5 Torr) Yield: 87 % The yields are typically between 83-87%. The purity is 100% based on $^{31}\text{P}\{^1\text{H}\}$ NMR.

$^{31}\text{P}\{^1\text{H}\}$ NMR (161.976 MHz, C_6D_6): -14.1 ppm (s) [lit. -15.4 ppm (s)].⁴

5.11 Synthesis of *rac*, *meso*-et,ph-P4-Ph Ligand

Method A

This procedure has been previously reported.⁴ The following procedure was carried out in a Schlenk flask covered with aluminum foil in order to exclude light. Solution of 3(I) (15.90 g, 54.3 mmol) in THF (40.0 mL) cooled to 0°C was slowly treated with 2.9 M solution of *i*PrMgBr in THF (18.7 ml, 54.3 mmol). Reaction was allowed to stir at 0°C for 6-8 hours. Next the flask was cooled to -25°C and solution of 2 (8.19 g, 27.2 mmol) in THF (40 mL) cooled to -25°C was added drop-wise. Reaction was allowed to slowly warm to room temperature and stir overnight. Degassed water (50 mL) was added to the yellow reaction mixture and stirring was continued for 15 minutes. The organic layer was removed by cannula and aqueous layer was extracted with diethyl ether (3 x 50 ml). Combined organic extracts were dried over Na_2SO_4 and concentrated *in vacuo*. Product purity was not determined via $^{31}\text{P}\{^1\text{H}\}$ NMR spectroscopy because some of the impurities show signals in the same region as et,ph-P4-Ph ligand. At this time unreacted 3(I) can be removed by short-path distillation *in vacuo*. Crude product mixture was purified on neutral alumina (4 x 12 cm column) eluting with CH_2Cl_2 . Purified product mixture consisted of a white pasty mass that contained a mixture of *rac* and *meso*-diastereomers (obtained by epimerization) of et,ph-P4-Ph in 89% purity on average. After separation of *rac* and *meso*-diastereomers the yield is 60-65%. The

meso-et,ph-P4-Ph is not obtained in pure form, because its recovered from the column along with unidentified phosphine impurities.

Method B

This procedure is similar to the one described above (Method A). The only difference is that reaction with 3(I) and *i*PrMgBr was allowed to stir at 0°C for 24 h. A sample from the crude reaction mixture was analyzed via $^{31}\text{P}\{^1\text{H}\}$ NMR to check for complete conversion of 3(I) to the corresponding Grignard reagent. The scale was: 3(I) (7.7 g, 26.3 mmol.) in THF (20 mL), *i*PrMgBr (8.92 mL of 2.9 M), 1 (3.90 g, 13.0 mmol) in THF (10 mL) in diethyl ether (25 mL). $^{31}\text{P}\{^1\text{H}\}$ NMR of the final product mixture showed that amount of phosphine impurities was greatly reduced by comparison to Method A product purity was not determined via $^{31}\text{P}\{^1\text{H}\}$ NMR spectroscopy because some of the impurities show signals in the same region as et,ph-P4-Ph ligand. After purification on neutral alumina a mixture of *rac* and *meso*-diastereomers of et,ph-P4-Ph (obtained by epimerization) was obtained in 89% purity on average. The *meso*-et,ph-P4-Ph is not obtained in a pure form, because its recovered from the column along with unidentified phosphine impurities.

Method C

To a flame dried Schlenk flask (flame dried) equipped with condenser were added 0.955g (39.3 mmol) Mg turning. The setup was evacuated and placed under nitrogen and allowed to stir for 3 days. At the end of that period solution of 3(Br) 7.41g (30.2 mmol) in 30 mL THF (1M) was slowly added to by cannula. The flask was then placed in the oil bath and allowed to stir for 2-3 h at 65-75°C until most of the Mg was consumed. Next solution of Grignard reagent was added dropwise to cooled (-35°C) solution of 2

(4.79g 15.9 mmol) in THF (1M, 16 mL). After addition was complete reaction flask was allowed to slowly warm up to 25°C and was kept stirring overnight. The work up was the same as described above (Method A). After work up the crude product mixture consisted of *meso*-et,ph-P4-Ph (small traces of *rac*-diastereomer present) 77%, unreacted 3(Br) 4%, and 19% unidentified phosphine impurities. The final product mixture after purification on neutral alumina (4 x 12 cm column) eluting with CH₂Cl₂ consisted of a white pasty mass that contained a mixture of *rac* and *meso*-diastereomers of et,ph-P4-Ph (obtained by epimerization) 96% and unreacted 3(Br) 4%. Unreacted 3(Br) can be separated via short path distillation *in vacuo* (bp 84-86°C (0.5 Torr)) without epimerization of the et,ph-P4-Ph ligand. After separation of *rac* and *meso* diastereomers via column chromatography each diastereomer is obtained in 100% purity. The ³¹P NMR values listed below were determined from an AA'BB' spin simulation using MestReNova (version 8.1.1) and manually optimized to fit the experimental spectrum of each diastereomer. A & A' represent the external phosphines (P_{ext}), while B & B' are the internal methylene bridged phosphorus centers (P_{int}).

³¹P{¹H} NMR *meso*-et,ph-P4-Ph (161.976 MHz, CD₂Cl₂): δ P_{ext} = -27.68, P_{int} = -31.42; J_{Pint-Pext} = 146 Hz, J_{Pint-Pext} = 111 Hz, J_{Pint-Pext} = 5 Hz, J_{Pint-Pext} = 1 Hz.

¹H NMR *meso*-et,ph-P4-Ph (400.130 MHz, CD₂Cl₂): δ 7.67 (ddt, *J* = 6.3, 3.1, 1.8 Hz, 2H), 7.59 (ddq, *J* = 8.7, 5.3, 1.9 Hz, 4H), 7.33 – 7.25 (m, 2H), 7.20 – 6.98 (m, 10H), 3.08 (dt, *J* = 13.2, 3.6 Hz, 1H), 2.80 (dt, *J* = 13.2, 4.2 Hz, 1H), 1.61 – 1.51 (m, 2H), 1.50 – 1.33 (m, 2H), 0.95 (dt, *J* = 14.9, 7.6 Hz, 3H), 0.77 (dt, *J* = 14.9, 7.6 Hz, 3H).

High resolution mass spectrometry *meso*-et,ph-P4-Ph: 561.2159 amu (calc, M+H⁺); 561.2168 amu (exp, M+H⁺)

$^{31}\text{P}\{^1\text{H}\}$ NMR *rac*-et,ph-P4-Ph (161.976 MHz, CD_2Cl_2): δ $\text{P}_{\text{ext}} = -27.35$, $\text{P}_{\text{int}} = -30.68$;

$^J\text{P}_{\text{int}}\text{-P}_{\text{ext}} = 142$ Hz, $^J\text{P}_{\text{int}}\text{-P}_{\text{int}} = 122$ Hz, $^J\text{P}_{\text{int2}}\text{-P}_{\text{ext}} = 2$ Hz, $^J\text{P}_{\text{ext}}\text{-P}_{\text{ext}} = 0$ Hz

^1H NMR *rac*-et,ph-P4-Ph (400. 130 MHz, Benzene- d_6): δ 7.73 (ddt, $J = 8.1, 4.7, 1.4$ Hz, 4H), 7.46 (dh, $J = 6.5, 1.5$ Hz, 2H), 7.25 (ddt, $J = 7.1, 2.9, 1.5$ Hz, 2H), 7.19 – 6.94 (m, 10H), 2.99 (t, $J_{\text{P-H}} = 3.4$ Hz, 2H), 1.61 – 1.32 (m, 4H), 0.94 (dt, $J = 14.9, 7.6$ Hz, 3H), 0.80 (dt, $J = 14.8, 7.6$ Hz, 3H).

High resolution mass spectrometry *rac*-et,ph-P4-Ph: 561.2159 amu (calc, $\text{M}+\text{H}^+$); 561.2157 amu (exp, $\text{M}+\text{H}^+$)

5.12 Separation *rac* and *meso*-et,ph-P4-Ph via Column Chromatography

To separate *rac* and *meso* diastereomers of et,ph-P4-Ph and the remaining 3(Br), 0.9 g. of the practically pure product mixture was subjected to a second chromatography on neutral alumina (Grade IV, 4×20 cm column) eluting with a 1:4 CH_2Cl_2 /hexane solvent mixture. A total of 53×10 mL fractions were collected and analyzed by TLC. Fractions 1-5 contained 3(Br), fractions 6-17 contained only solvent, fractions 17-34 contained *meso*-et,ph-P4-Ph, fractions 35-43 contained a mixture of *rac* and *meso*-diastereomers, and fractions 43-53 contained *rac*-et,ph-P4-Ph.

Important notes: The et,ph-P4,Ph slowly react with CH_2Cl_2 to give unidentified products that we are still characterizing. So it is important to remove CH_2Cl_2 solvent as soon as possible.

5.13 Synthesis of $\text{Pt}_2\text{Cl}_4(\text{rac-et,ph-P4-Ph})$, 4R

To a solution of *rac*-et,ph-P4-Ph (0.212 g. 0.378 mmol) in CH_2Cl_2 (25.0 ml) was added $\text{PtCl}_2(\text{cod})$ (0.284 g, 0.756 mmol). Solution was allowed to stir at 25°C for 16-18

hours and solvent was removed *in vacuo*. The residue was washed several times with hexane. The product was isolated as a light yellow powder (78%). Small amount of $\text{PtCl}_2(\text{cod})$ was still present, as observed via ^1H NMR.

^{31}P { ^1H } NMR (161.976 MHz, CD_2Cl_2): $P_{\text{ext}} = 49.7$ ppm (s), $^1J_{\text{PtP}} = 3483$ Hz; $P_{\text{int}} = 30.9$ (s) ($^1J_{\text{PtP}} = 3698$ Hz). Assignments for internal and terminal phosphorus atoms were made tentatively based on the previous assignments.

^1H NMR (400.130 MHz, CD_2Cl_2): 5.18 ppm (t, $J = 14$ Hz PCH_2P) (Figure 3.3.7).

Complex spectrum does not allow for full interpretation.

Crystals suitable for X-ray diffraction were grown by slow evaporation of a CH_3CN solution.

5.14 Synthesis of $\text{PtNiCl}_4(\text{rac-et,ph-P4-Ph})$, 5R

This reaction was carried out on a small scale. Stock solutions (0.03 M, 6.0 mL) of *rac-et,ph-P4-Ph* in DCM and $\text{Ni}_2\text{Cl}_4 \cdot 6\text{H}_2\text{O}$ in ethanol were prepared. To solution of *rac-et,ph-P4-Ph* (3.0 ml of 0.03M) in CH_2Cl_2 slowly was added solution of $\text{Ni}_2\text{Cl}_4 \cdot 6\text{H}_2\text{O}$ (3.0 ml of 0.03M) in ethanol. Reaction flask was carefully shaken by hand for a few minutes, followed by slow addition of $\text{PtCl}_2(\text{cod})$ (0.067 g. 0.18 mmol). Reaction flask was removed from the glove box and allowed to stir for 16 hours at 25°C. After removal of the solvents *in vacuo* the residue was dissolved in the minimal amount of CH_2Cl_2 and precipitated with hexanes. The product was isolated as an orange powder. Final % yield was not determined.

^{31}P { ^1H } NMR (161.976 MHz, C_6D_6): $P_{\text{ext}} = 66.6$ ppm (d, $^1J_{\text{PP}} = 75.1$ Hz), $P_{\text{int}} = 47.7$ (d, $^1J_{\text{PP}} = 75.1$ Hz), $P_{\text{ext}} = 49.74$ ppm (bs, $^1J_{\text{PtP}} = 3493$ Hz), $P_{\text{int}} = 31.84$ (bs, $^1J_{\text{PtP}} = 3644$ Hz).

Assignments for internal and terminal phosphorus atoms have been made tentatively based on the previous assignments.

Crystals suitable for X-ray diffraction were grown by slow evaporation of a CH₃CN solution.

¹H NMR (400. 130 MHz, CD₂Cl₂): 5.05 – 4.77 ppm (two m, PCH₂P). Complex spectrum does not allow for full interpretation.

5.15 Synthesis of [Rh₂(nbd)₂(*rac*-et,ph-P4-Ph)](BF₄)₂, 6R

This procedure is similar to that previously reported for the preparation of [*rac*, *meso*-Rh₂(nbd)₂(et,ph-P4-Ph)](BF₄)₂.⁶ Solution of *rac*-et,ph-P4-Ph (0.470 g, 0.834 mmol) in CH₂Cl₂ (2.5 ml) was added by cannula to a solution of [Rh(nbd)₂](BF₄) (0.613 g, 1.67 mmol) in CH₂Cl₂ (5.0 ml). Reaction was stirred for 1.5-2 hours, followed by removal of CH₂Cl₂ *in vacuo* to yield 6R as a red-brown powder in 87% yield. The yields for this step are typically 85-92%. Clean product was obtained by recrystallization from the minimal amount of acetone at – 40°C. Purification of 6R has not been optimized at this time, but we are able to obtain a small amount of the pure solid at a time via recrystallization from acetone at – 40°C.

³¹P {¹H} NMR (161.976 MHz, CD₂Cl₂): P_{ext} = 56.7 ppm (dd) (J_{Rh-P} = 154.3 Hz, J_{Pint-Pext} = 29.0 Hz), 55.8 ppm (dd) (J_{Rh-P} = 154.3 Hz, J_{Pint-Pext} = 29.0 Hz); P_{int} = 43.9 ppm (dd) (J_{Rh-P} = 160.6 Hz, J_{Pint-Pext} = 29.0 Hz), and 42.9 ppm (dd) (J_{Rh-P} = 160.6 Hz, J_{Pint-Pext} = 29.0 Hz). Assignments for internal and terminal phosphorus atoms have been made tentatively based on the previous assignments. ¹H NMR (400.130 MHz, CD₂Cl₂): 3.80 ppm (t, J_{PH} = 9.6 Hz PCH₂P). Complex spectrum does not allow for a full interpretation. Crystals suitable for X-ray diffraction were grown from acetone at – 40°C.

5.16 Additional Spectroscopic Data

$^{31}\text{P}\{^1\text{H}\}$ NMR: Simulation & Experimental

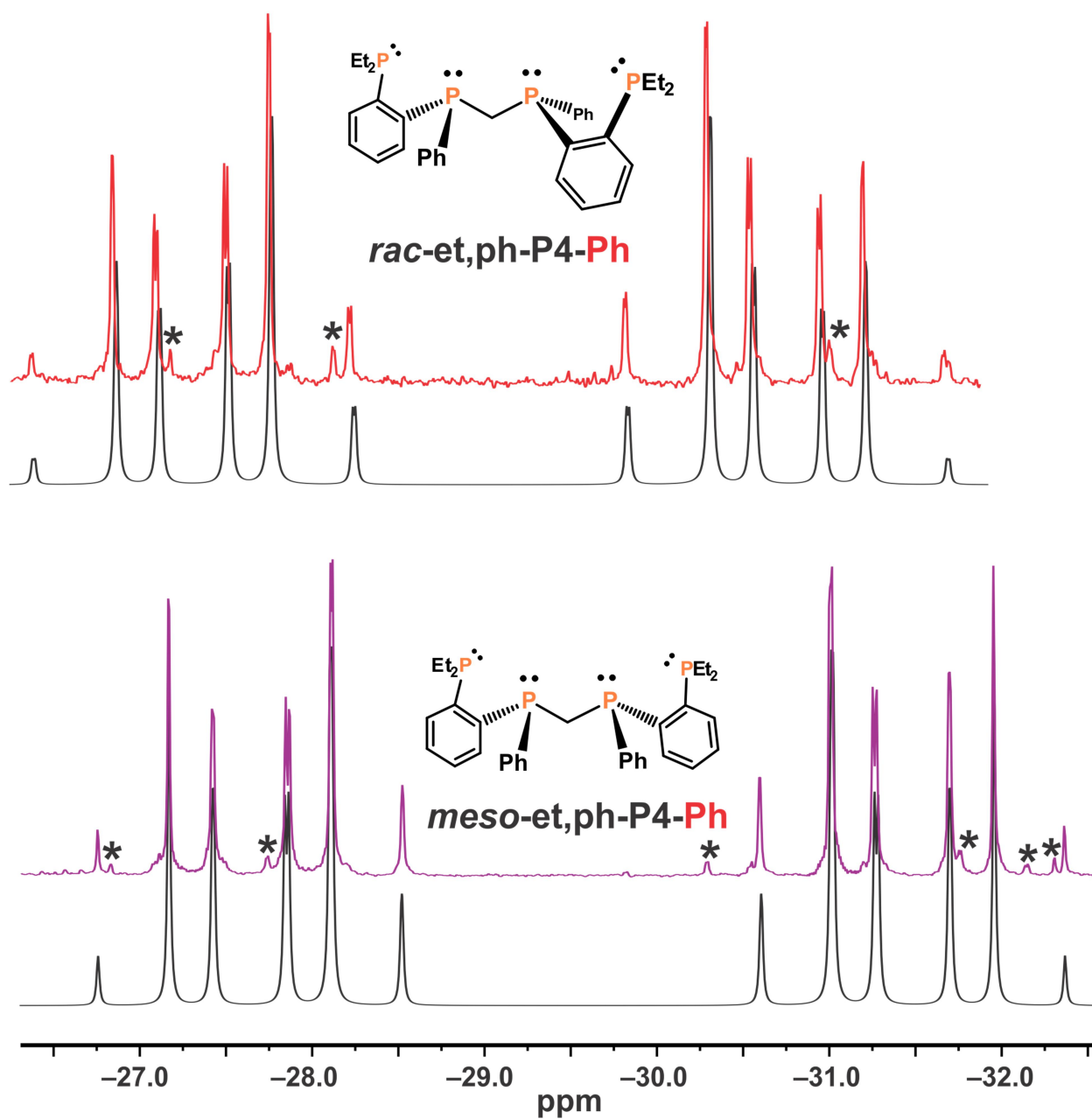


Figure 5.1 $^{31}\text{P}\{^1\text{H}\}$ NMR (experimental and simulated) *rac* and *meso*-et,ph-P4-Ph.

$^{31}\text{P}\{^1\text{H}\}$ NMR: Simulation & Experimental

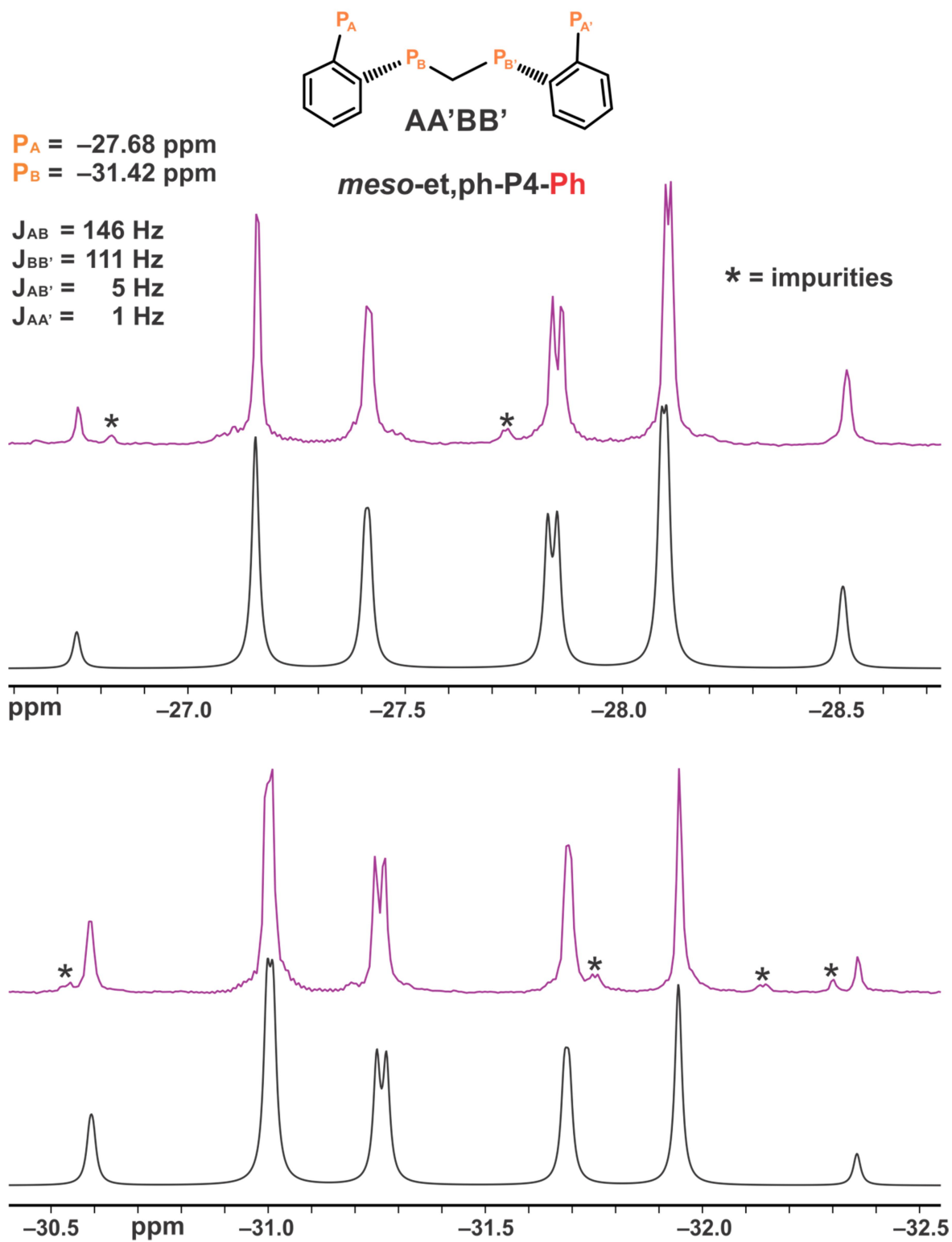


Figure 5.2 $^{31}\text{P}\{^1\text{H}\}$ NMR (experimental and simulated) *meso-et,ph-P4-Ph*

$^{31}\text{P}\{^1\text{H}\}$ NMR: Simulation & Experimental

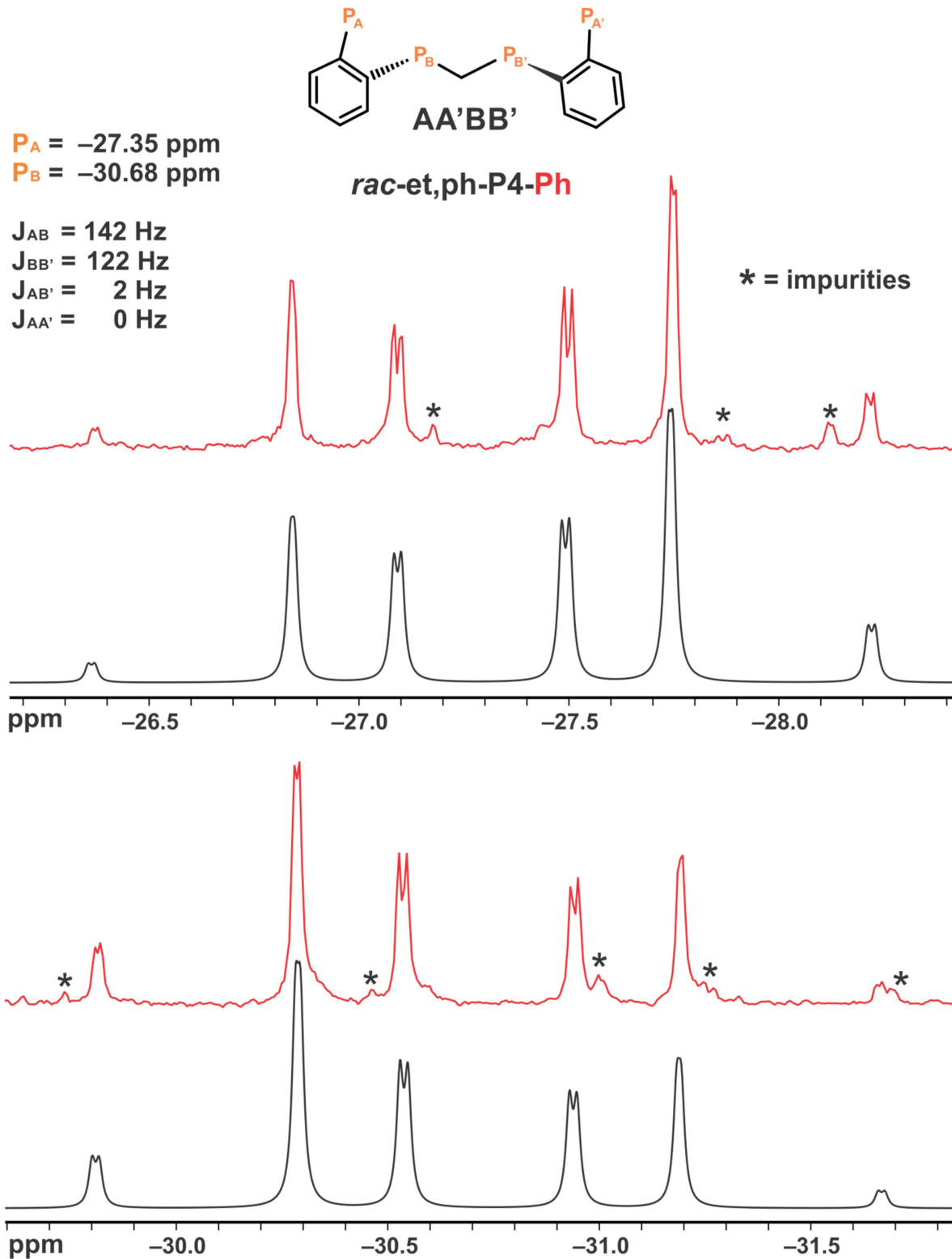


Figure 5.3 $^{31}\text{P}\{^1\text{H}\}$ NMR (experimental and simulated) *rac-et,ph-P4-Ph*.

^1H NMR (400.130 MHz)

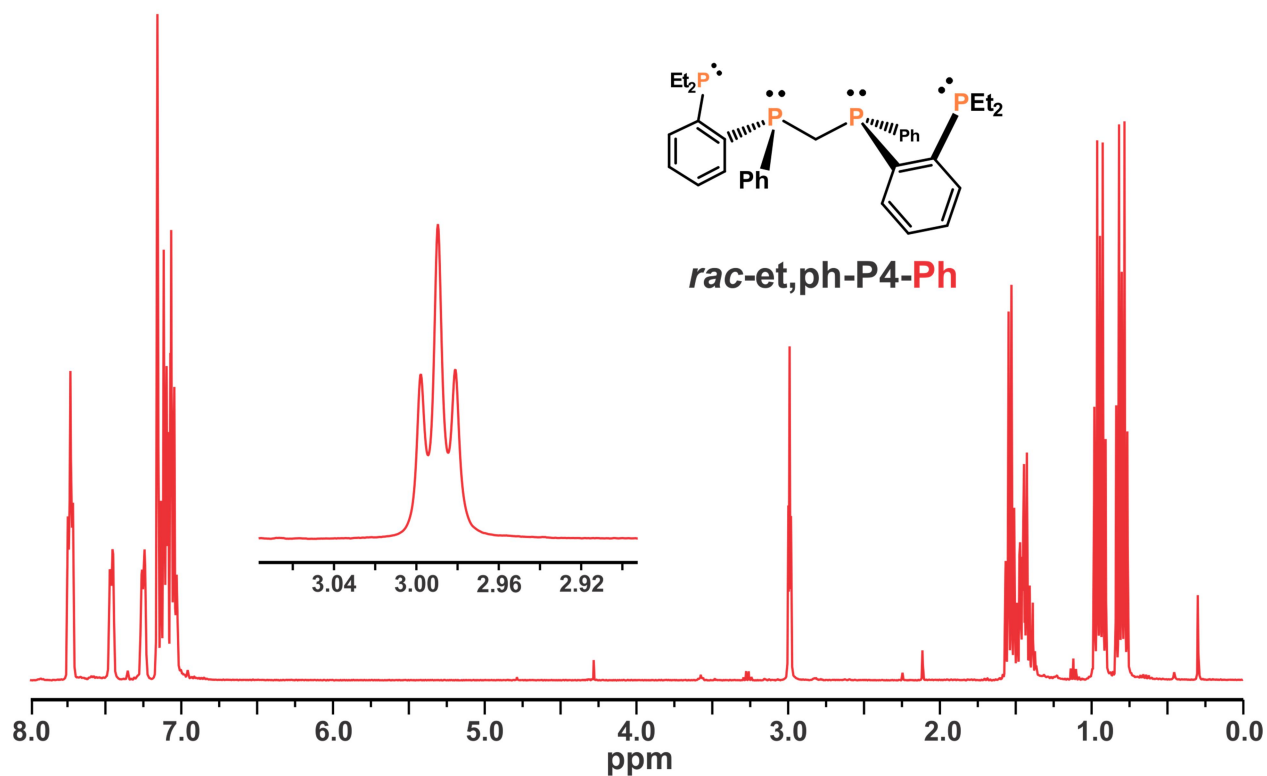
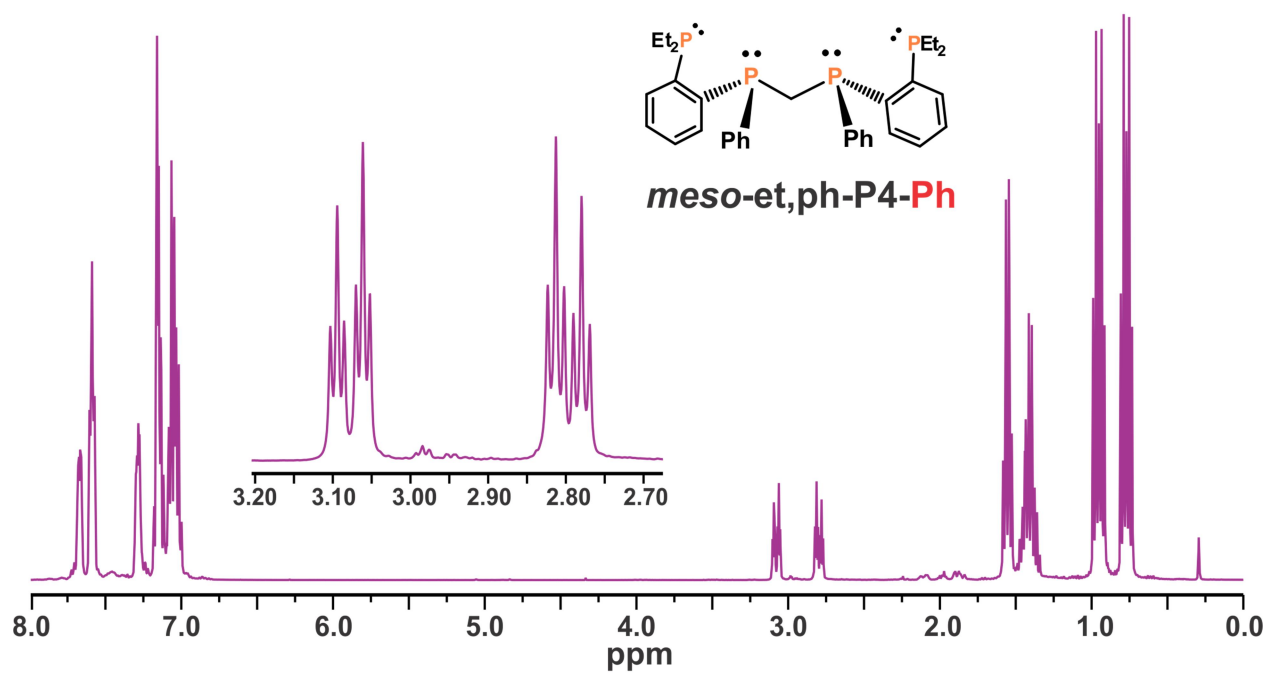
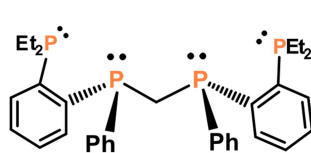


Figure 5.4 ^1H NMR of *rac* and *meso*-et,ph-P4-Ph.

^1H NMR (400.130 MHz)



***meso*-et,ph-P4-Ph**

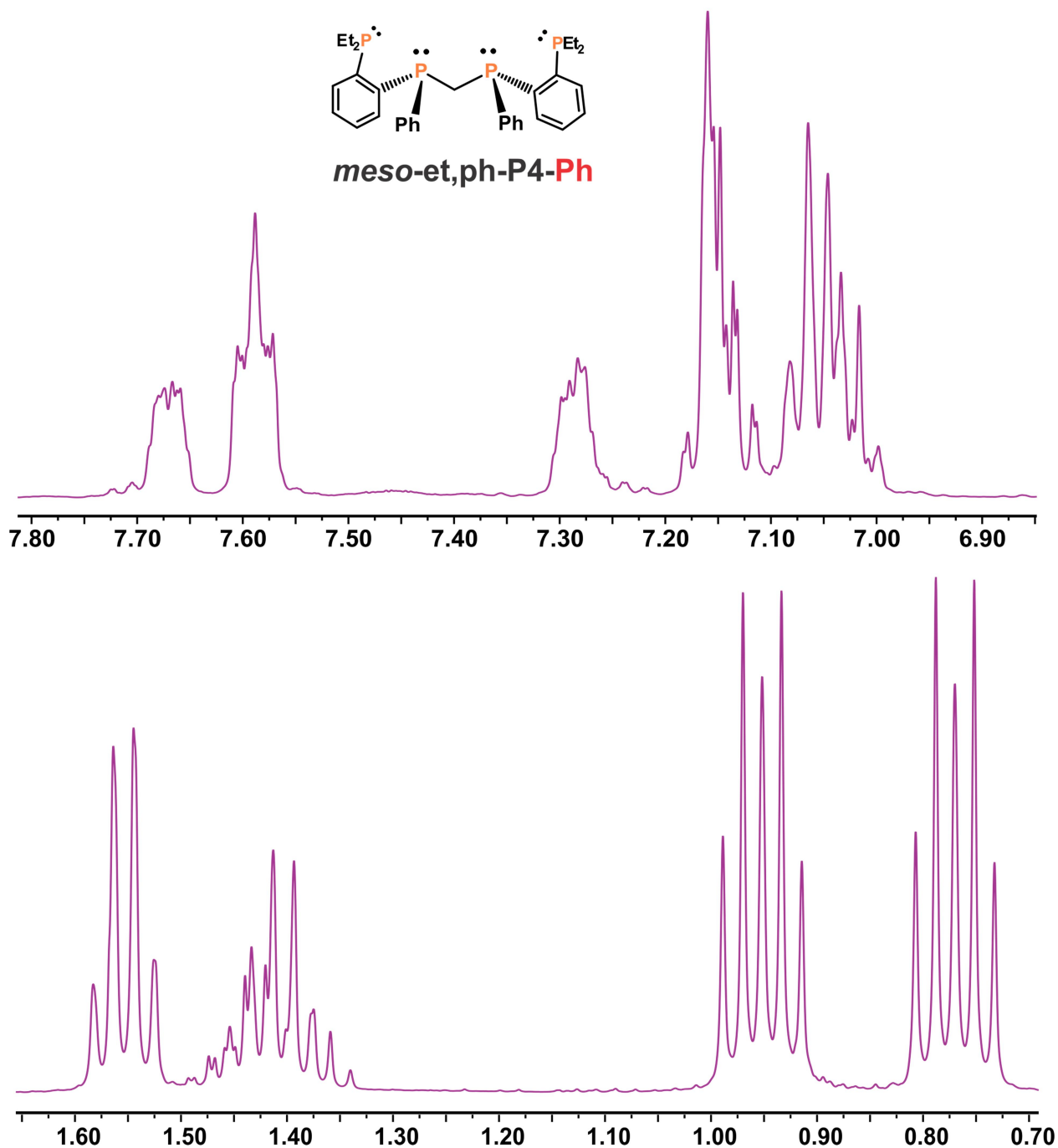


Figure 5.5 ^1H NMR of *meso*-et,ph-P4-Ph in C_6D_6 showing 7.80-6.80 ppm and 1.60-0.70 ppm regions.

^1H NMR (400.130 MHz)

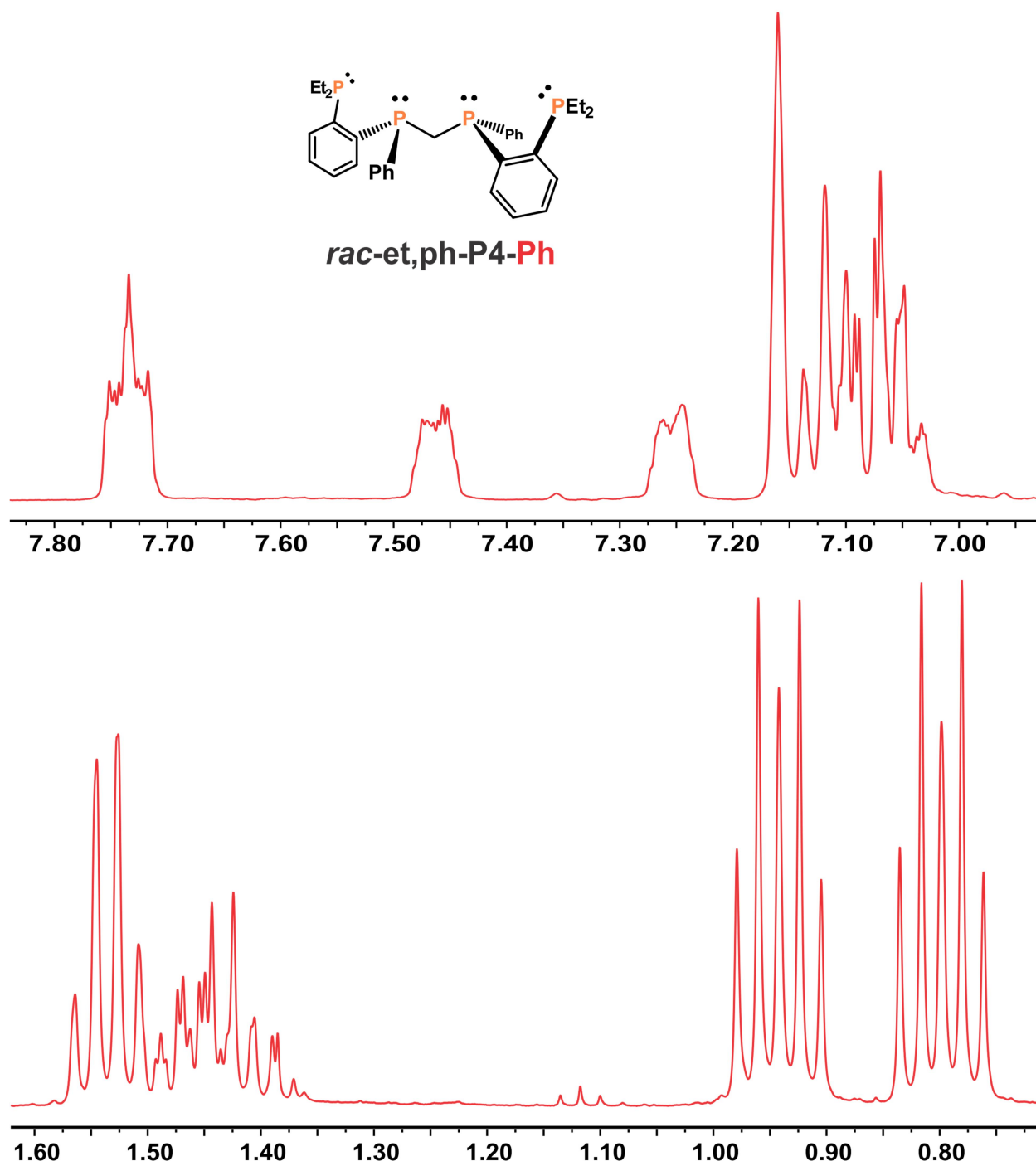


Figure 5.6 ^1H NMR of *rac*-et,ph-P4-Ph in C_6D_6 showing 7.80-6.80 ppm and 1.60-0.70ppm regions.

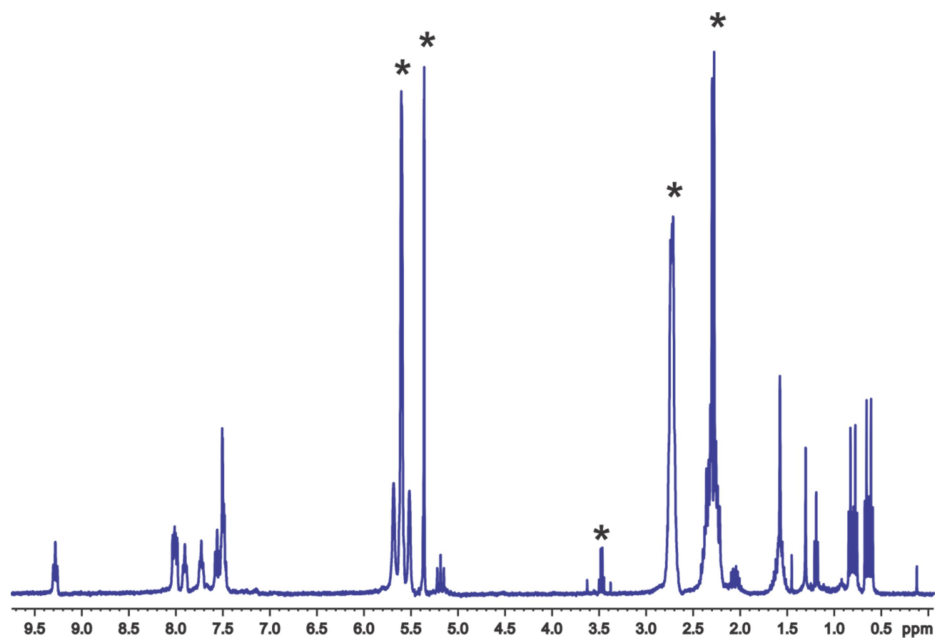


Figure 5.7. The ^1H NMR of $\text{rac-Pt}_2\text{Cl}_2(\text{et,ph-P4-Ph})$, 5R in CD_2Cl_2 . Asterisked peaks are due to unremoved $\text{PtCl}_2(\text{cod})$ and solvent impurities.

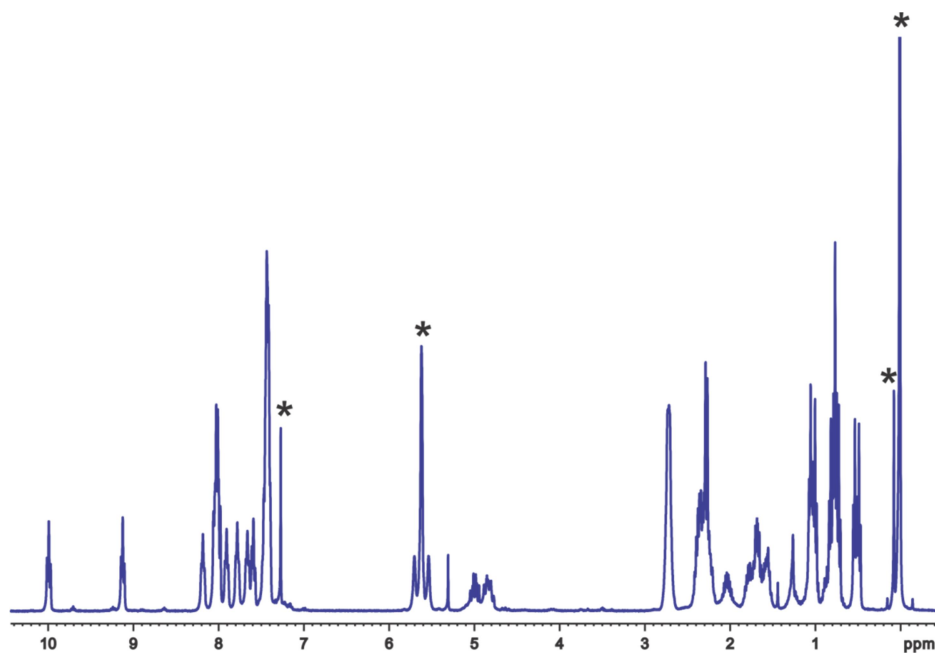


Figure 5.8. ^1H NMR of $\text{rac-NiPtCl}_4(\text{et,ph-P4-Ph})$ in CDCl_3 . Asterisked peaks are due to $\text{PtCl}_2(\text{cod})$ and solvent impurities.

5.17 References

1. Laneman, S. A.; Fronczek, F. R.; Stanley, G. G., Synthesis of binucleating tetratertiary phosphine ligand system and the structural characterization of both meso and racemic diastereomers of {bis[(diethylphosphinoethyl)phenylphosphino]methane}tetrachlorodinickel. *Inorganic Chemistry* **1989**, 28 (10), 1872-1878.
2. (a) Booth, G.; Chatt, J., Some complexes of ditertiary phosphines with nickel(II) and nickel(III). *J. Chem. Soc.* **1965**, (Copyright (C) 2010 American Chemical Society (ACS). All Rights Reserved.), 3238-41; (b) Venanzi, L. M., Tetrahedral nickel(II) complexes and the factors determining their formation. I. Bistriphenylphosphine nickel-(II) compounds. *J. Chem. Soc.* **1958**, (Copyright (C) 2010 American Chemical Society (ACS). All Rights Reserved.), 719-24.
3. Aubry, D. A.; Laneman, S. A.; Fronczek, F. R.; Stanley, G. G., Separating the Racemic and Meso Diastereomers of a Binucleating Tetrphosphine Ligand System through the Use of Nickel Chloride. *Inorganic Chemistry* **2001**, 40 (19), 5036-5041.
4. Monteil, A. R. Investigation into the Dirhodium-Catalyzed Hydroformylation of 1-Alkenes and Preparation of a Novel Tetrphosphine Ligand. Ph.D. Disseretation, Louisisana State University, 2006.
5. Weferling, N., Neue Methoden zur Chlorierung von Organophosphorverbindungen mit P-H-Funktionen. *Zeitschrift für anorganische und allgemeine Chemie* **1987**, 548 (5), 55-62.
6. Broussard, M. E.; Juma, B.; Train, S. G.; Peng, W.-J.; Laneman, S. A.; Stanley, G. G., A Bimetallic Hydroformylation Catalyst: High Regioselectivity and Reactivity Through Homobimetallic Cooperativity. *Science* **1993**, 260 (5115), 1784-1788.

Vita

Ekaterina Kalachnikova was born in Ekaterinburg, Russia, to Mr. Victor Kalachnikov and Mrs. Ludmila Kalachnikova. She earned her Bachelor's of Science degree, in chemistry in December, 2007 from University of South Alabama. In Fall 2008 she was excepted to Graduate School Doctoral program at Louisiana State University. She joined Prof. George Stanley research group, in the Spring 2009. Ekaterina plans to graduate with the degree of Doctor of Philosophy in chemistry from Louisiana State University in May 2015.